2013

Distributed Fault Diagnosis of Interconnected Nonlinear Uncertain Systems

Qi Zhang
Wright State University

Distributed Fault Diagnosis of Interconnected Nonlinear Uncertain Systems

A dissertation submitted in partial fulfillment of the
requirements for the degree of

Doctor of Philosophy

by

Qi Zhang

M.S., Wright State University, 2010
M.S., East China University of Science and Technology, Shanghai, China, 2009
B.S., East China University of Science and Technology, Shanghai, China, 2006

2013

Wright State University

WRIGHT STATE UNIVERSITY

The Graduate School

August 07, 2013

I HEREBY RECOMMEND THAT THE DISSERTATION PREPARED UNDER MY SUPERVISION BY **Qi Zhang** ENTITLED **Distributed Fault Diagnosis of Interconnected Nonlinear Uncertain Systems** BE ACCEPTED IN PARTIAL FULFILLMENT OF THE REQUIREMENTS FOR THE DEGREE OF **Doctor of Philosophy**.

_____

Xiaodong Zhang, Ph.D.
Dissertation Director

_____

Ramana V. Grandhi, Ph.D.
Director, Ph.D. in Engineering Program

_____

R. William Ayres, Ph.D.
Interim Dean, School of Graduate Studies

Committee on Final Examination

_____

Xiaodong Zhang, Ph.D.

_____

Kuldip S.Rattan, Ph.D.

_____

Raul Ordonez, Ph.D.

_____

Mark J. Mears, Ph.D.

_____

Zhiqiang Wu, Ph.D.

ABSTRACT

Zhang, Qi. Ph.D.in Engineering, Department of Electrical Engineering, Wright State University, 2013. *Distributed Fault Diagnosis of Interconnected Nonlinear Uncertain Systems*

Fault diagnosis is crucial in achieving safe and reliable operations of interconnected control systems. This dissertation presents a distributed fault detection and isolation (FDI) method for interconnected nonlinear uncertain systems. The contributions of this dissertation include the following: First, the detection and isolation problem of process faults in a class of interconnected input-output nonlinear uncertain systems is investigated. A novel fault detection and isolation scheme is devised, and the fault detectability and isolability conditions are rigorously investigated, characterizing the class of faults in each subsystem that are detectable and isolable by the proposed distributed FDI method. Second, a distributed sensor fault FDI scheme is developed in a class of interconnected input-output nonlinear systems where only the measurable part of state variables are directly affected by the interconnections between subsystems. A class of multimachine power systems is used as an application example to illustrate the effectiveness of the proposed approach. Third, the previous results are extended to a class of interconnected input-output nonlinear systems where both the unknown and the measurable part of system states of each subsystem are directly affected by the interconnections between subsystems. In this case, the fault propagation effect among subsystems directly affects the unknown part of state variables of each subsystem. Thus, the problem considered is more challenging than what is described above. Finally, a fault detection scheme is presented for a more general distributed nonlinear systems. With a removal of a restrictive limitation on the system model structure, the results described above are extended to a class of interconnected nonlinear uncertain systems with a more general structure.

In addition, the effectiveness of the above fault diagnosis schemes is illustrated by using simulations of interconnected inverted pendulums mounted on carts and multi-machine power systems. Different fault scenarios are considered to verify the diagnosis performances,

and the satisfactory performances of the proposed diagnosis scheme are validated by the good simulation results. Some interesting future research work is also discussed.

Contents

List of Figures

List of Tables

Acknowledgment

I would like to express my sincerest gratitude to my advisor Dr. Xiaodong Zhang for his outstanding guidance, constant encouragement and patience. I wish to thank Dr. Xiaodong Zhang for his valuable discussions and comments. I am also thankful to Dr. Kuldip Rattan, Dr. Raul Ordonez, Dr. Mark Mears and Dr. Zhiqiang Wu for their time and helpful feedback. Moreover, my warmest thanks go to my family for their love and support over the years.

Dedicated to

my family

Chapter 1

Introduction

Rapid progress in information technology is changing almost every aspect of how people live their lives. In the last decade, peoples' ability to access information has been greatly enhanced by significant improvements in computer hardware, software, and telecommunications. As an integration of the fast developing information technology and the traditional control technology, networked control systems have been applied in a broad range of areas in industry. Such systems are composed of a great number of locally distributed and dynamically interacting control components, including control units, sensors, and actuators. The information (sensor data, control signals, ect.) exchange among these control system components is accomplished via a communication network or direct interconnections. The primary advantages of distributed systems over the traditional centralized control systems include improved control performance, low cost, reduced computation resource requirements, reduced wiring or communication bandwidth requirements, simple installation and maintenance, and system agility. However, compared with tradition control systems, such distributed systems are more vulnerable to system faults, since the effect of a catastrophic failure in one subsystem will be quickly propagated to other subsystems due to interconnections or communications. In order to achieve reliable and safe operations of such distributed systems, the design of intelligent fault diagnosis technologies is a crucial step in the development of networked control system.

Recently, there have been significant research activities in the development of new methodologies of fault diagnosis in distributed networked control systems. However, most of these methods are based on a centralized architecture. In practice, due to the constraints on computational capabilities, wiring, and/or communication bandwidth, it is very difficult to address the problem of diagnosing faults in interconnected distributed systems using a centralized architecture. Also, limited research work has been done in the area of the fault diagnosis of distributed systems, in particular for distributed nonlinear uncertain systems This dissertation is motivated by the above significant issues. The research objective is to investigate the problem of distributed fault detection and isolation for interconnected nonlinear uncertain systems. The overall organization of the dissertation is as follows:

Chapter 2 presents a general introduction of networked control system and reviews the state of art of automated fault diagnosis techniques for distributed control systems.

Chapter 3 presents a distributed detection and isolation method for process faults in a class of interconnected nonlinear uncertain systems. A fault detection and isolation (FDI) component is designed for each subsystem in the interconnected system. A novel fault detection and isolation scheme is devised, and the fault detectability and isolability conditions are rigorously investigated, characterizing the class of faults in each subsystem that are detectable and isolable by the proposed distributed FDI method. Moreover, the stability and learning capability of the local adaptive fault isolation estimators designed for each subsystem is established. This chapter is based on the following paper:

- X. Zhang and Q. Zhang, "Distributed fault diagnosis in a class of interconnected nonlinear uncertain systems," *International Journal of Control* , vol. 85, no. 11, pp. 1644 -1662, 2012.

Chapter 4 presents a distributed sensor FDI scheme for a class of interconnected nonlinear systems, where only the measurable part of the state variables are directly affected by the interactions between subsystems. A multimachine power system is used as an illustrative example of the general method. In the multimachine power system, each generator

is interconnected with other generators through a transmission network. In the proposed distributed FDI scheme, a local FDI component is designed for each generator excitation system in the power system based on local measurements and certain communicated information from other FDI components associated with generators that are directly interconnected to the local generator. A fault detection and isolation scheme is developed and some of its properties, such as the fault detectability and isolability conditions are rigorously investigated. This chapter is based on the following paper:

- Q. Zhang and X. Zhang, "Distributed Sensor Fault Detection and Isolation for multimachine Power systems" , *International Journal of Robust and Nonlinear Control* , (under minor revision)

Chapter 5 presents a distributed sensor FDI method for a class of interconnected nonlinear uncertain systems. This chapter extends the results described in Chapter 4 by considering interconnected nonlinear systems where both the unknown part and the measurable parts of system states of each subsystem are directly affected by the interconnections. This chapter is based on the following paper:

- Q. Zhang and X. Zhang, "Distributed sensor fault detection and isolation in a class of interconnected nonlinear uncertain systems", *IFAC Annual Reviews in Control*, vol. 37, Issue 1, pp. 170-179, 2013.

Chapter 6 presents a distributed fault detection method for a class of interconnected nonlinear uncertain systems. This chapter extends previous results by considering more general nonlinear systems. Under certain assumptions, a distributed fault detection method is developed, and adaptive threshold for fault detection is derived, ensuring robustness with respect to interconnections among subsystems and modeling uncertainty. Moreover, the fault detectability conditions are rigorously investigated, characterizing the class of detectable process faults and sensor faults in each subsystem. This chapter is based on the following paper:

- Q. Zhang and X. Zhang, "A distributed detection scheme for process faults and sensor faults in a class of interconnected nonlinear uncertain systems," *the 2012 IEEE Conference on Decision and Control* , Maui, Hawaii, pp. 586-591, 2012. (Also in the preparation of submission to IEEE Transactions on Automatic Control)

Chapter 7 includes some concluding remarks and some discussion of future research directions as described.

Chapter 2

Literature Review: Research Motivation

In this chapter, a general introduction of networked control system is first presented. Then, an overview of the field of fault diagnosis is given, and some important concepts and definitions are introduced. In addition, we review some existing research work focusing on the areas of fault detection and isolation of distributed linear and nonlinear systems, respectively. Then, the research objectives of this dissertation are presented.

2.1 Introduction of Networked Control System

The networked control systems (NCS) are a class of spatially distributed control systems where all the system components (sensors, actuators and controllers) exchange information through a shared bandwidth, limited digital communication network [27, 7, 73]. As shown in Fig. 2.1, all the nodes in NCS (i.e., sensors, actuators and controllers) can be connected to each other through a communication network, and the complexity and cost of design and operation of the control systems can be significantly reduced [27, 30, 67, 44]. Moreover, since NCS have a flexible architecture and enhanced agility, with adding or removal of sensors, actuators or controllers in the overall system, low cost and reliable installation and

maintenance can be achieved.

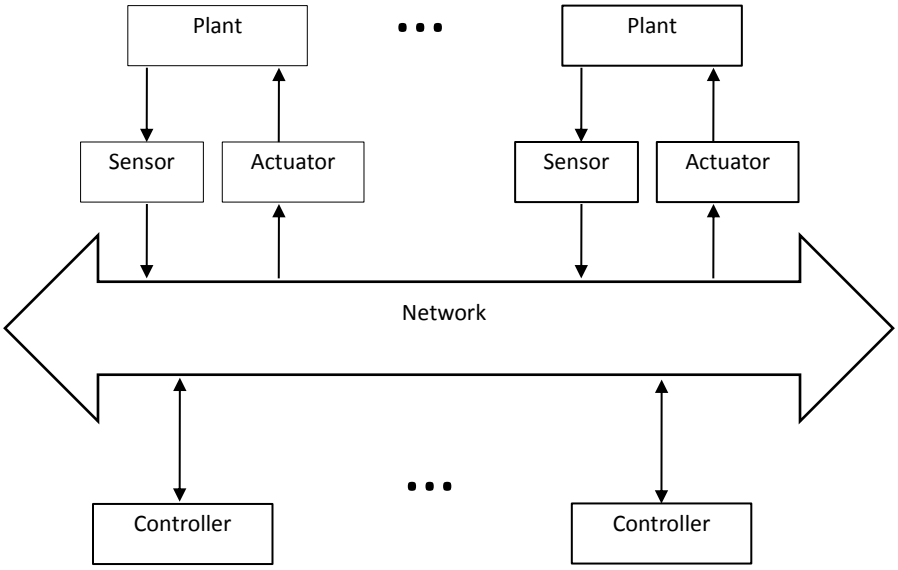

Figure 2.1: Typical Structure of Networked Control System.

In recent years, the area of NCS is attracting more and more attention, and there have been many applications of networked control system in different areas of the engineering field. Examples of such systems including automotive control systems [53, 38, 16], distributed jet engine control [1], cooperative control of a team of unmanned vehicles [45], haptics collaboration over the Internet [29, 31, 59], power generation and distribution systems [25], and water transport networks [13], etc.

In order to get more insight into the networked control system concept, the networked control system architecture of the Volvo XC90 [38] shown in Fig. 2.2 is considered as an illustrative example. The embedded distributed vehicle control system is considered as a networked control system composed of different types of subsystems (i.e., the electrical control units (ECUs) as shown in Table 2.1) and different types of communication networks. Specifically, the power train and chassis ECUs (e.g., TCM, ECM, BCM, etc) exchange the

information through a CAN bus (represented by red line) with a communication rate of 500 kbps. The body electronics ECUs (e.g., DDM, PDM, CCM, etc) are interconnected with each other via another type of CAN bus (represented by light blue line) with a communication rate of 125 kbps. In addition, the media oriented system transport (MOST) networks (represented by dark blue lines) connects the infotainment and telematics ECUs, and the slave nodes are connected into the corresponding ECU through local interconnect networks (LINs) which are denoted by dashed black lines.

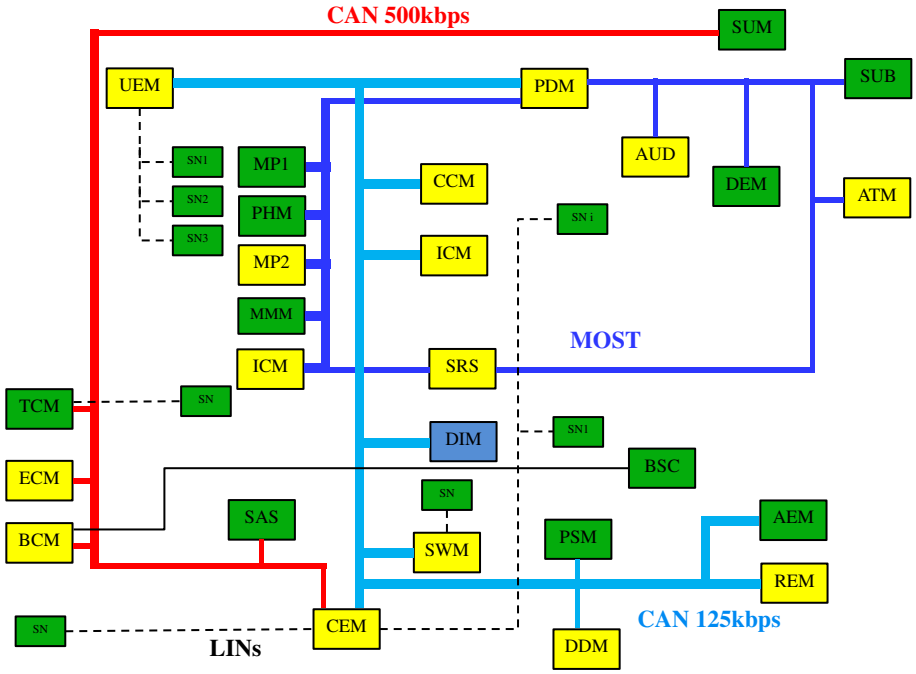

Figure 2.2: Distributed control architecture for the Volvo XC90.

Table 2.1 ECUs in the networked control system architecture of the Volvo XC90 [38]

Powertrain and chassis	**Body electronics**
TCM Transmission control module	CEM Central electronic module
ECM Engine control module	SWM Steering wheel module
BCM Brake control module	DDM Driver door module
BSC Body sensor cluster	REM Rear electronic module
SAS Steering angle sensor	CCM Climate control module
SUM Suspension module	PDM Passenger door module
AUD Audio module	
Infotainment/Telematics	
MP1,2 Media player 1 and 2	ICM Infotainment control
PHM Phone module	UEM Upper electronic module
MMM Multimedia module	DIM Driver information module
SUB Subwoofer	AEM Auxiliary electronic module
ATM Antenna tuner module	

Recently, significant research work has been done in area of NCS. Most of the results focus on the control problem [75], including

(1) Control of networks: in order to achieving efficient utilization of network resources of NCS, the problem of network resources scheduling is investigated([64, 10, 74]).

(2) Control over networks: because the data of all nodes of NCS is exchanged through unreliable communication links, a lot of work has been done in designing of feedback strategies adapted to NCS, while maintaining system stability or good control performance([23, 68, 12]).

(3) Multi-agent systems: some research work has been devoted to analyzing how network architecture and interactions between subsystems influence global control goals ([54, 55, 46]).

In order to achieve reliable and safe operations of NCS, the design of fault diagnosis and

accommodation schemes is also a crucial step. However, there has been limited research work on fault diagnosis of networked control system. Thus, the study of fault diagnosis and accommodation of NCS needs to be considered as one of the key future directions for networked control systems research.

In the last two decades, there have been significant research activities in the design and analysis of fault diagnosis and accommodation schemes ([3, 5, 24, 36, 22]). However, most of these existing methods consider traditional centralized control systems. Thus, the distributed fault diagnosis problem has attracted significantly increasing attention in recent years.

2.2 Overview of Automated Fault Diagnosis

A fault is defined as an unpermitted deviation of at least one characteristic property of a variable from an acceptable behavior. It may lead to a malfunction or failure of the system. The faults in the system can generally be classified into three types: component faults, actuator faults, and sensor faults.

1. A component fault typically represents a fault which leads to changes in the normal system dynamics. It can be modeled as an additive component fault or multiplicative component fault [24]. An additive component fault causes changes in the system outputs independent of known inputs. A multiplicative component fault is expressed as changes in plant parameters in a process. For example, in a vehicular electric power generation and storage system, damaged diodes in the rectifier in the alternator results in a component fault [80].

2. An actuator fault represents the discrepancies between the input command of an actuator and its actual output. For instance, in an aircraft control system, control surface damage can be considered as an actuator fault [33].

3. A sensor fault represents the deviation between the measured and the actual value of a plant's output variable.

Actuator faults and sensor faults are commonly modeled as additive faults in the system. Also, according to the time profiles of faults, faults can be classified as follows:

(i) abrupt fault , i.e., step-like change.

(ii) incipient faults. The magnitude of an incipient fault develops over a period of time. They are often modeled as a drift or time-varying change in the parameters of a system.

(iii) intermittent fault. In a system, the symptoms of an intermittent fault only show up at some time intervals or operating conditions, not all the time.

The fault diagnosis procedure monitors the system and generates information about the abnormal behavior of its components. In general, *fault detection*, *fault isolation* and *fault identification* are the three main steps of the fault diagnosis procedure [5]. The occurrence of a fault in a monitored system can be determined in the *fault detection* stage. The step of *fault isolation* ensures that we are able to retrieve some information about the fault such as fault type or location, and *fault identification* determines the size or nature of the fault. Next, we introduce some important properties for evaluating the performance of fault diagnosis schemes, including robustness, fault detectability and isolability.

(i) Robustness is the ability of the scheme to operate in the presence of noise, disturbance, and modeling errors, with few false alarms.

(ii) Detectability and isolability are characterized by the class of faults which can be successfully detected and isolated. A successful fault diagnosis scheme should be able to detect and isolate faults of reasonably small sizes.

2.3 Fault Diagnosis Methods of Distributed Linear Systems

Early research work in the area of fault diagnosis of distributed system focuses on linear systems [61, 28, 52]. The overlapping decomposition techniques proposed in [34] is used to decompose a large scale linear system into subsystems sharing some common state variables. Multiple decentralized observers are designed based on the subsystems, and differences between the same state as estimated by the different observer can be used to isolate the

fault. In [58, 45], a decentralized detection filter method is presented to estimate the states of the distributed linear system, and the absence of modeling uncertainty is assumed.

Recently, some research work [49, 50] have considered detection of malicious attacks in *cyber-physical systems* modeled as distributed linear systems. *Cyber-physical systems* is a class of distributed system consisting of physical processes of each subsystem as well as communication networks among all the subsystems. There are many examples of *cyber-physical systems* in industry, such as power generation and distribution networks, computer networks, sensor networks, and energy efficient buildings. Such distributed systems are vulnerable to malicious attacks in the communication link among subsystems, for example, the Davis-Besse nuclear plant suffered the SQL Slammer worm attack in January 2003 [42], and the StuxNet computer worm [17] attacked Iran's nuclear facilities in June 2010. As an example, a differential-algebraic model of the ith cyber- physical subsystem under attack is represented as follows [50]:

$$E_i\dot{x}_i(t) = A_i x_i(t) + \sum_{j\in N_i} A_{ij}x_j(t) + B_{K_i}u_{K_i}(t), \tag{2.1}$$

$$y_i(t) = C_i x_i(t) + D_{K_i}u_{K_i}(t)\ ,\ , \tag{2.2}$$

where $x_i(t) \in \Re_i^n$ and $y_i(t) \in \Re_i^m$ are the state vector and the output vector of the ith subsystem, respectively, and u_{K_i} represents the K_ith type of attack on the system dynamics or sensor outputs. N_i are the neighbors of the ith subsystem, A_i, B_{K_i}, D_{K_i} and C_i are known matrices with appropriate dimensions, and the matrix E_i is possibly singular.

Based upon a waveform relaxation technique [43, 8], in [11, 49, 50, 51], a distributed fault detection filter is proposed for each subsystem to detect any fault that may occur in the corresponding subsystem. Also, the attack isolation problem for a certain class of cyber-physical system has been considered in [49, 50], where a bank of distributed fault isolation estimators are designed for each subsystem to identify a fault defined in a fault set. Specifically, for the ith subsystem described in (2.2), the interconnections between subsystems (i.e. $\sum_{j\in N_i} A_{ij}x_j(t)$) is treated as an unknown input, and a bank of unknown input observers

are designed. Thus, the residual of each unknown input observer is insensitive to the interconnection term, and only sensitive to attacks in the ith subsystem. An isolation scheme is proposed to identify both the subsystem where actual fault occurred and the particular type of fault in that subsystem.

2.4 Fault Diagnosis Methods of Distributed Nonlinear Systems

In recent years, the area of distributed fault diagnosis of interconnected nonlinear system has attracted significantly increasing attention [20, 72, 18, 48, 19, 86, 4]. Consider a nonlinear dynamic system composed of M interconnected subsystems. A general system model is given by the following differential equations, for $i = 1, \cdots, M$

$$\begin{aligned} \dot{x}_i &= f_i(x_i, u_i) + g_i(x, u_i, u_j) + \eta_i(x_i, u_i, t) + \beta_{ix}(t - T_{0x})\phi_i(x_i, u_i) \\ y_i &= C_i x_i + \beta_{iy}(t - T_{0y})\theta_i(t) \end{aligned} \tag{2.3}$$

where $x_i \in \Re^{n_i}$, $u_i \in \Re^{m_i}$, $y_i \in \Re^{l_i}$ and $x \in \Re^n$ are the local state vector, input vector, and output vector of the ith subsystem ($n_i \geq l_i$), and state vector of the overall system, respectively, $f_i : \Re^{n_i} \times \Re^{m_i} \mapsto \Re^{n_i}$ represents the local nominal dynamics, $g_i : \Re^n \times \Re^{m_i} \times \Re^{m_j} \mapsto \Re^{n_i}$ represents the interconnection effect, $\eta_i : \Re^{n_i} \times \Re^{m_i} \times \Re^{+} \mapsto \Re^{n_i}$ is the modeling uncertainty. The term $\beta_{ix}(t - T_{0x})\phi_i(x_i, u_i)$ denotes the changes in the dynamics of the ith subsystem due to the occurrence of a process fault in the local subsystem. Specifically, the vector β_{ix} characterizes the time profile of a process fault occurring at some unknown time T_{0x}, and $\phi_i(x_i, u_i)$ represents the nonlinear process fault function. The changes in the dynamics of ith subsystem caused by a sensor fault are characterized by the term $\beta_{iy}(t - T_{0y})\theta_i(t)$. Specifically, the vector $\theta_i(t)$ denotes a time-varying bias on measurements caused by a sensor fault, and β_{iy} represents the time profile of the sensor fault, where T_{0y} is the sensor fault occurrence time.

In recent research work of the fault diagnosis of nonlinear distributed systems, the inter-

connection function g_i is often assumed to be partially known or satisfy certain conditions. For instance, the interconnection term is assumed to be linear in [45, 58], and the interconnection term is assumed to satisfy lipschitz conditions in [72]. In [20, 19, 47, 18, 48, 4], an on-line neural approximation model is used to estimate the interconnection term g_i, and an upper bound of the network approximation error is assumed to be known.

In [20, 18, 19], the overlapping decompositions strategy is applied to detect faults in large-scale nonlinear systems. The distributed system is decomposed into sets of interconnected subsystems sharing certain state variables. Based on the measurable local state and the transmitted variables from the neighboring subsystem, a local fault detector is designed for each subsystem. The interconnection between neighboring subsystems is approximated by the neural network and the approximation information is sent to the local fault detector in each subsystem. Moreover, a specially designed consensus-based estimator is used to make the diagnoser reach a common decision about the variables which are affected by faults. However, it is assumed that all the state variables are measurable. Additionally, the unknown interconnection term is approximated by a linearly parameterized adaptive approximator, and a bound on the approximation error is assumed to be known.

In [72], the sliding mode observer is used to address the problem of decentralized actuator fault detection and estimation for a class of nonlinear large-scale systems. A sliding mode observer is developed together with an appropriate coordinate transformation to find the sliding mode dynamics. Then, an equivalent output error injection is used to estimate the decentralized fault. The modeling uncertainty is assumed to have a certain structure and a non-linear bound. In [72], the modeling uncertainty is assumed to be structured with a known distribution matrix. Certain conditions on the uncertainty distribution matrix are assumed to allow decoupling the effect of modeling uncertainty. Also, the upper bound on the modeling uncertainty is assumed to satisfy a Lipschitz condition. When the above conditions are satisfied, [72] provides a powerful method for fault estimation. However, the modeling uncertainties in many practical systems are often unstructured. Additionally, the fault estimation method presented in [72] does not necessarily allow the isolation of faults

affecting the same state equation.

2.5 Research Motivation

In order to achieve safe and reliable operations of interconnected nonlinear controls systems at all times, despite the possible occurrence of faulty behaviors in some subsystems, the design of FDI schemes is a crucial step. First, an occurrence of any fault in any subsystem needs to be detected as early as possible. Then, fault isolation schemes are required to determine the particular fault type/location. Because of the fault effect propagation among subsystems, multiple subsystems may be affected by a fault in a local subsystem. Thus, a hierarchical fault isolation architecture needs to be considered in the FDI schemes, including : 1) determining the faulty subsystem where the fault actually occurred among the set of all subsystems. 2) determining the type of the fault among a set of known (or partially known) possible fault types in the faulty subsystem.

The distributed fault detection and isolation methods introduced in Section 2.4 are very interesting. However, the FDI problem for a general interconnected nonlinear uncertain systems remains open.

As described above, in the literature of fault diagnosis of distributed nonlinear systems, some research work considered the system with full-state measurements [20, 18, 19]. However, in practice, only a part of the states are available. As a result, it is important to consider the FDI problem of input-output systems with partial state measurements. Moreover, some research work assume the absence of modeling uncertainty (e.g., [58]) or structured modeling uncertainty (e.g., [72]). In the case of structured models of the modeling uncertainty, in order to achieve robustness, it is often assumed that the uncertainty distribution matrix satisfies certain rank conditions. Based on such assumptions, we can derive a system which is decoupled from the modeling uncertainties, but remain sensitive to the faults by using a suitable state transformation. However, the modeling uncertainty in many of practical systems are unstructured, thus, it is necessary to address the problem of unstructured

modeling uncertainty. Additionally, most of the research work introduced in Section 2.4 only focus on the fault detection problem of the distributed nonlinear systems. There are very limited results investigating the fault isolation problem of the distributed nonlinear systems.

The idea of using adaptive and learning techniques for fault diagnosis and accommodation has been proposed in (see, for instance, [39, 83, 37, 66, 70, 6]). However, most of these methods are based on a centralized fault diagnosis architecture. In practice, due to constraints on computational capabilities and communication bandwidth, it is very difficult to address the problem of diagnosing faults in interconnected systems using a centralized architecture. Thus, in this dissertation, fault diagnosis schemes with a distributed architecture are considered.

The first research objective of this dissertation is to investigate the detection and isolation problem of process faults in a class of interconnected input-output nonlinear systems with unstructured uncertainty. In such systems, it is assumed that system states of each subsytem can be decomposed into an unknown part and a measurable part by a state transformation, and the mearuable part of states may be directly affected by a set of process fault types which are partially known. Our goal is detect and identify which one has actually occurred in a faulty subsystem. In the proposed distributed FDI architecture, a FDI component is designed for each subsystem in the interconnected system. For each subsystem, its corresponding local FDI component is designed by utilizing local measurements and certain communicated information from neighboring FDI components associated with subsystems that are directly interconnected to the particular subsystem under consideration. A novel fault detection and isolation scheme is developed and some of its properties, such as the fault detectability and isolability conditions are rigorously investigated.

The second research objective of this dissertation is to study the sensor FDI problem for a class of interconnected input-output nonlinear systems with an unstructured modeling uncertainty. Because the effect of a faulty sensor in a subsystem may be propagated to other interconnected subsystems, distributed sensor FDI is a challenging problem, and our goal

is determining the faulty subsystem where the sensor fault actually occurred. A distributed sensor FDI scheme is developed for a class of interconnected nonlinear systems where only the measurable part of state variables are directly affected by the interactions between subsystems. A class of multimachine power systems is used as an application example to illustrate the effectiveness of the proposed method, and the method can be easily extended to other systems with the similar model structure. In the multimachine power system, each generator is interconnected with other generators through a transmission network, and it is assumed that the system state in each generator excitation control system can be decomposed into an unknown part and a measurable part. In the proposed distributed FDI scheme, a local FDI component is designed for each generator excitation system in the power system based on local measurements and certain communicated information from other FDI components associated with generators which are directly interconnected to the local generator. A fault detection and isolation scheme is developed and some of its properties, such as the fault detectability and isolability conditions are rigorously investigated.

The third research objective of this dissertation is to extend the above results on sensor fault diagnosis by considering a class of interconnected input-output nonlinear systems, where both the unknown part and the measurable part of system states of each subsystem are directly affected by the interconnection between subsystem. In this case, a fault propagation effect among subsystems directly affects the unknown part of state variables of each subsystem. Thus, the problem considered is more challenging than what is described above.

The fourth research objective of this dissertation is to consider the fault detection problem of more general distributed nonlinear systems. In the research work described above, it is assumed that the nonlinear system model satisfies certain structural assumptions. Specifically, it is assumed that the system state in each subsystem can be decomposed into an unknown part and a measurable part, with the unknown part assumed to be stable and not directly affected by faults. Under this task, we significantly extend the above research work by removing these restrictive limitations on system model structure and fault effects. Under certain assumptions, a distributed fault detection method is developed for a

class of interconnected nonlinear uncertain systems with a more general system structure. In the distributed detection scheme, a fault detection component is associated with each subsystem. Adaptive thresholds for fault detection are derived, ensuring robustness with respect to interconnections among subsystems and modeling uncertainty. Moreover, the fault detectability conditions are rigorously investigated, characterizing the class of detectable process faults and sensor faults in each subsystem.

Chapter 3

Distributed Process Fault Detection and Isolation in Interconnected Nonlinear Systems

A centralized FDI methodology for nonlinear uncertain systems has been developed in [83, 84]. The chapter significantly extends the previous results by developing a distributed FDI scheme for a class of interconnected nonlinear uncertain systems. The class of faults considered are nonlinear process faults which directly affect the dynamics of a particular subsystem and includes both abrupt and incipient faults, including components faults and actuator faults described in Section 2.2. Because of the interactions among subsystems and the limitation of information that is available for each subsystem, the problem of distributed FDI is very challenging. In the presented distributed FDI architecture, a fault diagnostic component is designed for each subsystem in the interconnected system by utilizing local measurements and certain communicated information from neighboring FDI components associated with its directly interconnected subsystems. Each local FDI component consists of a fault detection estimator (FDE) and a bank of nonlinear adaptive *fault isolation estimators* (FIEs), where each FIE is associated with a type of potential nonlinear fault associated

with the corresponding subsystem. Once a fault is detected in a particular subsystem, then the corresponding local FIEs are activated for the purpose of determining the particular type of fault that has occurred in the subsystem.

In the fault isolation scheme, a set of adaptive thresholds are designed in order to evaluate residuals generated from each FIE, and we can eliminate the possibility of the occurrence of a particular fault based on the fact that at least one of the residual components of the corresponding isolation estimator exceeds its threshold in finite time. Thus, if all but one of the faults are excluded, then a successful fault isolation can be achieved. In addition, a concept 'fault mismatch function' is applied in describing the similarity degree of two faults. If two faults are not sufficiently different, then they can not be isolated by using the proposed FDI method.

The distributed FDI method is presented with an analytical framework aiming at characterizing its important properties. Specifically, the analysis focuses on: (i) derivation of adaptive thresholds for distributed fault detection and fault isolation, ensuring the robustness property with respect to interactions among interconnected subsystems and modeling uncertainty; (ii) investigation of fault detectability and isolability conditions, characterizing the class of faults in each subsystem that are detectable and isolable by the proposed method; (iii) investigation of stability and learning capability of local adaptive fault isolation estimators designed for each subsytem.

The chapter is organized as follows. In Section 3.1, the problem of distributed FDI for a class of interconnected nonlinear uncertain systems is formulated. Section 3.2 describes the distributed FDI architecture and the design of local FDI component for each subsystem in the interconnected system. The design of adaptive thresholds for distributed fault isolation in each subsystem is presented in Section 3.4. Section 3.5 analyzes several important properties of the distributed FDI method, including fault detectability, fault isolability, and stability and learning capability of the adaptive fault isolation estimators. To illustrate the effectiveness of the diagnostic method, some simulation results of an example of interconnected inverted pendulums mounted on carts is presented in Section 3.6.

3.1 Problem Formulation

Consider a nonlinear dynamic system composed of M interconnected subsystems with the dynamics of the ith subsystem, $i = 1, \cdots, M$, being described by the following differential equation

$$\begin{aligned} \dot{z}_i &= A_i z_i + \zeta_i(z_i, u_i) + \varphi_i(z_i, u_i, t) + \beta_i(t - T_0) E_i \bar{f}_i(z_i, u_i) \\ &\quad + \textstyle\sum_{j=1}^{M} \left[h_{ij}(z_i, z_j, u_i, u_j) + d_{ij}(z_i, z_j, u_i, u_j) \right] \\ y_i &= \bar{C}_i z_i \end{aligned} \tag{3.1}$$

where $z_i \in \Re^{n_i}$, $u_i \in \Re^{m_i}$, and $y_i \in \Re^{l_i}$ are the state vector, input vector, and output vector of the ith subsystem ($n_i \geq l_i$), respectively, $\zeta_i : \Re^{n_i} \times \Re^{m_i} \mapsto \Re^{n_i}$, $\varphi_i : \Re^{n_i} \times \Re^{m_i} \times \Re^{+} \mapsto \Re^{n_i}$, $\bar{f}_i : \Re^{n_i} \times \Re^{m_i} \mapsto \Re^{q_i}$, d_{ij} and $h_{ij} : \Re^{n_i} \times \Re^{n_j} \times \Re^{m_i} \times \Re^{m_j} \mapsto \Re^{n_i}$ are smooth vector fields. Specifically, the model given by

$$\begin{aligned} \dot{z}_{Ni} &= A_i z_{Ni} + \zeta_i(z_{Ni}, u_i) \\ y_{Ni} &= \bar{C}_i z_{Ni} \end{aligned}$$

is the *known nominal* model of the ith subsystem with ζ_i being the known nonlinearity. The vector field φ_i in (3.1) represents the modeling uncertainty of the ith subsystem, and $\beta_i(t - T_0) E_i \bar{f}_i(z_i, u_i)$ denotes the changes in the dynamics of ith subsystem due to the occurrence of a fault in the local subsystem. Specifically, $\beta_i(t - T_0)$ is a step function representing the time profile of a fault which occurs at some unknown time T_0 (i.e., $\beta_i(t - T_0) = 0$ if $t < T_0$, and $\beta_i(t - T_0) = 1$ if $t \geq T_0$), $\bar{f}_i(z_i, u_i)$ is a nonlinear fault function, and E_i is a fault distribution matrix. Additionally, the vector fields h_{ij} and d_{ij} represent the direct interconnection between the ith subsystem and the jth subsystem. Specifically, h_{ij} is the known part of direct interconnection, while d_{ij} is the unknown part of the interconnection. It is noted that likely many functions h_{ij} and d_{ij} are identically zero in an interconnected system (i.e., many subsystems do not directly influence subsystem i). Moreover, $h_{ii} = 0$ and $d_{ii} = 0$ because the interconnection terms are only defined between two subsystems.

Assumption 3.1 *The constant matrices $E_i \in \Re^{n_i \times q_i}$ and $\bar{C}_i \in \Re^{l_i \times n_i}$ with $q_i \leq l_i$ are of*

full column rank and satisfies the condition $rank(\bar{C}_i E_i) = q_i$. *Additionally, all the invariant zeros of the system* (A_i, E_i, $\bar{C}_i$) *are in the left half plane.*

Then, under Assumption 3.1, for $i = 1, \cdots, M$, there exists a change of coordinates $x_i = [x_{i1}^\top \ x_{i2}^\top]^\top = T_i z_i$ with $x_{i1} \in \Re^{(n_i - l_i)}$ and $x_{i2} \in \Re^{l_i}$, such that [72]

- $T_i E_i = \begin{bmatrix} 0 \\ E_{i2} \end{bmatrix}$, where $E_{i2} \in \Re^{l_i \times q_i}$.
- $\bar{C}_i T_i^{-1} = [0 \ \ C_i]$, where $C_i \in \Re^{l_i \times l_i}$ is orthogonal.

Therefore, in the new coordinate system, the system model (3.1) is in the form of

$$\begin{aligned}
\dot{x}_{i1} &= \mathcal{A}_{i1} x_{i1} + \mathcal{A}_{i2} x_{i2} + \rho_{i1}(x_i, u_i) + \phi_{i1}(x_i, u_i, t) \\
&\quad + \sum_{j=1}^{M} \Big[H_{ij}^1(x_i, x_j, u_i, u_j) + D_{ij}^1(x_i, x_j, u_i, u_j) \Big] \\
\dot{x}_{i2} &= \mathcal{A}_{i3} x_{i1} + \mathcal{A}_{i4} x_{i2} + \rho_{i2}(x_i, u_i) + \phi_{i2}(x_i, u_i, t) + \beta_i(t - T_0) E_{i2} \bar{f}_i(x_i, u_i) \\
&\quad + \sum_{j=1}^{M} \Big[H_{ij}^2(x_i, x_j, u_i, u_j) + D_{ij}^2(x_i, x_j, u_i, u_j) \Big] \\
y_i &= C_i x_{i2} \,,
\end{aligned} \tag{3.2}$$

where $\begin{bmatrix} \mathcal{A}_{i1} & \mathcal{A}_{i2} \\ \mathcal{A}_{i3} & \mathcal{A}_{i4} \end{bmatrix} = T_i A_i T_i^{-1}$, $\begin{bmatrix} \rho_{i1} \\ \rho_{i2} \end{bmatrix} = T_i \zeta_i$, $\begin{bmatrix} \phi_{i1} \\ \phi_{i2} \end{bmatrix} = T_i \varphi_i$, $\begin{bmatrix} H_{ij}^1 \\ H_{ij}^2 \end{bmatrix} = T_i h_{ij}$, and $\begin{bmatrix} D_{ij}^1 \\ D_{ij}^2 \end{bmatrix} = T_i d_{ij}$. Let us define $\bar{x}_j$, $\bar{u}_j$, and $\bar{y}_j$ as the vectors comprising of the state variables, input signals, and output variables of those subsystems that have nonzero unknown interconnection terms D_{ij}^1 and D_{ij}^2 with respect to subsystem i, respectively. Then,

by allowing a more general structure of the fault function, we have

$$\begin{aligned}
\dot{x}_{i1} &= \mathcal{A}_{i1}x_{i1} + \mathcal{A}_{i2}x_{i2} + \rho_{i1}(x_i, u_i) + \eta_{i1}(x_i, \bar{x}_j, u_i, \bar{u}_j, t) + \sum_{j=1}^{M} H_{ij}^1(x_i, x_j, u_i, u_j) \\
\dot{x}_{i2} &= \mathcal{A}_{i3}x_{i1} + \mathcal{A}_{i4}x_{i2} + \rho_{i2}(x_i, u_i) + \eta_{i2}(x_i, \bar{x}_j, u_i, \bar{u}_j, t) + \beta_i(t - T_0)f_i(x_i, u_i) \\
&\quad + \sum_{j=1}^{M} H_{ij}^2(x_i, x_j, u_i, u_j) \\
y_i &= C_i x_{i2}\,,
\end{aligned} \tag{3.3}$$

where $\eta_{i1} \stackrel{\triangle}{=} \phi_{i1} + \sum_{j=1}^{M} D_{ij}^1$, $\eta_{i2} \stackrel{\triangle}{=} \phi_{i2} + \sum_{j=1}^{M} D_{ij}^2$, and $f_i : \Re^{n_i} \times \Re^{m_i} \mapsto \Re^{l_i}$ is a smooth vector field representing the *unstructured* nonlinear fault function in each subsystem under consideration, Clearly, (3.2) is a special case of (3.3) with $f_i(x_i, u_i) = E_{i2}\bar{f}_i$.

To formulate the fault isolation problem, it is assumed that there are N_i types of faults in the fault set associated with the ith subsystem, $i = 1, \cdots, M$. Specifically, the unknown fault function $f_i(x_i, u_i)$ in (3.3) is assumed to belong to a finite set of fault types given by

$$\mathcal{F}_i \stackrel{\triangle}{=} \left\{ f_i^1(x_i, u_i), \;\; \ldots, \;\; f_i^{N_i}(x_i, u_i) \right\}. \tag{3.4}$$

Each fault type f_i^s, $s = 1, \cdots, N_i$, is in the form of

$$f_i^s(x_i, u_i) \stackrel{\triangle}{=} \left[(\theta_{i1}^s(t))^\top g_{i1}^s(x_i, u_i), \cdots, (\theta_{il_i}^s(t))^\top g_{il_i}^s(x_i, u_i) \right]^\top, \tag{3.5}$$

where $\theta_{ip}^s(t)$, $p = 1, \cdots, l_i$, characterizing the unknown fault magnitude, is a parameter vector assumed to belong to a known compact and convex set Θ_{ip}^s (i.e., $\theta_{ip}^s(t) \in \Theta_{ip}^s$, $\forall t \geq 0$), and g_{ip}^s is a known smooth vector field representing the functional structure of the sth fault affecting the pth component of state vector x_{i2} of the ith subsystem. For instance, in the case of a leakage fault [83], $\theta_{ip}^s(t)$ characterizes the size of the leakage in a tank, and g_{ip}^s represents the functional structure of the fault affecting each state equation.

The fault isolation problem formulated above is motivated by practical considerations. In many engineering applications, based on the historical data and past experiences, the system

engineers often have a reasonably good idea of the types of faults that may occur in a particular system. Although different faults have possibly different nonlinear effects on the system dynamics, for a given type of fault, the uncertainty is often the magnitude of the fault. In [83], a well-known fault diagnosis benchmark example, the three-tank system, has been considered to motivate the definition of the fault set described by (3.2) and (3.3).

The objective of this chapter is to develop a robust distributed fault detection and isolation scheme for the class of interconnected nonlinear uncertain systems that can be transformed into (3.3). It is worth noting that the case of a new fault, which doesn't belong to the fault set (3.4), can also be determined based on the presented FDI method, if its fault functional structure is sufficiently different (as quantified in Section 3.5.2). Throughout the paper, the following assumptions are made:

Assumption 3.2 *The functions η_{i1} and η_{i2} in (3.3), representing the unstructured modeling uncertainty, are unknown nonlinear functions of x_i, $\bar{x}_j$, u_i, $\bar{u}_j$, and t, but bounded,*

$$|\eta_{i1}(x_i, \bar{x}_j, u_i, \bar{u}_j, t)| \leq \bar{\eta}_{i1}(y_i, \bar{y}_j, u_i, \bar{u}_j, t), \qquad |\eta_{i2}(x_i, \bar{x}_j, u_i, \bar{u}_j, t)| \leq \bar{\eta}_{i2}(y_i, \bar{y}_j, u_i, \bar{u}_j, t)\,, \tag{3.6}$$

where the the bounding functions $\bar{\eta}_{i1}$ and $\bar{\eta}_{i2}$ are known and uniformly bounded in the corresponding compact sets of admissible state variables, inputs, and outputs with appropriate dimensions, respectively.

Assumption 3.3 *The system state vector x_i of each subsystem remains bounded before and after the occurrence of a fault, i.e., $x_i(t) \in L_\infty$, $\forall t \geq 0$.*

Assumption 3.4 *The nonlinear terms $\rho_{i1}(x_i, u_i)$ and $\rho_{i2}(x_i, u_i)$ in (3.3) satisfy the following inequalities: $\forall u_i \in \mathcal{U}_i$ and $\forall x_i$, $\hat{x}_i \in \mathcal{X}_i$,*

$$|\rho_{i1}(x_i, u_i) - \rho_{i1}(\hat{x}_i, u_i)| \leq \sigma_{i1}|x_i - \hat{x}_i| \tag{3.7}$$

$$|\rho_{i2}(x_i, u_i) - \rho_{i2}(\hat{x}_i, u_i)| \leq \sigma_{i2}(y_i, u_i, \hat{x}_i)\,|x_i - \hat{x}_i| \tag{3.8}$$

where σ_{i1} is a known Lipschitz constant, $\sigma_{i2}(\cdot)$ is a known function that is uniformly

bounded, $\mathcal{X}_i \subset \Re^{n_i}$ *and* $\mathcal{U}_i \subset \Re^{m_i}$ *are compact sets of admissible state variables and inputs, respectively.*

Assumption 3.5 *The interconnection terms* H_{ij}^1 *and* H_{ij}^2 *satisfy the following condition, i.e.,* $\forall x_j,\ \hat{x}_j \in \mathcal{X}_j$,

$$|H_{ij}^1(x_i, x_j, u_i, u_j) - H_{ij}^1(\hat{x}_i, \hat{x}_j, u_i, u_j)| \leq \gamma_{ij}^1 |x_j - \hat{x}_j| \tag{3.9}$$

$$|H_{ij}^2(x_i, x_j, u_i, u_j) - H_{ij}^2(\hat{x}_i, \hat{x}_j, u_i, u_j)| \leq \gamma_{ij}^2(y_i, y_j, u_i, u_j)|x_j - \hat{x}_j| \tag{3.10}$$

where γ_{ij}^1 *is a known Lipschitz constant, and* γ_{ij}^2 *is a known and uniformly bounded function.*

Assumption 3.6 *The rate of change of each fault parameter vector* $\theta_{ip}^s(t)$ *in (3.5) (*$s = 1, \cdots, N_i,\ p = 1, \cdots, l_i$*) is uniformly bounded, i.e.,* $|\dot{\theta}_i^s(t)| \leq \alpha_i^s$ *for all* $t \geq 0$*, where* $\theta_i^s(t) \triangleq \left[\left(\theta_{i1}^s(t)\right)^\top, \cdots, \left(\theta_{il_i}^s(t)\right)^\top \right]^\top$*, and* α_i^s *is a known constant.*

Assumption 3.7 *The fault function* $f_i^s(x_i, u_i)$ *satisfy the following condition, i.e.,* $\forall x_j,\ \hat{x}_j \in \mathcal{X}_j$,

$$|f_i^s(x_i, u_i) - f_i^s(\hat{x}_i, u_i)| \leq \varpi_i^s(y_i, u_i)|x_i - \hat{x}_i| \tag{3.11}$$

where ϖ_i^s *is a known and uniformly bounded function.*

Assumption 3.2 characterizes the class of modeling uncertainty under consideration, including various modeling errors in the system's local dynamics (i.e., ϕ_{i1} and ϕ_{i2}) and the unknown part of interconnection between subsystems (i.e., D_{ij}^1 and D_{ij}^2). The bounds on the *unstructured* modeling uncertainty are needed in order to be able to distinguish between the effects of faults and modeling uncertainty (see [83, 84]). For instance, in the aircraft engine fault diagnosis application considered in [65], the modeling uncertainty is the deviation of the actual engine dynamics from a nominal engine model representing the dynamics of a new engine, which results from normal engine component degradation during its service life. Such normal component degradation can be modeled by small changes in certain engine component health parameters (e.g., efficiency and flow capacity of the fan,

compressor, and turbine). Therefore, the bounding function on the modeling uncertainty (i.e., $\bar{\eta}_{i1}$ and $\bar{\eta}_{i2}$) can be obtained by using the knowledge of possible normal degradation of these health parameters during a number of flights under the worst case scenario [56]. Additionally, it is worth noting that the modeling uncertainty considered in this paper is *unstructured*, while distributed fault diagnosis methods in the literature often assume the absence of modeling uncertainty (e.g., [58]) or *structured* modeling uncertainty (e.g., [72]). In the case of structured models of the modeling uncertainty, in order to achieve robustness, it is often assumed that certain rank conditions are satisfied by the uncertainty distribution matrix. On the other hand, the utilization of structured uncertainty with additional assumptions on the distribution matrix may allow the design of FDI schemes that completely decouple the fault from the modeling uncertainty.

Assumption 3.3 requires the boundedness of the state variables before and after the occurrence of a fault in each subsystem. Hence, it is assumed that the distributed feedback control system is capable of retaining the boundedness of the state variables of each subsystem even in the presence of a fault. This is a technical assumption required for well-posedness since the distributed FDI design under consideration does not influence the closed-loop dynamics and stability. The design of distributed fault-tolerant controllers is beyond the scope of this chapter. However, it is important to note that the proposed distributed FDI design does not depend on the structure of the distributed controllers.

Assumption 3.4 characterizes the type of known nonlinearities of the nominal system dynamics under consideration. Specifically, it is assumed $\rho_{i1}(x_i, u_i)$ is Lipschitz in u_i, and $\rho_{i2}(x_i, u_i)$ satisfies inequality (3.8). Note that condition (3.8) is more general than the Lipschitz condition (in this special case, σ_{i2} is a constant).

Assumption 3.5 requires the interconnection term H_{ij} between subsystems to satisfy a Lipschitz type of condition. Several examples of distributed nonlinear systems with Lipschitz interconnection terms have been considered in literature (see, for instance, the automated highway system [58, 62], interconnected inverted pendulums [32, 63]), and large-scale power systems [25]). Note that H_{ij} is a function of unknown state vectors x_j and x_i.

In Assumption 3.6, known bounds on the rate of change of the fault magnitude $\theta_i^s(t)$ are assumed. In practice, the rate bounds α_i^s can be set by exploiting some *a priori* knowledge on the fault developing dynamics. Note that the cases of abrupt faults and incipient faults are both covered by the fault model $\beta_i(t-T_0)f_i$ under consideration. Specifically, the fault time profile function $\beta_i(t-T_0)$ is a step function modeling abrupt characteristics of the fault, and the fault magnitude $\theta_i^s(t)$ represents the (possibly time-varying) fault magnitude. For instance, in the case of foreign object damage to the fan of an aircraft engine, the function $\beta_i(t-T_0)$ models the sudden and immediate effect of the damage, and $\theta_i^s(t)$ captures the possibly time-varying development of the fault magnitude following the initial sudden damage. In the specifical case of abrupt faults, we can simply set $\alpha_i^s = 0$ (i.e., θ_i^s is a vector of constants), and the function $\beta_i(t-T_0)$ models the abrupt behavior of the fault.

Assumption 3.7 assumes the fault function f_i satisfies the condition given by (3.11). This is needed for the design and analysis of the distributed adaptive FDI algorithm, since the fault function f_i is also a function of the unknown state variables x_i. In the special case that the fault is a function of measurable output y_i and known input u_i, we simply have $\varpi_i^s = 0$.

Remark 3.1 An interesting distributed fault estimation method was developed in [72] based on sliding mode observer techniques. The approach in [72] assumes a known bound on the fault function and utilizes a structured model of modeling uncertainty with additional assumptions on the distribution matrices of the modeling uncertainty, which allows completely decoupling faults from modeling uncertainty. In this chapter, we consider a different problem of distributed fault isolation for nonlinear systems with different fault models and unstructured modeling uncertainty based on adaptive estimation techniques. The objective is to detect the occurrence of any faults and to determine if one of the faults in the fault set (3.4) or a new fault that doesn't belong to (3.4) has occurred. In addition, in previous papers [82, 84], fault diagnosis schemes for nonlinear systems utilizing a *centralized* architecture were developed. In this research work, the problem of *distributed* fault diagnosis for

interconnected nonlinear systems is investigated. With the interconnection terms H_{ij}^1 and H_{ij}^2 among subsystems (see (3.3)) and the presence of unstructured modeling uncertainty, the design and analysis of distributed fault diagnosis methods is much more challenging than centralized fault diagnosis methods.

3.2 Distributed Fault Detection and Isolation Architecture

The distributed FDI architecture is comprised of M local FDI components, with one FDI component designed for each of the M subsystems. The objective of each FDI component is to detect and isolate faults in the corresponding local subsystem. Specifically, each local FDI component consists of a fault detection estimator (FDE) and a bank of N_i nonlinear adaptive *fault isolation estimators* (FIEs), where N_i is the number of different nonlinear fault types in the fault set $\mathcal{F}_i$ associated with the corresponding ith subsystem (see (3.4)), $i = 1, \cdots, M$. Under normal conditions, each local FDE monitors the corresponding local subsystem to detect the occurrence of any fault. If a fault is detected in a particular subsystem i, then the corresponding N_i local FIEs are activated for the purpose of determining the particular type of fault that has occurred in the subsystem.

The FDI architecture for each subsystem follows the generalized observer scheme (GOS) architectural framework well-documented in the fault diagnosis literature [3, 5]. The distributed nature of the presented FDI method can be better understood if compared with the conventional centralized FDI architecture. For M interconnected subsystems, $N_1 + N_2 + \cdots + N_M$ estimators are needed at the server node in the case of centralized FDI architecture. With the presented distributed FDI architecture, N_i estimators are needed at the ith subsystem. Hence, the computation is distributed across the subsytems in the network.

3.3 Distributed Fault Detection Method

In this section, we investigate the distributed fault detection method, including the designs of each local FDE for residual generation and the corresponding adaptive thresholds for residual evaluation.

3.3.1 Distributed Fault Detection Estimators

Based on the subsystem model described by (3.3), the FDE for each local subsystem is chosen as:

$$\begin{aligned}
\dot{\hat{x}}_{i1} &= \mathcal{A}_{i1}\hat{x}_{i1} + \mathcal{A}_{i2}C_i^{-1}y_i + \rho_{i1}(\hat{x}_i, u_i) + \sum_{j=1}^{M} H_{ij}^1(\hat{x}_i, \hat{x}_j, u_i, u_j) \\
\dot{\hat{x}}_{i2} &= \mathcal{A}_{i3}\hat{x}_{i1} + \mathcal{A}_{i4}\hat{x}_{i2} + \rho_{i2}(\hat{x}_i, u_i) + L_i(y_i - \hat{y}_i) + \sum_{j=1}^{M} H_{ij}^2(\hat{x}_i, \hat{x}_j, u_i, u_j) \\
\hat{y}_i &= C_i\hat{x}_{i2}\,,
\end{aligned} \tag{3.12}$$

where $\hat{x}_{i1}$, $\hat{x}_{i2}$, and $\hat{y}_i$ denote the estimated local state and output variables of the ith subsystem, $i = 1, \cdots, M$, respectively, $L_i \in \Re^{l_i \times l_i}$ is a design gain matrix, $\hat{x}_i \stackrel{\triangle}{=} [(\hat{x}_{i1})^\top \ (C_i^{-1}y_i)^\top]^\top$, and $\hat{x}_j \stackrel{\triangle}{=} [(\hat{x}_{j1})^\top \ (C_j^{-1}y_j)^\top]^\top$ (here $\hat{x}_{j1}$ is the estimate of state vector x_{j1} of the jth interconnected subsystem). The initial conditions are $\hat{x}_{i1}(0) = 0$ and $\hat{x}_{i2}(0) = C_i^{-1}y_i(0)$. It is worth noting that the distributed FDE (3.12) for the ith subsystem is constructed based on local input and output variables (i.e., u_i and y_i) and the communicated information $\hat{x}_j$ and u_j from the FDE associated with the jth interconnected subsystem. Note that many distributed estimation and diagnostic methods in literature allow certain communication among interconnected subsystems (see, e.g., [58, 60, 72, 20, 45]).

For each local FDE, let $\tilde{x}_{i1} \stackrel{\triangle}{=} x_{i1} - \hat{x}_{i1}$ and $\tilde{x}_{i2} \stackrel{\triangle}{=} x_{i2} - \hat{x}_{i2}$ denote the state estimation errors, and $\tilde{y}_i \stackrel{\triangle}{=} y_i - \hat{y}_i$ denote the output estimation error. Then, before fault occurrence

(i.e., for $t < T_0$), by using (3.3) and (3.12), the estimation error dynamics are given by

$$\begin{aligned}
\dot{\tilde{x}}_{i1} &= \mathcal{A}_{i1}\tilde{x}_{i1} + \rho_{i1}(x_i, u_i) - \rho_{i1}(\hat{x}_i, u_i) + \eta_{i1} \\
&\quad + \sum_{j=1}^{M} \left[H_{ij}^1(x_i, x_j, u_i, u_j) - H_{ij}^1(\hat{x}_i, \hat{x}_j, u_i, u_j) \right] \qquad (3.13) \\
\dot{\tilde{x}}_{i2} &= \bar{\mathcal{A}}_{i4}\tilde{x}_{i2} + \mathcal{A}_{i3}\tilde{x}_{i1} + \rho_{i2}(x_i, u_i) - \rho_{i2}(\hat{x}_i, u_i) + \eta_{i2} \\
&\quad + \sum_{j=1}^{M} \left[H_{ij}^2(x_i, x_j, u_i, u_j) - H_{ij}^2(\hat{x}_i, \hat{x}_j, u_i, u_j) \right] \qquad (3.14) \\
\tilde{y}_i &= C_i(x_{i2} - \hat{x}_{i2}) = C_i\tilde{x}_{i2}\,, \qquad (3.15)
\end{aligned}$$

where $\bar{\mathcal{A}}_{i4} \triangleq \mathcal{A}_{i4} - L_iC_i$. Note that, since C_i is nonsingular, we can always choose L_i to make $\bar{\mathcal{A}}_{i4}$ stable.

3.3.2 Adaptive Thresholds for Distributed Fault Detection

Next, we will investigate the design of adaptive thresholds for distributed fault detection in each subsystem. The following Lemma will be needed in the subsequent analysis:

Lemma 3.1 [35]. *Let* $\bar{p}(t)$, $\bar{q}(t) : [0, \infty) \mapsto \Re$. *Then*

$$\dot{\bar{p}}(t) \le -a\bar{p}(t) + \bar{q}(t), \quad \forall t \ge t_0 \ge 0$$

implies that

$$\bar{p}(t) \le e^{-a(t-t_0)}\bar{p}(t_0) + \int_{t_0}^{t} e^{-a(t-\tau)}\bar{q}(\tau)d\tau, \quad \forall t \ge t_0 \ge 0$$

for any finite constant a.

Then, a bounding function on the state estimation error vector

$$\tilde{x}_1(t) \triangleq [(\tilde{x}_{11})^\top, \cdots, (\tilde{x}_{i1})^\top, \cdots, (\tilde{x}_{M1})^\top]^\top \qquad (3.16)$$

before fault occurrence (i.e., for $0 \le t < T_0$) can be obtained. Specifically, we have the following results:

Lemma 3.2. *Consider the system described by (3.3) and the fault detection estimator*

described by (3.12). Assume that there exists a symmetric positive definite matrix $P_i \in \Re^{(n_i-l_i)\times(n_i-l_i)}$, *for* $i = 1, \cdots, M$, *such that,*

1. *the symmetric matrix*

$$R_i \stackrel{\triangle}{=} -\mathcal{A}_{i1}^{\top} P_i - P_i \mathcal{A}_{i1} - 2P_i P_i - 2\sigma_{i1}||P_i||I \; > \; 0\,, \tag{3.17}$$

   where I *is the identity matrix;*

2. *the matrix* $Q \in \Re^{M\times M}$, *whose entries are given by*

$$Q_{ij} = \begin{cases} \lambda_{min}(R_i)\,, & i = j \\ -||P_i||\gamma_{ij}^1 - ||P_j||\gamma_{ji}^1\,, & i \neq j,\; j \;=\; 1, \cdots,\, M\,, \end{cases} \tag{3.18}$$

   is positive definite, where γ_{ij}^1 *and* γ_{ji}^1 *are the Lipschitz constants introduced in (3.9).*

Then, for $0 \leq t < T_0$, *the state estimation error vector* $\tilde{x}_1(t)$ *defined by (3.16) satisfies the following inequality:*

$$|\tilde{x}_1|^2 \;\leq\; \frac{\bar{V}_0 e^{-ct}}{\lambda_{min}(P)} + \frac{1}{2\lambda_{min}(P)} \int_0^t e^{-c(t-\tau)} \sum_{i=1}^{M} |\bar{\eta}_{i1}|^2 \, d\tau\,, \tag{3.19}$$

where the matrix $P \stackrel{\triangle}{=} \mathrm{diag}\{P_1, \cdots, P_M\}$, *the constant* $c \stackrel{\triangle}{=} \lambda_{min}(Q)/\lambda_{max}(P)$, *and* $\bar{V}_0$ *is a positive constant to be defined later on.*

Proof: For the ith subsystem, let us consider a Lyapunov function candidate $V_i = {\tilde{x}_{i1}}^{\top} P_i \tilde{x}_{i1}$. The time derivative of V_i along the solution of (3.13) is given by

$$\begin{aligned} \dot{V}_i \;\; = \;\; & \tilde{x}_{i1}^{\top}(\mathcal{A}_{i1}^{\top} P_i + P_i \mathcal{A}_{i1})\tilde{x}_{i1} + 2\tilde{x}_{i1}^{\top} P_i \eta_{i1} + 2\tilde{x}_{i1}^{\top} P_i \sum_{j=1}^{M} \left[H_{ij}^1(x_i, x_j, u_i, u_j) - H_{ij}^1(\hat{x}_i, \hat{x}_j, u_i, u_j)\right] \\ & + 2\tilde{x}_{i1}^{\top} P_i \left[\rho_{i1}(x_i, u_i) - \rho_{i1}(\hat{x}_i, u_i)\right]\,. \end{aligned} \tag{3.20}$$

Note that

$$x_j - \hat{x}_j \;=\; \left[\begin{array}{c} x_{j1} - \hat{x}_{j1} \\ x_{j2} - C_j^{-1} y_j \end{array}\right] = \left[\begin{array}{c} \tilde{x}_{j1} \\ 0 \end{array}\right]. \tag{3.21}$$

Therefore, based on (3.9) and (3.21), we have

$$\begin{aligned} 2\tilde{x}_{i1}^{\top} P_i \sum_{j=1}^{M} \left[H_{ij}^1(x_i, x_j, u_i, u_j) - H_{ij}^1(\hat{x}_i, \hat{x}_j, u_i, u_j)\right] &\leq 2|\tilde{x}_{i1}| \cdot ||P_i|| \sum_{j=1}^{M} \gamma_{ij}^1 |x_j - \hat{x}_j| \\ &= 2||P_i|| \sum_{j=1}^{M} \gamma_{ij}^1 |\tilde{x}_{i1}|\,|\tilde{x}_{j1}|\,. \end{aligned} \tag{3.22}$$

Moreover, based on (3.7) and (3.21), we obtain

$$\begin{aligned} 2\tilde{x}_{i1}^{\top} P_i \left[\rho_{i1}(x_i, u_i) - \rho_{i1}(\hat{x}_i, u_i)\right] &\leq 2|\tilde{x}_{i1}| \cdot ||P_i||\,\sigma_{i1}\,|x_i - \hat{x}_i| \\ &= 2|\tilde{x}_{i1}| \cdot ||P_i||\,\sigma_{i1}\,|\tilde{x}_{i1}| \\ &= \tilde{x}_{i1}^{\top}\left[\,2\sigma_{i1}||P_i||I\,\right]\tilde{x}_{i1}\,. \end{aligned} \tag{3.23}$$

Additionally, we have

$$2\tilde{x}_{i1}^{\top} P_i \eta_{i1} \;\leq\; |2P_i\tilde{x}_{i1}|\,|\eta_{i1}| \;\leq\; 2\tilde{x}_{i1}^{\top} P_i P_i \tilde{x}_{i1} + \frac{1}{2}|\eta_{i1}|^2\,. \tag{3.24}$$

By using (3.20), (3.22), (3.23) and (3.24), we obtain

$$\dot{V}_i \leq \tilde{x}_{i1}^{\top}\left[\mathcal{A}_{i1}^{\top} P_i + P_i \mathcal{A}_{i1} + 2P_iP_i + 2\sigma_{i1}||P_i||\,I\right]\tilde{x}_{i1} + 2||P_i|| \sum_{j=1}^{M} \gamma_{ij}^1 |\tilde{x}_{i1}|\,|\tilde{x}_{j1}| + \frac{1}{2}|\eta_{i1}|^2\,. \tag{3.25}$$

Based on (3.17) and the inequality $\tilde{x}_{i1}^{\top} R_i \tilde{x}_{i1} \geq \lambda_{min}(R_i)|\tilde{x}_{i1}|^2$, where $\lambda_{min}(R_i)$ is the minimum eigenvalue of R_i, we obtain:

$$\dot{V}_i \;\leq\; -\lambda_{min}(R_i)\,|\tilde{x}_{i1}|^2 + 2||P_i|| \sum_{j=1}^{M} \gamma_{ij}^1 |\tilde{x}_{i1}|\,|\tilde{x}_{j1}| \;+\; \frac{1}{2}|\eta_{i1}|^2\,. \tag{3.26}$$

Now, let us consider the following overall Lyapunov function candidate for the intercon-

nected system: $V = \sum_{i=1}^{M} V_i = \sum_{i=1}^{M} \tilde{x}_{i1}{}^{\top} P_i \tilde{x}_{i1} = \tilde{x}_1^{\top} P \tilde{x}_1,$ where $P = \mathrm{diag}\{P_1, \cdots, P_M\}$. Therefore, from (3.26) and (3.18), we have

$$\begin{aligned} \dot{V} &\leq -\sum_{i=1}^{M} \lambda_{min}(R_i)|\tilde{x}_{i1}|^2 + \sum_{i=1}^{M}\sum_{j=1}^{M} 2||P_i||\,\gamma_{ij}^1 |\tilde{x}_{i1}|\,|\tilde{x}_{j1}| + \sum_{i=1}^{M} \frac{1}{2}|\eta_{i1}|^2 \\ &= -\big[|\tilde{x}_{11}| \;\; |\tilde{x}_{21}| \;\; \cdots \;\; |\tilde{x}_{M1}|\big] Q \begin{bmatrix} |\tilde{x}_{11}| \\ |\tilde{x}_{21}| \\ \vdots \\ |\tilde{x}_{M1}| \end{bmatrix} + \sum_{i=1}^{M} \frac{1}{2}|\eta_{i1}|^2 \end{aligned}$$

where the matrix Q is defined by (3.18). By using the Rayleigh principle (i.e., $\lambda_{min}(P)|\tilde{x}_1|^2 \leq V(t) \leq \lambda_{max}(P)|\tilde{x}_1|^2$) and the definition of $V(t)$, we have

$$\dot{V} \leq -\lambda_{min}(Q)|\tilde{x}_1|^2 + \sum_{i=1}^{M} \frac{1}{2}|\eta_{i1}|^2 \leq -\frac{\lambda_{min}(Q)}{\lambda_{max}(P)} V + \sum_{i=1}^{M} \frac{1}{2}|\eta_{i1}|^2 = -cV + \sum_{i=1}^{M} \frac{1}{2}|\eta_{i1}|^2 .$$

where $\tilde{x}_1$ and the constant c are defined in (3.16) and Lemma 3.2, respectively. Now, based on Lemma 3.1, it can be easily shown that

$$V(t) \leq V(0)e^{-ct} + \frac{1}{2}\int_0^t e^{-c(t-\tau)} \sum_{i=1}^{M} |\bar{\eta}_{i1}|^2 \, d\tau .$$

Note that we can always choose a positive constant $\bar{V}_0$ such that $V(0) < \bar{V}_0$. Thus, based on the definition of $V(t)$ and the Rayleigh principle, the proof of (3.19) can be immediately concluded. □

Remark 3.2: It is also worth noting that a necessary condition for (3.17) is that A_{i1} is Hurwitz. In addition, note that the linear matrix inequality (LMI) toolbox can be used to find a feasible solution to the matrix inequalities (3.17) and (3.18). Specifically, the following procedure can be adopted:

- By using the Schur complements, the nonlinear inequalities $-\mathcal{A}_{i1}^{\top} P_i - P_i \mathcal{A}_{i1} - 2P_i P_i -$

$2\sigma_{i1}\,||P_i||\,I > 0$ can be converted to a LMI form as

$$\begin{bmatrix} -\mathcal{A}_{i1}^{\top}P_i - P_i\mathcal{A}_{i1} - 2\sigma_{i1}\varsigma_i I & \sqrt{2}P_i \\ \sqrt{2}P_i & I \end{bmatrix} > 0 \tag{3.27}$$

and

$$\begin{bmatrix} \varsigma_i I & P_i \\ P_i & \varsigma_i I \end{bmatrix} > 0\,, \tag{3.28}$$

where ς_i is a positive constant. Then, a suitable solution of P_i can be obtained by solving (3.27) and (3.28) using the LMI toolbox.

- For the matrix P_i found in the above step, the matrix Q defined in (3.18) is verified. If Q is positive definite, the solution of P_i is valid.

Now, we analyze the output estimation error $\tilde{y}_i(t)$ (see (3.15)) of the ith subsystem. For $0 \le t < T_0$, the solution of (3.14) is given by

$$\begin{aligned}\tilde{x}_{i2}(t) &= \int_0^t e^{\bar{\mathcal{A}}_{i4}(t-\tau)}\left[\mathcal{A}_{i3}\tilde{x}_{i1}(\tau) + \eta_{i2}(x_i,\bar{x}_j,u_i,\bar{u}_j,t)\right]d\tau + \int_0^t e^{\bar{\mathcal{A}}_{i4}(t-\tau)}\left[\rho_{i2}(x_i,u_i) - \rho_{i2}(\hat{x}_i,u_i)\right]d\tau \\ &\quad + \int_0^t e^{\bar{\mathcal{A}}_{i4}(t-\tau)}\sum_{j=1}^{M}\left[H_{ij}^2(x_i,x_j,u_i,u_j) - H_{ij}^2(\hat{x}_i,\hat{x}_j,u_i,u_j)\right]d\tau\,.\end{aligned}$$

Therefore, for each component of the output estimation error, i.e., $\tilde{y}_{ip}(t) \triangleq C_{ip}\tilde{x}_{i2}(t)$, $p = 1,\cdots,l_i$, where C_{ip} is the pth row vector of matrix C_i, by applying the triangle inequality, we have

$$\begin{aligned}|\tilde{y}_{ip}(t)| \le &\left|\int_0^t C_{ip}e^{\bar{\mathcal{A}}_{i4}(t-\tau)}\sum_{\substack{j=1\\ j\neq i}}^{M}\left[H_{ij}^2(x_i,x_j,u_i,u_j) - H_{ij}^2(\hat{x}_i,\hat{x}_j,u_i,u_j)\right]d\tau\right| \\ &+\left|\int_0^t C_{ip}e^{\bar{\mathcal{A}}_{i4}(t-\tau)}\left[\mathcal{A}_{i3}\tilde{x}_{i1} + \eta_{i2}\right]d\tau\right| \\ &+\left|\int_0^t C_{ip}e^{\bar{\mathcal{A}}_{i4}(t-\tau)}\left[\rho_{i2}(x_i,u_i) - \rho_{i2}(\hat{x}_i,u_i)\right]d\tau\right|.\end{aligned} \tag{3.29}$$

Based on (3.8), (3.10), and (3.21), we have

$$\begin{aligned} |H_{ij}^2(x_i, x_j, u_i, u_j) - H_{ij}^2(\hat{x}_i, \hat{x}_j, u_i, u_j)| &\leq \gamma_{ij}^2 \, |\tilde{x}_{j1}| \\ |\rho_{i2}(x_i, u_i,) - \rho_{i2}(\hat{x}_i, u_i)| &\leq \sigma_{i2}(y_i, u_i, \hat{x}_{i1}) \, |\tilde{x}_{i1}| \, . \end{aligned} \tag{3.30}$$

Therefore, by using (3.29) and (3.30), we obtain

$$|\tilde{y}_{ip}(t)| \leq k_{ip} \int_0^t e^{-\lambda_{ip}(t-\tau)} \Big[[||\mathcal{A}_{i3}|| + \sigma_{i2}(y_i, u_i, \hat{x}_{i1})] \, |\tilde{x}_{i1}| + |\eta_{i2}| + \sum_{j=1}^{M} \gamma_{ij}^2 |\tilde{x}_{j1}| \Big] d\tau \, , \tag{3.31}$$

where k_{ip} and λ_{ip} are positive constants chosen such that $|C_{ip} e^{\bar{\mathcal{A}}_{i4} t}| \leq k_{ip} e^{-\lambda_{ip} t}$ (since $\bar{\mathcal{A}}_{i4}$ is stable, constants k_{ip} and λ_{ip} satisfying the above inequality always exist [35]). By letting

$$\varrho_i \stackrel{\triangle}{=} [\gamma_{i1}^2, \cdots, \gamma_{i(i-1)}^2, \, ||\mathcal{A}_{i3}|| + \sigma_{i2}, \, \gamma_{i(i+1)}^2, \cdots, \gamma_{iM}^2]^\top \, , \tag{3.32}$$

(that is, the components of ϱ_i are given by $\varrho_{ii} = ||\mathcal{A}_{i3}|| + \sigma_{i2}$, and $\varrho_{ij} = \gamma_{ij}^2$ for $j \neq i$), the inequality (3.31) can be rewritten as

$$\begin{aligned} |\tilde{y}_{ip}(t)| &\leq k_{ip} \int_0^t e^{-\lambda_{ip}(t-\tau)} \Big[\sum_{j=1}^{M} \varrho_{ij} |\tilde{x}_{j1}| + |\eta_{i2}| \Big] \, d\tau \\ &\leq k_{ip} \int_0^t e^{-\lambda_{ip}(t-\tau)} \Big[|\varrho_i| \, |\tilde{x}_1| + \bar{\eta}_{i2} \Big] d\tau \, . \end{aligned} \tag{3.33}$$

Now, based on (3.33) and (3.19), we obtain

$$|\tilde{y}_{ip}(t)| \leq k_{ip} \int_0^t e^{-\lambda_{ip}(t-\tau)} \big[|\varrho_i| \, \chi(\tau) + \bar{\eta}_{i2} \big] d\tau \, . \tag{3.34}$$

where

$$\chi(t) \stackrel{\triangle}{=} \left\{ \frac{\bar{V}_0 e^{-ct}}{\lambda_{min}(P)} + \frac{1}{2\lambda_{min}(P)} \int_0^t e^{-c(t-\tau)} \sum_{i=1}^{M} |\bar{\eta}_{i1}|^2 \, d\tau \right\}^{1/2} . \tag{3.35}$$

Therefore, based on the above analysis, we have the following

Distributed Fault Detection Decision Scheme: *The decision on the occurrence of a fault (detection) in the ith subsystem is made when the modulus of at least one component of*

the output estimation error (i.e., $\tilde{y}_{ip}(t)$) generated by the local FDE exceeds its corresponding threshold $\nu_{ip}(t)$ given by

$$\nu_{ip}(t) \triangleq k_{ip} \int_0^t e^{-\lambda_{ip}(t-\tau)} \left[|\varrho_i| \, \chi(\tau) + \bar{\eta}_{i2} \right] d\tau \,. \tag{3.36}$$

The fault detection time T_d is defined as the first time instant such that $|\tilde{y}_{ip}(T_d)| > \nu_{ip}(T_d)$, for some $T_d \geq T_0$ and some $p \in \{1, \cdots, l_i\}$, that is, $T_d \triangleq \inf \bigcup_{p=1}^{l_i} \{ t \geq 0 : \ |\tilde{y}_{ip}(t)| > \nu_{ip}(t) \}$.

The above design and analysis is summarized by the following technical result:

Theorem 3.1 (Robustness): *For the interconnected nonlinear uncertain system described by (3.3), the distributed fault detection method, characterized by FDE (3.12) and adaptive thresholds (3.36) designed for each local subsystem, ensures that each residual component $y_{ip}(t)$ generated by the local FDEs remains below its corresponding adaptive threshold $\nu_{ip}(t)$ prior to the occurrence of a fault (i.e., for $t < T_0$).*

Remark 3.3 It is worth noting that $\nu_{ip}(t)$ given by (3.36) is an adaptive threshold for fault detection, which has obvious advantage over a constant one. Moreover, the threshold $\nu_{ip}(t)$ can be easily implemented using linear filtering techniques [83]. Additionally, the constants $\bar{V}_0$ in (3.35) is a (possibly conservative) bound for the unknown initial conditions $V(0)$. However, note that, since the effect of this bound decreases exponentially (i.e., it is multiplied by e^{-ct}), the practical use of such a conservative bound will not significantly affect the performance of the distributed fault detection algorithm.

3.4 Distributed Fault Isolation Method

3.4.1 Distributed Fault Isolation estimators

As described above, each local FDI component consists of a FDE and a bank of FIEs. Now, assume that a fault is detected in the ith subsystem at some time T_d; accordingly, at $t = T_d$ the FIEs in the local FDI component designed for the ith subsystem are activated. Each FIE is designed based on the functional structure of one potential fault type in the local

subsystem. Specifically, the following N_i nonlinear adaptive estimators are used as isolation estimators: for $s = 1, \cdots, N_i$,

$$\begin{aligned}
\dot{\hat{x}}^s_{i1} &= \mathcal{A}_{i1}\hat{x}^s_{i1} + \mathcal{A}_{i2}C_i^{-1}y_i + \rho_{i1}(\hat{x}^s_i, u_i) + \sum_{j=1}^{M} H^1_{ij}(\hat{x}^s_i, \hat{x}_j, u_i, u_j) \\
\dot{\hat{x}}^s_{i2} &= \mathcal{A}_{i3}\hat{x}^s_{i1} + \mathcal{A}_{i4}\hat{x}^s_{i2} + \rho_{i2}(\hat{x}^s_i, u_i) + L^s_i(y_i - \hat{y}^s_i) + \hat{f}^s_i(\hat{x}^s_i, u_i, \hat{\theta}^s_i) + \Omega^s_i\dot{\hat{\theta}}^s_i \\
&\quad + \sum_{j=1}^{M} H^2_{ij}(\hat{x}^s_i, \hat{x}_j, u_i, u_j) \\
\dot{\Omega}^s_i &= \bar{\mathcal{A}}_{i4}\Omega^s_i + G^s_i(\hat{x}^s_i, u_i) \\
\hat{y}^s_i &= C_i\hat{x}^s_{i2}\,,
\end{aligned} \tag{3.37}$$

where $\hat{x}^s_{i1}$, $\hat{x}^s_{i2}$, and $\hat{y}^s_i$ denote the estimated state and output variables provided by the sth local FIE, respectively, $L^s_i \in \Re^{l_i \times l_i}$ is a design gain matrix (for simplicity of presentation and without loss of generality, we let $L^s_i = L_i$), $\hat{x}^s_i \triangleq [(\hat{x}^s_{i1})^\top\ (C_i^{-1}y_i)^\top]^\top$, and $\hat{x}_j \triangleq [(\hat{x}_{j1})^\top\ (C_j^{-1}y_j)^\top]^\top$. The function $\hat{f}^s_i(\hat{x}^s_i, u_i, \hat{\theta}^s_i) \triangleq [(\hat{\theta}^s_{i1})^\top g^s_{i1}(\hat{x}^s_i, u_i), \cdots, (\hat{\theta}^s_{il_i})^\top g^s_{il_i}(\hat{x}^s_i, u_i)]$ provides the adaptive structure for approximating the unknown fault function $f^s_i(x_i, u_i)$ described by (3.5), and $\hat{\theta}^s_{ip}$ ($i = 1, \cdots, M$, and $p = 1, \cdots, l_i$) is the adjustable parameter vector. The initial conditions are $\hat{x}^s_{i1}(T_d) = 0$, $\hat{x}^s_{i2}(T_d) = 0$, and $\Omega^s_i(T_d) = 0$. It is noted that, according to (3.5), the fault approximation model $\hat{f}^s_i$ is linear in the adjustable weights $\hat{\theta}^s_i$. Consequently, the gradient matrix $G^s_i(\hat{x}^s_i, u_i) \triangleq \partial\hat{f}^s_i(\hat{x}^s_i, u_i, \hat{\theta}^s_i)\,/\,\partial\hat{\theta}^s_i = \mathrm{diag}\,[(g^s_{i1}(\hat{x}^s_i, u_i))^\top, \cdots, (g^s_{il_i}(\hat{x}^s_i, u_i))^\top]$ does not depend on $\hat{\theta}^s_i$. Note that the distributed FIEs (3.37) for each local subsystem are constructed based on local measurements (i.e., u_i and y_i) and the communicated information $\hat{x}_j$ and u_j from the FDI component associated with the jth directly interconnected subsystem.

The adaptation in the isolation estimators arises due to the unknown fault magnitude $\theta^s_i \triangleq \left[(\theta^s_{i1})^\top, \cdots, (\theta^s_{il_i})^\top\right]^\top$. The adaptive law for adjusting $\hat{\theta}^s_i$ is derived using the Lyapunov synthesis approach (see for example [35]). Specifically, the learning algorithm is chosen as follows

$$\dot{\hat{\theta}}^s_i = \mathcal{P}_{\Theta^s_i}\left\{\Gamma\Omega^{s\top}_i C_i^\top \tilde{y}^s_i\right\}, \tag{3.38}$$

where $\tilde{y}_i^s(t) \triangleq y_i(t) - \hat{y}_i^s(t)$ denotes the output estimation error generated by the sth FIE for the local subsystem, $\Gamma > 0$ is a symmetric, positive-definite learning rate matrix, and $\mathcal{P}_{\Theta_i^s}$ is the projection operator restricting $\hat{\theta}_i^s$ to the corresponding *known* set Θ_i^s (in order to guarantee stability of the learning algorithm in the presence of modeling uncertainty, as described in [35, 15]).

The distributed fault isolation decision scheme is based on the following intuitive principle: if fault s occurs in the ith subsystem, $i = 1, \cdots, M$, at time T_0 and is detected at time T_d, then a set of adaptive threshold functions $\{\mu_{ip}^s(t),\, p = 1, \cdots, l_i,\, s = 1, \cdots, N_i\}$ can be designed for the matched sth isolation estimator of the ith subsystem, such that each component of its output estimation error satisfies $|\tilde{y}_{ip}^s(t)| \leq \mu_{ip}^s(t)$, for all $t \geq T_d$. Consequently, such a set of adaptive thresholds $\mu_{ip}^s(t)$ with $s = 1, \cdots, N_i$ can be associated with the output estimation error of each local isolation estimator. In the fault isolation procedure, if, for a particular local isolation estimator $r \in \{1, \cdots, N_i\} \backslash \{s\}$, there exists some $p \in \{1, \cdots, l_i\}$, such that the pth component of its output estimation error satisfies $|\tilde{y}_{ip}^r(t)| > \mu_{ip}^r(t)$ for some finite time $t > T_d$, then the possibility of the occurrence of fault r can be excluded. Based on this intuitive idea, the following fault isolation decision scheme is devised:

Distributed Fault Isolation Decision Scheme: *If, for each* $r \in \{1, \cdots, N_i\} \backslash \{s\}$*, there exist some finite time* $t^r > T_d$ *and some* $p \in \{1, \cdots, l_i\}$*, such that* $|\tilde{y}_{ip}^r(t^r)| > \mu_{ip}^r(t^r)$*, then the occurrence of fault* s *in the* i*th subsystem is concluded.*

Remark 3.4 It is worth noting that the presented FDI method is capable of identifying not only faults defined in the partially unknown fault class $\mathcal{F}$ (see (3.4)) but also the case of new faults that do not belong to $\mathcal{F}$ (in this case, at least one component of the residuals generated by each FIE would exceed its threshold). In addition to the output estimation error, the parameter estimation $\hat{\theta}_i^s$ might also provide some information for fault isolation. However, note that a necessary condition to ensure that the parameter estimation $\hat{\theta}_i^s$ converges to its actual value θ_i^s is the persistency of excitation of signals (see [35, 15]), which is in general too restrictive in many practical applications. Here we do *not* assume persistency of excitation.

3.4.2 Adaptive Thresholds for Distributed Fault Isolation

The threshold functions $\mu_{ip}^s(t)$ clearly play a key role in the proposed distributed fault isolation decision scheme. The following lemma provides a bounding function for each component of the output estimation error of the matched sth local isolation estimator in the case that fault s occurs in the ith subsystem.

Lemma 3.3 *If fault s in the ith subsystem is detected at time T_d, where $s \in \{1, \cdots, N_i\}$ and $i \in \{1, \cdots, M\}$, then for all $t > T_d$, each component of the output estimation error $\tilde{y}_{ip}^s(t)$ associated with the matched sth local isolation estimator satisfies*

$$|\tilde{y}_{ip}^s(t)| \leq k_{ip} \int_{T_d}^{t} e^{-\lambda_{ip}(t-\tau)} \left[|\bar{\varrho}_i| \chi(\tau) + \bar{\eta}_{i2} + \alpha_i^s ||\Omega_i^s|| \right] d\tau + k_{ip}\omega_{i2} e^{-\lambda_{ip}(t-T_d)} + |(C_{ip}\Omega_i^s)^\top| |\tilde{\theta}_i^s| , \tag{3.39}$$

where $\tilde{y}_{ip}^s(t) \triangleq y_{ip}(t) - \hat{y}_{ip}^s(t)$, $p = 1, \cdots l_i$, $\chi(t)$ is given in (3.35), $\tilde{\theta}_i^s(t) \triangleq \hat{\theta}_i^s(t) - \theta_i^s(t)$ represents the fault parameter vector estimation error, ω_{i2} is a positive constant satisfying $|x_{i2}^s(T_d)| \leq \omega_{i2}$, and $\bar{\varrho}_i$ is defined later on..

Proof: Denote the state estimation error of the sth local isolation estimator for the ith subsystem by $\tilde{x}_{i1}^s(t) \triangleq x_{i1}(t) - \hat{x}_{i1}^s(t)$ and $\tilde{x}_{i2}^s(t) \triangleq x_{i2}(t) - \hat{x}_{i2}^s(t)$. By using (3.37) and (3.3), in the presence of fault s in the ith subsystem, the state estimation error of the matched sth local FIE satisfies, for $t > T_d$,

$$\begin{aligned}
\dot{\tilde{x}}_{i1}^s &= \mathcal{A}_{i1}\tilde{x}_{i1}^s + \eta_{i1} + \rho_{i1}(x_i, u_i) - \rho_{i1}(\hat{x}_i^s, u_i) \\
&\quad + \sum_{j=1}^{M} \left[H_{ij}^1(x_i, x_j, u_i, u_j) - H_{ij}^1(\hat{x}_i^s, \hat{x}_j, u_i, u_j) \right] \qquad (3.40) \\
\dot{\tilde{x}}_{i2}^s &= \bar{\mathcal{A}}_{i4}\tilde{x}_{i2}^s + \mathcal{A}_{i3}\tilde{x}_{i1}^s + \eta_{i2} + \rho_{i2}(x_i, u_i) - \rho_{i2}(\hat{x}_i^s, u_i) + f_i^s(x_i, u_i) - \hat{f}_i^s(\hat{x}_i^s, u_i, \hat{\theta}_i^s) \\
&\quad - \Omega_i^s \dot{\hat{\theta}}_i^s + \sum_{j=1}^{M} \left[H_{ij}^2(x_i, x_j, u_i, u_j) - H_{ij}^2(\hat{x}_i^s, \hat{x}_j, u_i, u_j) \right] , \qquad (3.41)
\end{aligned}$$

where $\bar{\mathcal{A}}_{i4}$ is defined in (3.14). Note that

$$\begin{aligned} f_i^s(x_i,u_i)-\hat{f}_i^s(\hat{x}_i^s,u_i) &= G_i^s(x_i,u_i)\theta_i - G_i^s(\hat{x}_i^s,u_i)\theta_i + G_i^s(\hat{x}_i^s,u_i)\theta_i - G_i^s(\hat{x}_i^s,u_i)\hat{\theta}_i \\ &= f_i^s(x_i,u_i) - f_i^s(\hat{x}_i^s,u_i) - G_i^s(\hat{x}_i^s,u_i)\tilde{\theta}_i\,. \end{aligned} \tag{3.42}$$

By using $G_i^s(\hat{x}_i^s,u_i) = \dot{\Omega}_i^s - \bar{\mathcal{A}}_{i4}\Omega_i^s$ (see (3.37)), we have

$$\begin{aligned} \dot{\tilde{x}}_{i2}^s = \bar{\mathcal{A}}_{i4}\left(\tilde{x}_{i2}^s + \Omega_i^s\tilde{\theta}_i^s\right) + \mathcal{A}_{i3}\tilde{x}_{i1}^s + \eta_{i2} - \frac{d}{dt}(\Omega_i^s\tilde{\theta}_i^s) + \rho_{i2}(x_i,u_i) - \rho_{i2}(\hat{x}_i^s,u_i) - \Omega_i^s\dot{\theta}_i^s \\ +\sum_{j=1}^{M}\left[H_{ij}^2(x_i,x_j,u_i,u_j) - H_{ij}^2(\hat{x}_i^s,\hat{x}_j,u_i,u_j)\right] + f_i^s(x_i,u_i) - f_i^s(\hat{x}_i^s,u_i)\,. \end{aligned}$$

By letting $\bar{x}_{i2}^s \triangleq \tilde{x}_{i2}^s + \Omega_i^s\tilde{\theta}_i^s$, the above equation can be rewritten as

$$\begin{aligned} \dot{\bar{x}}_{i2}^s &= \bar{\mathcal{A}}_{i4}\bar{x}_{i2}^s + \mathcal{A}_{i3}\tilde{x}_{i1}^s + \sum_{j=1}^{M}\left[H_{ij}^2(x_i,x_j,u_i,u_j) - H_{ij}^2(\hat{x}_i^s,\hat{x}_j,u_i,u_j)\right] + f_i^s(x_i,u_i) - f_i^s(\hat{x}_i^s,u_i) \\ &\quad +\rho_{i2}(x_i,u_i) - \rho_{i2}(\hat{x}_i^s,u_i) + \eta_{i2} - \Omega_i^s\dot{\theta}_i^s(t)\,. \end{aligned} \tag{3.43}$$

The solution of (3.43), for $t > T_d$, is given by

$$\begin{aligned} \bar{x}_{i2}^s(t) = \int_{T_d}^{t} e^{\bar{\mathcal{A}}_{i4}(t-\tau)}\left[\mathcal{A}_{i3}\tilde{x}_{i1}^s + \eta_{i2} - \Omega_i^s\dot{\theta}_i^s\right]d\tau + \int_{T_d}^{t} e^{\bar{\mathcal{A}}_{i4}(t-\tau)}\left[\rho_{i2}(x_i,u_i) - \rho_{i2}(\hat{x}_i^s,u_i)\right]d\tau \\ + \int_{T_d}^{t} e^{\bar{\mathcal{A}}_{i4}(t-\tau)}\sum_{j=1}^{M}\left[H_{ij}^2(x_i,x_j,u_i,u_j) - H_{ij}^2(\hat{x}_i^s,\hat{x}_j,u_i,u_j)\right]d\tau \\ + \int_{T_d}^{t} e^{\bar{\mathcal{A}}_{i4}(t-\tau)}\left[f_i^s(x_i,u_i) - f_i^s(\hat{x}_i^s,u_i)\right]d\tau + e^{\bar{\mathcal{A}}_{i4}(t-T_d)}\bar{x}_{i2}^s(T_d)\,. \end{aligned} \tag{3.44}$$

By using (3.37), (3.3), and the definition of $\bar{x}_{i2}^s(t)$, each component of the output estimation error is given by:

$$\tilde{y}_{ip}^s(t) = C_{ip}\tilde{x}_{i2}^s(t) = C_{ip}\left(\bar{x}_{i2}^s(t) - \Omega_i^s\tilde{\theta}_i^s\right)\,. \tag{3.45}$$

Now, based on (3.44) and (3.45), as well as Assumptions 3.2, 3.4 and 3.5, after following some similar reasoning logic as reported in the derivation of the adaptive thresholds for

fault detection (see (3.21), (3.30), and (3.31)), it can be shown that

$$
\begin{aligned}
|\tilde{y}_{ip}^s(t)| \;\leq\; & k_{ip}\int_{T_d}^{t} e^{-\lambda_{ip}(t-\tau)}\Big[\,||\mathcal{A}_{i3}||\,|\tilde{x}_{i1}^s| \;+\; \bar{\eta}_{i2} + \alpha_i^s||\Omega_i^s|| + \sum_{j=1}^{M}\gamma_{ij}^2|\tilde{x}_{j1}|\,\Big]d\tau \;+\; |(C_{ip}\Omega_i^s)^\top|\,|\tilde{\theta}_i^s| \\
& + k_{ip}\int_{T_d}^{t} e^{-\lambda_{ip}(t-\tau)}\Big[\,\sigma_{i2}|\tilde{x}_{i1}^s| \;+\; \varpi_i^s|\tilde{x}_{i1}^s|\,\Big]d\tau \;+\; k_{ip}e^{-\lambda_{ip}(t-T_d)}|\bar{x}_{i2}^s(T_d)|\,,
\end{aligned}
$$

where the constants k_{ip} and λ_{ip} are defined in (3.31). using $\tilde{x}_1$ as defined in (3.16) respectively,

$$
\bar{\varrho}_i \stackrel{\triangle}{=} [\gamma_{i1}^2,\,\cdots,\,\gamma_{i(i-1)}^2,\,||\mathcal{A}_{i3}|| + \sigma_{i2} + \varpi_i^s,\,\gamma_{i(i+1)}^2,\,\cdots,\gamma_{iM}^2]^\top\,, \tag{3.46}
$$

we have

$$
|\tilde{y}_{ip}^s(t)| \leq k_{ip}\int_{T_d}^{t} e^{-\lambda_{ip}(t-\tau)}\big[\,|\bar{\varrho}_i|\,|\tilde{x}_1| + \bar{\eta}_{i2} + \alpha_i^s||\Omega_i^s||\,\big]d\tau \;+\; |(C_{ip}\Omega_i^s)^\top|\,|\tilde{\theta}_i^s| \;+\; k_{ip}e^{-\lambda_{ip}(t-T_d)}|\bar{x}_{i2}^s(T_d)|\,.
$$

Note that (3.40) is in the same form as (3.13). Thus, by using the results of Lemma 3.2 (i.e., (3.39)), the above inequality becomes

$$
|\tilde{y}_{ip}^s(t)| \leq k_{ip}\int_{T_d}^{t} e^{-\lambda_{ip}(t-\tau)}\big[\,|\bar{\varrho}_i|\,\chi + \bar{\eta}_{i2} + \alpha_i^s||\Omega_i^s||\,\big]d\tau + k_{ip}|\bar{x}_{i2}^s(T_d)|e^{-\lambda_{ip}(t-T_d)} + |(C_{ip}\Omega_i^s)^\top|\,|\tilde{\theta}_i^s|\,.
$$

Where χ is defined by (3.35). Now, inequality (3.39) follows directly from the initial condition $\hat{x}_{i2}^s(T_d) = 0$, $\Omega_i^s(T_d) = 0$, and $|x_{i2}^s(T_d)| \leq \omega_{i2}$.

□

Although Lemma 3.3 provides an upper bound on the output estimation error of the sth local estimator for subsystem i, the right-hand side of (3.39) cannot be directly used as a threshold function for fault isolation, because $\tilde{\theta}_i^s(t)$ is not available (we do not assume the condition of persistency of excitation as described in Remark 3.4) . However, since the estimate $\hat{\theta}_i^s$ belongs to the known compact set Θ_i^s, we have $\left|\theta_i^s - \hat{\theta}_i^s(t)\right| \leq \kappa_i^s(t)$ for a suitable $\kappa_i^s(t)$ depending on the geometric properties of set Θ_i^s (see [82, 83]). Hence, based

on the above discussions, the following threshold function is chosen:

$$\mu_{ip}^{s}(t) \quad = k_{ip} \int_{T_d}^{t} e^{-\lambda_{ip}(t-\tau)} \left[\, |\bar{\varrho}_i| \, \chi + \bar{\eta}_{i2} + \alpha_i^s ||\Omega_i^s|| \, \right] d\tau + \; k_{ip}\omega_{i2} e^{-\lambda_{ip}(t-T_d)} + |(C_{ip}\, \Omega_i^s)^\top| \, \kappa_i^s(t) \, . \tag{3.47}$$

Remark 3.5 Note that the adaptive threshold $\mu_{ip}^{s}(t)$ can be easily implemented on-line using linear filtering techniques [82, 83]. The constant bound ω_{i2} is a (possibly conservative) bound for the unknown initial conditions $x_{i2}^{s}(T_d)$. However, note that, since the effect of this bound decreases exponentially (i.e., it is multiplied by $e^{-\lambda_{ip}(t-T_d)}$, the practical use of such a conservative bound will not affect significantly the performance of the distributed fault isolation algorithm.

Remark 3.6 As we can see, the adaptive threshold function described by (3.47) is influenced by several sources of uncertainty entering the fault isolability problem, such as modeling uncertainty (i.e., η_{i1}, η_{i2}), fault parametric uncertainty κ_i^s, unknown fault development rate α_i^s, and unknown initial conditions (i.e., $\bar{V}_0$ and ω_{i2}). Intuitively, the smaller the uncertainty (resulting in a smaller threshold $\mu_{ip}^{s}(t)$), the easier the task of isolating the faults. On the other hand, as clarified in Section 3.5.2, the capability to isolate a fault depends not only on the threshold $\mu_{ip}^{s}(t)$, but also on the degree that the types of faults in each subsystem are mutually "different".

3.5 Analytical Properties of the Distributed FDI Method

As is well known in the fault diagnosis literature, there is an inherent tradeoff between robustness and fault sensitivity. In this section, we analyze the fault sensitivity property of the the distributed fault diagnosis method, including fault detectability and isolability. In addition, the stability and learning capability of the adaptive fault isolation estimators are also investigated.

3.5.1 Fault Detectability Condition

The following theorem characterizes (in a non-closed form) the class of faults that are detectable by the proposed distributed fault detection method.

Theorem 3.2 (Fault Detectability): *For the distributed fault detection method described by (3.12) and (3.36), suppose that fault s occurs in the ith subsystem at time T_0, where $s \in \{1, \cdots, N_i\}$ and $i \in \{1, \cdots, M\}$. Then, if there exist some time instant $T_d > T_0$ and some $p \in \{1, \cdots, l_i\}$, such that the fault function $f_i(x_i, u_i)$ satisfies*

$$\left| \int_{T_0}^{T_d} C_{ip} e^{\bar{\mathcal{A}}_{i4}(T_d - \tau)} f_i(x_i(\tau), u_i(\tau)) d\tau \right| \;\geq\; 2\nu_{ip}(T_d)\,, \tag{3.48}$$

the fault will be detected at time $t = T_d$, i.e., $|\tilde{y}_{ip}(T_d)| > \nu_{ip}(T_d)$.

Proof: In the presence of a fault (i.e., for $t \geq T_0$), base on (3.3) and (3.12), the dynamics of the state estimation error $\tilde{x}_{i1} \stackrel{\triangle}{=} x_{i1} - \hat{x}_{i1}$ and $\tilde{x}_{i2} \stackrel{\triangle}{=} x_{i2} - \hat{x}_{i2}$ satisfies

$$\begin{aligned} \dot{\tilde{x}}_{i1} &= \mathcal{A}_{i1}\tilde{x}_{i1} + \eta_{i1} + \sum_{j=1}^{M} \left[H_{ij}^1(x_i, x_j, u_i, u_j) - H_{ij}^1(\hat{x}_i, \hat{x}_j, u_i, u_j) \right] \\ &\quad + \rho_{i1}(x_i, u_i) - \rho_{i1}(\hat{x}_i, u_i) \qquad (3.49) \\ \dot{\tilde{x}}_{i2} &= \bar{\mathcal{A}}_{i4}\tilde{x}_{i2} + \mathcal{A}_{i3}\tilde{x}_{i1} + \eta_{i2} + \beta_i f_i + \sum_{j=1}^{M} \left[H_{ij}^2(x_i, x_j, u_i, u_j) - H_{ij}^2(\hat{x}_i, \hat{x}_j, u_i, u_j) \right] \\ &\quad + \rho_{i2}(x_i, u_i) - \rho_{i2}(\hat{x}_i, u_i) \qquad (3.50) \end{aligned}$$

Therefore, for each component of the output estimation error, i.e., $\tilde{y}_{ip}(t) \stackrel{\triangle}{=} C_{ip}\tilde{x}_{i2}(t)$, $p = 1, \cdots, l_i$, we have

$$\begin{aligned} \tilde{y}_{ip}(t) &= \int_0^t C_{ip} e^{\bar{\mathcal{A}}_{i4}(t-\tau)} \left[\mathcal{A}_{i3}\tilde{x}_{i1} + \eta_{i2} + \beta_i f_i(x_i, u_i) \right] d\tau \\ &\quad + \int_0^t C_{ip} e^{\bar{\mathcal{A}}_{i4}(t-\tau)} \left[\rho_{i2}(x_i, u_i) - \rho_{i2}(\hat{x}_i, u_i) \right] d\tau \\ &\quad + \int_0^t C_{ip} e^{\bar{\mathcal{A}}_{i4}(t-\tau)} \sum_{j=1}^{M} \left[H_{ij}^2(x_i, x_j, u_i, u_j) - H_{ij}^2(\hat{x}_i, \hat{x}_j, u_i, u_j) \right] d\tau\,. \end{aligned}$$

Note that (3.49) is in the same form as (3.13). Therefore, from Lemma 3.2, we have

$|\tilde{x}_1(t)| \leq \chi(t)$, where $\chi(t)$ is defined in (3.35). Then, by applying the triangle inequality and (3.30), we obtain:

$$\begin{aligned} |\tilde{y}_{ip}(t)| &\geq \left| \int_0^t C_{ip} e^{\bar{\mathcal{A}}_{i4}(t-\tau)} \beta_i f_i(x_i, u_i) d\tau \right| - k_{ip} \int_0^t e^{-\lambda_{ip}(t-\tau)} \Big[||\mathcal{A}_{i3}||\, |\tilde{x}_{i1}| + |\eta_{i2}| \\ &\quad + \sum_{j=1}^{M} \gamma_{ij}^2 |\tilde{x}_{j1}| + \sigma_{i2} |\tilde{x}_{i1}| \Big] d\tau \\ &\geq \left| \int_0^t C_{ip} e^{\bar{\mathcal{A}}_{i4}(t-\tau)} \beta_i f_i(x_i, u_i) d\tau \right| - k_{ip} \int_0^t e^{-\lambda_{ip}(t-\tau)} \big[\, |\varrho_i|\, \chi + \bar{\eta}_{i2} \,\big] d\tau \ , \quad (3.51) \end{aligned}$$

where ϱ_i is defined in (3.32). By substituting (3.36) into (3.51), we have

$$|\tilde{y}_{ip}(t)| \geq \left| \int_0^t C_{ip} e^{\bar{\mathcal{A}}_{i4}(t-\tau)} \beta_i f_i(x_i(\tau), u_i(\tau)) d\tau \right| - \nu_{ip}(t) \quad (3.52)$$

Based on the property of the step function β_i, if there exists $T_d > T_0$, such that condition (3.48) is satisfied, then it is concluded that $|\tilde{y}_{ip}(T_d)| > \nu_{ip}(T_d)$, i.e., the fault is detected at time $t = T_d$. □

Remark 3.7 Note that the integral on the left-hand side of (3.48) represents the filtered fault function. In qualitative terms, the fault detectability theorem states that if the magnitude of the filtered fault function on the time interval $[T_0, T_d]$ becomes sufficiently large, then the fault in the ith subsystem can be detected. The result also shows that if a fault function $f_i(x_i, u_i)$ changes sign over time then it may be difficult (or impossible) to detect.

3.5.2 Fault Isolability Analysis

For our purpose, a fault in each subsystem is considered to be *isolable* if the distributed fault isolation scheme is able to reach a correct decision in finite time. Intuitively, faults are isolable if they are *mutually different* according to a certain measure quantifying the difference in the effects that different faults have on measurable outputs and on the estimated quantities in the isolation scheme. To quantify this concept, we introduce the *fault mismatch*

function between the sth fault and the rth fault in the ith subsystem, for $i = 1, \cdots, M$:

$$h_{ip}^{sr}(t) \stackrel{\triangle}{=} C_{ip}\left(\Omega_i^s \theta_i^s \; - \; \Omega_i^r \hat{\theta}_i^r\right), \tag{3.53}$$

where $r, s = 1, \cdots, N_i$, $r \neq s$ and $p = 1, \cdots, l_i$. From a qualitative point of view, $h_{ip}^{sr}(t)$ can be interpreted as a filtered version of the difference between the actual fault function $G_i^s \theta_i^s$ and its estimate $G_i^r \hat{\theta}_i^r$ associated with the rth local isolation estimator whose structure does not match the actual fault s in the local subsystem. Recalling that each local FIE is designed based on the functional structure of one of the nonlinear faults in the fault class associated with the local subsystem. Consequently, if fault s occurs, its estimate $G_i^r \hat{\theta}_i^r$ generated by FIE r is determined by the structure of FIE r, which in turn is determined by fault r. Therefore, the fault mismatch function $h_{ip}^{sr}(t)$, defined as the ability of the rth local FIE to learn fault s in the local subsystem, offers a measure of the difference between fault s and fault r associated with the local subsystem.

The following theorem characterizes the class of isolable faults in each subsystem:

Theorem 3.3 *Consider the distributed fault isolation scheme described by (3.37) and (3.47). Suppose that fault s ($s = 1, \cdots, N_i$), occurring in the ith subsystem at time T_0, is detected at time T_d. Then, fault s is isolable if, for each $r \in \{1, \cdots, N_i\} \backslash \{s\}$, there exist some time $t^r > T_d$ and some $p \in \{1, \cdots, l_i\}$, such that the fault mismatch function $h_{ip}^{sr}(t^r)$ satisfies*

$$\begin{aligned} |h_{ip}^{sr}(t^r)| \;\; \geq \;\; & 2k_{ip} \int_{T_d}^{t^r} e^{-\lambda_{ip}(t^r - \tau)} \left[\, |\bar{\varrho}_i| \chi + \bar{\eta}_{i2} \, \right] d\tau \; + \; k_{ip} \int_{T_d}^{t^r} e^{-\lambda_{ip}(t^r - \tau)} \left[\, \alpha_i^s ||\Omega_i^s|| \; + \; \alpha_i^r ||\Omega_i^r|| \, \right] d\tau \\ & + |(C_{ip} \Omega_i^r)^\top| \kappa_i^r + \; 2\omega_{i2} k_{ip} e^{-\lambda_{ip}(t^r - T_d)} \, . \end{aligned} \tag{3.54}$$

Proof: Denote the state estimation errors of the rth local isolation estimator for subsystem i by $\tilde{x}_{i1}^r(t) \stackrel{\triangle}{=} x_{i1}(t) - \hat{x}_{i1}^r(t)$ and $\tilde{x}_{i2}^r(t) \stackrel{\triangle}{=} x_{i2}(t) - \hat{x}_{i2}^r(t)$. By using (3.37) and (3.3), in the

presence of fault s in the ith subsystem, for $t > T_d$, we have

$$\begin{aligned}
\dot{\tilde{x}}^r_{i1} &= \mathcal{A}_{i1}\tilde{x}^r_{i1} + \rho_{i1}(x_i, u_i) - \rho_{i1}(\hat{x}^r_i, u_i) + \eta_{i1} \\
&\quad + \sum_{j=1}^{M} \left[H^1_{ij}(x_i, x_j, u_i, u_j) - H^1_{ij}(\hat{x}^r_i, \hat{x}_j, u_i, u_j) \right] \qquad (3.55) \\
\dot{\tilde{x}}^r_{i2} &= \bar{\mathcal{A}}_{i4}\tilde{x}^r_{i2} + \mathcal{A}_{i3}\tilde{x}^r_{i1} + \eta_{i2} + \sum_{j=1}^{M} \left[H^2_{ij}(x_i, x_j, u_i, u_j) - H^2_{ij}(\hat{x}^r_i, \hat{x}_j, u_i, u_j) \right] + \rho_{i2}(x_i, u_i) \\
&\quad - \rho_{i2}(\hat{x}^r_i, u_i) + G^s_i(x_i, u_i)\theta^s_i - G^s_i(\hat{x}^s_i, u_i)\theta^s_i + G^s_i(\hat{x}^s_i, u_i)\theta^s_i - G^r_i(\hat{x}^r_i, u_i)\hat{\theta}^r_i - \Omega^r_i\dot{\hat{\theta}}^r_i \qquad (3.56)
\end{aligned}$$

By substituting $G^s_i(\hat{x}^s_i, u_i) = \dot{\Omega}^s_i - \bar{\mathcal{A}}_{i4}\,\Omega^s_i$ and $G^r_i(\hat{x}^r_i, u_i) = \dot{\Omega}^r_i - \bar{\mathcal{A}}_{i4}\,\Omega^r_i$ into (3.56), we obtain

$$\begin{aligned}
\dot{\tilde{x}}^r_{i2} = \bar{\mathcal{A}}_{i4}\left(\tilde{x}^r_{i2} + \Omega^r_i\hat{\theta}^r_i - \Omega^s_i\theta^s_i\right) + \mathcal{A}_{i3}\tilde{x}^r_{i1} + \eta_{i2} - \Omega^s\dot{\theta}^s_i - \frac{d}{dt}\left(\Omega^r_i\hat{\theta}^r_i - \Omega^s_i\theta^s_i\right) \\
+ \sum_{j=1}^{M} \left[H^2_{ij}(x_i, x_j, u_i, u_j) - H^2_{ij}(\hat{x}^r_i, \hat{x}_j, u_i, u_j) \right] + \rho_{i2}(x_i, u_i) - \rho_{i2}(\hat{x}^r_i, u_i) \\
+ f^s_i(x_i, u_i) - f^s_i(\hat{x}^s_i, u_i)\,.
\end{aligned}$$

By defining $\bar{x}^r_{i2}(t) \triangleq \tilde{x}^r_{i2}(t) + \Omega^r_i\hat{\theta}^r_i - \Omega^s_i\theta^s_i$, the above equation can be rewritten as follows

$$\begin{aligned}
\dot{\tilde{x}}^r_{i2} &= \bar{\mathcal{A}}_{i4}\bar{x}^r_{i2} + \mathcal{A}_{i3}\tilde{x}^r_{i1} + \sum_{j=1}^{M} \left[H^2_{ij}(x_i, x_j, u_i, u_j) - H^2_{ij}(\hat{x}^r_i, \hat{x}_j, u_i, u_j) \right] + \eta_{i2} - \Omega^s_i\dot{\theta}^s_i \\
&\quad + \rho_{i2}(x_i, u_i) - \rho_{i2}(\hat{x}^r_i, u_i) + f^s_i(x_i, u_i) - f^s_i(\hat{x}^s_i, u_i)\,. \qquad (3.57)
\end{aligned}$$

The pth component of the output estimation error generated by the rth local FIE for subsystem i (i.e., $\tilde{y}^r_{ip}(t) \triangleq y_{ip}(t) - \hat{y}^r_{ip}(t)$, $p = 1, \cdots l_i$) is given by

$$\tilde{y}^r_{ip}(t) = C_{ip}\tilde{x}^r_{i2}(t) = C_{ip}(\bar{x}^r_{i2}(t) - \Omega^r_i\hat{\theta}^r_i + \Omega^s_i\theta^s_i) = C_{ip}\bar{x}^r_{i2}(t) + h^{sr}_{ip}(t).$$

By applying the triangle inequality, we have

$$|\tilde{y}^r_{ip}(t)| \geq |h^{sr}_{ip}(t)| - |C_{ip}\bar{x}^r_{i2}(t)|\,. \qquad (3.58)$$

Note that (3.57) is in a similar form as (3.43). Therefore, by using (3.57) and (3.58) and by following similar reasoning logic reported in the proof of Lemma 3.3, we have

$$\begin{aligned}|\tilde{y}_{ip}^r(t)| &\geq |h_{ip}^{sr}(t)| - \int_{T_d}^t |C_{ip}e^{\bar{\mathcal{A}}_{i4}(t-\tau)}|\Big[\,|\bar{\varrho}_i|\chi(\tau) + |\eta_2| + |\Omega^s\dot{\theta}_i^s|\,\Big]d\tau - |C_{ip}e^{\bar{\mathcal{A}}_{i4}(t-T_d)}|\,|x_{i2}^r(T_d)|\,. \\ &\geq |h_{ip}^{sr}(t)| - k_{ip}\int_{T_d}^t e^{-\lambda_{ip}(t-\tau)}\Big[\,|\bar{\varrho}_i|\chi(\tau) + |\bar{\eta}_2| + |\Omega^s\dot{\theta}_i^s|\,\Big]d\tau - k_{ip}e^{-\lambda_{ip}(t-T_d)}|x_{i2}^r(T_d)|\,.\end{aligned}$$

Now by taking into account the corresponding adaptive threshold $\mu_{ip}^r(t)$ given by (3.47) we can conclude that, if condition (3.54) is satisfied at time $t = t^r$, we obtain $|\tilde{y}_{ip}^r(t^r)| > \mu_{ip}^r(t^r)$, which implies that the possibility of the occurrence of fault r in subsystem i can be excluded at time $t = t^r$.

□

Remark 3.8 According to the above theorem, if, for each $r \in \{1, \cdots, N_i\}\backslash\{s\}$, the fault mismatch function $h_{ip}^{sr}(t^r)$ satisfies condition (3.54) for some time $t^r > 0$, then the pth component of the output estimation error generated by the rth FIE of subsystem i would exceed its corresponding adaptive threshold at time $t = t^r$, i.e., $|\tilde{y}_{ip}^r(t^r)| > \mu_{ip}^r(t^r)$, hence excluding the occurrence of fault r in subsystem i. Therefore, Theorem 3.3 characterizes (in a non-closed form) the class of nonlinear faults that are isolable in each subsystem by the proposed robust distributed FDI scheme.

3.5.3 Stability and Learning Capability

We now investigate the *stability and learning properties* of the adaptive fault isolation estimators, which are described by the following result:

Theorem 3.4 *Suppose that fault s, occurring in the ith subsystem, is detected at time T_d, where $s \in \{1, \cdots, N_i\}$ and $i \in \{1, \cdots, M\}$. Then, the distributed fault isolation scheme described by (3.37), (3.38) and (3.47) guarantees that,*

- *for each local fault isolation estimator q, $q = 1, \cdots, N_i$, the estimate variables $\hat{x}_{i1}^q(t)$, $\hat{x}_{i2}^q(t)$, and $\hat{\theta}_i^q(t)$ are uniformly bounded;*

- *there exist a positive constant $\bar{\kappa}_i$ and a bounded function $\bar{\xi}_i^s(t)$, such that, for all finite time $t_f > T_d$, the output estimation error of the matched sth local isolation estimator satisfies*

$$\int_{T_d}^{t_f} |\tilde{y}_i^s(t)|^2 dt \;\leq\; \bar{\kappa}_i + 2\int_{T_d}^{t_f} |\bar{\xi}_i^s(t)|^2 dt\,. \tag{3.59}$$

Proof. Let us first address the signal boundedness property. The state estimation error and output estimation error of the qth FIE for the ith subsystem are defined as $\tilde{x}_{i1}^q(t) \stackrel{\triangle}{=} x_{i1}(t) - \hat{x}_{i1}^q(t)$, $\tilde{x}_{i2}^q(t) \stackrel{\triangle}{=} x_{i2}(t) - \hat{x}_{i2}^q(t)$, and $\tilde{y}_i^q \stackrel{\triangle}{=} y_i(t) - \hat{y}_i^q(t)$, respectively. By using (3.37) and (3.3), for $t > T_d$, the output estimation error is $\tilde{y}_i^q = C_i\tilde{x}_{i2}^q$, and the state estimation error satisfies

$$\begin{aligned}
\dot{\tilde{x}}_{i1}^q &= \mathcal{A}_{i1}\tilde{x}_{i1}^q + \eta_{i1} + \rho_{i1}(x_i,u_i) - \rho_{i1}(\hat{x}_i^q,u_i) \\
&\quad + \sum_{j=1}^{M}\left[H_{ij}^1(x_i,x_j,u_i,u_j) - H_{ij}^1(\hat{x}_i^q,\hat{x}_j,u_i,u_j)\right] \qquad (3.60)\\
\dot{\tilde{x}}_{i2}^q &= \bar{\mathcal{A}}_{i4}\tilde{x}_{i2}^q + \mathcal{A}_{i3}\tilde{x}_{i1}^q + \eta_{i2} + \rho_{i2}(x_i,u_i) - \rho_{i2}(\hat{x}_i^q,u_i) + G_i^s(x_i,u_i)\theta_i^s - G_i^s(\hat{x}_i^s,u_i)\theta_i^s \\
&\quad + G_i^s(\hat{x}_i^s,u_i)\theta_i^s - G_i^q(\hat{x}_i^q,u_i)\hat{\theta}_i^q - \Omega_i^q\dot{\hat{\theta}}_i^q \\
&\quad + \sum_{j=1}^{M}\left[H_{ij}^2(x_i,x_j,u_i,u_j) - H_{ij}^2(\hat{x}_i^q,\hat{x}_j,u_i,u_j)\right]\,. \qquad (3.61)
\end{aligned}$$

By substituting $G_i^s(\hat{x}_i^s,u_i) = \dot{\Omega}_i^s - \bar{\mathcal{A}}_{i4}\Omega_i^s$ and $G_i^q(\hat{x}_i^q,u_i) = \dot{\Omega}_i^q - \bar{\mathcal{A}}_{i4}\Omega_i^q$ (see (3.37)) into (3.61), and by defining $\bar{x}_{i2}^q \stackrel{\triangle}{=} \tilde{x}_{i2}^q - \Omega_i^s\theta_i^s + \Omega_i^q\hat{\theta}_i^q$, we obtain

$$\begin{aligned}
\dot{\bar{x}}_{i2}^q &= \bar{\mathcal{A}}_{i4}\bar{x}_{i2}^q + \mathcal{A}_{i3}\tilde{x}_{i1}^q + \rho_{i2}(x_i,u_i) - \rho_{i2}(\hat{x}_i^q,u_i) + f_i^s(x_i,u_i) - f_i^s(\hat{x}_i^s,u_i) + \eta_{i2} \\
&\quad + \sum_{j=1}^{M}\left[H_{ij}^2(x_i,x_j,u_i,u_j) - H_{ij}^2(\hat{x}_i^q,\hat{x}_j,u_i,u_j)\right] - \Omega_i^s\dot{\theta}_i^s\,. \qquad (3.62)
\end{aligned}$$

Note that (3.60) is in the same form as (3.13). Therefore, based on the results of Lemma 3.2 (i.e., (3.39)) and Assumptions 3.2 and 3.3, we have $\tilde{x}_{i1}^q \in L_\infty$, $\tilde{x}_{j1} \in L_\infty$, and $\hat{x}_{i1}^q \in L_\infty$. Additionally, based on similar reasoning logic as report in the proof of Lemma 3.2 (see (3.30)), we know that $\rho_{i2}(x_i,u_i) - \rho_{i2}(\hat{x}_i^q,u_i)$, $H_{ij}^2(x_i,x_j,u_i,u_j) - H_{ij}^2(\hat{x}_i^q,\hat{x}_j,u_i,u_j)$, and

$f_i^s(x_i,u_i) - f_i^s(\hat{x}_i^s,u_i)$ are bounded. Moreover, due to the use of parameter projection (see (3.38)), we have $\hat{\theta}_i^q \in L_\infty$. Furthermore, because η_{i2}, Ω_i^s, and $\dot{\theta}_i^s$ are bounded (Assumption 3.2 and Assumption 3.6) and $\bar{\mathcal{A}}_{i4}$ is a stable matrix, by using (3.62) we can obtain $\bar{x}_{i2}^q \in L_\infty$. Owing to the definition of $\bar{x}_2^q$, we conclude that $\tilde{x}_2^q \in L_\infty$ and $\hat{x}_2^q \in L_\infty$. This concludes the first part of the theorem.

Now, let us prove the second part of the theorem concerning the learning capability of the local FIE in the case that it matches the occurred sth fault in the local subsystem, i.e., $q = s$. In this case, the solution of (3.62) can be written as $\bar{x}_{i2}^s(t) = \xi_{i1}^s(t) + \xi_{i2}^s(t)$, $\forall t \geq T_d$, where ξ_{i1}^s and ξ_{i2}^s are the solutions of the following differential equations, respectively,

$$\begin{aligned}
\dot{\xi}_{i1}^s &= \bar{\mathcal{A}}_{i4}\xi_{i1}^s + \mathcal{A}_{i3}\tilde{x}_{i1}^s + \rho_{i2}(x_i,u_i) - \rho_{i2}(\hat{x}_i^s,u_i) + \sum_{j=1}^{M}\Big[H_{ij}^2(x_i,x_j,u_i,u_j) - H_{ij}^2(\hat{x}_i^s,\hat{x}_j,u_i,u_j)\Big] \\
&\quad + \eta_{i2} + f_i^s(x_i,u_i) - f_i^s(\hat{x}_i^s,u_i) - \Omega_i^s\dot{\theta}_i^s\,, \quad \xi_{i1}^s(T_d) = 0 \\
\dot{\xi}_{i2}^s &= \bar{\mathcal{A}}_{i4}\xi_{i2}^s\,, \quad \xi_{i2}^s(T_d) = \tilde{x}_{i2}^s(T_d) = x_{i2}^s(T_d)\,.
\end{aligned}$$

Using the definition of $\bar{x}_{i2}^s$, we have $\tilde{x}_{i2}^s = \xi_{i1}^s(t) + \xi_{i2}^s(t) - \Omega_i^s\tilde{\theta}_i^s$. Therefore,

$$\tilde{y}_i^s(t) = C_i\tilde{x}_{i2}^s = C_i[\xi_{i1}^s(t) + \xi_{i2}^s(t)] - C_i\Omega_i^s\tilde{\theta}_i^s\,. \tag{3.63}$$

Now, consider a Lyapunov function candidate $V_i = \frac{1}{2\Gamma^s}(\tilde{\theta}_i^s)^2 + \int_t^\infty |C_i\xi_{i2}^s(\tau)|^2 d\tau$. The time derivative of V_i along the solution of (3.38) is given by $\dot{V}_i = \frac{1}{\Gamma^s}\tilde{\theta}_i^s\mathcal{P}_{\Theta^s}\left\{\Gamma^s{\Omega_i^s}^\top C_i^\top\tilde{y}_i^s\right\} - |C_i\xi_{i2}^s|^2 - \frac{1}{\Gamma^s}\tilde{\theta}_i^s\dot{\theta}_i^s$. Clearly, since $\theta_i^s \in \Theta^s$, when the projection operator $\mathcal{P}$ is in effect, it always results in smaller parameter errors that will decrease $\dot{V}_i$ [35, 82]. Therefore, by using (3.63) and completing the squares, we obtain

$$\begin{aligned}
\dot{V}_i &\leq (\tilde{y}_i^s)^\top C_i\Omega_i^s\tilde{\theta}_i^s - |C_i\xi_{i2}^s|^2 - \frac{1}{\Gamma^s}\tilde{\theta}_i^s\dot{\theta}_i^s \\
&= (\tilde{y}_i^s)^\top(-\tilde{y}_i^s + C_i\xi_{i1}^s + C_i\xi_{i2}^s) - |C_i\xi_{i2}^s|^2 - \frac{1}{\Gamma^s}\tilde{\theta}_i^s\dot{\theta}_i^s \\
&\leq -\frac{|\tilde{y}_i^s|^2}{2} + |C_i\xi_{i1}^s|^2 + \frac{1}{\Gamma^s}|\tilde{\theta}_i^s|\,|\dot{\theta}_i^s|\,.
\end{aligned} \tag{3.64}$$

Let $\bar{\xi}_i^s \triangleq \left(|C_i\xi_{i1}^s|^2 + \frac{1}{\Gamma^s}|\tilde{\theta}_i^s||\dot{\theta}_i^s|\right)^{\frac{1}{2}}$. By integrating (3.64) from $t = T_d$ to $t = t_f$, we obtain $\int_{T_d}^{t_f}|\tilde{y}_i^s(t)|^2\,dt \leq \bar{\kappa}_i + 2\int_{T_d}^{t_f}|\bar{\xi}_i^s(t)|^2\,dt$, where $\bar{\kappa}_i \triangleq \sup_{t_f\geq T_d}\{2[V_i(T_d) - V_i(t_f)]\}$.

□

Theorem 3.4 guarantees the boundedness of all the variables involved in the local adaptive FIEs in the case that a fault is detected in the corresponding subsystem. Moreover, the performance measure given by (3.59) shows that the ability of the matched local isolation estimator to learn the post-fault system dynamics is limited by the extended L_2 norm of $\bar{\xi}_i^s(t)$, which, in turn, is related to the modeling uncertainties η_{i1} and η_{i2}, the parameter estimation error $\tilde{\theta}_i^s$, and the rate of change of the time–varying bias θ_i^s.

3.6 Simulation Results

In this section, a simulation example of interconnected inverted pendulums mounted on carts [32] shown in Figure 3.1 is given to illustrate the effectiveness of the distributed FDI algorithm.

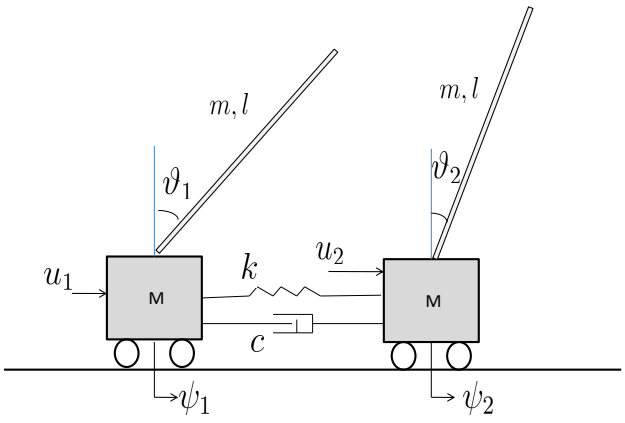

Figure 3.1: Interconnected inverted pendulums mounted on carts

Specifically, we consider two identical inverted pendulums mounted on carts, which are

connected by springs and dampers. Each cart is linked by a transmission belt to a drive wheel driven by a DC motor. As described in [32], the equations of motion are

$$\begin{aligned}
(M+m)\ddot{\psi}_1 + F_\psi\dot{\psi}_1 + ml\ddot{\vartheta}_1 cos\vartheta_1 - ml(\dot{\vartheta}_1)^2 sin\vartheta_1 &= u_1 + s_1 \\
J\ddot{\vartheta}_1 + F_\vartheta\dot{\vartheta}_1 - mlgsin\vartheta_1 + ml\ddot{\psi}_1 cos\vartheta_1 &= 0 \\
(M+m)\ddot{\psi}_2 + F_\psi\dot{\psi}_2 + ml\ddot{\vartheta}_2 cos\vartheta_2 - ml(\dot{\vartheta}_2)^2 sin\vartheta_2 &= u_2 + s_2 \\
J\ddot{\vartheta}_2 + F_\vartheta\dot{\vartheta}_2 - mlgsin\vartheta_2 + ml\ddot{\psi}_2 cos\vartheta_2 &= 0
\end{aligned}$$

where, in each subsystem, ψ_i $(i = 1, 2)$ is the position of the cart, ϑ_i is the angle of the pendulum, u_i is the input force, respectively. The interconnection forces due to springs and dampers are $s_1 = k(\psi_2 - \psi_1) + c(\dot{\psi}_2 - \dot{\psi}_1)$, $s_2 = k(\psi_1 - \psi_2) + c(\dot{\psi}_1 - \dot{\psi}_2)$, where k and c are the spring constant and the damping constant, respectively. Additionally, J is the moment of inertial, M is the mass of the cart, m is rod mass, l is rod length, g is the gravitational acceleration, F_ϑ and F_ψ are the friction coefficients. The model parameters are: $M = 5\,\mathrm{kg}$, $m = 0.535\,\mathrm{kg}$, $J = 0.062\,\mathrm{kg\,m^2}$, $l = 0.365\,\mathrm{m}$, $F_\psi = 6.2\,\mathrm{kg/s}$, $F_\vartheta = 0.09\,\mathrm{kg\,m^2}$ and $g = 9.8\,\mathrm{m/s^2}$, $k = 1$, and $c = 0.02$.

For each subsystem, we assume the cart position (ψ_i), pendulum angle (ϑ_i), and pendulum angular velocity $(\dot{\vartheta}_i)$ are measurable. By using a change of coordinates defined by $z_i = [z_{i1}\ z_{i2}\ z_{i3}\ z_{i4}]^\top = T_i[\psi_i\ \vartheta_i\ \dot{\psi}_i\ \dot{\vartheta}_i]^\top$ with

$$T = \begin{bmatrix} -1.5 & 0 & 1 & 0.3175/\cos\vartheta_i \\ 1 & 0 & 0 & 0 \\ 0 & 1 & 0 & 1 \\ 0 & 0 & 0 & 1 \end{bmatrix} \tag{3.65}$$

a system state space model is obtained as

$$\left[\begin{array}{c} \dot{z}_{i1} \\ \hline \dot{z}_{i2} \\ \dot{z}_{i3} \\ \dot{z}_{i4} \end{array}\right] = \left[\begin{array}{c|ccc} -1.5 & -2.25 & 0 & 0 \\ \hline 1 & 1.5 & 0 & 0 \\ 0 & 0 & 0 & 1 \\ 0 & 0 & 0 & 0 \end{array}\right] \left[\begin{array}{c} z_{i1} \\ \hline z_{i2} \\ z_{i3} \\ z_{i4} \end{array}\right] + \left[\begin{array}{c} \zeta_{i1}(z_i, u_i) \\ \hline \zeta_{i2}(z_i, u_i) \\ 0 \\ \zeta_{i4}(z_i, u_i) \end{array}\right] + h_{ij} + \varphi_i + d_{ij} \quad (3.66)$$

$$y_i = \left[\begin{array}{cccc} 0 & 1 & 0 & 0 \\ 0 & 0 & 1 & 0 \\ 0 & 0 & 0 & 1 \end{array}\right] \left[\begin{array}{c} z_{i1} \\ z_{i2} \\ z_{i3} \\ z_{i4} \end{array}\right],$$

where the nominal nonlinear dynamics are $\zeta_{i2} = \frac{-0.3175 z_{i4}}{cos z_{i3}}$,

$$\begin{aligned} \zeta_{i1} &= \frac{ml(\cos z_{i3})^2(F_\vartheta z_{i4} - mlg \sin z_{i3}) - 0.3175(m+M)(F_\vartheta z_{i4} - mgl \sin z_{i3})}{\cos z_{i3}[J(M+m) - (ml \cos z_{i3})^2]} \\ &\quad + \frac{0.4763 z_{i4}}{\cos z_{i3}} + \frac{0.3175 z_{i4} \sin z_{i3}}{(\cos z_{i3})^2} \end{aligned}$$

$$\begin{aligned} \zeta_{i4} &= \frac{ml \cos z_{i3} \left[ml(z_{i4})^2 \sin z_{i3} - (F_\psi + c)(z_{i1} + 1.5 z_{i2} - 0.3175 z_{i4}) - k z_{i2} + u_i\right]}{(ml \cos z_{i3})^2 - J(M+m)} \\ &\quad + \frac{(M+m)(F_\vartheta z_{i4} - mgl \sin z_{i3})}{(ml \cos z_{i3})^2 - J(M+m)} \end{aligned}$$

and the known interconnection term is

$$h_{ij} = \left[\begin{array}{ccc} 0 & 0 & 0 \end{array} \quad \frac{mlcosz_{i3}[k z_{j2} + c(z_{j1} + 1.5 z_{j2} - 0.3175 z_{j4})]}{(mlcosz_{i3})^2 - J(M+m)} \right]^\top.$$

Note that the effects of modeling uncertainty (i.e., φ_i and d_{ij}) have been included in the above model. Specifically, two sources of modeling uncertainty are considered: (i) up to 80% inaccuracy in the friction constant F_ϑ (corresponding to φ_i in (3.66) and (3.1)); (ii) up to 10% inaccuracy in the spring constant k in the interconnection force (corresponding to d_{ij} in (3.66) and (3.1)).

In addition, the following two types of faults are considered in each subsystem:

1. *An actuator fault.* A simple multiplicative actuator fault by letting $u_i = \bar{u}_i + \theta_i^1 \bar{u}_i$ is considered, where $\bar{u}_i$ is the nominal control input in the non-fault case, and $\theta_i^1 \in [-1 \;\; 0]$ is the unknown fault magnitude. For instance, the case $\theta_i^1 = 0$ represents the normal operation condition, while the case $\theta_i^1 = -1$ corresponds to a complete failure of the actuator. Hence, based on the system and fault models given by (3.66) and (3.5), the actuator fault can be described by $f_i^1 \triangleq [0 \quad 0 \quad \theta_i^1 g_i^1(z_i, u_i)]^\top$, where $g_i^1 = \frac{mlu_i \cos z_{i3}}{(ml\cos z_{i3})^2 - J(M+m)}$ and $\theta_i^1 \in [-1 \; 0]$.

2. *A process fault causing extra abnormal friction applied to the cart.* Specifically, as a result of the fault, the viscous friction constant F_ψ increases by up to three times of its nominal value. Then, the fault function is in the form of $f_i^2 \triangleq [0 \;\; 0 \;\; \theta_i^2 g_i^2(z_i)]^\top$, where $g_i^2 = \frac{3mlF_\psi \, z_{i1} \cos z_{i3}}{(ml\cos z_{i3})^2 - J(M+m)}$ and $\theta_i^2 \in [-1 \;\; 0]$ represents significance of extra friction.

Clearly, the above system model is in the form of (3.3) with $x_{i1} = z_{i1}$, $x_{i2} = [z_{i2} \; z_{i3} \; z_{i4}]^\top$, $\rho_{i1} = \zeta_{i1}$, $\rho_{i2} = [\zeta_{i2} \;\; 0 \;\; \zeta_{i4}]^\top$, and $H_{ij} = h_{ij}$. Also, it can be easily seen that Assumptions 3.2-3.7 are satisfied. Specifically, based on the change of coordinates defined above, we have

$$\bar{\eta}_{i1} = \left| \frac{0.8F_\vartheta y_{i3}[ml(\cos y_{i2})^2 - 0.3175(M+m)]}{\cos y_{i2}[J(M+m) - (ml\cos y_{i2})^2]} \right| ,$$

$$\bar{\eta}_{i2} = \frac{|0.8(M+m)F_\vartheta y_{i3}| \; + \; |0.1kml\cos y_{i2}(y_{j1} - y_{i1})|}{J(M+m) - (ml\cos y_{i2})^2} ,$$

$\gamma_{21}^1 = \gamma_{12}^1 = 0$, $\gamma_{12}^2 = \frac{cml\,|\cos y_{12}|}{J(M+m)-(ml\cos y_{12})^2}$ and $\gamma_{21}^2 = \frac{cml\,|\cos y_{22}|}{J(M+m)-(ml\cos y_{22})^2}$, $\sigma_{i1} = 0$ and $\sigma_{i2} = \frac{(F_\psi + c)ml\,|\cos y_{i2}|}{J(M+m)-(ml\cos y_{i2})^2}$, $\varpi_i^1 = 0$, and $\varpi_i^2 = \frac{3mlF_\psi|\cos z_{i3}|}{J(M+m)-(ml\cos z_{i3})^2}$.

The initial condition of each cart-pendulum subsystem is set to $x_i = [0 \;\; 0 \;\; 0 \;\; 0]^\top$. For simplicity, the input to each subsystem consists of two parts: a stabilizing part based on state feedback design and a sinusoidal signal causing each subsystem to deviate from steady-state linear dynamics. In the simulation, the actual modeling uncertainties used are: (i) 40% inaccuracy in the friction constant F_ϑ; (ii) 8% inaccuracy in the spring constant k in the interconnection force.

The gain matrix L_i of the estimators is chosen such that the poles of matrix $\bar{\mathcal{A}}_{i4}$ are located at -1.7 , -2.5 and -2.2, respectively. Consequently, the related design constants are $k_{i1} = k_{i2} = k_{i3} = 1$, $\lambda_{i1} = -1.7$, $\lambda_{i2} = -2.5$ and $\lambda_{i3} = -2.2$. Additionally, we choose the matrix $P = [0.5\ 0\ ;\ 0\ 0.5]$ (i.e., $P_i = 0.5$, see Lemma 3.2). Thus, $Q = [1\ \ 0; 0\ \ 1]$, which results in $c = 2$. The learning rate of the adaptive algorithm for fault parameters estimation in the FIE1 and FIE2 is set to 1 and 0.1, respectively.

First, we consider an *an actuator fault* (fault type 1, as defined in section 3.2) in subsystem 1. Figure 3.2 and Figure 3.3 show the fault detection results when a partial actuator fault with $\theta_1^1 = -0.25$ occurs to subsystem 1 at $T_0 = 5$ second. Note that, since the dynamics of z_{i3} in each subsystem is not affected by the faults or modeling uncertainty under consideration, we only focus on the residuals and thresholds associated with y_{i1} and y_{i3}. As can be seen from Figure 3.3, both the residuals generated by FDE 2 (i.e., local FDE associated with subsystem 2) always remain below their thresholds, while the residual associated with y_{13} generated by FDE 1 (i.e., the local FDE designed for subsystem 1) almost immediately exceeds its threshold after fault occurrence (see Figure 3.3). Therefore, the actuator fault in subsystem 1 is timely detected. Then, the two local FIEs associated with subsystem 1 are activated to determine the particular fault type that has occurred. Selected fault isolation residuals and the corresponding thresholds generated by the two local FIEs for subsystem 1 are shown in Figure 3.4. It is obvious that the residual associated with y_{13} generated by local FIE 2 exceeds the threshold at approximately $t = 5.88$ second, while both residuals generated by local FIE 1 always remain below their thresholds, indicating the isolation of fault f_1^1 (i.e., actuator fault in subsystem 1). It is worth noting that for local FIE 2, only the residual and threshold associated with y_{13} are shown, since it is sufficient to exclude the possibility of occurrence of f_1^2 based on the presented fault isolation decision scheme. In addition, Figure 3.5 and Figure 3.6 show the actuator fault effect on the angle and the angle velocity of the subsystem 1.

As another illustrative example, we consider a *process fault causing extra abnormal friction applied to the cart* in the second subsystem. Figure 3.7 and Figure 3.8 show the simulation

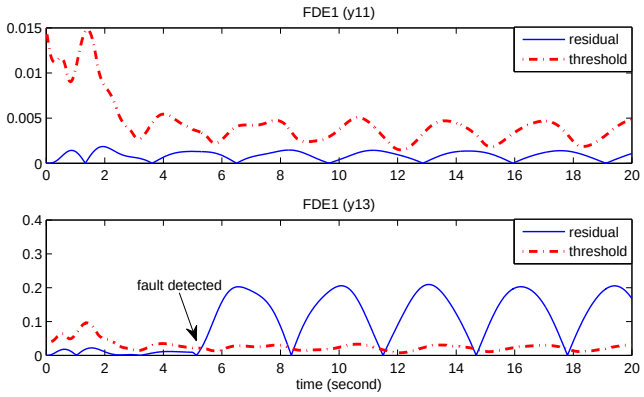

Figure 3.2: The case of an actuator fault in subsystem 1: fault detection residuals (solid and blue line) associated with y_{11} and y_{13} and their thresholds (dashed and red line) generated by the local FDE for subsystem 1.

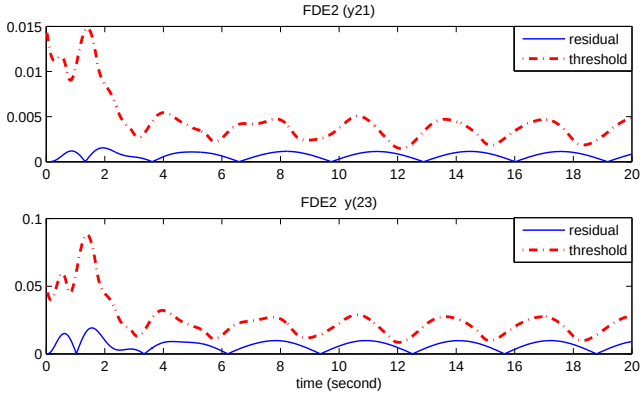

Figure 3.3: The case of an actuator fault in subsystem 1: the fault detection residuals (solid and blue line) associated with y_{21} and y_{23} and their thresholds (dashed and red line) generated by the local FDE for subsystem 2.

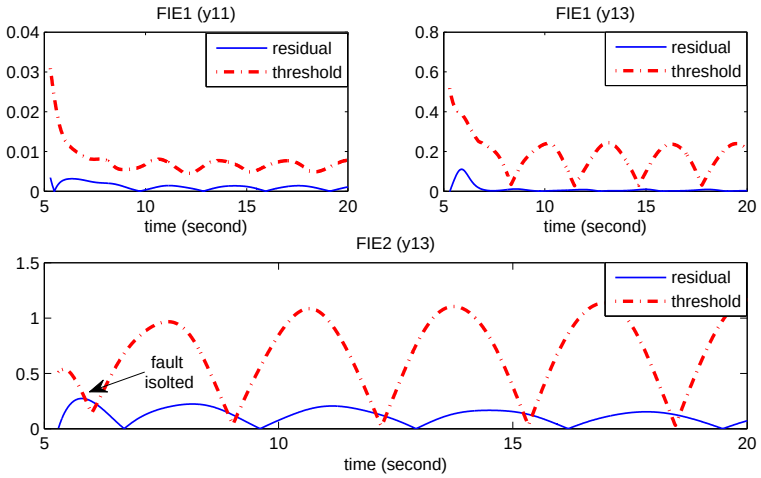

Figure 3.4: The case of an actuator fault in subsystem 1: selected fault isolation residuals (solid and blue line) and their thresholds (dashed and red line) generated by the two local FIEs associated with subsystem 1.

results of fault detection when such a fault with $\theta_2^2 = -0.5$ occurs to the second subsystem at $T_0 = 5$ second. Figure 3.9 shows the results of fault isolation. Again, the fault is successfully detected and isolated.

Moreover, a *completely unknown fault* is considered in subsystem 1. Specifically, as a result of the fault, the dynamics of the angle velocity is affected by a sinusoidal signal. Then, the fault function is in the form of $f_i^{unknown} \triangleq [0 \quad 0 \quad \cos(t)]^\top$. Figure 3.10 and Figure 3.11 show the fault detection results when this unknown fault occurs to subsystem 1 at $T_0 = 5$ second. As can be seen from Figure 3.11, both the residuals generated by FDE 2 (i.e., local FDE associated with subsystem 2) always remain below their thresholds, while the residual associated with y_{13} generated by FDE 1 (i.e., the local FDE designed for subsystem 1) almost immediately exceeds its threshold after fault occurrence (see Figure 3.10). Therefore, the unknown fault in subsystem 1 is timely detected. Then, the two local FIEs associated with subsystem 1 are activated to determine the particular fault type that has occurred. Selected fault isolation residuals and the corresponding thresholds generated by the two local FIEs for subsystem 1 are shown in Figure 3.12 and Figure 3.13. It is obvious that the residuals in both FIEs exceed the corresponding thresholds. Thus, based on the isolation logic, the

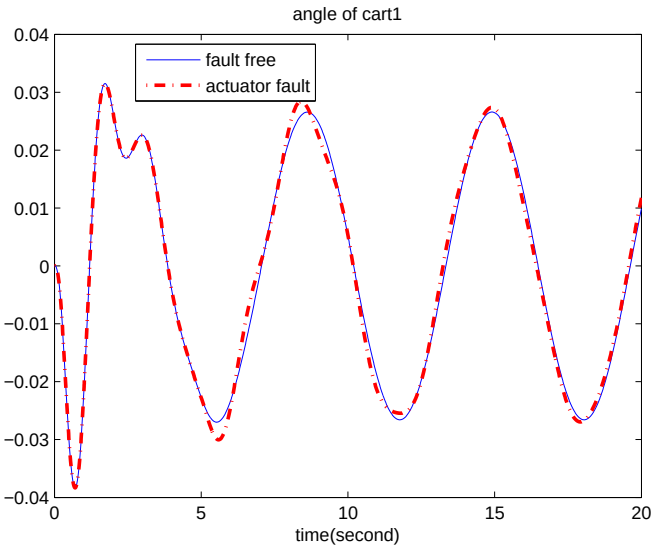

Figure 3.5: The case of an actuator fault in subsystem 1: the signal of the angle in the fault free case (solid and blue line) and the signal of the angle in the actuator fault case (dashed and red line) of subsystem 1.

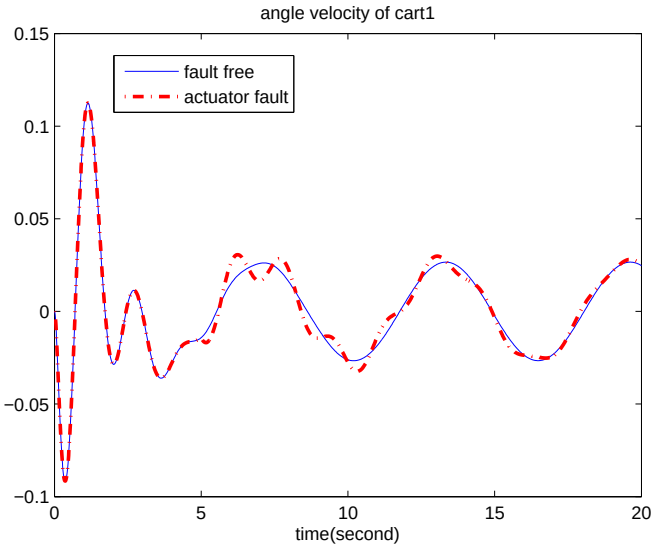

Figure 3.6: The case of an actuator fault in subsystem 1: the signal of the angle velocity in the fault free case (solid and blue line) and the signal of the angle velocity in the actuator fault case (dashed and red line) of subsystem 1.

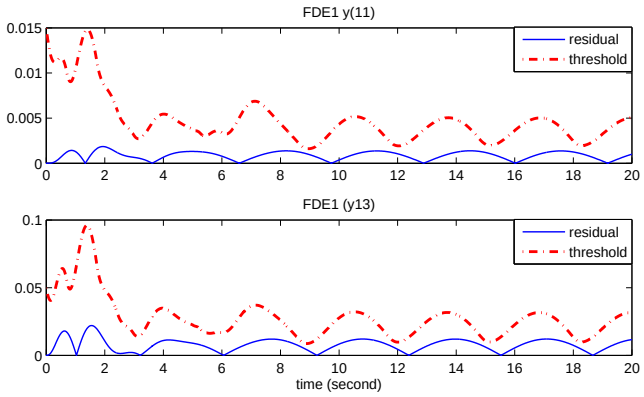

Figure 3.7: The case of a process fault in subsystem 2: fault detection residuals (solid and blue line) associated with y_{11} and y_{13} and their thresholds (dashed and red line) generated by the local FDE for subsystem 1.

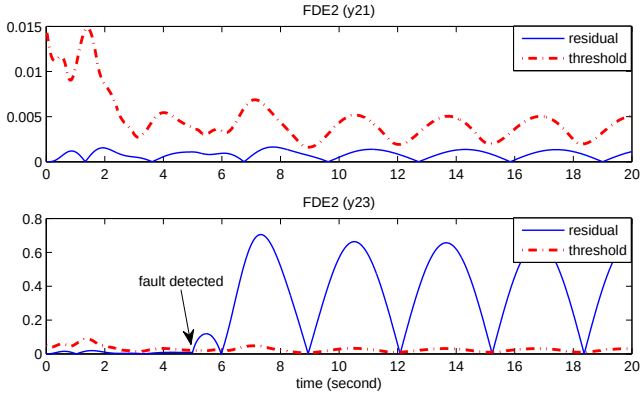

Figure 3.8: The case of a process fault in subsystem 2: the fault detection residuals (solid and blue line) associated with y_{21} and y_{23} and their thresholds (dashed and red line) generated by the local FDE for subsystem 2.

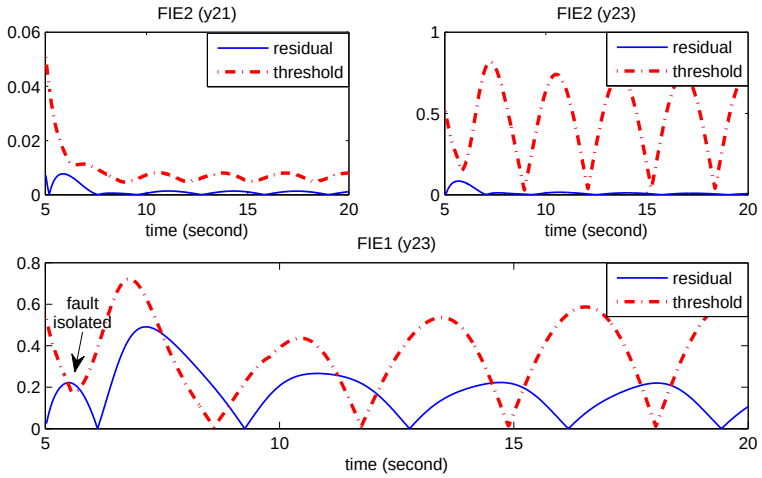

Figure 3.9: The case of a process fault in subsystem 2: selected fault isolation residuals (solid and blue line) and their thresholds (dashed and red line) generated by the two local FIEs associated with subsystem 2.

possibilities of the occurrence of the two predefined faults are excluded, the decision of the occurrence of an unknown type fault which is not included in the fault set is made.

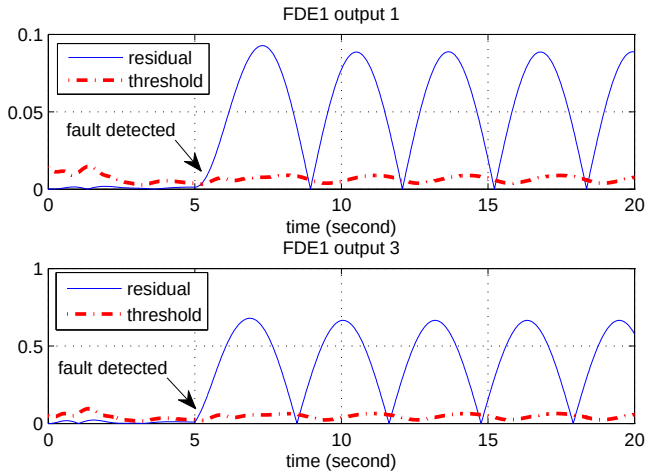

Figure 3.10: The case of a complete unknown fault in subsystem 1: fault detection residuals (solid and blue line) associated with y_{11} and y_{13} and their thresholds (dashed and red line) generated by the local FDE for subsystem 1.

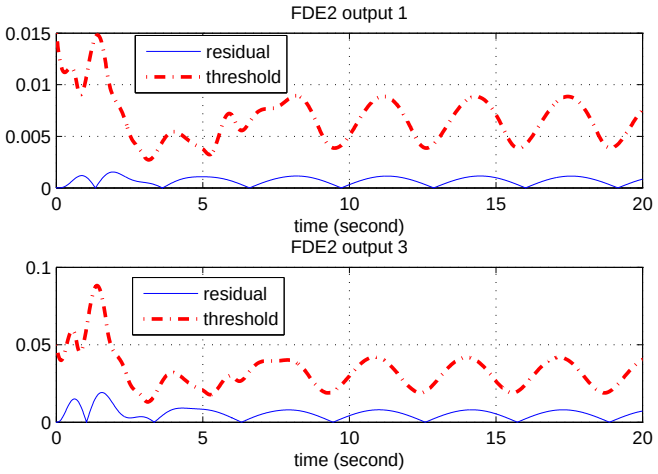

Figure 3.11: The case of a complete unknown fault in subsystem 1: the fault detection residuals (solid and blue line) associated with y_{21} and y_{23} and their thresholds (dashed and red line) generated by the local FDE for subsystem 2.

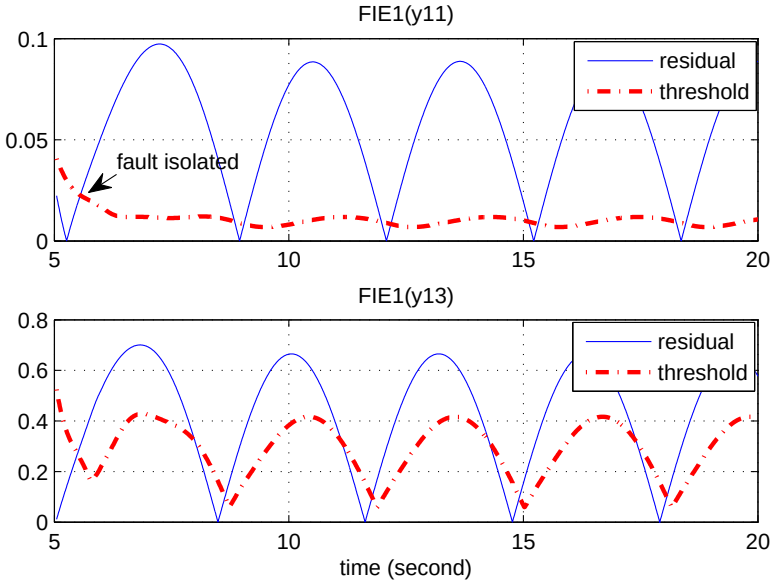

Figure 3.12: The case of a complete unknown fault in subsystem 1: selected fault isolation residuals (solid and blue line) and their thresholds (dashed and red line) generated by FIE 1 associated with subsystem 1.

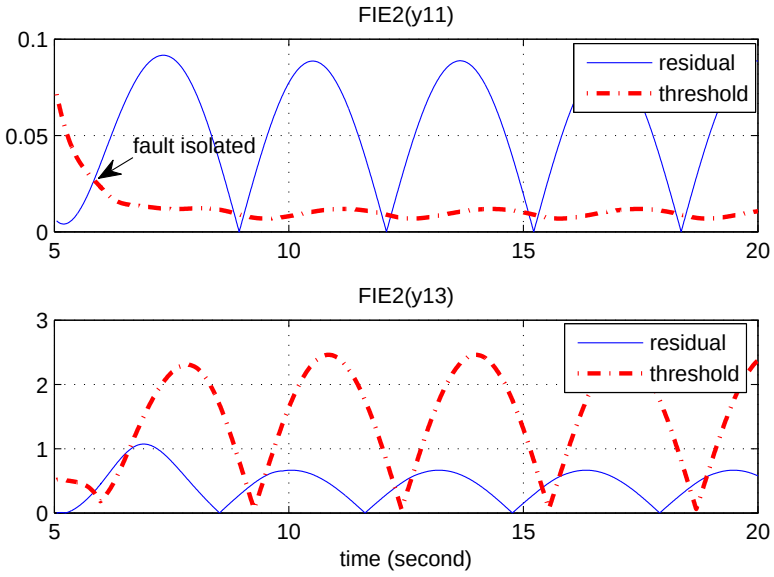

Figure 3.13: The case of a complete unknown fault in subsystem 1: selected fault isolation residuals (solid and blue line) and their thresholds (dashed and red line) generated by FIE 2 associated with subsystem 1.

Chapter 4

Distributed Sensor Fault Detection and Isolation in Multimachine Power Systems

The distributed fault diagnosis scheme presented in Chapter 3 only considers the process faults in a class of distributed nonlinear systems. In real world applications, the reliable operations of interconnected control systems also greatly rely on the health of sensors. For instance, a sensor fault may lead to poor tracking performance, or even affect the stability of the overall distributed system, since the fault effect may be propagated to other subsystems through interconnections. Moreover, a faulty sensor output may also cause wrong diagnostic and prognostic decisions, resulting in mistaken replacement of system components or mission abortion. Hence, sensor fault diagnosis is a critical issue in distributed interconnected control systems.

This chapter presents a distributed sensor FDI scheme for a class of interconnected nonlinear systems, where only the measurable part of the state variables are directly affected by the interconnections between subsystems. A multimachine power systems is used as an application example. The general theory can be easily extended to other systems with

the similar model structure. In a multimachine power systems, each generator is interconnected with other generators through a transmission network, where the interactions between directly interconnected generators are nonlinear. Because of the interconnection among generators and the limited sensor data that are available for each local system, the problem of distributed sensor FDI is very challenging. In the proposed distributed FDI architecture, a fault diagnostic component is designed for each generator in the interconnected system by exploiting local measurements and suitable communicated information from neighboring FDI components associated with its directly interconnected generators. In each FDI component, adaptive thresholds for distributed FDI are derived, ensuring robustness with respect to nonlinear interconnection and unstructured modeling uncertainty under certain conditions. Furthermore, the fault detectability and isolability properties are investigated, characterizing the class of sensor faults that are detectable and isolable by the distributed FDI method. In addition, the stability and learning capability of the local adaptive fault isolation estimators designed for each generator is derived. A simulation example of a two-machine power system is used to illustrate the effectiveness of the proposed method.

The chapter is organized as follows. In Section 4.1, the problem of distributed FDI for multimachine power systems is formulated. Section 4.2 describes the distributed FDI architecture, the design of adaptive thresholds for distributed fault detection and isolation in each generator, and the fault detectability of the distributed sensor FDI method. Section 4.3 analyzes several important properties of the distributed fault isolation method, including fault isolability, stability and learning capability. To illustrate the effectiveness of the diagnostic method, some simulation results using the example of a two-machine power system are presented in Section 4.4.

4.1 Problem Formulation

We consider a multimachine power system consisting of M generators interconnected through a transmission network. A complete model of each generator includes the mechanical equations describing the motion of the generator rotor, the generator electrical equations representing the dynamics of the generator windings, and the electrical equations describing the interconnections between the generator and the transmission network. Based on the classic dynamic model of power systems given in [2], a model for the ith generator with excitation control in the multimachine power system can be described by the following equations (see [25, 26]):

1. Mechanical Equations

$$\dot{\delta}_i = \omega_i \,, \tag{4.1}$$

$$\dot{\omega}_i = -\frac{D_i}{2H_i}\omega_i + \frac{\omega_0}{2H_i}(P_{mi0} - P_{ei}) + d_i \,, \tag{4.2}$$

2. Generator electrical dynamics:

$$\dot{E}'_{qi} = \frac{1}{T'_{doi}}(E_{fi} - E_{qi}) \,, \tag{4.3}$$

3. Electrical equations:

$$
\begin{aligned}
E_{qi} &= E_{qi}^{'} + (x_{di} - x_{di}^{'})I_{di}, \\
E_{fi} &= k_{ci}u_{fi}, \\
P_{ei} &= \sum_{j=1}^{M} E_{qi}^{'}E_{qj}^{'}B_{ij}\sin(\delta_i - \delta_j), \\
Q_{ei} &= -\sum_{j=1}^{M} E_{qi}^{'}E_{qj}^{'}B_{ij}\cos(\delta_i - \delta_j), \\
I_{di} &= -\sum_{j=1}^{M} E_{qj}^{'}B_{ij}\cos(\delta_i - \delta_j), \\
I_{qi} &= \sum_{j=1}^{M} E_{qj}^{'}B_{ij}\sin(\delta_i - \delta_j), \\
E_{qi} &= x_{adi}I_{fi}, \\
V_{ti} &= \sqrt{(E_{qi}^{'} - x_{di}^{'}I_{di})^2 + (x_{di}^{'}I_{qi})^2}.
\end{aligned}
$$

The notation for the above generator model, given in the Appendix A, is the same as in [25].

In this chapter, we focus on the sensor fault FDI problem of the excitation loop of each generator in the multimachine power system. Thus, by using the direct feedback linearizable compensation for the power system as in [26], we obtain

$$
\begin{aligned}
\dot{\delta}_i &= \omega_i \\
\dot{\omega}_i &= -\tfrac{D_i}{2H_i}\omega_i - \tfrac{\omega_0}{2H_i}\Delta P_{ei} \\
\Delta\dot{P}_{ei} &= -\tfrac{1}{T_{doi}^{'}}\Delta P_{ei} + \tfrac{1}{T_{doi}^{'}}v_{fi} + E_{qi}^{'}\sum_{j=1}^{M}\dot{E}_{qj}^{'}B_{ij}\sin(\delta_i - \delta_j) - E_{qi}^{'}\sum_{j=1}^{M}E_{qj}^{'}B_{ij}\cos(\delta_i - \delta_j)\omega_j\,],
\end{aligned}
$$

where ω_i is the relative speed of the ith generator, δ_i is the power angle of the ith generator, and $\Delta P_{ei} = P_{ei} - P_{mi0}$ with P_{ei} being the electrical power and P_{mi0} being the mechanical input power, respectively. Since only the excitation loop is under consideration, P_{mi0} is a constant. By defining the state vector as $x_i = [x_{i1}\ x_{i2}^{\top}\ ]^{\top} = [\omega_i\ \delta_i\ \Delta P_{ei}]^{\top}$ with $x_{i1} = \omega_i$,

$x_{i2} = [\delta_i \ \Delta P_{ei}]^\top$ and by assuming the states δ_i and ΔP_{ei} to be measurable, we can obtain a model of the excitation loop of the ith generator, $i = 1, \cdots, M$ as follows:

$$\begin{aligned} \dot{x}_{i1} &= \mathcal{A}_{i1}x_{i1} + \mathcal{A}_{i2}x_{i2} + d_i(x_i, u_i, t) \\ \dot{x}_{i2} &= \mathcal{A}_{i3}x_{i1} + \mathcal{A}_{i4}x_{i2} + G_i\frac{v_{fi}}{T'_{doi}} + \eta_i(x_i, u_i, t) + G_i\sum_{j=1}^{M}\gamma_{ij}h_{ij}(x_i, x_j) \\ y_i &= x_{i2} + \beta_i(t - T_i)\theta_i(t)\,, \end{aligned} \tag{4.4}$$

where $v_{fi} \in \Re$ and $y_i \in \Re^2$ represent the control input and output, respectively, $\mathcal{A}_{i1} = -\frac{D_i}{2H_i}$, $\mathcal{A}_{i2} = [\,0 \quad \frac{\omega_0}{2H_i}\,]$, $\mathcal{A}_{i3} = [\,1 \quad -E'^2_{qi}B_{ii}\,]^\top$, $\mathcal{A}_{i4} = [\,0 \quad 0; 0 \quad -\frac{1}{T'_{doi}}\,]$, $G_i = [\,0 \quad 1\,]^\top$. The term $G_i\gamma_{ij}h_{ij}$ represents the direct interconnection between the ith generator and the jth generator. Specifically, $h_{ij}(x_i, x_j) \stackrel{\triangle}{=} E'_{qi}\dot{E}'_{qj}B_{ij}\sin(\delta_i - \delta_j) - E'_{qi}E'_{qj}B_{ij}\cos(\delta_i - \delta_j)x_{j1}$, and γ_{ij} is a constant with a value of either 1 or 0 (i.e., if the jth generator is directly connected to the ith generator, then $\gamma_{ij} = 1$. Otherwise, $\gamma_{ij} = 0$). Note that, $\gamma_{ii} = 0$ because the interconnection term is only defined between two generators.

The functions d_i and η_i in (4.4) represent the modeling uncertainties, and $\beta_i(t - T_i)\theta_i(t)$ denotes a sensor bias fault [81, 79]. Specifically, $\beta_i(t - T_i)$ is a step function representing the time profile of the sensor fault which occurs at some unknown time T_i, and the vector $\theta_i(t) \in \Re^2$ represents the unknown time-varying sensor bias affecting the output of the ith generator. Therefore, the sensor fault can be either an abrupt or incipient one. It is assumed that only one of the M generators possibly has faulty sensors at a given time.

The objective of this chapter is to develop a robust distributed sensor bias FDI scheme for multimachine power systems that can be represented by (4.4). Specifically, the distributed FDI algorithm detects the occurrence of a sensor fault and determines the particular generator with faulty sensors. Throughout the chapter, the following assumptions are made:

Assumption 4.1. *The functions d_i and η_i in (4.4), representing the unstructured modeling uncertainty, are unknown nonlinear functions of x_i, u_i, and t, but bounded,*

$$|d_i(x_i,u_i,t)| \le \bar{d}_i(y_i,u_i,t),\ |\eta_{i1}(x_i,u_i,t)| \le \bar{\eta}_{i1}(y_i,u_i,t),\ |\eta_{i2}(x_i,u_i,t)| \le \bar{\eta}_{i2}(y_i,u_i,t)\,, \tag{4.5}$$

where η_{i1} and η_{i2} represent the first and the second component of η_i, respectively, and the the bounding functions $\bar{d}_i$, $\bar{\eta}_{i1}$, and $\bar{\eta}_{i2}$ are known and uniformly bounded in the corresponding compact sets of admissible state variables, inputs, and outputs with appropriate dimensions, respectively.

Assumption 4.2. *The state vector x_i of each subsystem remains bounded before and after the occurrence of a fault, i.e., $x_i(t) \in L_\infty$, $\forall t \ge 0$.*

Assumption 4.3. *The rate of change of the possible time-varying sensors bias is uniformly bounded. i.e., $|\dot{\theta}_i(t)| \le \alpha_i$ for all $t \ge 0$, where α_i is a known positive constant.*

Assumption 4.1 characterizes the class of modeling uncertainty under consideration. The bound on the modeling uncertainty is needed in order to be able to distinguish between the effects of faults and modeling uncertainty (see [83, 84]). The modeling uncertainty in the multimachine power system can be a variety of sources affecting the dynamics of each machine, such as a consistent load change, increase of the mechanical input power in each machine, or parametric uncertainties. For instance, the disturbance effect on the power system frequency is considered in [25].

Assumption 4.2 requires the boundedness of the state variables before and after the occurrence of a fault in each subsystem. Hence, it is assumed that the distributed feedback control system is capable of retaining the boundedness of the state variables of each subsystem even in the presence of a sensor fault. This is a technical assumption required for well-posedness since the distributed FDI design under consideration does not influence the closed-loop dynamics and stability. The design of distributed fault-tolerant controllers is beyond the scope of this paper. However, it is important to note that the proposed distributed FDI design does not depend on the structure of the distributed controllers.

Assumption 4.3 gives a known bound on the rate of change of the sensor fault magnitude $\theta_i(t)$. In practice, the rate bound α_i can be set by exploiting some *a priori* knowledge on the fault developing dynamics. Note that both abrupt fault and incipient fault are considered in the paper for multimachine power systems. Specifically, the fault time profile function $\beta_i(t - T_i)$ is a step function modeling abrupt characteristics of the sensor bias, and the fault magnitude $\theta_i(t)$ represents the (possibly time-varying) sensor bias magnitude. In the specifical case of abrupt faults, we can simply set $\alpha_i = 0$ (i.e., θ_i is a vector of constants).

Remark 4.1. Note that the FDI method presented in this chapter can be easily extended to other nonlinear systems, where the interconnections only directly affect the measurable part of the state vector. Specifically, it can be extended to a general system model described as follows:

$$\begin{aligned} \dot{z}_{i1} &= \mathcal{A}_{i1} z_{i1} + \mathcal{A}_{i2} z_{i2} + \psi_{i1}(y_i, u_i) + \eta_{i1}(z_i, u_i, t) \\ \dot{z}_{i2} &= \mathcal{A}_{i3} z_{i1} + \mathcal{A}_{i4} z_{i2} + \rho_{i2}(z_i, u_i) + \psi_{i2}(y_i, u_i) + \eta_{i2}(z_i, u_i, t) + \sum_{j=1}^{M} H_{ij}(z_j, u_j) \\ y_i &= C_i z_{i2} + \beta_i(t - T_0)\theta_i(t)\,, \end{aligned} \tag{4.6}$$

where $[\, z_{i1}^\top \quad z_{i2}^\top \,]^\top$, u_i, and y_i are the state vector, input vector, and output vector of the ith subsystem, respectively, ψ_{i1}, ρ_{i2} and ψ_{i2} represent nonlinearities, $\eta_{i1}(z_i, u_i, t)$ and $\eta_{i2}(z_i, u_i, t)$ represent modeling uncertainties, and $H_{ij}(z_j, u_j)$ represents the interconnection from the jth directly interconnected subsystem, $\mathcal{A}_{i1}$, $\mathcal{A}_{i2}$, $\mathcal{A}_{i3}$, $\mathcal{A}_{i4}$ and C_i are known matrices with appropriate dimensions, and θ_i represents a sensor fault.

4.2 Distributed Fault Detection and Isolation Architecture

The distributed FDI architecture is made of M local FDI components, with one FDI component designed for each of the M generators. Specifically, each local FDI component consists of a FDE and a nonlinear adaptive FIE. Under normal conditions, each local FDE monitors the corresponding local generator to detect the occurrence of any fault. If a sensor fault is detected, then the FIEs are activated for the purpose of isolating the particular generator

where the sensor fault has actually occurred.

The FDI architecture for each generator follows the generalized observer scheme (GOS) architectural framework well-documented in the fault diagnosis literature [3, 5]. The distributed nature of the presented FDI method can be better understood if compared with the conventional centralized FDI architecture. For M interconnected generators, $M+1$ estimators are needed at the server node in the case of centralized FDI architecture. Moreover, each generator needs to transmit data to the server node. With the distributed FDI architecture, only a pair of local FDE and FIE is needed at the ith generator. Hence, the computation is distributed in the network. Additionally, data communication is only required among the FDI components associated with generators that are directly interconnected.

In order to get a deeper insight into the distributed FDI architecture described above, we refer to Figure 4.1. For the sake of simplicity, an example of three interconnected generators is considered. Without loss of generality, we assume that there exit direct interconnections in two pairs of generators (i.e., generators 1 and 2, and generators 2 and 3). Thus, the distributed FDI architecture consists of three local FDI components, and the information exchange is conducted between FDI components 1 and 2, and FDI components 2 and 3, respectively.

4.2.1 Distributed Fault Detection Method

In this section, we describe the distributed fault detection method, including the design of each local FDE for residual generation and adaptive thresholds for residual evaluation.

Based on the generator model described by (4.4), the FDE for each local generator is chosen as:

$$\begin{aligned}
\dot{\hat{x}}_{i1} &= \mathcal{A}_{i1}\hat{x}_{i1} + \mathcal{A}_{i2}y_i \\
\dot{\hat{x}}_{i2} &= \mathcal{A}_{i3}\hat{x}_{i1} + \mathcal{A}_{i4}\hat{x}_{i2} + G_i\frac{v_{fi}}{T'_{doi}} + L_i(y_i - \hat{y}_i) + G_i\sum_{j=1}^{M}\gamma_{ij}h_{ij}(\hat{x}_i, \hat{x}_j) \qquad (4.7) \\
\hat{y}_i &= \hat{x}_{i2}
\end{aligned}$$

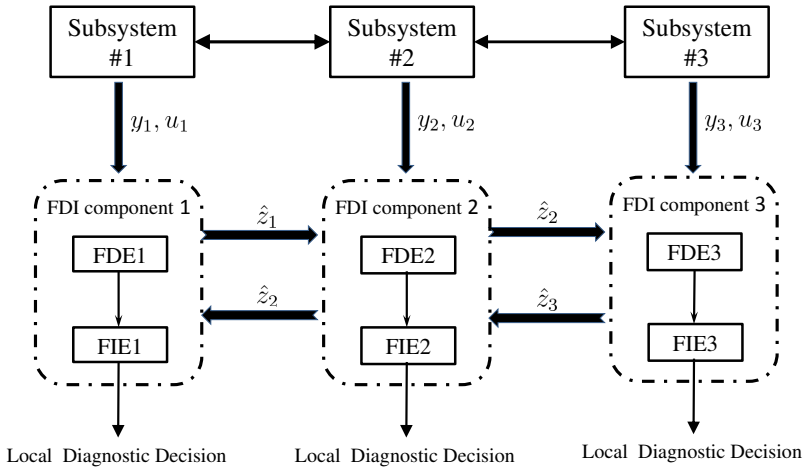

Figure 4.1: Example of distributed FDI architecture for three interconnected generators.

where $\hat{x}_{i1}$, $\hat{x}_{i2}$, and $\hat{y}_i$ denote the estimated local state and output variables of the ith generator, $i = 1, \cdots, M$, respectively, L_i is an estimator gain, $\hat{x}_i \stackrel{\triangle}{=} [\hat{x}_{i1} \quad y_i^\top]^\top$, and $\hat{x}_j \stackrel{\triangle}{=} [\hat{x}_{j1} \quad y_j^\top]^\top$ (here $\hat{x}_{j1}$ is the estimate of state variable x_{j1} of the jth interconnected generator). The initial conditions are $\hat{x}_{i1}(0) = 0$ and $\hat{x}_{i2}(0) = y_i(0)$. It is worth noting that the local FDE (4.7) for the ith generator is constructed based on local input and output variables (i.e., v_{fi} and y_i) and certain communicated information from the FDE associated with the jth directly interconnected generator (for instance, $\hat{x}_j$). Note that this structure is consistent with several others in the literature on distributed estimation and diagnosis in which information exchanges among subsystems are considered (see, e.g., [58, 60, 72, 20, 21]).

For each local FDE, let $\tilde{x}_{i1} \stackrel{\triangle}{=} x_{i1} - \hat{x}_{i1}$ and $\tilde{x}_{i2} \stackrel{\triangle}{=} x_{i2} - \hat{x}_{i2}$ denote the state estimation errors, and $\tilde{y}_i \stackrel{\triangle}{=} y_i - \hat{y}_i$ denote the output estimation error, respectively. Then, before fault occurrence (i.e., for $0 \leq t < T_i$), by using (4.4) and (4.7), the estimation error dynamics are

given by

$$\dot{\tilde{x}}_{i1} = \mathcal{A}_{i1}\tilde{x}_{i1} + d_i \tag{4.8}$$

$$\dot{\tilde{x}}_{i2} = \bar{\mathcal{A}}_{i4}\tilde{x}_{i2} + \mathcal{A}_{i3}\tilde{x}_{i1} + G_i\sum_{j=1}^{M}\gamma_{ij}[h_{ij}(x_i, x_j) - h_{ij}(\hat{x}_i, \hat{x}_j)] + \eta_i \tag{4.9}$$

$$\tilde{y}_i = x_{i2} - \hat{x}_{i2} = \tilde{x}_{i2} \tag{4.10}$$

where $\bar{\mathcal{A}}_{i4} \stackrel{\triangle}{=} \mathcal{A}_{i4} - L_i$. Specifically, the estimate gain matrix $L_i \in \Re^{2\times 2}$ can be chosen to make $\bar{\mathcal{A}}_{i4} = \text{diag}\{-\lambda_{i1},\ -\lambda_{i2}\}$ with the positive scalars λ_{i1} and λ_{i2}. By using (4.8) and (4.5), and by applying the triangle inequality, we obtain

$$|\tilde{x}_{i1}| \le \omega_{i0}e^{\mathcal{A}_{i1}t} + \int_0^t e^{\mathcal{A}_{i1}(t-\tau)}\bar{d}_i(y_i, u_i, \tau)d\tau\,, \tag{4.11}$$

where ω_{i0} is a constant bound for $|x_{i1}(0)|$, such that $|\tilde{x}_{i1}(0)| = |x_{i1}(0)| \le \omega_{i0}$ (Note $\hat{x}_{i1}(0) = 0$).

Now, we analyze the output estimation error $\tilde{y}_i(t)$ (see (4.10)) of the ith generator. For $0 \le t < T_i$, based on (4.9), we know the estimation errors of δ_i and ΔP_{ei} (i.e. $\tilde{x}_{i2}$) is given by

$$\begin{aligned}\tilde{x}_{i2}(t) = \int_0^t e^{\bar{\mathcal{A}}_{i4}(t-\tau)}\Big\{&\mathcal{A}_{i3}\tilde{x}_{i1}(\tau) + G_i\sum_{j=1}^{M}\gamma_{ij}[h_{ij}(x_i(\tau), x_j(\tau)) - h_{ij}(\hat{x}_i(\tau), \hat{x}_j(\tau))] \\ &+\eta_i(x_i(\tau), u_i(\tau), \tau)\Big\}d\tau\,.\end{aligned}$$

Note that for the interconnection effect from the jth directly connected generator, we have

$$|h_{ij}(x_i, x_j) - h_{ij}(\hat{x}_j, \hat{x}_j)| = |E'_{qi}E'_{qj}B_{ij}\cos(y_{i1} - y_{j1})(x_{j1} - \hat{x}_{j1})| \le |E'_{qi}E'_{qj}B_{ij}\cos(y_{i1} - y_{j1})|\,|\tilde{x}_{j1}|\,.$$

Therefore, based on the system model (4.4), for each component of the output estimation

error, (i.e., $\tilde{y}_{ip}(t), p = 1,\ 2$), we have

$$
\begin{aligned}
&|\tilde{y}_{i1}(t)| \leq \int_0^t e^{-\lambda_{i1}(t-\tau)}(|\tilde{x}_{i1}| + \eta_{i1})\, d\tau \leq \int_0^t e^{-\lambda_{i1}(t-\tau)}(\chi_i(\tau) + \bar{\eta}_{i1})\, d\tau\,, \\
&|\tilde{y}_{i2}(t)| \leq \int_0^t e^{-\lambda_{i2}(t-\tau)}\left[|E_{qi}^{'2} B_{ii}|\, \chi_i(\tau) + \bar{\eta}_{i2}(\tau) + \sum_{j=1}^{M} \gamma_{ij} |E_{qi}^{'} E_{qj}^{'} B_{ij} \cos(y_{i1}(\tau) - y_{j1}(\tau))|\, \chi_j(\tau)\right] d\tau\,,
\end{aligned}
\tag{4.12}
$$

where

$$
\chi_i(t) \stackrel{\triangle}{=} \omega_{i0} e^{\mathcal{A}_{i1} t} + \int_0^t e^{\mathcal{A}_{i1}(t-\tau)} \bar{d}_i(y_i, u_i, \tau) d\tau \ \ , i = 1,\, 2,\, \cdots M. \tag{4.13}
$$

Therefore, based on the above discussions, we have the following

Distributed Fault Detection Decision Scheme: *The decision on the occurrence of a fault (detection) in the ith generator is made when the modulus of at least one component of the output estimation error (i.e., $\tilde{y}_{ip}(t)$, $p = 1,\, 2$) generated by the local FDE exceeds its corresponding threshold $\nu_{ip}(t)$ given by*

$$
\begin{aligned}
\nu_{i1}(t) &\stackrel{\triangle}{=} \int_0^t e^{-\lambda_{i1}(t-\tau)}(\,\chi_i + \bar{\eta}_{i1})\, d\tau\,, \\
\nu_{i2}(t) &\stackrel{\triangle}{=} \int_0^t e^{-\lambda_{i2}(t-\tau)}\left[|E_{qi}^{'2} B_{ii}|\, \chi_i + \bar{\eta}_{i2} + \sum_{j=1}^{M} \gamma_{ij} |E_{qi}^{'} E_{qj}^{'} B_{ij} \cos(y_{i1} - y_{j1})|\, \chi_j\right] d\tau\,,
\end{aligned}
\tag{4.14}
$$

where $\chi_i(t)$ and $\chi_j(t)$ are defined by (4.13). The fault detection time T_d is defined as the first time instant such that $|\tilde{y}_{ip}(T_d)| > \nu_{ip}(T_d)$, for some $T_d \geq T_i$ and some $p \in \{1,\, 2\}$, that is, $T_d \stackrel{\triangle}{=} \inf \bigcup_{p=1}^{2} \{\, t \geq 0 :\ |\tilde{y}_{ip}(t)| > \nu_{ip}(t)\}$.

Remark 4.2. Note that $\nu_{ip}(t)$ given by (4.14) is an adaptive threshold for fault detection, which has obvious advantage over a constant one. Moreover, the threshold $\nu_{ip}(t)$ can be easily implemented using linear filtering techniques [83].

4.2.2 Fault Detectability Condition

The following theorem characterizes (in a non-closed form) the class of sensor faults that are detectable by the proposed distributed fault detection method.

Theorem 4.1 (Fault Detectability): *For the distributed fault detection method de-*

scribed by (4.7) and (4.14), suppose that a sensor fault occurs in the ith subsystem at time T_i, where $i \in \{1, \cdots, M\}$. Then, if there exist some time instant $T_d > T_i$ and some $p \in \{1,\ 2\}$, such that the sensor bias θ_i satisfies the following condition

$$\begin{aligned}
&\left| \int_{T_i}^{T_d} e^{-\lambda_{ip}(T_d-\tau)}(C_{ip}\mathcal{A}_{i3}\frac{\mathcal{A}_{i2}}{\mathcal{A}_{i1}} - C_{ip}L_i)\theta_i d\tau + \theta_{ip} \right| \\
&- \quad G_{ip}\int_{T_i}^{T_d} e^{-\lambda_{i2}(T_d-\tau)}\sum_{j=1}^{M}\gamma_{ij}(|E_{qi}^{'}E_{qj}^{'}B_{ij}\hat{x}_{j1}| + |E_{qi}^{'}\dot{E}_{qj}^{'}B_{ij}|)\,|\theta_{i1}|d\tau \\
&\geq \quad 2\nu_{ip}(T_d) + \int_{T_i}^{T_d} e^{-\lambda_{ip}(T_d-\tau)}\Bigg[|C_{ip}\mathcal{A}_{i3}||\frac{\mathcal{A}_{i2}}{\mathcal{A}_{i1}^2}\alpha_i|(1-e^{\mathcal{A}_{i1}(\tau-T_i)}) \\
&\quad +G_{ip}\sum_{j=1}^{M}\gamma_{ij}|E_{qi}^{'}E_{qj}^{'}B_{ij}|(1-|\cos(y_{i1}-y_{j1})|)\chi_j\Bigg]d\tau, \qquad (4.15)
\end{aligned}$$

where θ_{ip} is the pth component of θ_i, $C_{ip}^{\top} \in \Re^2$ is a constant vector with all entries being 0 except the pth entry (taking the value of 1), and G_{ip} is the pth component of G_i defined in (4.4), then the sensor fault will be detected at time $t = T_d$, i.e., $|\tilde{y}_{ip}(T_d)| > \nu_{ip}(T_d)$.

Proof: In the presence of a sensor fault (i.e., for $t \geq T_i$) in the ith generator, base on (4.4) and (4.7), the dynamics of the state estimation error $\tilde{x}_{i1} \stackrel{\triangle}{=} x_{i1} - \hat{x}_{i1}$ and $\tilde{x}_{i2} \stackrel{\triangle}{=} x_{i2} - \hat{x}_{i2}$ of the ith FDE satisfies

$$\dot{\tilde{x}}_{i1} = \mathcal{A}_{i1}\tilde{x}_{i1} - \mathcal{A}_{i2}\beta_i\theta_i + d_i \qquad (4.16)$$

$$\dot{\tilde{x}}_{i2} = \bar{\mathcal{A}}_{i4}\tilde{x}_{i2} + \mathcal{A}_{i3}\tilde{x}_{i1} + \eta_i - L_i\beta_i\theta_i + G_i\sum_{j=1}^{M}\gamma_{ij}\left[h_{ij}(x_i,x_j) - h_{ij}(\hat{x}_i,\hat{x}_j)\right]. \qquad (4.17)$$

Let $\xi_i \stackrel{\triangle}{=} \tilde{x}_{i1} - \frac{\mathcal{A}_{i2}}{\mathcal{A}_{i1}}\beta_i\theta_i$; from (4.16), we have

$$\dot{\xi}_i = \mathcal{A}_{i1}\xi_i + d_i - \frac{\mathcal{A}_{i2}}{\mathcal{A}_{i1}}\beta_i\dot{\theta}_i\,. \qquad (4.18)$$

Then, based on (4.18) and by using the triangular inequality, we obtain

$$\begin{aligned} |\xi_i(t)| &\leq \omega_{i0}e^{\mathcal{A}_{i1}t} + \int_0^t e^{\mathcal{A}_{i1}(t-\tau)}\bar{d}_i(y_i,u_i,\tau)d\tau + \left|\int_0^t e^{\mathcal{A}_{i1}(t-\tau)}\frac{\mathcal{A}_{i2}}{\mathcal{A}_{i1}}\beta_i\dot{\theta}_i d\tau\right| \\ &\leq \chi_i(t) + |\frac{\mathcal{A}_{i2}}{\mathcal{A}_{i1}^2}\beta_i\alpha_i|(1-e^{\mathcal{A}_{i1}(t-T_i)})\,, \end{aligned} \tag{4.19}$$

where α_i and $\chi_i(t)$ are defined in Assumption 4.3 and (4.13), respectively.

Now, let us consider the output estimation error. For the second component of the output estimation error (i.e., $\tilde{y}_{i2} = y_{i2} - \hat{y}_{i2}$), based on (4.17) and (4.4), we have

$$\begin{aligned} \tilde{y}_{i2}(t) &= C_{i2}\tilde{x}_{i2} + \beta_i C_{i2}\theta_i \\ &= \int_0^t e^{-\lambda_{i2}(t-\tau)}\Big[-E_{qi}^{'2}B_{ii}\,\tilde{x}_{i1} + \eta_{i2} - C_{i2}L_i\beta_i\theta_i + \sum_{j=1}^{M}\gamma_{ij}[h_{ij}(x_i,x_j) - h_{ij}(\hat{x}_i,\hat{x}_j)]\Big]d\tau \\ &\quad +\beta_i C_{i2}\theta_i\,. \end{aligned}$$

By using the definition of ξ_i (i.e., $\xi_i \stackrel{\triangle}{=} \tilde{x}_{i1} - \frac{\mathcal{A}_{i2}}{\mathcal{A}_{i1}}\beta_i\theta_i$) and applying again the triangular inequality, we have

$$\begin{aligned} |\tilde{y}_{i2}(t)| &\geq \left|\int_0^t e^{-\lambda_{i2}(t-\tau)}\big[-E_{qi}^{'2}B_{ii}\xi_i + (\frac{-E_{qi}^{'2}B_{ii}\mathcal{A}_{i2}}{\mathcal{A}_{i1}} - C_{i2}L_i)\beta_i\theta_i\big]d\tau + \beta_i C_{i2}\theta_i\right| \\ &\quad - \int_0^t e^{-\lambda_{i2}(t-\tau)}(\bar{\eta}_{i2} + \sum_{j=1}^{M}\gamma_{ij}|h_{ij}(x_i,x_j) - h_{ij}(\hat{x}_i,\hat{x}_j)|)d\tau \\ &\geq \left|\int_0^t e^{-\lambda_{i2}(t-\tau)}(\frac{-E_{qi}^{'2}B_{ii}\mathcal{A}_{i2}}{\mathcal{A}_{i1}} - C_{i2}L_i)\beta_i\theta_i d\tau + \beta_i C_{i2}\theta_i\right| - \int_0^t e^{-\lambda_{i2}(t-\tau)}|E_{qi}^{'2}B_{ii}|\,|\xi_i|d\tau \\ &\quad - \int_0^t e^{-\lambda_{i2}(t-\tau)}(\bar{\eta}_{i2} + \sum_{j=1}^{M}\gamma_{ij}|h_{ij}(x_i,x_j) - h_{ij}(\hat{x}_i,\hat{x}_j)|)d\tau\,. \end{aligned} \tag{4.20}$$

For the interconnection effect from the jth FDE, we have

$$\begin{aligned} h_{ij}(x_i,x_j) - h_{ij}(\hat{x}_i,\hat{x}_j) &= -E_{qi}^{'}E_{qj}^{'}B_{ij}[\cos(y_{i1} - \beta_i\theta_{i1} - y_{j1})x_{j1} - \cos(y_{i1} - y_{j1})\hat{x}_{j1}] \\ &\quad +E_{qi}^{'}\dot{E}_{qj}^{'}B_{ij}[\sin(y_{i1} - \beta_i\theta_{i1} - y_{j1}) - \sin(y_{i1} - y_{j1})]. \end{aligned} \tag{4.21}$$

The first term of the right hand side of (4.21) can be rewritten as follows:

$$\begin{aligned}
&-E_{qi}^{'}E_{qj}^{'}B_{ij}[\cos(y_{i1}-\beta_i\theta_{i1}-y_{j1})x_{j1}-\cos(y_{i1}-y_{j1})\hat{x}_{j1}] \\
=\ &-E_{qi}^{'}E_{qj}^{'}B_{ij}[\cos(y_{i1}-\beta_i\theta_{i1}-y_{j1})x_{j1}-\cos(y_{i1}-y_{j1})\hat{x}_{j1}+\cos(y_{i1}-\beta_i\theta_{i1}-y_{j1})\hat{x}_{j1} \\
&-\cos(y_{i1}-\beta_i\theta_{i1}-y_{j1})\hat{x}_{j1}] \\
=\ &-E_{qi}^{'}E_{qj}^{'}B_{ij}\Big\{\cos(y_{i1}-\beta_i\theta_{i1}-y_{j1})\tilde{x}_{j1}+[\cos(y_{i1}-\beta_i\theta_{i1}-y_{j1}) \\
&-\cos(y_{i1}-y_{j1})]\hat{x}_{j1}\Big\}. \qquad (4.22)
\end{aligned}$$

Note that $|\cos(y_{i1}-\beta_i\theta_{i1}-y_{j1})-\cos(y_{i1}-y_{j1})| \le |\beta_i\theta_i|$ and $|\sin(y_{i1}-\beta_i\theta_{i1}-y_{j1})-\sin(y_{i1}-y_{j1})| \le |\beta_i\theta_i|$. Thus, based on (4.21) and (4.22), we have

$$|h_{ij}(x_i,x_j)-h_{ij}(\hat{x}_i,\hat{x}_j)| \le |E_{qi}^{'}E_{qj}^{'}B_{ij}|(|\tilde{x}_{j1}|+|\beta_i\theta_{i1}|\,|\hat{x}_{j1}|)+|E_{qi}^{'}\dot{E}_{qj}^{'}B_{ij}|\,|\beta_i\theta_{i1}|\,. \qquad (4.23)$$

Based on (4.23), (4.20) and (4.19), we have

$$\begin{aligned}
|\tilde{y}_{i2}(t)| \ \ge\ & \left|\int_0^t e^{-\lambda_{i2}(t-\tau)}\Big(\frac{-E_{qi}^{'2}B_{ii}\mathcal{A}_{i2}}{\mathcal{A}_{i1}}-C_{i2}L_i\Big)\beta_i\theta_i d\tau+\beta_i\theta_{i2}\right| \\
&-\int_0^t e^{-\lambda_{i2}(t-\tau)}|E_{qi}^{'2}B_{ii}|\,\Big|\frac{\mathcal{A}_{i2}}{\mathcal{A}_{i1}^2}\beta_i\alpha_i\Big|(1-e^{\mathcal{A}_{i1}(\tau-T_i)})d\tau \\
&-\int_0^t e^{-\lambda_{i2}(t-\tau)}\sum_{j=1}^{M}\gamma_{ij}(|E_{qi}^{'}E_{qj}^{'}B_{ij}\hat{x}_{j1}|+|E_{qi}^{'}\dot{E}_{qj}^{'}B_{ij}|)\,|\beta_i\theta_{i1}|d\tau \\
&-\int_0^t e^{-\lambda_{i2}(t-\tau)}\left[|E_{qi}^{'2}B_{ii}|\,\chi_i+\bar{\eta}_{i2}+\sum_{j=1}^{M}\gamma_{ij}|E_{qi}^{'}E_{qj}^{'}B_{ij}|\,\chi_j\right]d\tau\,, \qquad (4.24)
\end{aligned}$$

where χ_i and χ_j are defined in (4.13). Based on the detection threshold given in (4.14), by

using the property of the step function $\beta_i(t-T_i)$, (4.24) can be rewritten as

$$
\begin{aligned}
|\tilde{y}_{i2}(t)| \;\geq\; & \left| \int_{T_i}^{t} e^{-\lambda_{i2}(t-\tau)} \left(\frac{-E_{qi}^{'2} B_{ii} \mathcal{A}_{i2}}{\mathcal{A}_{i1}} - C_{i2} L_i\right) \theta_i d\tau + \theta_{i2} \right| \\
& - \int_{T_i}^{t} e^{-\lambda_{i2}(t-\tau)} \left[|E_{qi}^{'2} B_{ii}| \left[\chi_i + |\frac{\mathcal{A}_{i2}}{\mathcal{A}_{i1}^2} \alpha_i| (1 - e^{\mathcal{A}_{i1}(\tau - T_i)})\right] + \bar{\eta}_{i2} + \sum_{j=1}^{M} \gamma_{ij} |E_{qi}^{'} E_{qj}^{'} B_{ij}| \, \chi_j \right] d\tau \\
& - \int_{T_i}^{t} e^{-\lambda_{i2}(t-\tau)} \sum_{j=1}^{M} \gamma_{ij} \left(|E_{qi}^{'} E_{qj}^{'} B_{ij} \hat{x}_{j1}| + |E_{qi}^{'} \dot{E}_{qj}^{'} B_{ij}|\right) |\theta_{i1}| d\tau. \qquad (4.25)
\end{aligned}
$$

Additionally, for the first component of output estimation error (i.e., $\tilde{y}_{i1}$), by following the similar reasoning logic as reported above, we have

$$
|\tilde{y}_{i1}(t)| \geq \left| \int_{T_i}^{t} e^{-\lambda_{i1}(t-\tau)} \left(\frac{\mathcal{A}_{i2}}{\mathcal{A}_{i1}} - C_{i1} L_i\right) \theta_i d\tau + \theta_{i1} \right| - \int_{T_i}^{t} e^{-\lambda_{i1}(t-\tau)} \left[\chi_i + |\frac{\mathcal{A}_{i2}}{\mathcal{A}_{i1}^2} \alpha_i| (1 - e^{\mathcal{A}_{i1}(\tau - T_i)}) + \bar{\eta}_{i1}\right] d\tau \,. \qquad (4.26)
$$

Based on (4.25) and (4.26), it can be easily seen that if there exists $T_d > T_i$, such that condition (4.15) is satisfied, then it is concluded that $|\tilde{y}_{ip}(T_d)| > \nu_{ip}(T_d)$, i.e., the fault is detected at time $t = T_d$.

□

The above analysis for the general case of incipient faults can be specified to the important case of abrupt faults. Specifically, we have the following results:

Corollary 4.1: *For the distributed fault detection method described by (4.7) and (4.14), suppose that a constant sensor bias occurs in the ith generator at time T_i, where $i \in \{1, \cdots, M\}$. Then, if there exist some time instant $T_d > T_i$ and some $p \in \{1,\ 2\}$, such that the constant sensor bias θ_i satisfies the following conditions:*

$$
|\theta_i| \geq \frac{N_{ip}(T_d) + 2\nu_{ip}(T_d)}{\sigma_{ip}(T_d)} \,, \qquad (4.27)
$$

where

$$\begin{aligned}\sigma_{ip} &\triangleq \left|\tfrac{C_{ip}}{\lambda_{ip}}(\tfrac{\mathcal{A}_{i3}\mathcal{A}_{i2}}{\mathcal{A}_{i1}} - L_i + I)(1 - e^{-\lambda_{ip}(T_d - T_i)})\right| \\ &\quad -G_{ip}\textstyle\int_{T_i}^{T_d} e^{-\lambda_{i2}(T_d-\tau)}\sum_{j=1}^{M}\gamma_{ij}(|E'_{qi}E'_{qj}B_{ij}\hat{x}_{j1}| + |E'_{qi}\dot{E}'_{qj}B_{ij}|)\,|C_{i1}|d\tau \\ N_{ip} &\triangleq \textstyle\int_{T_i}^{T_d} e^{-\lambda_{ip}(T_d-\tau)}G_{ip}\sum_{j=1}^{M}\gamma_{ij}|E'_{qi}E'_{qj}B_{ij}|(1 - |\cos(y_{i1} - y_{j1})|)\chi_j\, d\tau\,,\end{aligned}$$

and I is the identity matrix, then the sensor fault will be detected at time $t = T_d$, i.e., $|\tilde{y}_{ip}(T_d)| > \nu_{ip}(T_d)$.

Remark 4.3. According to Corollary 4.1, in the case of abrupt sensor faults, if the sensor bias magnitude θ_i is sufficiently large (i.e., it satisfies (4.27)) for some $T_d > T_i$, then the fault will be detected at T_d. Thus, Corollary 4.1 characterizes the class of abrupt sensor faults that are detectable by the distributed sensor fault detection method.

Remark 4.4. In the presence of a sensor fault in one of the generators of the power system, the fault effect may be propagated to other FDI components due to their interconnections through the transmission network. As a result, multiple residuals generated by several local FDEs may exceed their thresholds, indicating the occurrence of a sensor fault. Clearly, among a set of interconnected generators, the isolation of the particular generator where the sensor fault has actually occurred is an important research issue, which is investigated next.

4.2.3 Distributed Fault Isolation Method

Now, assume that a sensor bias fault occurred in sth generator is detected at some time T_d; accordingly, at $t = T_d$, the FIEs are activated. For $s = 1, \cdots, M$, the local FIE associated

with the sth generator is chosen as

$$\dot{\hat{x}}_{s1} = \mathcal{A}_{s1}\hat{x}_{s1} + \mathcal{A}_{s2}(y_s - \hat{\theta}_s) + \Omega_{s1}\dot{\hat{\theta}}_s \tag{4.28}$$

$$\dot{\hat{x}}_{s2} = \mathcal{A}_{s3}\hat{x}_{s1} + \mathcal{A}_{s4}\,\hat{x}_{s2} + G_s\frac{v_{fs}}{T'_{dos}} + L_s(y_s - \hat{y}_s) + \Omega_{s2}\dot{\hat{\theta}}_s + G_s\sum_{j=1}^{M}\gamma_{sj}h_{sj}(\hat{x}_s, \hat{x}_j) \tag{4.29}$$

$$\dot{\Omega}_{s1} = \mathcal{A}_{s1}\Omega_{s1} - \mathcal{A}_{s2} \tag{4.30}$$

$$\dot{\Omega}_{s2} = \bar{\mathcal{A}}_{s4}\Omega_{s2} - L_s \tag{4.31}$$

$$\hat{y}_s = \hat{x}_{s2} + \hat{\theta}_s\,, \tag{4.32}$$

where $\hat{x}_{s1}$, $\hat{x}_{s2}$, and $\hat{y}_s$ denote the estimated state and output variables provided by the local FIE, respectively, L_s is a design gain matrix (see (4.7)), $\hat{x}_s \stackrel{\triangle}{=} [\hat{x}_{s1} \quad (y_s - \hat{\theta}_s)^\top]^\top$, $\hat{x}_j \stackrel{\triangle}{=} [\hat{x}_{j1} \quad y_j^\top]^\top$, $\hat{x}_{j1}$ is from jth FDE, and $\hat{\theta}_s$ is the estimated sensor bias provided by the local isolation estimator. The initial conditions are $\hat{x}_{s1}(T_d) = 0$, $\hat{x}_{s2}(T_d) = 0$, $\Omega_{s1}(T_d) = 0$, and $\Omega_{s2}(T_d) = 0$. Note that the distributed FIE described by (4.28)-(4.32) for each local generator is constructed based on local measurements (i.e., v_{fs} and y_s) and certain communicated information (for instance, $\hat{x}_j$) from the FDI component associated with the jth directly interconnected generator.

The adaptive law for adjusting $\hat{\theta}_s$ is derived using the Lyapunov synthesis approach (see, for example, [35]). Specifically, the learning algorithm is given by

$$\dot{\hat{\theta}}_s = \mathcal{P}_{\Theta_s}\left\{\Gamma_s(\Omega_{s2} + I)^\top\tilde{y}_s\right\}, \tag{4.33}$$

where $\tilde{y}_s(t) \stackrel{\triangle}{=} y_s(t) - \hat{y}_s(t)$ denotes the output estimation error generated by the FIE associated with the sth generator, $\Gamma_s > 0$ is a symmetric, positive-definite learning rate matrix, and $\mathcal{P}_{\Theta_s}$ is the projection operator restricting $\hat{\theta}_s$ to the corresponding *known* set Θ_s (in order to guarantee stability of the learning algorithm in the presence of modeling uncertainty, as described in [35, 15]), and I is the identity matrix.

The distributed fault isolation decision scheme is based on the following intuitive principle: if a sensor fault occurs in the sth generator at time T_s and is detected at time T_d, then a

set of adaptive threshold functions $\{\mu_{sp}(t),\, p = 1,\, 2\,\}$ can be designed for the corresponding local isolation estimator, such that each component of its output estimation error satisfies $|\tilde{y}_{sp}(t)| \leq \mu_{sp}(t)$, for all $t \geq T_d$. Consequently, such a set of adaptive thresholds $\mu_{sp}(t)$, with $s = 1, \cdots, M$, can be associated with the output estimation error of each local isolation estimator. In the fault isolation procedure, if, for a particular local isolation estimator $r \in \{1, \cdots, M\}\backslash\{s\}$, there exists some $p \in \{1,\, 2\,\}$, such that the pth component of its output estimation error satisfies $|\tilde{y}_{rp}(t)| > \mu_{rp}(t)$ for some finite time $t > T_d$, then the possibility of the occurrence of the sensor fault in rth generator can be excluded. Based on this intuitive idea, we have the following

Distributed Fault Isolation Decision Scheme: *If, for each* $r \in \{1, \cdots, M\}\backslash\{s\}$*, there exist some finite time* $t^r > T_d$ *and some* $p \in \{1,\, 2\,\}$*, such that* $|\tilde{y}_{rp}(t^r)| > \mu_{rp}(t^r)$*, then the occurrence of the sensor bias fault in the* s*th generator is concluded.*

Remark 4.5. Note that the isolation of the faulty generator is conducted locally. In the distributed FDI architecture (see, for instance, Figure 4.1), a local FIE is associated with each generator. For a particular local generator, if at least one component of the residual generated by the local FIE exceed its threshold, then the case of a fault in the local generator is excluded. On the other hand, if all local FIE residual components remain below their corresponding thresholds, then the local FDI component determines that the local generator is faulty.

4.2.4 Adaptive Thresholds for Distributed Fault Isolation

The threshold functions $\mu_{sp}(t)$ clearly play a key role in the proposed distributed fault isolation decision scheme. To derive the adaptive threshold, we analyze the output estimation error of the matched sth local isolation estimator in the case that a sensor bias fault occurs to the sth generator.

Let us denote the state estimation error of the sth local isolation estimator associated with the sth generator by $\tilde{x}_{s1}(t) \stackrel{\triangle}{=} x_{s1}(t) - \hat{x}_{s1}(t)$ and $\tilde{x}_{s2}(t) \stackrel{\triangle}{=} x_{s2}(t) - \hat{x}_{s2}(t)$ and the output estimation error by $\tilde{y}_s \stackrel{\triangle}{=} y_s - \hat{y}_s$, respectively. By using (4.28)-(4.32) and (4.4), in the

presence of a sensor fault in the sth generator, for $t > T_d$, we have

$$\begin{aligned}
\dot{\tilde{x}}_{s1} &= \mathcal{A}_{s1}\tilde{x}_{s1} + \mathcal{A}_{s2}\tilde{\theta}_s - \Omega_{s1}\dot{\hat{\theta}}_s + d_s \qquad (4.34)\\
\dot{\tilde{x}}_{s2} &= \bar{\mathcal{A}}_{s4}\tilde{x}_{s2} + \mathcal{A}_{s3}\tilde{x}_{s1} + \eta_s + L_s\tilde{\theta}_s - \Omega_{s2}\dot{\hat{\theta}}_s \\
&\quad + G_s\sum_{j=1}^{M}\gamma_{sj}[h_{sj}(x_s, x_j) - h_{sj}(\hat{x}_s, \hat{x}_j)]\,, \qquad (4.35)
\end{aligned}$$

where $\bar{\mathcal{A}}_{s4}$ is defined in (4.9).

The following lemma provides a bounding function for the output estimation error corresponding to the local isolation estimator associated with the sth generator, in the case that a sensor fault occurs in this generator.

Lemma 4.1. *If a sensor fault in the sth generator is detected at time T_d, where $s \in \{1, \cdots, M\}$, then for all $t > T_d$, the pth component of the output estimation error generated by the local FIE for the sth generator satisfies*

$$\begin{aligned}
|\tilde{y}_{sp}(t)| \;\leq\; & \int_{T_d}^{t} e^{-\lambda_{sp}(t-\tau)}\Big[|C_{sp}\mathcal{A}_{s3}|(\rho_s + |\Omega_{s1}\tilde{\theta}_s|) + \bar{\eta}_{sp} + |C_{sp}\Omega_{s2}|\;\alpha_s \\
& + G_{sp}(\sum_{j=1}^{M}\gamma_{sj}|E'_{qs}E'_{qj}B_{sj}|\,\chi_j + \sum_{j=1}^{M}\gamma_{sj}(|\phi_{sj}| + |\psi_{sj}|)\tilde{\theta}_{s1})\Big]d\tau + \omega_{s2}e^{-\lambda_{sp}(t-T_d)} \\
& + |(C_{sp}\Omega_{s2} + C_{sp})^{\top}|\,|\tilde{\theta}_s|\,, \qquad (4.36)
\end{aligned}$$

where

$$\begin{aligned}
\phi_{sj}(t) &\triangleq E'_{qs}\dot{E}'_{qj}B_{sj}\sin(y_{s1} - y_{j1}) - E'_{qs}E'_{qj}B_{sj}\hat{x}_{j1}\cos(y_{s1} - y_{j1}) \\
\psi_{sj}(t) &\triangleq E'_{qs}\dot{E}'_{qj}B_{sj}\cos(y_{s1} - y_{j1}) + E'_{qs}E'_{qj}B_{sj}\hat{x}_{j1}\sin(y_{s1} - y_{j1})\,,
\end{aligned}$$

$\tilde{\theta}_s(t) \triangleq \hat{\theta}_s(t) - \theta_s(t)$ represents the fault parameter estimation error, θ_{s1} is the first component of θ_s, ω_{s2} is a positive constant satisfying $|x_{s2}(T_d)| \leq \omega_{s2}$, $C_{sp}^{\top} \in \Re^2$ is a constant vector with all entries being 0 except the pth entry (taking the value of 1), $\chi_j(t)$ is defined in (4.13),

$$\rho_s(t) \triangleq \int_{T_d}^{t} e^{\mathcal{A}_{s1}(t-\tau)}\big(\bar{d}_s(y_s, u_s, \tau) + |\Omega_{s1}|\alpha_s\big)d\tau + \bar{\omega}_{s0}e^{\mathcal{A}_{s1}(t-T_d)}\,, \qquad (4.37)$$

and $\bar{\omega}_{s0}$ is a constant bound satisfying $|\tilde{x}_{s1}(T_d)| \leq \bar{\omega}_{s0}$.

Proof: Consider the state estimation error $\tilde{x}_{s1}$ described by (4.34). By substituting $A_{s2} = -\dot{\Omega}_{s1} + \mathcal{A}_{s1}\Omega_{s1}$ (see (4.30)) into (4.34) and by letting $\bar{x}_{s1} \stackrel{\triangle}{=} \tilde{x}_{s1} + \Omega_{s1}\tilde{\theta}_s$, we obtain

$$\dot{\bar{x}}_{s1} = \mathcal{A}_{s1}\bar{x}_{s1} - \Omega_{s1}\dot{\theta}_s + d_s\,. \tag{4.38}$$

Therefore, the solution of (4.38) is given by

$$\bar{x}_{s1} \;=\; \int_{T_d}^{t} e^{\mathcal{A}_{s1}(t-\tau)}\big(d_s(x_s,u_s,\tau) - \Omega_{s1}\dot{\theta}_s\big)d\tau + e^{\mathcal{A}_{s1}(t-T_d)}\bar{x}_{s1}(T_d)\,. \tag{4.39}$$

By using (4.4), (4.39), Assumption 4.3, the definition of $\bar{x}_{s1}$, and the triangular inequality, we obtain

$$|\tilde{x}_{s1}| \;\le\; |\bar{x}_{s1}| + |\Omega_{s1}\tilde{\theta}_s| \;\le\; \rho_s + |\Omega_{s1}\tilde{\theta}_s|\,, \tag{4.40}$$

where ρ_s is defined in (4.37).

Now, let us consider the output estimation error $\tilde{y}_s$. By substituting $L_s = -\dot{\Omega}_{s2} + \bar{\mathcal{A}}_{s4}\Omega_{s2}$ (see (4.31)) into (4.35) and by letting $\bar{x}_{s2} \stackrel{\triangle}{=} \tilde{x}_{s2} + \Omega_{s2}\tilde{\theta}_s$, we obtain

$$\dot{\bar{x}}_{s2} = \bar{\mathcal{A}}_{s4}\bar{x}_{s2} + \mathcal{A}_{s3}\tilde{x}_{s1} + \eta_s - \Omega_{s2}\dot{\theta}_s + G_s\sum_{j=1}^{M}\gamma_{sj}\left[h_{sj}(x_s,x_j) - h_{sj}(\hat{x}_s,\hat{x}_j)\right]\,. \tag{4.41}$$

Define each component of the output estimation error generated by the sth FIE as $\tilde{y}_{sp} \stackrel{\triangle}{=} y_{sp} - \hat{y}_{sp}$, $p = 1,\, 2$. By using (4.32), (4.4), and the definition of $\bar{x}_{s2}(t)$, we have

$$\tilde{y}_{sp}(t) = C_{sp}\tilde{x}_{s2}(t) - C_{sp}\tilde{\theta}_s = C_{sp}\bar{x}_{s2}(t) - (C_{sp}\Omega_{s2} + C_{sp})\tilde{\theta}_s\,. \tag{4.42}$$

Next, let us consider the second component of the output estimation error (i.e., $\tilde{y}_{s2}$). Based on (4.41) and (4.42) as well as Assumptions 4.1 and 4.3, it can be shown that

$$\begin{aligned}|\tilde{y}_{s2}(t)| \;\le\; & \int_{T_d}^{t} e^{-\lambda_{s2}(t-\tau)}\Big[|E_{qs}'^{2}B_{ss}|\,|\tilde{x}_{s1}| + \bar{\eta}_{s2} + |C_{s2}\Omega_{s2}|\;\alpha_s + \sum_{j=1}^{M}\gamma_{sj}|h_{sj}(x_s,x_j) \\ & -h_{sj}(\hat{x}_s,\hat{x}_j)|\Big]d\tau + \omega_{s2}e^{-\lambda_{s2}(t-T_d)} + |(C_{s2}\Omega_{s2} + C_{s2})^{\top}|\,|\tilde{\theta}_s|\,,\end{aligned} \tag{4.43}$$

where ω_{s2} is a constant bound for $|x_{s2}(T_d)|$, such that $|\tilde{x}_{s2}(T_d)| = |x_{s2}(T_d)| \leq \omega_{s2}$ (Note $\hat{x}_{s2}(T_d) = 0$). Note that in the presence of a sensor fault in the sth generator, we have

$$\begin{aligned} h_{sj}(x_s, x_j) - h_{sj}(\hat{x}_s, \hat{x}_j) &= -E'_{qs}E'_{qj}B_{sj}[\cos(y_{s1} - \theta_{s1} - y_{j1})x_{j1} - \cos(y_{s1} - \hat{\theta}_{s1} - y_{j1})\hat{x}_{j1}] \\ &\quad + E'_{qs}\dot{E}'_{qj}B_{sj}[\sin(y_{s1} - \theta_{s1} - y_{j1}) - \sin(y_{s1} - \hat{\theta}_{s1} - y_{j1})] \\ &= -E'_{qs}E'_{qj}B_{sj}\Big\{[\cos(y_{s1} - \theta_{s1} - y_{j1}) - \cos(y_{s1} - \hat{\theta}_{s1} - y_{j1})]\hat{x}_{j1} \\ &\quad + \cos(y_{s1} - \theta_{s1} - y_{j1})\tilde{x}_{j1}\Big\} \\ &\quad + E'_{qs}\dot{E}'_{qj}B_{sj}[\sin(y_{s1} - \theta_{s1} - y_{j1}) - \sin(y_{s1} - \hat{\theta}_{s1} - y_{j1})]. \end{aligned}$$

Then, after some algebra manipulations, we have

$$\begin{aligned} h_{sj}(x_s, x_j) - h_{sj}(\hat{x}_s, \hat{x}_j) &= -E'_{qs}E'_{qj}B_{sj}\cos(y_{s1} - \theta_{s1} - y_{j1})\tilde{x}_{j1} + \phi_{sj}(\cos\theta_{s1} - \cos\hat{\theta}_{s1}) \\ &\quad - \psi_{sj}(\sin\theta_{s1} - \sin\hat{\theta}_{s1})\,, \end{aligned}$$

where ϕ_{sj} and ψ_{sj} are given in (4.36). Thus, by using the triangle inequality, we obtain

$$|h_{sj}(x_s, x_j) - h_{sj}(\hat{x}_j, \hat{x}_j)| \leq |E'_{qs}E'_{qj}B_{sj}||\tilde{x}_{j1}| + (|\phi_{sj}| + |\psi_{sj}|)|\tilde{\theta}_{s1}|\,. \tag{4.44}$$

Note that as defined in (4.29), $\hat{x}_j \stackrel{\triangle}{=} [\,\hat{x}_{j1} \;\; y_j^\top\,]^\top$ with $\hat{x}_{j1}$ being the state estimation provided by the jth FDE. Therefore, $\tilde{x}_{j1}$ in (4.44) satisfies

$$\dot{\tilde{x}}_{j1} = \mathcal{A}_{j1}\tilde{x}_{j1} + d_j\,. \tag{4.45}$$

Because (4.45) is in the same form of (4.8), we have $|\tilde{x}_{j1}(t)| \leq \chi_j(t)$, where χ_j is defined in (4.13).

Based on (4.43), (4.44) and (4.40), we have

$$|\tilde{y}_{s2}(t)| \leq \int_{T_d}^{t} e^{-\lambda_{s2}(t-\tau)}\Big[|E_{qs}^{'2}B_{ss}|(\rho_s+|\Omega_{s1}\tilde{\theta}_s|)+\bar{\eta}_{s2}+|C_{s2}\Omega_{s2}|\ \alpha_s+\sum_{j=1}^{M}\gamma_{sj}|E_{qs}^{'}E_{qj}^{'}B_{sj}|\,\chi_j$$
$$+\sum_{j=1}^{M}\gamma_{sj}(|\phi_{sj}|+|\psi_{sj}|)|\tilde{\theta}_{s1}|\Big]d\tau+\omega_{s2}e^{-\lambda_{s2}(t-T_d)}+|(C_{s2}\Omega_{s2}+C_{s2})^{\top}|\,|\tilde{\theta}_s|\,. \quad (4.46)$$

Analogously, for the first component of output estimation error (i.e., $\tilde{y}_{s1}$), by following the similar reasoning logic as reported above, we have

$$|\tilde{y}_{s1}(t)| \leq \int_{T_d}^{t} e^{-\lambda_{s1}(t-\tau)}\Big[\rho_s+|\Omega_{s1}\tilde{\theta}_s|+|C_{s1}\Omega_{s2}|\ \alpha_s+\bar{\eta}_{s1}\Big]d\tau+|(C_{s1}\Omega_{s2}+C_{s1})^{\top}|\,|\tilde{\theta}_s|+\omega_{s2}e^{-\lambda_{s1}(t-T_d)}\,. \quad (4.47)$$

Now the (4.36) follows directly from (4.46) and (4.47).

□

Although Lemma 4.1 provides a bounding function for the output estimation error corresponding to the local isolation estimator associated with the sth generator, in the case that a sensor fault occurs in the sth generator, it cannot be directly used as a threshold function for fault isolation, because $\tilde{\theta}_s(t)$ is not available (we do not assume the condition of persistency of excitation in this paper). However, as the estimate $\hat{\theta}_s$ belongs to the known compact set Θ_s, we have $\left|\theta_{sp}-\hat{\theta}_{sp}(t)\right| \leq \kappa_{sp}(t)$, $p=1,\ 2$, for a suitable $\kappa_s(t) \stackrel{\triangle}{=} [\,\kappa_{s1}(t)\ \ \kappa_{s2}(t)\,]^{\top}$ depending on the geometric properties of set Θ_s (see, e.g., [84]). Hence, the following threshold function for fault isolation can be chosen:

$$\mu_{sp}(t) = \int_{T_d}^{t} e^{-\lambda_{sp}(t-\tau)}\Big[|C_{sp}\mathcal{A}_{s3}|(\rho_s+|\Omega_{s1}|\kappa_s)+\bar{\eta}_{sp}+|C_{sp}\Omega_{s2}|\ \alpha_s+G_{sp}\sum_{j=1}^{M}\gamma_{sj}|E_{qs}^{'}E_{qj}^{'}B_{sj}|\,\chi_j$$
$$+G_{sp}\sum_{j=1}^{M}\gamma_{sj}(|\phi_{sj}|+|\psi_{sj}|)\kappa_{s1}\Big]d\tau+\omega_{s2}e^{-\lambda_{sp}(t-T_d)}+|(C_{sp}\Omega_{sp}+C_{sp})^{\top}|\,\kappa_s\,. \quad (4.48)$$

Remark 4.6. Note that the adaptive threshold $\mu_{sp}(t)$ can be easily implemented on-line using linear filtering techniques (see [83]). The constant bounds $\bar{\omega}_{s0}$ and ω_{s2} are (possibly conservative) bounds for the unknown initial conditions $x_{s1}(T_d)$ and $x_{s2}(T_d)$, respectively.

However, note that, since the effect of these bounds decreases exponentially (i.e., $\bar{\omega}_{s0}$ is multiplied by $e^{\mathcal{A}_{s1}(t-T_d)}$, and ω_{s2} is multiplied by $e^{-\lambda_{sp}(t-T_d)}$, the practical use of such conservative bounds will not affect significantly the performance of the distributed fault isolation algorithm.

4.3 Analytical Properties of the Distributed Fault Isolation Method

As is well known in the fault diagnosis literature, there is an inherent tradeoff between robustness and fault sensitivity. In this section, we analyze the fault isolability of the distributed sensor fault diagnosis method. In addition, the stability and learning capability of the adaptive isolation estimators are also investigated.

4.3.1 Fault Isolability Analysis

For our purpose, a fault in each generator is considered to be *isolable* if the distributed fault isolation scheme is able to reach a correct decision in finite time. Intuitively, faults are isolable if they are *mutually different* according to a certain measure quantifying the difference in the effects that different faults have on measurable outputs and on the estimated quantities in the isolation scheme. To quantify this concept, we introduce the *fault mismatch function* [83] between a sensor fault occurred in the sth generator and a sensor fault occurred in the rth generator:

$$\begin{aligned} h_p^{rs}(t) \triangleq\ & (C_{rp}\Omega_{r2}+C_{rp})\hat{\theta}_r - G_{rp}\int_{T_d}^{t} e^{-\lambda_{rp}(t-\tau)}\sum_{j=1}^{M}\gamma_{rj}[\phi_{rj}(\cos\vartheta_j^s-\cos\hat{\theta}_{r1}) \\ & +\psi_{rj}(\sin\vartheta_j^s+\sin\hat{\theta}_{r1})]d\tau, \end{aligned} \tag{4.49}$$

where ϕ_{rj} and ψ_{rj} are defined in (4.36), $r,s=1,\cdots,M$, $r\neq s$, $p\in\{1,\ \ 2\}$, $\hat{\theta}_{r1}$ is the first component of $\hat{\theta}_r$, and $\vartheta^s\in R^M$ is a vector with only its sth component being non-zero (i.e., $\vartheta_s^s=\theta_{s1}$ and $\vartheta_r^s=0$), respectively. From a qualitative point of view, $h_p^{rs}(t)$ can be

interpreted as a filtered version of the difference between the effect of a sensor fault in the sth generator on the rth FIE and the estimated sensor fault provided by the rth FIE whose structure does not match the actual fault scenario. Therefore, the fault mismatch function $h_p^{rs}(t)$, defined as the ability of the rth local FIE to learn the effect of the sensor fault in the sth generator, offers a measure of the difference between the sensor fault occurred in the sth generator and the sensor fault occurred in the rth generator.

The following theorem characterizes in an implicit way the class of isolable faults in each generator:

Theorem 4.2. (Fault Isolability) *Consider the distributed fault isolation scheme described by (4.28)- (4.32) and (4.48). Suppose that a sensor fault occurring in the sth generator is detected at time T_d. Then, fault s is isolable if, for each $r \in \{1, \cdots, M\}\backslash\{s\}$, there exist some time $t^r > T_d$ and some $p \in \{1, \ 2\}$ such that the fault mismatch function $h_p^{rs}(t^r)$ satisfies*

$$\begin{aligned} |h_p^{rs}(t^r)| \ \geq \ & \int_{T_d}^{t} e^{-\lambda_{rp}(t-\tau)} \Bigg\{ |C_{rp}\mathcal{A}_{r3}| \left(\chi_r + |\Omega_{r1}\hat{\theta}_r|\right) + \bar{\eta}_{rp} + G_{rp}\Bigg[\sum_{j=1}^{M} \gamma_{rj} |E_{qr}^{'} E_{qj}^{'} B_{rj}| \, |\chi_j| \\ & + \gamma_{rs} |E_{qr}^{'} E_{qs}^{'} B_{rs}| \left(|\frac{\mathcal{A}_{s2}}{\mathcal{A}_{s1}^2}\alpha_s|(1 - e^{\mathcal{A}_{s1}(\tau - T_s)}) + |\frac{\mathcal{A}_{s2}}{\mathcal{A}_{s1}}\theta_s| \right) \Bigg] \Bigg\} d\tau \\ & + \omega_{r2} e^{-\lambda_{rp}(t-T_d)} + \mu_{rp}(t) \, . \end{aligned} \tag{4.50}$$

Proof: Denote the state estimation errors of the rth local isolation estimator associated with the rth generator by $\tilde{x}_{r1}(t) \stackrel{\triangle}{=} x_{r1}(t) - \hat{x}_{r1}(t)$ and $\tilde{x}_{r2}(t) \stackrel{\triangle}{=} x_{r2}(t) - \hat{x}_{r2}(t)$. By using (4.28)-(4.32) and (4.4), in the presence of a sensor fault in the sth generator, for $t > T_d$, we have

$$\dot{\tilde{x}}_{r1} = \mathcal{A}_{r1}\tilde{x}_{r1} + \mathcal{A}_{r2}\hat{\theta}_r - \Omega_{r1}\dot{\hat{\theta}}_r + d_r \tag{4.51}$$

$$\begin{aligned} \dot{\tilde{x}}_{r2} = \ & \bar{\mathcal{A}}_{r4}\tilde{x}_{r2} + \mathcal{A}_{r3}\tilde{x}_{r1} + L_r\hat{\theta}_r - \Omega_{r2}\dot{\hat{\theta}}_r + \eta_r \\ & + G_r \sum_{j=1}^{M} \gamma_{rj} \left[h_{rj}(x_r, x_j) - h_{rj}(\hat{x}_r, \hat{x}_j) \right] . \end{aligned} \tag{4.52}$$

Then, based on (4.51), by using the same reasoning logic as reported in the proof of Lemma 4.1 (see (4.38)), we have

$$\dot{\bar{x}}_{r1} = \mathcal{A}_{r1}\bar{x}_{r1} + d_r \tag{4.53}$$

$$\dot{\bar{x}}_{r2} = \bar{\mathcal{A}}_{r4}\bar{x}_{r2} + \mathcal{A}_{r3}\tilde{x}_{r1} + \eta_r + G_r\sum_{j=1}^{M}\gamma_{rj}\left[h_{rj}(x_r, x_j) - h_{rj}(\hat{x}_r, \hat{x}_j)\right], \tag{4.54}$$

where $\bar{x}_{r1} \stackrel{\triangle}{=} \tilde{x}_{r1} + \Omega_{r1}\hat{\theta}_r$ and $\bar{x}_{r2} \stackrel{\triangle}{=} \tilde{x}_{r2} + \Omega_{r2}\hat{\theta}_r$. Note that (4.53) is in the same form as (4.45). Therefore, from the proof of Lemma 4.1 and the definition of $\bar{x}_{r1}$, we obtain

$$|\tilde{x}_{r1}| \leq |\bar{x}_{r1}| + |\Omega_{r1}\hat{\theta}_r| \leq \chi_r + |\Omega_{r1}\hat{\theta}_r|, \tag{4.55}$$

where χ_r is defined in (4.13).

Now, let us analyze the estimation error of the interconnection term $\sum_{j=1}^{M}\gamma_{rj}[h_{rj}(x_r, x_j) - h_{rj}(\hat{x}_r, \hat{x}_j)]$ in (4.52). First, note that in the presence of a sensor fault in the sth generator,

we have

$$
\begin{aligned}
h_{rs}(x_r, x_s) - h_{rs}(\hat{x}_r, \hat{x}_s) &= E'_{qr}\dot{E}'_{qs}B_{rs}[\sin(y_{r1} - (y_{s1} - \vartheta^s_s)) - \sin(y_{r1} - \hat{\theta}_{r1} - y_{s1})] \\
&\quad -E'_{qr}E'_{qs}B_{rs}[\cos(y_{r1} - (y_{s1} - \vartheta^s_s))x_{s1} - \cos(y_{r1} - \hat{\theta}_{r1} - y_{s1})\hat{x}_{s1}] \\
&= E'_{qr}\dot{E}'_{qs}B_{rs}[\sin(y_{r1} - y_{s1} + \vartheta^s_s) - \sin(y_{r1} - \hat{\theta}_{r1} - y_{s1})] \\
&\quad -E'_{qr}E'_{qs}B_{rs}\Big\{[\cos(y_{r1} - y_{s1} + \vartheta^s_s) - \cos(y_{r1} - \hat{\theta}_{r1} - y_{s1})]\hat{x}_{s1} \\
&\quad + \cos(y_{r1} - y_{s1} + \vartheta^s_s)\tilde{x}_{s1}\Big\} \\
&= [E'_{qr}\dot{E}'_{qs}B_{rs}\sin(y_{r1} - y_{s1}) - E'_{qr}E'_{qs}B_{rs}\hat{x}_{s1}\cos(y_{r1} - y_{s1})] \cdot \\
&\quad (\cos\vartheta^s_s - \cos\hat{\theta}_{r1}) \\
&\quad +[E'_{qr}\dot{E}'_{qs}B_{rs}\cos(y_{r1} - y_{s1}) + E'_{qr}E'_{qs}B_{rs}\hat{x}_{s1}\sin(y_{r1} - y_{s1})] \cdot \\
&\quad (\sin\vartheta^s_s + \sin\hat{\theta}_{r1}) - E'_{qr}E'_{qs}B_{rs}\cos(y_{r1} - y_{s1} + \vartheta^s_s)\tilde{x}_{s1} \\
&= \phi_{rs}(\cos\vartheta^s_s - \cos\hat{\theta}_{r1}) + \psi_{rs}(\sin\vartheta^s_s + \sin\hat{\theta}_{r1}) \\
&\quad -E'_{qr}E'_{qs}B_{rs}\cos(y_{r1} - y_{s1} + \vartheta^s_s)\tilde{x}_{s1}\,, \qquad (4.56)
\end{aligned}
$$

where ϕ_{rs} and ψ_{rs} are defined in (4.36).

Second, the estimation error of the interconnection effect from the kth healthy generator, $k \in \{1, \cdots, M\}\backslash\{s,\, r\}$, can be represented as follows

$$
\begin{aligned}
\sum_{\substack{k=1\\k\neq s}}^{M}\gamma_{rk}[h_{rk}(x_r, x_k) - h_{rk}(\hat{x}_r, \hat{x}_k)] &= \sum_{\substack{k=1\\k\neq s}}^{M}\gamma_{rk}E'_{qr}\dot{E}'_{qk}B_{rk}\Big[\sin(y_{r1} - (y_{k1} - \vartheta^s_k)) \\
&\quad - \sin(y_{r1} - \hat{\theta}_{r1} - y_{k1})\Big] \\
&\quad -\sum_{\substack{k=1\\k\neq s}}^{M}\gamma_{rk}E'_{qr}E'_{qk}B_{rk}\Big[\cos(y_{r1} - (y_{k1} - \vartheta^s_k))x_{k1} \\
&\quad - \cos(y_{r1} - \hat{\theta}_{r1} - y_{k1})\hat{x}_{k1}\Big]\,.
\end{aligned}
$$

By using a similar reasoning logic reported as in (4.56), we have

$$\sum_{\substack{k=1\\k\neq s}}^{M}\gamma_{rk}[h_{rk}(x_r,x_k)-h_{rk}(\hat{x}_r,\hat{x}_k)] = \sum_{\substack{k=1\\k\neq s}}^{M}\gamma_{rk}\Big[\phi_{rk}(\cos\vartheta_k^s-\cos\hat{\theta}_{r1})+\psi_{rk}(\sin\vartheta_k^s+\sin\hat{\theta}_{r1}) -E_{qr}^{'}E_{qk}^{'}B_{rk}\cos(y_{r1}-y_{k1}+\vartheta_k^s)\tilde{x}_{k1}\Big], \quad (4.57)$$

where ϕ_{rk} and ψ_{rk} are defined in (4.36), and ϑ_k^s is the kth component of ϑ^s defined in (4.49). Therefore, based on (4.56) and (4.57), we can obtain

$$\sum_{j=1}^{M}\gamma_{rj}[h_{rj}(x_r,x_j)-h_{rj}(\hat{x}_r,\hat{x}_j)] = \sum_{j=1}^{M}\gamma_{rj}[\phi_{rj}(\cos\vartheta_j^s-\cos\hat{\theta}_{r1})+\psi_{rj}(\sin\vartheta_j^s+\sin\hat{\theta}_{r1}) -E_{qr}^{'}E_{qj}^{'}B_{rj}\cos(y_{r1}-y_{j1}+\vartheta_j^s)\tilde{x}_{j1}]. \quad (4.58)$$

Then, based on (4.58) and (4.54), we have

$$\dot{\tilde{x}}_{r2} = \bar{\mathcal{A}}_{r4}\bar{x}_{r2}+\mathcal{A}_{r3}\tilde{x}_{r1}+\eta_r+G_r\sum_{j=1}^{M}\gamma_{rj}\Big\{\phi_{rj}(\cos\vartheta_j^s-\cos\hat{\theta}_{r1})+\psi_{rj}(\sin\vartheta_j^s+\sin\hat{\theta}_{r1}) -E_{qr}^{'}E_{qj}^{'}B_{rj}\cos(y_{r1}-y_{j1}+\vartheta_j^s)\tilde{x}_{j1}\Big\}. \quad (4.59)$$

Now, let us consider the pth component of the output estimation error (i.e., $\tilde{y}_{rp}\stackrel{\triangle}{=}y_{rp}-\hat{y}_{rp}$). By using (4.32), (4.4), and the definition of $\bar{x}_{r2}(t)$, we have

$$\tilde{y}_{rp}(t)=C_{rp}\tilde{x}_{r2}(t)-C_{rp}\hat{\theta}_r=C_{rp}\bar{x}_{r2}(t)-(C_{rp}\Omega_{r2}+C_{rp})\hat{\theta}_r\,.$$

Thus, based on the above equation and (4.59), we can obtain

$$\tilde{y}_{rp}(t) = G_{rp}\int_{T_d}^{t}e^{-\lambda_{rp}(t-\tau)}\sum_{j=1}^{M}\gamma_{rj}[\phi_{rj}(\cos\vartheta_j^s-\cos\hat{\theta}_{r1})+\psi_{rj}(\sin\vartheta_j^s+\sin\hat{\theta}_{r1})]d\tau +\int_{T_d}^{t}e^{-\lambda_{rp}(t-\tau)}[C_{rp}\mathcal{A}_{r3}\tilde{x}_{r1}+\eta_{rp}-G_{rp}\sum_{j=1}^{M}\gamma_{rj}E_{qr}^{'}E_{qj}^{'}B_{rj}\cos(y_{r1}-y_{j1}+\vartheta_j^s)\tilde{x}_{j1}]d\tau -(C_{rp}\Omega_{r2}+C_{rp})\hat{\theta}_r+C_{rp}\tilde{x}_{r2}(T_d)e^{-\lambda_{rp}(t-T_d)}\,. \quad (4.60)$$

Therefore, based on (4.59) and (4.60), by using the triangle inequality, we can obtain

$$|\tilde{y}_{rp}(t)| \geq |h_p^{rs}(t)| - \int_{T_d}^{t} e^{-\lambda_{rp}(t-\tau)}[|C_{rp}\mathcal{A}_{r3}|\,|\tilde{x}_{r1}| + \bar{\eta}_{rp} + G_{rp}\sum_{j=1}^{M}\gamma_{rj}|E_{qr}^{'}E_{qj}^{'}B_{rj}|\,|\tilde{x}_{j1}|\,]d\tau + \omega_{r2}e^{-\lambda_{rp}(t-T_d)}\,. \tag{4.61}$$

In the presence of a sensor fault in the sth generator, based on some similar reasoning logic as reported in the proof of Lemma 4.1 (see (4.45)), and (4.19), we can obtain

$$|\tilde{x}_{s1}| \leq \chi_s + |\frac{\mathcal{A}_{s2}}{\mathcal{A}_{s1}^2}\alpha_s|(1 - e^{\mathcal{A}_{s1}(t-T_s)}) + |\frac{\mathcal{A}_{s2}}{\mathcal{A}_{s1}}\theta_s|\,, \tag{4.62}$$

and

$$|\tilde{x}_{j1}| \leq \chi_j\,, \qquad\qquad r \in \{1, \cdots, M\}\backslash\{s\}, \tag{4.63}$$

where χ_j is defined in (4.13). Therefore, based on (4.61), (4.62), (4.63), and (4.55), we have

$$\begin{aligned} |\tilde{y}_{rp}(t)| \geq\ & |h_p^{rs}(t)| - \int_{T_d}^{t} e^{-\lambda_{rp}(t-\tau)}\Big\{|C_{rp}\mathcal{A}_{r3}|\,(\chi_r + |\Omega_{r1}\hat{\theta}_r|) + \bar{\eta}_{rp} \\ & + G_{rp}\Big[\sum_{j=1}^{M}\gamma_{rj}|E_{qr}^{'}E_{qj}^{'}B_{rj}|\,|\chi_j| \\ & + \gamma_{rs}|E_{qr}^{'}E_{qs}^{'}B_{rs}|\,\big(|\frac{\mathcal{A}_{s2}}{\mathcal{A}_{s1}^2}\alpha_s|(1 - e^{\mathcal{A}_{s1}(\tau-T_s)}) + |\frac{\mathcal{A}_{s2}}{\mathcal{A}_{s1}}\theta_s|\big)\Big]\Big\}d\tau \\ & - \omega_{r2}e^{-\lambda_{rp}(t-T_d)}\,. \end{aligned} \tag{4.64}$$

Therefore, by taking into account the corresponding adaptive threshold μ_{rp} given in (4.48) for the FIE associated with the rth generator, we can conclude that, if condition (4.50) is satisfied at time $t = t^r$, we obtain $|\tilde{y}_{rp}(t^r)| > \mu_{rp}(t^r)$, which implies that the possibility of the occurrence of a sensor fault in rth generator can be excluded at time $t = t^r$.

□

Remark 4.7. According to the above theorem, if, for each $r \in \{1, \cdots, M\}\backslash\{s\}$, the fault mismatch function $h_p^{rs}(t^r)$ satisfies condition (4.50) for some time $t^r > 0$, then the pth component of the output estimation error generated by the rth FIE associated with

the rth generator would exceed its corresponding adaptive threshold at time $t = t^r$, i.e., $|\tilde{y}_{rp}(t^r)| > \mu_{rp}(t^r)$, hence excluding the occurrence of a sensor fault in the rth generator. Therefore, Theorem 4.2 characterizes (in a non-closed form) the class of sensor faults that are isolable in each generator by the proposed robust distributed FDI scheme.

4.3.2 Stability and Learning Capability

We now investigate the *stability and learning properties* of the adaptive fault isolation estimators, which are described by the following result:

Theorem 4.3. (Stability and Learning Capability): *Suppose that a sensor fault occurs in the sth generator at time T_s, where $s \in \{1, \cdots, M\}$. Then, the distributed fault isolation scheme described by (4.28)-(4.32) and (4.48) guarantees that,*

- *for each local fault isolation estimator q, $q = 1, \cdots, M$, the estimate variables $\hat{x}_{q1}(t)$, $\hat{x}_{q2}(t)$, and $\hat{\theta}_q(t)$ are uniformly bounded;*
- *there exist a positive constant $\bar{\kappa}_s$ and a bounded function $\bar{\zeta}_s(t)$, such that, for all finite time $t_f > T_d$, the output estimation error of the matched sth local isolation estimator satisfies*

$$\int_{T_d}^{t_f} |\tilde{y}_s(t)|^2 dt \leq \bar{\kappa}_s + 2\int_{T_d}^{t_f} |\bar{\zeta}_s(t)|^2 dt\,. \tag{4.65}$$

Proof: Let us first address the signal boundedness property. The state estimation error and output estimation error of the FIE for the qth generator are defined as $\tilde{x}_{q1} \stackrel{\triangle}{=} x_{q1}(t) - \hat{x}_{q1}(t)$, $\tilde{x}_{q2}(t) \stackrel{\triangle}{=} x_{q2}(t) - \hat{x}_{q2}(t)$, and $\tilde{y}_q \stackrel{\triangle}{=} y_q(t) - \hat{y}_q(t)$, respectively. First, let us consider the FIE associated with sth generator (i.e., $q = s$). By using the similar reasoning logic as reported in the proof of Lemma 4.1 (see (4.38) and (4.41)), we have

$$\dot{\tilde{x}}_{q1} = \mathcal{A}_{q1}\bar{x}_{q1} - \Omega_{q1}\dot{\theta}_q + d_q \tag{4.66}$$

$$\dot{\tilde{x}}_{q2} = \bar{\mathcal{A}}_{q4}\bar{x}_{q2} + \mathcal{A}_{q3}\tilde{x}_{q1} + \eta_q - \Omega_{q2}\dot{\theta}_q + G_q\sum_{j=1}^{M}\gamma_{qj}\left[h_{qj}(x_q, x_j) - h_{qj}(\hat{x}_q, \hat{x}_j)\right]\,, \tag{4.67}$$

where $\bar{x}_{q1} \stackrel{\triangle}{=} \tilde{x}_{q1} + \Omega_{q1}\tilde{\theta}_q$ and $\bar{x}_{q2} \stackrel{\triangle}{=} \tilde{x}_{q2} + \Omega_{q2}\tilde{\theta}_q$.

Since d_q, Ω_{q1} and $\dot{\theta}_q$ are bounded (Assumption 4.1 and Assumption 4.3) and $\mathcal{A}_{q1}$ is stable, we obtain $\bar{x}_{q1} \in L_\infty$ based on (4.66). Moreover, due to the use of parameter projection (see (4.33)), we have $\hat{\theta}_q \in L_\infty$. Therefore, based on Assumption 4.2 and the definition of $\bar{x}_{q1}$, we know that $\tilde{x}_{q1} \in L_\infty$, and $\hat{x}_{q1} \in L_\infty$. Then, based on a similar analysis of the dynamics of the state estimation error $\tilde{x}_{j1} \triangleq x_{j1} - \hat{x}_{j1}$ of the jth FDE, we have $\tilde{x}_{j1} \in L_\infty$ and $\hat{x}_{j1} \in L_\infty$. Thus, we know ϕ_{qj} and ψ_{qj} are bounded (see, (4.36)). Additionally, based on a similar reasoning logic as reported in the proof of Lemma 4.1 (see (4.44)), we know that and $h_{qj}(x_q, x_j) - h_{qj}(\hat{x}_q, \hat{x}_j)$ is bounded. Furthermore, because η_q, Ω_{q2} and $\dot{\theta}_q$ are bounded (Assumption 4.1 and Assumption 4.3) and $\bar{\mathcal{A}}_{q4}$ is stable, by using (4.67), we can obtain $\bar{x}_{q2} \in L_\infty$. Owing to the definition of $\bar{x}_{q2}$, we conclude that $\tilde{x}_{q2} \in L_\infty$ and $\hat{x}_{q2} \in L_\infty$.
Now, let us consider the FIEs associated with healthy generators (i.e., $q \in \{1, \cdots, M\} \backslash \{s\}$,). By using the similar reasoning logic as reported in the proof of Theorem 4.2 (see (4.53) and (4.54)), we have

$$\begin{aligned} \dot{\bar{x}}_{q1} &= \mathcal{A}_{q1}\bar{x}_{q1} + d_q & (4.68) \\ \dot{\bar{x}}_{q2} &= \bar{\mathcal{A}}_{q4}\bar{x}_{q2} + \mathcal{A}_{q3}\tilde{x}_{q1} + \eta_q + G_q \sum_{j=1}^{M} \gamma_{qj} \left[h_{qj}(x_q, x_j) - h_{qj}(\hat{x}_q, \hat{x}_j) \right] , & (4.69) \end{aligned}$$

where $\bar{x}_{q1} \triangleq \tilde{x}_{q1} + \Omega_{q1}\hat{\theta}_q$ and $\bar{x}_{q2} \triangleq \tilde{x}_{q2} + \Omega_{q2}\hat{\theta}_q$. Then, based on a similar reasoning logic as reported above, we can conclude that $\hat{\theta}_q \in L_\infty$, $\hat{x}_{q1} \in L_\infty$ and $\hat{x}_{q2} \in L_\infty$. This concludes the first part of the theorem.
Now, let us prove the second part of the theorem concerning the learning capability of the qth FIE in the case that it matches the occurred sensor fault in the sth generator, i.e., $q = s$. In this case, the solution of (4.67) can be written as $\bar{x}_{s2}(t) = \zeta_{s1}(t) + \zeta_{s2}(t)$, $\forall t \geq T_d$, where ζ_{s1} and ζ_{i2} are the solutions of the following differential equations, respectively:

$$\begin{aligned} \dot{\zeta}_{s1} &= \bar{\mathcal{A}}_{s4}\zeta_{s1} + \mathcal{A}_{s3}\tilde{x}_{s1} + \eta_s - \Omega_{s2}\dot{\theta}_s + G_s \sum_{j=1}^{M} \gamma_{sj} \left[h_{sj}(x_s, x_j) - h_{sj}(\hat{x}_s, \hat{x}_j) \right] , \quad \zeta_{s1}(T_d) = 0 \\ \dot{\zeta}_{s2} &= \bar{\mathcal{A}}_{s4}\zeta_{s2} , \quad \zeta_{s2}(T_d) = \tilde{x}_{s2}(T_d) = x_{s2}(T_d) . \end{aligned} \tag{4.70}$$

Using the definition of $\bar{x}_{s2}$, we have $\tilde{x}_{s2} = \zeta_{s1}(t) + \zeta_{s2}(t) - \Omega_{s2}\tilde{\theta}_s$. Therefore,

$$\tilde{y}_s(t) = \tilde{x}_{s2} - \tilde{\theta}_s = [\zeta_{s1}(t) + \zeta_{s2}(t)] - (\Omega_{s2} + I)\tilde{\theta}_s\,. \tag{4.71}$$

Now, consider a Lyapunov function candidate $V_s = \frac{1}{2\Gamma_s}\tilde{\theta}_s^\top\tilde{\theta}_s + \int_t^\infty |\zeta_{s2}(\tau)|^2 d\tau$. The time derivative of V_s along the solution of (4.33) is given by $\dot{V}_s = \frac{1}{\Gamma_s}\tilde{\theta}_s^\top \mathcal{P}_{\Theta_s}\left\{\Gamma_s(\Omega_{s2} + I)^\top \tilde{y}_s\right\} - |\zeta_{s2}|^2 - \frac{1}{\Gamma_s}\tilde{\theta}_s^\top\dot{\theta}_s$. Clearly, since $\theta_s \in \Theta_s$, when the projection operator $\mathcal{P}$ is in effect, it always results in smaller parameter errors that will decrease $\dot{V}_s$ [35, 15]. Therefore, by using (4.71) and completing the squares, we obtain

$$\begin{aligned}
\dot{V}_s &\leq \tilde{\theta}_s^\top(\Omega_{s2} + I)^\top\tilde{y}_s - |\zeta_{s2}|^2 - \frac{1}{\Gamma_s}\tilde{\theta}_s^\top\dot{\theta}_s \quad = \quad \tilde{y}_s^\top\left(-\tilde{y}_s + \zeta_{s1} + \zeta_{s2}\right) - |\zeta_{s2}|^2 - \frac{1}{\Gamma_s}\tilde{\theta}_s^\top\dot{\theta}_s \\
&\leq -\frac{|\tilde{y}_s|^2}{2} + |\zeta_{s1}|^2 + \frac{1}{\Gamma_s}|\tilde{\theta}_s|\,|\dot{\theta}_s|\,.
\end{aligned} \tag{4.72}$$

Let $\bar{\zeta}_s \triangleq \left(|\zeta_{s1}|^2 + \frac{1}{\Gamma_s}|\tilde{\theta}_s||\dot{\theta}_s|\right)^{\frac{1}{2}}$. By integrating (4.72) from $t = T_d$ to $t = t_f$, we obtain $\int_{T_d}^{t_f}|\tilde{y}_s(t)|^2\,dt \leq \bar{\kappa}_s + 2\int_{T_d}^{t_f}|\bar{\zeta}_s(t)|^2\,dt$, where $\bar{\kappa}_s \triangleq \sup_{t_f \geq T_d}\{2[V_s(T_d) - V_s(t_f)]\}$.

□

Theorem 4.3 guarantees the boundedness of all the variables involved in the local adaptive FIE in the case that a sensor fault is detected in the corresponding generator. Moreover, the performance measure given by (4.65) shows that the ability of the matched local isolation estimator to learn the post-fault system dynamics is limited by the extended L_2 norm of $\bar{\zeta}_s(t)$, which, in turn, is related to the modeling uncertainties d_s and η_s, the parameter estimation error $\tilde{\theta}_s$, the rate of change of the time–varying bias θ_s, and the estimation error of the interconnection.

4.4 Simulation Results

A two-machine infinite bus power system [25, 26] as shown in Figure 4.2 is used to demonstrate the effectiveness of the proposed distributed fault detection and isolation method. The voltage and the angle of the infinite bus are assumed to be constant under all condi-

tions, and the infinite bus is assumed to absorb infinite power. The parameters of the two

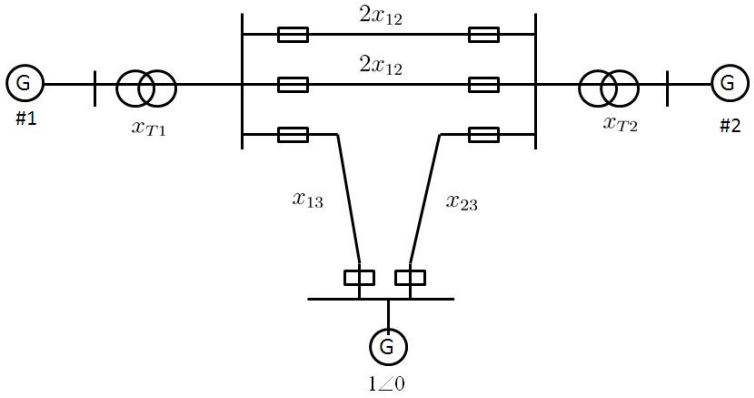

Figure 4.2: A two-machine infinite bus power system [26]

generators and the transmission line are give in Table 4.1.

Table 4.1 System parameters

	Generator 1	Generator 2
x_d (p.u.)	1.863	2.36
$x_d^{'}$ (p.u.)	0.257	0.319
x_{ad} (p.u.)	1.712	1.712
$T_{do}^{'}$ (p.u.)	6.9	7.96
$H(s)$	4	5.1
$D(p.u.)$	5	3
k_c	1	1
$x_{12}(p.u.)$	0.55	
$x_{13}(p.u.)$	0.53	
$x_{23}(p.u.)$	0.6	
$\omega_0(rad/s)$	314.159	

Based on the parameters given in Table 1, by defining the state variables as $x_i = [x_{i1}\ x_{i2}^{\top}]^{\top} = [\omega_i\ \ \delta_i\ \ \Delta P_{ei}]^{\top}$ with $i = 1, 2$, we can obtain a state space model of the system consisting of

two generators as follows:

$$\left[\begin{array}{c} \dot{x}_{11} \\ \hline \dot{x}_{12} \end{array}\right] = \left[\begin{array}{c|cc} -0.625 & 0 & -39.27 \\ \hline 1 & 0 & 0 \\ -E_{q1}^{'2}B_{11} & 0 & -0.1449 \end{array}\right] \left[\begin{array}{c} x_{11} \\ \hline x_{12} \end{array}\right] + \left[\begin{array}{c} 0 \\ \hline 0 \\ 1 \end{array}\right] 0.1449\, v_{f1} + \left[\begin{array}{c} 0 \\ \hline 0 \\ 1 \end{array}\right] h_{12}$$

$$y_1 = \left[\begin{array}{ccc} 0 & 1 & 0 \\ 0 & 0 & 1 \end{array}\right] x_1\,,$$

$$\left[\begin{array}{c} \dot{x}_{21} \\ \hline \dot{x}_{22} \end{array}\right] = \left[\begin{array}{c|cc} -0.2941 & 0 & -30.8 \\ \hline 1 & 0 & 0 \\ -E_{q2}^{'2}B_{22} & 0 & -0.1256 \end{array}\right] \left[\begin{array}{c} x_{21} \\ \hline x_{22} \end{array}\right] + \left[\begin{array}{c} 0 \\ \hline 0 \\ 1 \end{array}\right] 0.1256\, v_{f2} + \left[\begin{array}{c} 0 \\ \hline 0 \\ 1 \end{array}\right] h_{21}$$

$$y_2 = \left[\begin{array}{ccc} 0 & 1 & 0 \\ 0 & 0 & 1 \end{array}\right] x_2\,,$$

where the interconnection terms h_{12} and h_{21} are given by:

$$h_{12}(\delta,\omega) = E_{q1}^{'}\dot{E}_{q2}^{'}B_{12}\sin(\delta_1-\delta_2) - E_{q1}^{'}E_{q2}^{'}B_{12}\cos(\delta_1-\delta_2)\omega_2$$

$$h_{21}(\delta,\omega) = E_{q2}^{'}\dot{E}_{q1}^{'}B_{21}\sin(\delta_2-\delta_1) - E_{q2}^{'}E_{q1}^{'}B_{21}\cos(\delta_2-\delta_1)\omega_1\,,$$

and the known variables $E_{qi}^{'}$ and B_{ij}, $i, j = 1, 2$, can be calculated on-line based on the machine dynamics [25].

In this two-machine infinite bus power simulation example, two sources of modeling uncertainty are considered: (i) up to 5% disturbance effect on the power system frequency (i.e., $f_i = (1/2\pi)\omega_i$); (ii) up to 5% reduction in the direct axis transient short-circuit time constant $T_{doi}^{'}$. Therefore, we have $\bar{d}_i = \left|\frac{0.05\omega_i}{2\pi}\right|$, $\bar{\eta}_{i1} = 0$, and $\bar{\eta}_{i2} = \frac{0.0526}{T_{doi}^{'}}\,|v_{fi} - \Delta P_{ei}|$. The initial condition of machine 1 and machine 2 are set to $x_1 = x_2 = [\,0\;\;0\;\;0\,]^{\top}$. For simplicity, the input to each subsystem consists of two parts: a stabilizing part based on state feedback

design and a sinusoidal signal causing each subsystem to deviate from steady-state linear dynamics. In the simulation, the actual modeling uncertainties used are: (i) 4% disturbance effect on the power system frequency; (ii) 2% reduction in the direct axis transient short-circuit time constant $T_{doi}^{'}$.

The gain matrix L_i of the estimators is chosen such that the poles of matrix $\bar{\mathcal{A}}_{i4}$ are located at -1.7 and -2.5, respectively. Consequently, the related design constants are $\lambda_{i1} = -1.7$ and $\lambda_{i2} = -2.5$. Additionally, in the fault isolation module, FIE1 and FIE2 are two FIEs which are associated with the first generator and the second generator, respectively. The learning rates of the adaptive algorithm for fault parameters estimation in FIE1 and FIE2 are 1 and 0.05 for both FIE1 and FIE2.

We consider the case of a constant sensor bias which may occur to one of the two generators. Figure 4.3 and Figure 4.4 show the fault detection results when a constant bias with $\theta_2 = [\,0.03 \;\; 0.001\,]^\top$ occurs to the second generator at $T_2 = 5$ second. Specifically, the fault detection residuals (solid line) associated with δ_i and ΔP_i and the corresponding thresholds (dashed line) generated by each local FDE are shown in Figure 4.3 and Figure 4.4, respectively. As can be seen, the fault is detected almost immediately by each FDE. Then, the two local FIEs are activated to determine the particular faulty generator. The fault isolation residuals (solid line) and the corresponding thresholds (dashed line) generated by the FIE1 and FIE2 are shown in Figure 4.5 and Figure 4.6, respectively. It can be seen that the residual associated with output ΔP_1 generated by FIE 1 (i.e. the FIE associated with the first generator) exceeds its threshold at approximately $t = 6$ second. Meanwhile, both of the two residual components (solid line) generated by FIE 2 always remain below their thresholds (dashed line), as shown in Figure 4.6. Thus, the sensor fault in the second generator is correctly isolated.

In addition, the case of a sensor fault $\theta_1 = [\,0.02 \;\; 0.001\,]^\top$ in the first generator has also been considered. Specifically, Figure 4.7 and Figure 4.8 show fault detection results when the fault occurs to the first generator at $T_1 = 5$ second. Figure 4.9 and Figure 4.10 show the results of fault isolation. Again, the sensor bias is successfully detected and isolated.

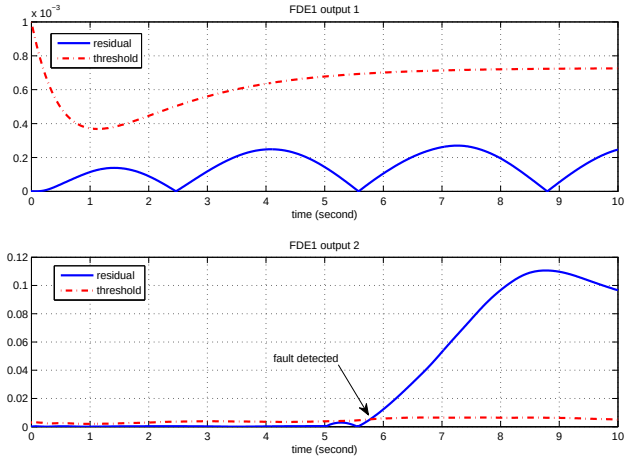

Figure 4.3: The case of a sensor bias in the second generator: the fault detection residuals (solid and blue line) associated with y_{11} and y_{12} and their thresholds (dashed and red line) generated by the local FDE for the first generator

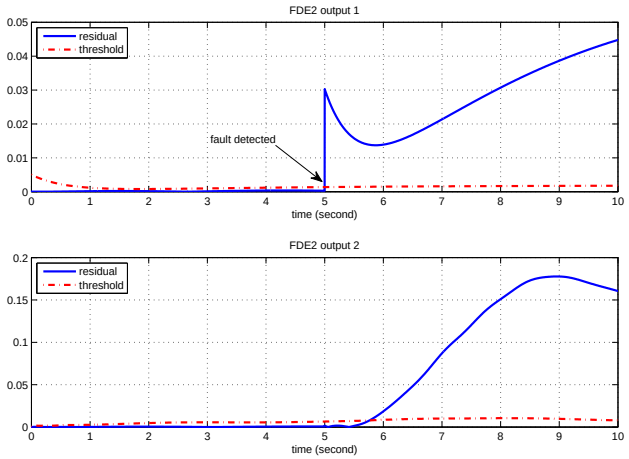

Figure 4.4: The case of a sensor bias in the second generator: the fault detection residuals (solid and blue line) associated with y_{21} and y_{22} and their thresholds (dashed and red line) generated by the local FDE for the second generator

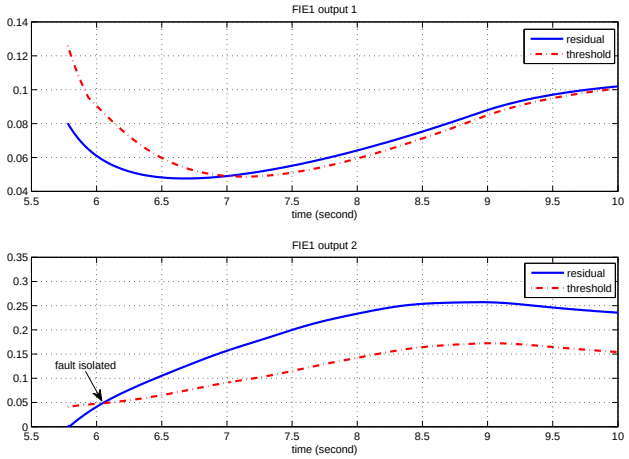

Figure 4.5: The case of a sensor bias in the second generator: the fault isolation residuals (solid and blue line) and their thresholds (dashed and red line) generated by local FIE1 associated with the first generator

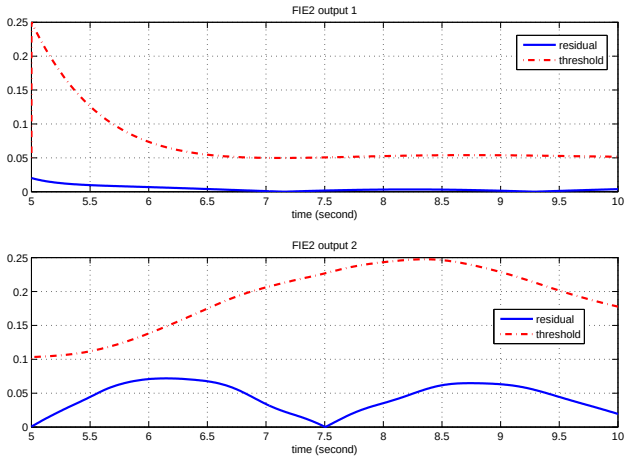

Figure 4.6: The case of a sensor bias in the second generator: the fault isolation residuals (solid and blue line) and their thresholds (dashed and red line) generated by local FIE2 associated with the second generator

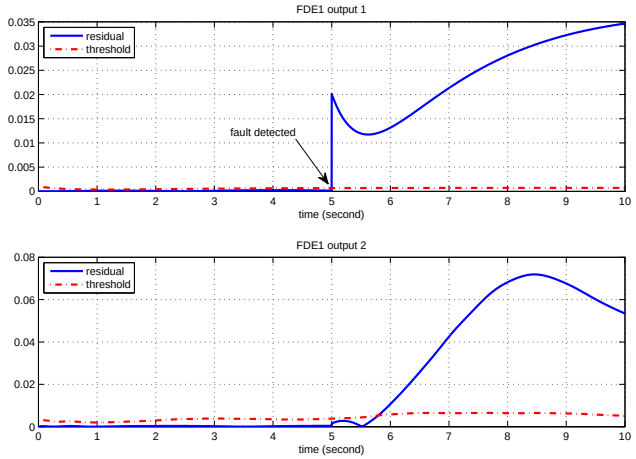

Figure 4.7: The case of a sensor bias in the first generator : the fault detection residuals (solid and blue line) associated with y_{11} and y_{12} and their thresholds (dashed and red line) generated by the local FDE for the first generator.

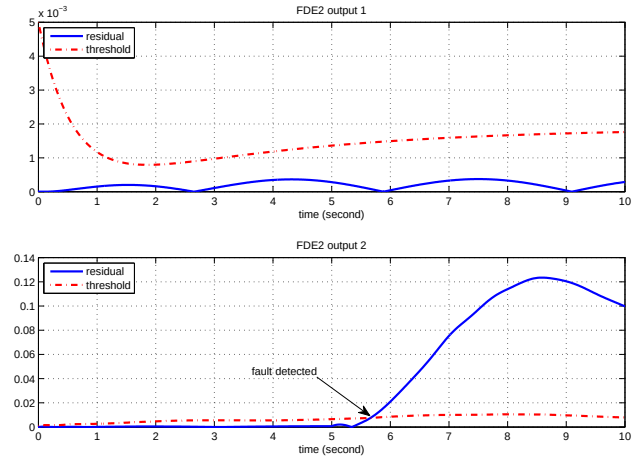

Figure 4.8: The case of a sensor bias in the first generator: the fault detection residuals (solid and blue line) associated with y_{21} and y_{22} and their thresholds (dashed and red line) generated by the local FDE for the second generator.

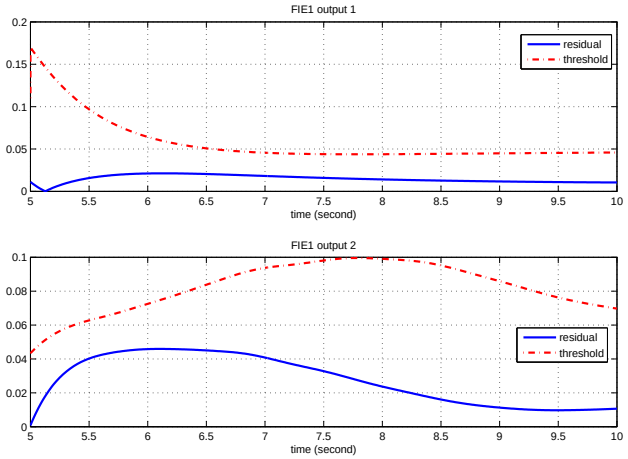

Figure 4.9: The case of a sensor bias in the first generator: the fault isolation residuals (solid and blue line) and their thresholds (dashed and red line) generated by the local FIE 1 associated with the first generator.

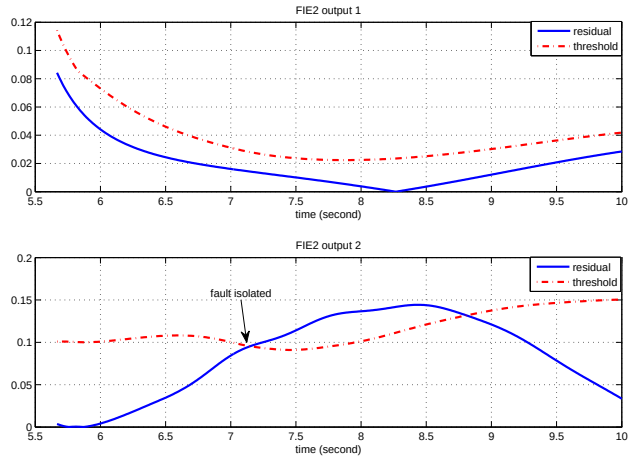

Figure 4.10: The case of a sensor bias in the first generator: the fault isolation residuals (solid and blue line) and their thresholds (dashed and red line) generated by the local FIE 2 associated with the second generator.

Chapter 5

Distributed Sensor Fault Diagnosis in a Class of Interconnected Nonlinear Uncertain Systems

The distributed fault diagnosis schemes for sensor faults in a class of input-output interconnected nonlinear systems have been presented in Chapter 4. In such systems, it is assumed that the system state in each subsystem can be decomposed into an unknown part and a measurable part, and there is no interconnection term in the dynamic equation of the unknown part of states. These assumptions may result in some possibly limiting requirements in applications. In this chapter, we extend the results described in Chapter 4 by considering a class of input-output interconnected nonlinear systems, where both unknown part and measurable part of system states of each subsystem are directly affected by the interconnection between other directly interconnected subsystems and this local subsystem. We are aiming to determine the particular subsystem with faulty sensors in the presence of propagated fault effect. In the presented distributed FDI architecture, a fault diagnostic component is designed for each subsystem in the interconnected system by utilizing local measurements and certain communicated information from neighboring FDI components

associated with its directly interconnected subsystems. Each local FDI component consists of a FDE and a nonlinear adaptive FIE. Once a sensor fault is detected, then the FIEs are activated for the purpose of isolating the particular subsystem where the sensor fault has actually occurred. In the fault isolation stage, the output estimation error of each FIE is evaluated with a set of adaptive thresholds, which can be implemented on-line using linear filtering techniques. The occurrence of sensor fault in a particular subsystem is excluded if at least one component of the output estimation error associated with the corresponding FIE exceeds its threshold at some finite time. The subsystem with actual local faulty sensors can be isolated if we can successfully exclude the occurrences of sensor faults for all subsystems but one. The chapter focuses on the derivation of adaptive thresholds for distributed sensor fault detection and fault isolation, respectively, ensuring robustness with respect to interactions among interconnected subsystems and modeling uncertainty. Additionally, the fault detectability condition and the stability and learning property of the distributed adaptive fault isolation method are investigated. An example of interconnected inverted pendulums mounted on carts is used to illustrate the effectiveness of the proposed scheme.

The organization of this chapter is as follows In Section 5.1, the sensor FDI problem for a class of interconnected nonlinear uncertain systems is formulated. Section 5.2 describes the distributed FDI architecture and the design of local FDI component for each subsystem in the interconnected system. The design of adaptive thresholds for distributed fault isolation is presented in Section 5.3. Section 5.4 investigates two important analytical properties of the distributed FDI method, including the fault detectability condition and the stability and learning capability of the distributed adaptive fault isolation method. To illustrate the effectiveness of the FDI method, simulation results of an example of interconnected inverted pendulums mounted on carts is presented in Section 5.5.

5.1 Problem Formulation

Consider a nonlinear dynamic system composed of M interconnected subsystems with the dynamics of the ith subsystem, $i = 1, \cdots, M$, being described by the following differential equation

$$\begin{aligned} \dot{x}_i &= A_i x_i + E_i \zeta_i(x_i, u_i) + D_i \varphi_i(x_i, u_i, t) + g_i(y_i, u_i) + \textstyle\sum_{j=1}^{M} h_{ij}(x_j, u_j) \\ y_i &= \bar{C}_i x_i + \beta_i(t - T_0)\theta_i(t) \end{aligned} \tag{5.1}$$

where $x_i \in \Re^{n_i}$, $u_i \in \Re^{m_i}$, and $y_i \in \Re^{l_i}$ are the state vector, input vector, and output vector of the ith subsystem ($n_i \geq l_i$), respectively, $E_i \in \Re^{n_i \times q_i}$ and $D_i \in \Re^{n_i \times r_i}$ are constant matrices, and $\zeta_i : \Re^{n_i} \times \Re^{m_i} \mapsto \Re^{q_i}$, $g_i : \Re^{l_i} \times \Re^{m_i} \mapsto \Re^{n_i}$, $\varphi_i : \Re^{n_i} \times \Re^{m_i} \times \Re^{+} \mapsto \Re^{r_i}$, $h_{ij} : \Re^{n_j} \times \Re^{m_j} \mapsto \Re^{n_i}$ are smooth vector fields. Specifically, the model given by

$$\begin{aligned} \dot{x}_{Ni} &= A_i x_{Ni} + E_i \zeta_i(x_{Ni}, u_i) + g_i(y_{Ni}, u_i) \\ y_{Ni} &= \bar{C}_i x_{Ni} \end{aligned}$$

is the *known nominal* model of the ith subsystem with ζ_i and g_i being the known nonlinearities. The vector field φ_i in (5.1) represents the modeling uncertainty of the ith subsystem, and $\beta_i(t - T_0)\theta_i(t)$ denotes a sensor bias fault. Specifically, $\beta_i(t - T_0)$ is a step function representing the time profile of the sensor fault which occurs at some unknown time T_0. The vector $\theta_i(t) \in \Re^{l_i}$ represents the unknown time-varying sensor bias affecting the output of subsystem i. Therefore, the sensor fault can be either an abrupt or incipient one. It is assumed that the sensor fault only occurs to one of the M subsystems at any time. Additionally, the vector fields h_{ij} represents the direct interconnection between the ith subsystem and the jth subsystem. Note that $h_{ii}(x_i, u_i) = 0$, because the interconnection term is only defined for two different subsystems. Also, it is noted that likely many functions h_{ij} are identically zero, since many subsystems may not be directly interconnected.

Assumption 5.1 *The constant matrices $E_i \in \Re^{n_i \times q_i}$, $D_i \in \Re^{n_i \times r_i}$, and $\bar{C}_i \in \Re^{l_i \times n_i}$ with $q_i \leq l_i$ are of full column rank and satisfies the conditions of $rank(\bar{C}_i E_i) = q_i$ and*

$rank(\bar{C}_i D_i) = r_i$.

Then, under Assumption 5.1, there exists a change of coordinates $z_i = [z_{i1}^\top \;\; z_{i2}^\top]^\top = T_i x_i$ with $z_{i1} \in \Re^{(n_i - l_i)}$ and $z_{i2} \in \Re^{l_i}$, such that ([72])

- $T_i E_i = \begin{bmatrix} 0 \\ E_{i2} \end{bmatrix}$, $T_i D_i = \begin{bmatrix} 0 \\ D_{i2} \end{bmatrix}$, where $E_{i2} \in \Re^{l_i \times q_i}$, and $D_{i2} \in \Re^{l_i \times r_i}$.
- $\bar{C}_i T_i^{-1} = [0 \;\; C_i]$, where $C_i \in \Re^{l_i \times l_i}$ is orthogonal.

Therefore, in the new coordinate system, by considering more general structures of the system nonlinearity and modeling uncertainty, we have

$$\begin{aligned} \dot{z}_{i1} &= \mathcal{A}_{i1} z_{i1} + \mathcal{A}_{i2} z_{i2} + \psi_{i1}(y_i, u_i) + \sum_{j=1}^{M} H_{ij}^1(z_j, u_j) \\ \dot{z}_{i2} &= \mathcal{A}_{i3} z_{i1} + \mathcal{A}_{i4} z_{i2} + \rho_{i2}(z_i, u_i) + \psi_{i2}(y_i, u_i) + \eta_i(z_i, u_i, t) + \sum_{j=1}^{M} H_{ij}^2(z_j, u_j) \\ y_i &= C_i z_{i2} + \beta_i(t - T_0)\theta_i(t)\,, \end{aligned} \tag{5.2}$$

where $\begin{bmatrix} \mathcal{A}_{i1} & \mathcal{A}_{i2} \\ \mathcal{A}_{i3} & \mathcal{A}_{i4} \end{bmatrix} = T_i A_i T_i^{-1}$, $\begin{bmatrix} \psi_{i1} \\ \psi_{i2} \end{bmatrix} = T_i g_i$, and $\begin{bmatrix} H_{ij}^1 \\ H_{ij}^2 \end{bmatrix} = T_i h_{ij}$, and the smooth vector fields $\rho_{i2} : \Re^{n_i} \times \Re^{m_i} \mapsto \Re^{l_i}$ and $\eta_i : \Re^{n_i} \times \Re^{m_i} \times \Re^{+} \mapsto \Re^{l_i}$ represent the unstructured system nonlinearity and modeling uncertainty in the z_{i2} state equation, respectively.

The objective of this chapter is to develop a robust distributed sensor bias FDI scheme for interconnected nonlinear systems that can be transformed into (5.2). Specifically, the distributed FDI algorithm aims to determine the particular subsystem with faulty sensors. Throughout this chapter, the following assumptions are made:

Assumption 5.2 *The unstructured modeling uncertainty, represented by η_i in (5.2), is an unknown nonlinear function of z_i, u_i, and t, but bounded, i.e.,*

$$|\eta_i(z_i, u_i, t)| \;\le\; \bar{\eta}_i(y_i, u_i, t)\,, \tag{5.3}$$

where the bounding function $\bar{\eta}_i$ is known and uniformly bounded in the corresponding

compact sets of admissible state variables, inputs, and outputs, respectively.

Assumption 5.3 *The system state vector z_i of each subsystem remains bounded before and after the occurrence of a fault, i.e., $z_i(t) \in L_\infty$, $\forall t \geq 0$.*

Assumption 5.4 *The nonlinear terms $\rho_{i2}(z_i, u_i)$ satisfy the following condition: $\forall u_i \in \mathcal{U}_i$ and $\forall z_i,\ \hat{z}_i \in \mathcal{Z}_i$,*

$$|\rho_{i2}(z_i, u_i) - \rho_{i2}(\hat{z}_i, u_i)| \leq \sigma_{i2}(y_i, u_i)\ |z_i - \hat{z}_i| \tag{5.4}$$

where σ_{i2} is a known and uniformly bounded function, $\mathcal{Z}_i \subset \Re^{n_i}$ and $\mathcal{U}_i \subset \Re^{m_i}$ are compact sets of admissible state variables and inputs, respectively.

Assumption 5.5 *The interconnection terms satisfy the following condition, i.e., $\forall z_i,\ \hat{z}_i \in \mathcal{Z}_i$, and $\forall z_j,\ \hat{z}_j \in \mathcal{Z}_j$,*

$$|H^1_{ij}(z_j, u_j) - H^1_{ij}(\hat{z}_j, u_j)| \leq \gamma^1_{ij}|z_j - \hat{z}_j| \tag{5.5}$$

$$|H^2_{ij}(z_j, u_j) - H^2_{ij}(\hat{z}_j, u_j)| \leq \gamma^2_{ij}(y_i, u_i)|z_j - \hat{z}_j| \tag{5.6}$$

where γ^1_{ij} is a known Lipschitz constant, γ^2_{ij} is a known and uniformly bounded function, and $\mathcal{Z}_i \subset \Re^{n_i}$ and $\mathcal{Z}_j \subset \Re^{n_j}$ are compact sets of admissible state variables for subsystems i and j, respectively.

Assumption 5.6 *The rate of change of the possibly time-varying sensors bias is uniformly bounded, i.e., $|\dot{\theta}_i(t)| \leq \alpha_i$ for all $t \geq 0$. Also, the sensor bias magnitude θ_i is uniformly bounded, i.e., $|\theta_i(t)| \leq \bar{\theta}_i$.*

Assumption 5.2 characterizes the class of modeling uncertainty under consideration. The bound on the modeling uncertainty is needed in order to be able to distinguish between the effects of faults and modeling uncertainty ([14, 83]).

Assumption 5.3 requires the boundedness of the state variables before and after the occurrence of a fault in each subsystem. Hence, it is assumed that the distributed feedback control system is capable of retaining the boundedness of the state variables of each subsystem even in the presence of a fault. This is a technical assumption required for well-posedness since the distributed FDI design under consideration does not influence the closed-loop dynamics

and stability. The design of distributed fault-tolerant controllers is beyond the scope of this chapter. However, it is important to note that the proposed distributed FDI design does not depend on the structure of the distributed controllers.

Assumption 5.4 characterizes the type of known nonlinearities of the nominal system dynamics under consideration. It is needed for deriving the adaptive thresholds for fault detection and isolation.

Assumption 5.5 requires the interconnection terms to satisfy Lipschitz condition. Several examples of distributed nonlinear systems with Lipschitz interconnection terms have been considered in literature, including automated highway system (see, e.g., [58, 62]), interconnected inverted pendulums given in [32], and large-scale power systems as described in [25].

5.2 Distributed Fault Detection and Isolation Architecture

The distributed FDI architecture is comprised of M local FDI components, with one FDI component designed for each of the M subsystems. Specifically, each local FDI component consists of a FDE and an adaptive FIE. Under normal conditions, each local FDE monitors the corresponding local subsystem to detect the occurrence of any fault. If a sensor fault is detected, then the FIEs are activated for the purpose of isolating the particular subsystem where the sensor fault has actually occurred.

The example depicted in Figure 4.1 can be used to illustrate the distributed FDI architecture described above. In Figure 4.1, a system composed of three interconnected subsystems is considered. Without loss of generality, we assume that there exist direct interconnections in two pairs of subsystems (i.e., subsystems 1 and 2, and subsystems 2 and 3). Thus, the distributed FDI architecture consists of three local FDI components, and the information exchange is conducted between FDI component 1 and 2, and FDI components 2 and 3, respectively. An example of three interconnected inverted pendulums mounted on carts, which has a similar system structure as shown in Figure 4.1, will be considered in Section

5.5.

5.2.1 Distributed Fault Detection Method

In this section, we describe the distributed fault detection method, including the design of each local FDE for residual generation and adaptive thresholds for residual evaluation. Based on the subsystem model described by (5.2), the FDE for each local subsystem is chosen as:

$$\begin{aligned}
\dot{\hat{z}}_{i1} &= \mathcal{A}_{i1}\hat{z}_{i1} + \mathcal{A}_{i2}C_i^{-1}y_i + \psi_{i1}(y_i,u_i) + \sum_{j=1}^{M} H_{ij}^1(\hat{z}_j,u_j) \\
\dot{\hat{z}}_{i2} &= \mathcal{A}_{i3}\hat{z}_{i1} + \mathcal{A}_{i4}\hat{z}_{i2} + \psi_{i2}(y_i,u_i) + \rho_{i2}(\hat{z}_i,u_i) + L_i(y_i-\hat{y}_i) + \sum_{j=1}^{M} H_{ij}^2(\hat{z}_j,u_j) \\
\hat{y}_i &= C_i\hat{z}_{i2}\,,
\end{aligned} \tag{5.7}$$

where $\hat{z}_{i1}$, $\hat{z}_{i2}$, and $\hat{y}_i$ denote the estimated local state and output variables of the ith subsystem, $i = 1,\cdots,M$, respectively, $L_i \in \Re^{l_i\times l_i}$ is a design gain matrix, $\hat{z}_i \stackrel{\triangle}{=} [(\hat{z}_{i1})^\top \ (C_i^{-1}y_i)^\top]^\top$, and $\hat{z}_j \stackrel{\triangle}{=} [(\hat{z}_{j1})^\top \ (C_j^{-1}y_j)^\top]^\top$ (here $\hat{z}_{j1}$ is the estimate of state vector z_{j1} of the jth interconnected subsystem). The initial conditions are $\hat{z}_{i1}(0) = 0$ and $\hat{z}_{i2}(0) = C_i^{-1}y_i(0)$.
For each local FDE, let $\tilde{z}_{i1} \stackrel{\triangle}{=} z_{i1} - \hat{z}_{i1}$ and $\tilde{z}_{i2} \stackrel{\triangle}{=} z_{i2} - \hat{z}_{i2}$ denote the state estimation errors, and $\tilde{y}_i \stackrel{\triangle}{=} y_i - \hat{y}_i$ denote the output estimation error. Then, before fault occurrence (i.e., for $t < T_0$), by using (5.2) and (5.7), the estimation error dynamics are given by

$$\dot{\tilde{z}}_{i1} = \mathcal{A}_{i1}\tilde{z}_{i1} + \sum_{j=1}^{M}\left[H_{ij}^1(z_j,u_j) - H_{ij}^1(\hat{z}_j,u_j)\right] \tag{5.8}$$

$$\dot{\tilde{z}}_{i2} = \bar{\mathcal{A}}_{i4}\tilde{z}_{i2} + \mathcal{A}_{i3}\tilde{z}_{i1} + \rho_{i2}(z_i,u_i) - \rho_{i2}(\hat{z}_i,u_i) + \eta_i + \sum_{j=1}^{M}\left[H_{ij}^2(z_j,u_j) - H_{ij}^2(\hat{z}_j,u_j)\right] \tag{5.9}$$

$$\tilde{y}_i = C_i(z_{i2}-\hat{z}_{i2}) = C_i\tilde{z}_{i2}\,, \tag{5.10}$$

where $\bar{\mathcal{A}}_{i4} \stackrel{\triangle}{=} \mathcal{A}_{i4} - L_iC_i$. Note that, since C_i is nonsingular, we can always choose L_i to

make $\bar{\mathcal{A}}_{i4}$ stable. We define a state estimation error vector as:

$$\tilde{z}_1(t) \stackrel{\triangle}{=} [(\tilde{z}_{11})^\top, \cdots, (\tilde{z}_{i1})^\top, \cdots, (\tilde{z}_{M1})^\top]^\top \tag{5.11}$$

Next, we will investigate the design of adaptive thresholds for distributed fault detection in each subsystem. First, a bounding function on the state estimation error vector $\tilde{z}_1$ can be obtained for $0 \leq t < T_0$ (i.e., before fault occurrence).

Lemma 5.1 *Consider the interconnected systems described by (5.2) and the fault detection estimators described by (5.7). Assume that there exists a symmetric positive definite matrix* $\bar{P}_i \in \Re^{(n_i-l_i)\times(n_i-l_i)}$, *for* $i = 1, \cdots, M$, *such that,*

1. *the symmetric matrix* $\bar{R}_i \stackrel{\triangle}{=} -\mathcal{A}_{i1}^\top \bar{P}_i - \bar{P}_i \mathcal{A}_{i1} > 0$,

2. *the matrix* $\bar{Q} \in \Re^{M\times M}$, *whose entries are given by*

$$\bar{Q}_{ij} = \begin{cases} \lambda_{min}(\bar{R}_i), & i = j \\ -||\bar{P}_i||\gamma_{ij}^1 - ||\bar{P}_j||\gamma_{ji}^1, & i \neq j,\ j = 1, \cdots, M \end{cases}$$

is positive definite, where γ_{ij}^1 *and* γ_{ji}^1 *are the Lipschitz constants introduced in (5.5), and* $\lambda_{min}(\bar{R}_i)$ *is the smallest eigenvalue of* $\bar{R}_i$.

Then, for $0 \leq t < T_0$, *the state estimation error vector* $\tilde{z}_1(t)$ *defined by (5.11) satisfies the following inequality:*

$$|\tilde{z}_1(t)| \leq \chi(t), \tag{5.12}$$

where $\chi(t) = \frac{\bar{V}_0 e^{-ct}}{\lambda_{min}(\bar{P})}$, *the matrix* $\bar{P} \stackrel{\triangle}{=} \text{diag}\{\bar{P}_1, \cdots, \bar{P}_M\}$, *the constant* $c \stackrel{\triangle}{=} \lambda_{min}(\bar{Q})/\lambda_{max}(\bar{P})$, *and* $\bar{V}_0$ *is a positive constant.*

Proof: The proof of the above lemma follows a similar reasoning logic as reported in the proof of Lemma 3.2 in Chapter 3, and it is omitted here.

Now, let us consider each component of the output estimation error, i.e., $\tilde{y}_{ip}(t) \stackrel{\triangle}{=} C_{ip}\tilde{z}_{i2}(t)$, $p = 1, \cdots, l_i$, where C_{ip} is the pth row vector of matrix C_i. Based on (5.4), (5.6) and (5.12),

after following a similar reasoning logic in [85], we have

$$|\tilde{y}_{ip}(t)| \leq k_{ip} \int_0^t e^{-\lambda_{ip}(t-\tau)} \big[|\varrho_i| \, \chi(\tau) \; + \; \bar{\eta}_i \big] d\tau \,, \tag{5.13}$$

where k_{ip} and λ_{ip} are positive constants chosen such that $|C_{ip} e^{\bar{\mathcal{A}}_{i4} t}| \leq k_{ip} e^{-\lambda_{ip} t}$ (since $\bar{\mathcal{A}}_{i4}$ is stable, constants k_{ip} and λ_{ip} satisfying the above inequality always exist, as described by [35]), and

$$\varrho_i \stackrel{\triangle}{=} [\gamma_{i1}^2, \cdots, \gamma_{i(i-1)}^2, ||\mathcal{A}_{i3}|| + \sigma_{i2}, \gamma_{i(i+1)}^2, \cdots, \gamma_{iM}^2]^\top \,, \tag{5.14}$$

(that is, the entries of ϱ_i are given by $\varrho_{ii} = ||\mathcal{A}_{i3}|| + \sigma_{i2}$, and $\varrho_{ij} = \gamma_{ij}^2$ for $j \neq i$).
Therefore, according to (5.13), the occurrence of a sensor fault is detected when the modulus of at least one component of the output estimation error (i.e., $\tilde{y}_{ip}(t)$), generated by the one or more local FDEs, exceeds its corresponding threshold $\nu_{ip}(t)$ given by

$$\nu_{ip}(t) \stackrel{\triangle}{=} k_{ip} \int_0^t e^{-\lambda_{ip}(t-\tau)} \big[|\varrho_i| \, \chi(\tau) \; + \; \bar{\eta}_i \big] d\tau \,. \tag{5.15}$$

Remark 5.1 In the presence of a sensor fault in one subsystem, the fault effect may be propagated to other subsystems due to their interconnections. As a result, multiple residuals generated by several local FDEs associated with different subsystems may exceed their thresholds, indicating the occurrence of a sensor fault. Thus, the determination of the particular subsystem where the sensor fault has actually occurred among subsystems affected by the fault is necessary for successful sensor fault diagnosis, which is investigated next.

5.2.2 Distributed Fault Isolation Method

Now, assume that a sensor bias fault occurred in sth subsystem is detected at some time T_d; accordingly, at $t = T_d$, the FIEs are activated. For $s = 1, \cdots, M$, the local FIE associated

with the sth subsystem is chosen as

$$\dot{\hat{z}}_{s1} = \mathcal{A}_{s1}\hat{z}_{s1} + \mathcal{A}_{s2}C_s^{-1}(y_s - \hat{\theta}_s) + \psi_{s1}(y_s, u_s) + \Omega_{s1}\dot{\hat{\theta}}_s + \sum_{j=1}^{M} H_{sj}^1(\hat{z}_j, u_j) \quad (5.16)$$

$$\dot{\hat{z}}_{s2} = \mathcal{A}_{s3}\hat{z}_{s1} + \mathcal{A}_{s4}\hat{z}_{s2} + \psi_{s2}(y_s, u_s) + \rho_{s2}(\hat{z}_s, u_s) + L_s(y_s - \hat{y}_s) + \Omega_{s2}\dot{\hat{\theta}}_s + \sum_{j=1}^{M} H_{sj}^2(\hat{z}_j, u_j) \quad (5.17)$$

$$\dot{\Omega}_{s1} = \mathcal{A}_{s1}\Omega_{s1} - \mathcal{A}_{s2}C_s^{-1} \quad (5.18)$$

$$\dot{\Omega}_{s2} = \bar{\mathcal{A}}_{s4}\Omega_{s2} - L_s \quad (5.19)$$

$$\hat{y}_s = C_s\hat{z}_{s2} + \hat{\theta}_s \quad (5.20)$$

where $\hat{z}_{s1}$, $\hat{z}_{s2}$, and $\hat{y}_s$ denote the estimated state and output variables provided by the local FIE, respectively, $L_s \in \Re^{l_s \times l_s}$ is a design gain matrix (for simplicity of presentation and without loss of generality, we let $L_s = L_i$), $\hat{z}_s \triangleq [(\hat{z}_{s1})^\top \ (C_s^{-1}(y_s - \hat{\theta}_s))^\top]^\top$, $\hat{z}_j \triangleq [(\hat{z}_{j1} - \Omega_{j1}\hat{\theta}_j)^\top \ (C_j^{-1}y_j)^\top]^\top$, and $\hat{\theta}_s$ is the estimated sensor bias provided by the local isolation estimator. The initial conditions are $\hat{z}_{s1}(T_d) = 0$, $\hat{z}_{s2}(T_d) = 0$, $\Omega_{s1}(T_d) = 0$, and $\Omega_{s2}(T_d) = 0$.

The adaptation in the isolation estimators arises due to the unknown fault magnitude θ_s. The adaptive law for adjusting $\hat{\theta}_s$ is derived using the Lyapunov synthesis approach (see, for example, [35]). Specifically, the learning algorithm is given by

$$\dot{\hat{\theta}}_s = \mathcal{P}_{\Theta_s}\left\{\Gamma(C_s\Omega_{s2} + I)^\top\tilde{y}_s\right\}, \quad (5.21)$$

where $\tilde{y}_s(t) \triangleq y_s(t) - \hat{y}_s(t)$ denotes the output estimation error generated by the FIE for the sth subsystem, $\Gamma > 0$ is a symmetric, positive-definite learning rate matrix, and $\mathcal{P}_{\Theta_s}$ is the projection operator restricting $\hat{\theta}_s$ to the corresponding *known* set Θ_s (in order to guarantee stability of the learning algorithm in the presence of modeling uncertainty (as described in [35, 15]).

The distributed fault isolation decision scheme is based on the following intuitive principle:

if a sensor fault occurs in the sth subsystem at time T_0 and is detected at time T_d, then a set of adaptive threshold functions $\{\mu_{sp}(t),\, p = 1, \cdots, l_s\}$ can be designed for the corresponding local isolation estimator, such that each component of its output estimation error satisfies $|\tilde{y}_{sp}(t)| \leq \mu_{sp}(t)$, for all $t \geq T_d$. Consequently, such a set of adaptive thresholds $\mu_{sp}(t)$, with $s = 1, \cdots, M$, can be associated with the output estimation error of each local isolation estimator. In the fault isolation procedure, if, for a particular local isolation estimator $r \in \{1, \cdots, M\}\backslash\{s\}$, there exists some $p \in \{1, \cdots, l_r\}$, such that the pth component of its output estimation error satisfies $|\tilde{y}_{rp}(t)| > \mu_{rp}(t)$ for some finite time $t > T_d$, then the possibility of the occurrence of the sensor fault in rth subsystem can be excluded. Thus, we have the following

Distributed Fault Isolation Decision Scheme: *If, for each $r \in \{1, \cdots, M\}\backslash\{s\}$, there exist some finite time $t^r > T_d$ and some $p \in \{1, \cdots, l_r\}$, such that $|\tilde{y}_{rp}(t^r)| > \mu_{rp}(t^r)$, then the occurrence of the sensor bias fault in the sth subsystem is concluded.*

Clearly, the distributed fault isolation logic follows the well-known generalized observer scheme (GOS) architectural framework.

5.3 Adaptive Thresholds for Distributed Fault Isolation

The threshold functions $\mu_{sp}(t)$ clearly play a key role in the proposed distributed fault isolation decision scheme. Denote the state estimation error generated by the local isolation estimator for the sth subsystem by $\tilde{z}_{s1}(t) \stackrel{\triangle}{=} z_{s1}(t) - \hat{z}_{s1}(t)$ and $\tilde{z}_{s2}(t) \stackrel{\triangle}{=} z_{s2}(t) - \hat{z}_{s2}(t)$. By using (5.16)-(5.20) and (5.2), in the presence of a sensor fault in the sth subsystem, for $t > T_d$, we have

$$\dot{\tilde{z}}_{s1} = \mathcal{A}_{s1}\tilde{z}_{s1} + \mathcal{A}_{s2}C_s^{-1}\tilde{\theta}_s + \sum_{j=1}^{M}\left[H_{sj}^1(z_j, u_j) - H_{sj}^1(\hat{z}_j, u_j)\right] - \Omega_{s1}\dot{\hat{\theta}}_s \tag{5.22}$$

$$\begin{aligned}\dot{\tilde{z}}_{s2} =& \bar{\mathcal{A}}_{s4}\tilde{z}_{s2} + \mathcal{A}_{s3}\tilde{z}_{s1} + \eta_s + \rho_{s2}(z_s, u_s) - \rho_{s2}(\hat{z}_s, u_s) + L_s\tilde{\theta}_s - \Omega_{s2}\dot{\hat{\theta}}_s \\ &+ \sum_{j=1}^{M}\left[H_{sj}^2(z_j, u_j) - H_{sj}^2(\hat{z}_j, u_j)\right]\end{aligned} \tag{5.23}$$

where $\tilde{\theta}_s = \hat{\theta}_s - \theta_s$ is the parameter estimation error, and $\bar{\mathcal{A}}_{s4}$ is defined in (5.9). By substituting $\mathcal{A}_{s2}C_s^{-1} = -\dot{\Omega}_{s1} + \mathcal{A}_{s1}\Omega_{s1}$ (see (5.18)) into (5.22) and by letting $\bar{z}_{s1} \stackrel{\triangle}{=} \tilde{z}_{s1} + \Omega_{s1}\tilde{\theta}_s$, we have

$$\dot{\bar{z}}_{s1} = \mathcal{A}_{s1}\bar{z}_{s1} + \sum_{j=1}^{M}\left[H_{sj}^1(z_j, u_j) - H_{sj}^1(\hat{z}_j, u_j)\right] - \Omega_{s1}\dot{\theta}_s. \tag{5.24}$$

Let us define a vector of state estimation errors as:

$$\bar{z}_1(t) \stackrel{\triangle}{=} [(\bar{z}_{11})^\top, \cdots, (\bar{z}_{s1})^\top, \cdots, (\bar{z}_{M1})^\top]^\top, \tag{5.25}$$

where for $s = 1, \cdots, M$, $\bar{z}_{s1}$ is defined in (5.24). Then, we have the following result:

Lemma 5.2 *Consider the interconnected systems described by (5.2) and the fault isolation estimators described by (5.16)-(5.20). In the presence of a sensor fault in sth subsystem, if there exists a symmetric positive definite matrix $P_i \in \Re^{(n_i-l_i)\times(n_i-l_i)}$, for $i = 1, \cdots, M$, such that,*

1. *the symmetric matrix*

$$R_i \stackrel{\triangle}{=} -\mathcal{A}_{i1}^\top P_i - P_i\mathcal{A}_{i1} - 2P_iP_i > 0\,, \tag{5.26}$$

2. *the matrix $Q \in \Re^{M\times M}$, whose entries are given by*

$$Q_{ij} = \begin{cases} \lambda_{min}(R_i)\,, & j = i \\ -||P_i||\gamma_{ij}^1 - ||P_i||\gamma_{ji}^1\,, & j \neq i,\ j = 1, \cdots, M \end{cases} \tag{5.27}$$

is positive definite, where γ_{ij}^1 and γ_{ji}^1 are the Lipschitz constants defined in (5.5).

Then, the state estimation error vector $\bar{z}_1(t)$ defined by (5.25) satisfies

$$|\bar{z}_1(t)| \leq \chi_s(t), \quad \text{for } t > T_d\,, \tag{5.28}$$

where

$$\chi_s(t) = \left\{ \frac{\bar{V}_0 e^{-b(t-T_d)}}{\lambda_{min}(P)} + \frac{1}{2\lambda_{min}(P)} \int_{T_d}^{t} e^{-b(t-\tau)} \left[||\Omega_{s1}||^2 \alpha_s^2 + \sum_{j=1}^{M} \left[\gamma_{js}^1 \bar{\theta}_s (||\Omega_{s1}|| + ||C_s^{-1}||) \right]^2 \right] d\tau \right\}^{\frac{1}{2}}, \tag{5.29}$$

the matrix $P \triangleq \text{diag}\{P_1, \cdots, P_M\}$, *the constant* $b \triangleq \lambda_{min}(Q)/\lambda_{max}(P)$, *and* $\bar{V}_0$ *is a constant to be defined later on in the proof.*

Proof: The proof consists of three parts. First, let us consider the Lyapunov function candidate $V_s = \bar{z}_{s1}^\top P_s \bar{z}_{s1}$. The time derivative of V_s along the solution of (5.24) is given by

$$\dot{V}_s = \bar{z}_{s1}^\top (\mathcal{A}_{s1}^\top P_s + P_s \mathcal{A}_{s1}) \bar{z}_{s1} - 2\bar{z}_{s1}^\top P_s \Omega_{s1} \dot{\theta}_s + 2\bar{z}_{s1}^\top P_s \sum_{j=1}^{M} \left[H_{sj}^1(z_j, u_j) - H_{sj}^1(\hat{z}_j, u_j) \right] \tag{5.30}$$

Note that, for the interconnected jth subsystem, where $j \in \{1, \cdots, M\} \backslash \{s\}$, we have

$$z_j - \hat{z}_j = \begin{bmatrix} z_{j1} - \hat{z}_{j1} + \Omega_{j1} \hat{\theta}_j \\ z_{j2} - C_j^{-1} y_j \end{bmatrix} = \begin{bmatrix} \bar{z}_{j1} \\ 0 \end{bmatrix}, \tag{5.31}$$

where $\bar{z}_{j1}$ is defined in (5.24) (note that $\bar{z}_{j1} = \tilde{z}_{j1} + \Omega_{j1} \tilde{\theta}_j = \tilde{z}_{j1} + \Omega_{j1} \hat{\theta}_j$). Therefore, based on (5.31) and (5.5), we have

$$2\bar{z}_{s1} P_s \sum_{j=1}^{M} [H_{sj}^1(z_j, u_j) - H_{sj}^1(\hat{z}_j, u_j)] \leq 2||P_s|| \sum_{j=1}^{M} \gamma_{sj}^1 |\bar{z}_{s1}| \, |\bar{z}_{j1}|. \tag{5.32}$$

Also, we have

$$2\, \bar{z}_{s1}^\top P_s \Omega_{s1} \dot{\theta}_s \leq |2P_s \bar{z}_{s1}| \, |\Omega_{s1} \dot{\theta}_s| \leq 2\bar{z}_{s1}^\top P_s P_s \bar{z}_{s1} + \frac{1}{2} |\Omega_{s1} \dot{\theta}_s|^2 . \tag{5.33}$$

By using (5.30), (5.32) and (5.33), we have

$$\dot{V}_s \leq \bar{z}_{s1}^\top \left[\mathcal{A}_{s1}^\top P_s + P_s \mathcal{A}_{s1} + 2P_s P_s \right] \bar{z}_{s1} + \frac{1}{2} |\Omega_{s1} \dot{\theta}_s|^2 + 2||P_s|| \sum_{j=1}^{M} \gamma_{sj}^1 |\bar{z}_{s1}| |\bar{z}_{j1}|.$$

According to (5.26) and the inequality $\bar{z}_{s1}^{\top} R_s \bar{z}_{s1} \geq \lambda_{min}(R_s)|\bar{z}_{s1}|^2$, where $\lambda_{min}(R_s)$ is the minimum eigenvalue of R_s, we have

$$\dot{V}_s \leq -\lambda_{min}(R_s)|\bar{z}_{s1}|^2 + 2||P_s|| \sum_{j=1}^{M} \gamma_{sj}^1 |\bar{z}_{s1}||\bar{z}_{j1}| + \frac{1}{2}|\Omega_{s1}\dot{\theta}_s|^2 \,. \tag{5.34}$$

Second, for the interconnected rth subsystem, where $r \in \{1, \cdots, M\} \backslash \{s\}$, based on (5.16) and (5.2), we have

$$\dot{\bar{z}}_{r1} = \mathcal{A}_{r1}\bar{z}_{r1} + \sum_{j=1}^{M} \left[H_{rj}^1(z_j, u_j) - H_{rj}^1(\hat{z}_j, u_j) \right] \,. \tag{5.35}$$

Note that the difference between (5.35) and (5.24) is because in the case the sensor fault is assumed to be in the sth subsystem. For subsystem r, we also define a Lyapunov function candidate $V_r = \bar{z}_{r1}^{\top} P_r \bar{z}_{r1}$. The time derivative of V_r along the solution of (5.35) is given by

$$\begin{aligned} \dot{V}_r = \; & \bar{z}_{r1}^{\top}(\mathcal{A}_{r1}^{\top} P_r + P_r \mathcal{A}_{r1})\bar{z}_{r1} + 2\bar{z}_{r1}^{\top} P_r \left[H_{rs}^1(z_s, u_s) - H_{rs}^1(\hat{z}_s, u_s) \right] \\ & + 2\bar{z}_{r1}^{\top} P_r \sum_{\substack{k=1 \\ k \neq s}}^{M} \left[H_{rk}^1(z_k, u_k) - H_{rk}^1(\hat{z}_k, u_k) \right] \,. \end{aligned} \tag{5.36}$$

Note that for the interconnection terms in (5.36), we have

$$z_s - \hat{z}_s \; = \; \begin{bmatrix} z_{s1} - \hat{z}_{s1} + \Omega_{s1}\hat{\theta}_s \\ z_{s2} - C_s^{-1} y_s \end{bmatrix} \; = \; \begin{bmatrix} \bar{z}_{s1} + \Omega_{s1}\theta_s \\ -C_s^{-1}\theta_s \end{bmatrix} \,, \tag{5.37}$$

and

$$z_k - \hat{z}_k \; = \; \begin{bmatrix} z_{k1} - \hat{z}_{k1} + \Omega_{k1}\hat{\theta}_k \\ z_{k2} - C_k^{-1} y_k \end{bmatrix} \; = \; \begin{bmatrix} \bar{z}_{k1} \\ 0 \end{bmatrix} \,, \tag{5.38}$$

where $\bar{z}_{k1} \; = \; \hat{z}_{k1} + \Omega_{k1}\hat{\theta}_k \; = \; \hat{z}_{k1} + \Omega_{k1}\tilde{\theta}_k$. Then based on (5.37) and (5.38), we have

$$2\bar{z}_{r1} P_r \sum_{\substack{k=1 \\ k \neq s}}^{M} \left[H_{rk}^1(z_k, u_k) - H_{rk}^1(\hat{z}_k, u_k) \right] \leq 2||P_k|| \sum_{\substack{k=1 \\ k \neq s}}^{M} \gamma_{rk}^1 |\bar{z}_{r1}| \, |\bar{z}_{k1}|, \tag{5.39}$$

and

$$2\bar{z}_{r1}P_r\left[H^1_{rs}(z_s,u_s)-H^1_{rs}(\hat{z}_s,u_s)\right] \leq 2||P_r||\gamma^1_{rs}|\bar{z}_{r1}||\bar{z}_{s1}|+2\bar{z}^\top_{r1}P_rP_r\bar{z}_{r1}+ \\ +\frac{1}{2}\left[\gamma^1_{rs}(|\Omega_{s1}\theta_s|+|C_s^{-1}\theta_s|)\right]^2. \quad (5.40)$$

Therefore, based on (5.39), (5.40), (5.36) and (5.26), after some algebraic manipulations, it can be shown that

$$\dot{V}_r \leq -\lambda_{min}(R_r)|\bar{z}_{r1}|^2+2||P_r||\sum_{j=1}^{M}\gamma^1_{rj}|\bar{z}_{r1}||\bar{z}_{j1}|+\frac{1}{2}\left[\gamma^1_{rs}(|\Omega_{s1}\theta_s|+|C_s^{-1}\theta_s|)\right]^2. \quad (5.41)$$

Finally, we consider an overall Lyapunov function candidate $V=\sum_{i=1}^{M}V_i=\sum_{i=1}^{M}\bar{z}^\top_{i1}P_i\bar{z}_{i1}=\bar{z}_1^\top P\bar{z}_1$ for the interconnected systems, where $P=\text{diag}\{P_1,\cdots,P_M\}$ and $\bar{z}_1$ is defined in (5.25). From (5.34) and (5.41), we have

$$\begin{aligned}\dot{V} &\leq -\sum_{i=1}^{M}\lambda_{min}(R_i)|\tilde{z}_{i1}|^2+\sum_{i=1}^{M}\sum_{j=1}^{M}2||P_i||\gamma^1_{ij}|\tilde{z}_{i1}||\tilde{z}_{j1}| \\ &\quad +\frac{1}{2}\left[|\Omega_{s1}\dot{\theta}_s|^2+\sum_{j=1}^{M}\left[\gamma^1_{js}(|\Omega_{s1}\theta_s|+|C_s^{-1}\theta_s|)\right]^2\right] \\ &= -\left[|\bar{z}_{11}|\ \ |\bar{z}_{21}|\ \ \cdots\ \ |\bar{z}_{M1}|\right]Q\left[|\bar{z}_{11}|\ \ |\bar{z}_{21}|\ \ \cdots\ \ |\bar{z}_{M1}|\right]^\top \\ &\quad +\frac{1}{2}|\Omega_{s1}\dot{\theta}_s|^2+\frac{1}{2}\sum_{j=1}^{M}\left[\gamma^1_{js}(|\Omega_{s1}\theta_s|+|C_s^{-1}\theta_s|)\right]^2,\end{aligned}$$

where the matrix Q is defined by (5.27). By applying the Rayleigh principle (i.e., $\lambda_{min}(Q)|\bar{z}_1|^2\leq\bar{z}_1^\top Q\bar{z}_1\leq\lambda_{max}(Q)|\bar{z}_1|^2$), we have

$$\dot{V}\leq -bV+\frac{1}{2}|\Omega_{s1}\dot{\theta}_s|^2+\frac{1}{2}\sum_{j=1}^{M}\left[\gamma^1_{js}(|\Omega_{s1}\theta_s|+|C_s^{-1}\theta_s|)\right]^2,$$

where the constant b is defined in (5.29). Now, based on Lemma 3.2.4 in [35] and Assumption

4.6, it can be shown that

$$V(t) \leq \frac{1}{2}\int_{T_d}^{t} e^{-b(t-\tau)}\Big\{\sum_{j=1}^{M}\left[\gamma_{js}^{1}\bar{\theta}_s(||\Omega_{s1}||+||C_s^{-1}||)\right]^2+||\Omega_{s1}||^2\alpha_s^2\Big\}d\tau+V(0)e^{-b(t-T_d)}\,. \quad (5.42)$$

Note that a positive constant $\bar{V}_0$ can be always chosen such that $V(0) < \bar{V}_0$. By using the definition of $V(t)$ and the Rayleigh principle, the proof of (5.28) can be concluded.

□

The following lemma provides a bounding function for the output estimation error generated by the local isolation estimator associated with the sth subsystem, in the case that a sensor fault occurs in the sth subsystem.

Lemma 5.3 *If a sensor fault in the sth subsystem is detected at time T_d, where $s \in \{1, \cdots, M\}$, then for all $t > T_d$, the pth component of the output estimation error generated by the local FIE for the sth subsystem satisfies*

$$\begin{aligned}|\tilde{y}_{sp}(t)| \;\leq\; & k_{sp}\int_{T_d}^{t} e^{-\lambda_{sp}(t-\tau)}\Big[\left(\sigma_{s2}+||\mathcal{A}_{s3}||\right)|\Omega_{s1}\tilde{\theta}_s|+|\varrho_s|\,\chi_s(\tau)+\sigma_{s2}|C_s^{-1}\tilde{\theta}_s| \\ & +\bar{\eta}_s+\alpha_s||\Omega_{s2}||\Big]d\tau+|C_{sp}\Omega_{s2}\tilde{\theta}_s+\tilde{\theta}_{sp}|+k_{sp}\omega_{s2}e^{-\lambda_{sp}(t-T_d)}, \end{aligned} \quad (5.43)$$

where $\tilde{\theta}_s(t) \triangleq \hat{\theta}_s(t)-\theta_s(t)$ is the fault parameter estimation error, ω_{s2} is a positive constant satisfying $|z_{s2}(T_d)| \leq \omega_{s2}$, $\tilde{\theta}_{sp}$ is the pth component of $\tilde{\theta}_s$, and ϱ_s is defined in (5.14).

Proof: Consider the the state estimation error $\tilde{z}_{s2}$ described by (5.23). By substituting $L_s = -\dot{\Omega}_{s2}+\bar{\mathcal{A}}_{s4}\Omega_{s2}$ (see (5.19)) into (5.23) and by letting $\bar{z}_{s2} \triangleq \tilde{z}_{s2}+\Omega_{s2}\tilde{\theta}_s$, we obtain

$$\begin{aligned}\dot{\bar{z}}_{s2} \;=\; & \bar{\mathcal{A}}_{s4}\bar{z}_{s2}+\mathcal{A}_{s3}\tilde{z}_{s1}+\rho_{s2}(z_s,u_s)-\rho_{s2}(\hat{z}_s,u_s)-\Omega_{s2}\dot{\theta}_s+\eta_s \\ & +\sum_{j=1}^{M}\left[H_{sj}^2(z_j,u_j)-H_{sj}^2(\hat{z}_j,u_j)\right]\,. \end{aligned} \quad (5.44)$$

Define each component of the output estimation error generated by the sth FIE as $\tilde{y}_{sp} \triangleq$

$y_{sp} - \hat{y}_{sp}$, with $p = 1, \cdots, l_s$. By using (5.20), (5.2), and the definition of $\bar{z}_{s2}(t)$, we have

$$\tilde{y}_{sp}(t) = C_{sp}\tilde{z}_{s2}(t) - \tilde{\theta}_{sp} = C_{sp}\left(\bar{z}_{s2}(t) - \Omega_{s2}\tilde{\theta}_s\right) - \tilde{\theta}_{sp}\,. \tag{5.45}$$

Note that in the presence of a sensor fault in subsystem s, we have

$$z_s - \hat{z}_s \;=\; \left[\begin{array}{c} z_{s1} - \hat{z}_{s1} \\ z_{s2} - C_s^{-1}(y_s - \hat{\theta}_s) \end{array}\right] = \left[\begin{array}{c} \tilde{z}_{s1} \\ C_s^{-1}\tilde{\theta}_s \end{array}\right]. \tag{5.46}$$

By using (5.46) and (5.31), we have

$$\begin{array}{rcl} |H_{sj}^2(z_j, u_j) - H_{sj}^2(\hat{z}_j, u_j)| & \leq & \gamma_{sj}^2|\bar{z}_{j1}| \\ |\rho_{s2}(z_s, u_s) - \rho_{s2}(\hat{z}_s, u_s)| & \leq & \sigma_{s2}|\tilde{z}_{s1}| + \sigma_{s2}|C_s^{-1}\tilde{\theta}_s|\,. \end{array} \tag{5.47}$$

Based on (5.47), (5.45), and the definition of $\bar{z}_{s1}$, and by following some similar reasoning logic as reported in the derivation of adaptive thresholds for fault detection, we have

$$\begin{array}{rcl} |\tilde{y}_{sp}(t)| & \leq & k_{sp}\displaystyle\int_{T_d}^{t} e^{-\lambda_{sp}(t-\tau)}\Big[(||\mathcal{A}_{s3}|| \; + \sigma_{s2})(|\bar{z}_{s1}| + |\Omega_{s1}\tilde{\theta}_s|) \\ & & \quad + \displaystyle\sum_{j=1}^{M}\gamma_{sj}^2\,|\bar{z}_{j1}| + \sigma_{s2}|C_s^{-1}\tilde{\theta}_s| + \bar{\eta}_s + |\Omega_{s2}\dot{\theta}_s|\Big]d\tau \\ & & \quad + |C_{sp}\Omega_{s2}\tilde{\theta}_s + \tilde{\theta}_{sp}| + k_{sp}|\bar{z}_{s2}(T_d)|e^{-\lambda_{sp}(t-T_d)}\,, \end{array} \tag{5.48}$$

where the constants k_{sp} and λ_{sp} are introduced in (5.13), and ω_{s2} is an upper bound of $|z_{s2}(T_d)|$ such that $|\tilde{z}_{s2}(T_d)| = |z_{s2}(T_d)| \leq \omega_{s2}$. Now, by using (5.14), (5.48), Lemma 5.2, and Assumption 5.6, the proof of (5.43) can be concluded.

□

Although Lemma 5.3 provides a bounding function for the output estimation error corresponding to the local isolation estimator associated with the sth subsystem, in the case that a sensor fault occurs in the sth subsystem. Lemma 5.3 cannot be directly used as a threshold function for fault isolation, because $\tilde{\theta}_s(t)$ is not available (we do not assume the

condition of persistency of excitation in this paper). However, as the estimate $\hat{\theta}_s$ belongs to the known compact set Θ_s, we have $\left|\theta_s - \hat{\theta}_s(t)\right| \leq \kappa_s(t)$, for a suitable $\kappa_s(t)$ depending on the geometric properties of set Θ_s (see, e.g., [83]). Hence, the following threshold function for fault isolation can be chosen:

$$\begin{aligned}\mu_{sp}(t) &= k_{sp}\int_{T_d}^{t} e^{-\lambda_{sp}(t-\tau)}\Big[(||\mathcal{A}_{s3}||+\sigma_{s2})||\Omega_{s1}||\kappa_s+|\varrho_s|\chi_s(\tau)+\sigma_{s2}||C_s^{-1}||\kappa_s+\bar{\eta}_s+||\Omega_{s2}||\alpha_s\Big]d\tau \\ &\quad +|C_{sp}\Omega_{s2}+F_{sp}|\kappa_s + k_{sp}\omega_{s2}e^{-\lambda_{sp}(t-T_d)}\,. \end{aligned} \tag{5.49}$$

where $F_{sp}^{\top} \in \Re^{l_s}$ is a constant vector with all entries being 0 except the pth entry (taking the value of 1). The above design and analysis is summarized as follows:

Theorem 5.1 : *Consider a sensor fault in subsystem s is detected at time T_d, where $s = 1, \cdots, M$. Then, the distributed fault isolation scheme, characterized by the distributed fault isolation estimators (5.16) - (5.20) and the adaptive thresholds (5.49), guarantees that each component of the output estimation error generated by the local isolation estimator associated with subsystem s satisfies $|\tilde{y}_{sp}(t)| \leq \mu_{sp}(t)$, for all $p = 1, \cdots, l_s$, and $t \geq T_d$.*

5.4 Analytical Properties

In this section, we analyze two important properties of the distributed FDI method, including fault detectability as well as stability and learning capability of the adaptive fault isolation method.

5.4.1 Fault Detectability Analysis

As is well known in the fault diagnosis literature, there is an inherent tradeoff between robustness and fault detectability. The following theorem characterizes (in a non-closed form) the class of sensor faults that are detectable by the proposed distributed FDI method.

Theorem 5.2 (Fault Detectability): *For the distributed fault detection method described by (5.7) and (5.15), suppose that a sensor fault occurs in the ith subsystem at time T_0, where $i \in \{1, \cdots, M\}$. Assume there exists a symmetric positive definite matrix*

$\hat{P}_i \in \Re^{(n_i-l_i)\times(n_i-l_i)}$, *for* $i = 1, \cdots, M$, *such that,*

1. *the symmetric matrix*

$$\hat{R}_i \stackrel{\triangle}{=} -\mathcal{A}_{i1}^{\top}\hat{P}_i - \hat{P}_i\mathcal{A}_{i1} - 2\hat{P}_i\hat{P}_i > 0\,, \tag{5.50}$$

2. *the matrix* $\hat{Q} \in \Re^{M\times M}$, *whose entries are given by*

$$\hat{Q}_{ij} = \begin{cases} \lambda_{min}(\hat{R}_i)\,, & j = i \\ -||\hat{P}_i||\gamma_{ij}^1 - ||\hat{P}_j||\gamma_{ji}^1\,, & j \neq i,\ j\ =\ 1, \cdots,\ M \end{cases} \tag{5.51}$$

is positive definite, where γ_{ij}^1 *and* γ_{ji}^1 *are the Lipschitz constants defined in (5.5).*

Then, the sensor fault will be detected if there exist some time instant $T_d > T_0$ *and some* $p \in \{1, \cdots l_i\}$, *such that the sensor bias* θ_i *satisfies the following condition*

$$\left|\theta_{ip} - C_{ip}\int_{T_0}^{T_d} e^{\bar{\mathcal{A}}_{i4}(T_d-\tau)}L_i\theta_i d\tau\right| - k_{ip}\int_{T_0}^{T_d} e^{-\lambda_{ip}(T_d-\tau)}\left[|\varrho_i|\,\xi_i\ ||C_i^{-1}\theta_i||_{2\bar{d}} + \sigma_{i2}|C_i^{-1}\theta_i|\right]d\tau$$
$$> \nu_{ip} + N_i(T_d), \tag{5.52}$$

where θ_{ip} *is the pth component of* θ_i, $||(\cdot)||_{2\bar{d}}$ *is the exponentially weighted* L_2 *norm defined in the time interval* $[T_0\,,\ T_d]$ *(see [35]),* ϱ_i *is defined in (5.14), the constant* $\bar{d} \stackrel{\triangle}{=} \lambda_{min}(\hat{Q})/\lambda_{max}(\hat{P})$, *the matrix* $\hat{P} \stackrel{\triangle}{=} \mathrm{diag}\{\hat{P}_1, \cdots, \hat{P}_M\}$, $N_i(T_d) \stackrel{\triangle}{=} k_{ip}\int_{T_0}^{T_d} e^{-\lambda_{ip}(T_d-\tau)}\big[|\varrho_i|\,\phi(\tau) + \bar{\eta}_i\big]d\tau$ *with* $\phi(t) \stackrel{\triangle}{=} \left\{\frac{\bar{V}_0 e^{-\bar{d}t}}{\lambda_{min}(\hat{P})}\right\}^{\frac{1}{2}}$, *and* ξ_i *is a constant to be defined later on in the proof.*

Proof: In the presence of a sensor fault (i.e., for $t \geq T_0$) in the ith subsystem, base on (5.2) and (5.7), the dynamics of the state estimation error $\tilde{z}_{i1} \stackrel{\triangle}{=} z_{i1} - \hat{z}_{i1}$ and $\tilde{z}_{i2} \stackrel{\triangle}{=} z_{i2} - \hat{z}_{i2}$ of the ith FDE satisfies

$$\dot{\tilde{z}}_{i1} = \mathcal{A}_{i1}\tilde{z}_{i1} - \mathcal{A}_{i2}C_i^{-1}\beta_i\theta_i + \sum_{j=1}^{M}\left[H_{ij}^1(z_j, u_j) - H_{ij}^1(\hat{z}_i, u_j)\right] \tag{5.53}$$

$$\dot{\tilde{z}}_{i2} = \bar{\mathcal{A}}_{i4}\tilde{z}_{i2} + \mathcal{A}_{i3}\tilde{z}_{i1} + \rho_{i2}(z_i, u_i) - \rho_{i2}(\hat{z}_i, u_i) + \eta_i - L_i\beta_i\theta_i$$
$$+\sum_{j=1}^{M}\left[H_{ij}^2(z_j, u_j) - H_{ij}^2(\hat{z}_j, u_j)\right]\,. \tag{5.54}$$

First, we consider the Lyapunov function candidate $V_i = \tilde{z}_{i1}^\top \hat{P}_i \tilde{z}_{i1}$. By using a similar reasoning logic as shown in the proof of Lemma 5.2 , we can obtain the time derivative of V_i along the solution of (5.53) as follows:

$$\dot{V}_i \leq -\lambda_{min}(\hat{R}_i)|\tilde{z}_{i1}|^2 + 2\,||\hat{P}_i|| \sum_{j=1}^{M} \gamma_{ij}^1 |\tilde{z}_{i1}||\tilde{z}_{j1}| + \frac{1}{2}|\mathcal{A}_{i2} C_i^{-1} \beta_i \theta_i|^2 \,. \tag{5.55}$$

Second, for the interconnected nth subsystem, where $n \in \{1, \cdots, M\} \backslash \{i\}$, we also define a Lyapunov function candidate $V_n = \tilde{z}_{n1}^\top \hat{P}_n \tilde{z}_{n1}$. It can be shown that

$$\dot{V}_n \leq -\lambda_{min}(\hat{R}_n)|\tilde{z}_{n1}|^2 + 2||\hat{P}_n|| \sum_{j=1}^{M} \gamma_{nj}^1 |\tilde{z}_{n1}|\,|\tilde{z}_{j1}| + \frac{1}{2}[\,\gamma_{ni}^1 |C_i^{-1}\beta_i\theta_i|\,]^2, \tag{5.56}$$

where $\hat{R}_n$ is defined in (5.50).

Finally, we consider an overall Lyapunov function candidate $V = \sum_{j=1}^{M} V_j = \sum_{j=1}^{M} \tilde{z}_{j1}^\top \hat{P}_j \tilde{z}_{j1} = \tilde{z}_1^\top \hat{P} \tilde{z}_1$ for the interconnected systems, where $\hat{P} = \text{diag}\{\hat{P}_1, \cdots, \hat{P}_M\}$ and $\tilde{z}_1$ is defined in (5.11). Based on (5.55) and (5.56), and by following a similar reasoning logic as reported in the proof of Lemma 4.2, we have

$$\dot{V} \leq -\bar{d} V + \frac{1}{2}\Big[\sum_{j=1}^{M} (\gamma_{ji}^1 |C_i^{-1}\beta_i\theta_i|)^2 + ||\mathcal{A}_{i2}||^2 \; |C_i^{-1}\beta_i\theta_i|^2 \Big],$$

where the constant $\bar{d}$ is defined in the theorem. Now, let us consider $\tilde{z}_1$ defined in (5.11). Based on Lemma 4.1, it can be shown that

$$\begin{aligned} |\tilde{z}_1|^2 &\leq \frac{V_0 e^{-\bar{d}t}}{\lambda_{min}(\hat{P})} + \int_0^t e^{-\bar{d}(t-\tau)} \xi_i^2 |C_i^{-1}\beta_i\theta_i|^2 \, d\tau \\ &= \phi^2 + \xi_i^2 (||C_i^{-1}\beta_i\theta_i||_{2\bar{d}})^2 \,, \end{aligned} \tag{5.57}$$

where $\xi_i \triangleq \left\{ \frac{||\mathcal{A}_{i2}||^2 + \sum_{j=1}^{M} (\gamma_{ji}^1)^2}{2\lambda_{min}(\hat{P})} \right\}^{\frac{1}{2}}$, ϕ is defined in the theorem, and the positive constant V_0 is chosen such that $V(0) < V_0$. Based on (5.57), we can obtain

$$|\tilde{z}_1(t)| \leq \phi(t) + \xi_i ||C_i^{-1}\beta_i\theta_i(t)||_{2\bar{d}} \,. \tag{5.58}$$

Now, let us consider each component of the output estimation error, (i.e., $\tilde{y}_{ip} = y_{ip} - \hat{y}_{ip}$, $p = 1, \cdots l_i$). Based on (5.7) and (5.2), we have

$$\begin{aligned}
\tilde{y}_{ip}(t) = \;& C_{ip}\tilde{z}_{i2} + \beta_i\theta_{ip} \\
= \;& C_{ip}\int_0^t e^{\bar{\mathcal{A}}_{i4}(t-\tau)}\Big\{\mathcal{A}_{i3}\,\tilde{z}_{i1} + \rho_{i2}(z_i,u_i) - \rho_{i2}(\hat{z}_i,u_i) + \eta_i \\
& -L_i\beta_i\theta_i + \sum_{j=1}^{M}[H_{ij}^2(z_j,u_j) - H_{ij}^2(\hat{z}_j,u_j)]\Big\}d\tau + \beta_i\theta_{ip}\,.
\end{aligned}$$

Additionally, by using (5.58) and by applying the triangular inequality, we obtain

$$\begin{aligned}
|\tilde{y}_{ip}(t)| \;\geq\; & \left|C_{ip}\int_0^t e^{\bar{\mathcal{A}}_{i4}(t-\tau)}(-L_i\beta_i\theta_i)d\tau + \beta_i\theta_{ip}\right| \\
& -k_{ip}\int_0^t e^{-\lambda_{ip}(t-\tau)}\left[|\varrho_i|\,\xi_i||C_i^{-1}\beta_i\theta_i||_{2\bar{d}} + \sigma_{i2}|C_i^{-1}\beta_i\theta_i|\right]d\tau \\
& -k_{ip}\int_0^t e^{-\lambda_{ip}(t-\tau)}(|\varrho_i|\,\phi + \bar{\eta}_i)d\tau, \qquad (5.59)
\end{aligned}$$

where ϱ_i is defined in (5.14). Now, based on (5.59) and the step function β_i, it can be easily seen that if there exists $T_d > T_0$, such that condition (5.52) is satisfied, then it is concluded that $|\tilde{y}_{ip}(T_d)| > \nu_{ip}(T_d)$, i.e., the fault is detected at time $t = T_d$.

5.4.2 Stability and Learning Capability

Theorem 5.3 (Stability and Learning Capability): *Suppose that a sensor fault occurs in the sth subsystem at time T_0, where $s \in \{1, \cdots, M\}$. Then, the distributed fault isolation scheme described by (5.16)-(5.20) and (5.49) guarantees that,*

- *for each local fault isolation estimator q, $q = 1, \cdots, M$, the estimate variables $\hat{z}_{q1}(t)$, $\hat{z}_{q2}(t)$, and $\hat{\theta}_q(t)$ are uniformly bounded;*
- *there exist a positive constant $\bar{\kappa}_s$ and a bounded function $\bar{\zeta}_s(t)$, such that, for all finite time $t_f > T_d$, the output estimation error of the matched sth local isolation estimator*

satisfies

$$\int_{T_d}^{t_f} |\tilde{y}_s(t)|^2 dt \;\leq\; \bar{\kappa}_s + 2\int_{T_d}^{t_f} |\bar{\zeta}_s(t)|^2 dt\,. \tag{5.60}$$

where $\bar{\zeta}_s(t)$ *and* $\bar{\kappa}_s$ *are related to the modeling uncertainty, the estimation errors.*

Proof. Let us consider the signal boundedness property. The state estimation error and output estimation error of the FIE associated with the qth subsystem are defined as $\tilde{z}_{q1} \triangleq z_{q1}(t) - \hat{z}_{q1}(t)$, $\tilde{z}_{q2}(t) \triangleq z_{q2}(t) - \hat{z}_{q2}(t)$, and $\tilde{y}_q \triangleq y_q(t) - \hat{y}_q(t)$, respectively.

First, consider the FIE associated with sth subsystem (i.e., $q = s$). By using (5.24) and the similar reasoning logic as reported in the proof of Lemma 5.3 (see (5.44)), respectively, we obtain

$$\dot{\bar{z}}_{q1} = \mathcal{A}_{q1}\bar{z}_{q1} + \sum_{j=1}^{M}\left[H_{qj}^1(z_j,u_j) - H_{qj}^1(\hat{z}_j,u_j)\right] - \Omega_{q1}\dot{\theta}_q \tag{5.61}$$

$$\begin{aligned}\dot{\bar{z}}_{q2} &= \bar{\mathcal{A}}_{q4}\bar{z}_{q2} + \mathcal{A}_{q3}\tilde{z}_{q1} + \eta_q - \Omega_{q2}\dot{\theta}_q + \rho_{q2}(z_q,u_q) \\ &\quad - \rho_{q2}(\hat{z}_q,u_q) + \sum_{j=1}^{M}\left[H_{qj}^2(z_j,u_j) - H_{qj}^2(\hat{z}_j,u_j)\right],\end{aligned} \tag{5.62}$$

where $\bar{z}_{q1} \triangleq \tilde{z}_{q1} + \Omega_{q1}\tilde{\theta}_q$ and $\bar{z}_{q2} \triangleq \tilde{z}_{q2} + \Omega_{q2}\tilde{\theta}_q$. Note that (5.61) is in the same form as (5.24). Thus, based on the results of Lemma 5.2 (i.e., (5.28)), Assumption 5.2 and Assumption 5.6, we have $\bar{z}_{q1} \in L_\infty$ and $\bar{z}_{j1} \in L_\infty$. Moreover, due to the use of parameter projection (see (5.21)), we have $\hat{\theta}_q \in L_\infty$ and $\hat{\theta}_j \in L_\infty$. Therefore, based on Assumption 5.3 and the definition of $\bar{z}_{q1}$ and $\bar{z}_{j1}$, we know that $\tilde{z}_{q1} \in L_\infty$, $\tilde{z}_{j1} \in L_\infty$, $\hat{z}_{q1} \in L_\infty$ and $\hat{z}_{j1} \in L_\infty$. Additionally, based on Lemma 4.3, we know that $\rho_{q2}(z_q,u_q) - \rho_{q2}(\hat{z}_q,u_q)$ and $H_{qj}^2(z_j,u_j) - H_{qj}^2(\hat{z}_j,u_j)$ are bounded. Furthermore, because η_q, Ω_{q2} and $\dot{\theta}_q$ are bounded (Assumption 5.2 and Assumption 5.6) and $\bar{\mathcal{A}}_{q4}$ is stable, by using (5.62), we can obtain $\bar{z}_{q2} \in L_\infty$. Owning to the definition of $\bar{z}_{q2}$, we conclude that $\tilde{z}_{q2} \in L_\infty$ and $\hat{z}_{q2} \in L_\infty$.

Second, let us consider the FIEs associated with healthy subsystems (i.e., $q \in \{1,\cdots,M\}\backslash\{s\}$,). By using the similar reasoning logic as reported in the proof of Lemma 5.2 and Lemma 5.3

(see (5.35) and (5.44)), we have

$$\begin{aligned}
\dot{\bar{z}}_{q1} &= \mathcal{A}_{q1}\bar{z}_{q1} + \sum_{j=1}^{M}\left[H_{qj}^{1}(z_j,u_j) - H_{qj}^{1}(\hat{z}_j,u_j)\right] \\
\dot{\bar{z}}_{q2} &= \bar{\mathcal{A}}_{q4}\bar{z}_{q2} + \mathcal{A}_{q3}\tilde{z}_{q1} + \eta_q + \rho_{q2}(z_q,u_q) - \rho_{q2}(\hat{z}_q,u_q) + \sum_{j=1}^{M}\left[H_{qj}^{2}(z_j,u_j) - H_{qj}^{2}(\hat{z}_j,u_j)\right] ,
\end{aligned}$$

where $\bar{z}_{q1} \stackrel{\triangle}{=} \tilde{z}_{q1} + \Omega_{q1}\hat{\theta}_q$ and $\bar{z}_{q2} \stackrel{\triangle}{=} \tilde{z}_{q2} + \Omega_{q2}\hat{\theta}_q$. Then, based on a similar reasoning logic as reported above, we can conclude that $\bar{z}_{q1} \in L_\infty$, $\hat{\theta}_q \in L_\infty$, $\hat{z}_{q1} \in L_\infty$, $\bar{z}_{q2} \in L_\infty$, and $\hat{z}_{q2} \in L_\infty$. This concludes the first part of the theorem.

Next, in the case that the qth FIE matches the occurred sensor fault in the sth subsystem, i.e., $q = s$, the proof of the second part of the theorem concerning the learning capability of the qth FIE follows similar reasoning logic in [85] and is omitted here due to space limitation.

□

Theorem 5.3 guarantees the boundedness of all the variables involved in the local adaptive FIEs in the presence of a sensor fault in the sth subsystem. Moreover, the performance measure given by (5.60) shows that the ability of the matched local isolation estimator to learn the post-fault system dynamics is limited by the L_2 norm of $\bar{\zeta}_s(t)$, which, in turn, is related to the modeling uncertainty η_s, the parameter estimation error $\tilde{\theta}_s$, the rate of change of the time–varying bias θ_s, and the estimation error of the interconnection term.

5.5 Simulation Results

In this section, a simulation example of interconnected inverted pendulums mounted on carts [32] shown in Figure 3.1 is chosen to illustrate the effectiveness of the distributed FDI algorithm. Specifically, we consider three identical inverted pendulums mounted on carts, which are connected by springs and dampers. Each cart is linked by a transmission belt to

a drive wheel driven by a DC motor. As described in [32], the equations of motion are

$$\begin{aligned}(M+m)\ddot{\psi}_i + F_\psi\dot{\psi}_i + ml\ddot{\vartheta}_i cos\vartheta_i - ml(\dot{\vartheta}_i)^2 sin\vartheta_i &= u_i + s_i \\ J\ddot{\vartheta}_i + F_\vartheta\dot{\vartheta}_i - mlgsin\vartheta_i + ml\ddot{\psi}_i cos\vartheta_i &= 0\end{aligned}$$

where, for each subsystem, ψ_i $(i = 1, 2, 3)$ is the position of the cart, ϑ_i is the angle of the pendulum, u_i is the input force to the carts, respectively. The interconnection forces due to springs and dampers are $s_1 = k(\psi_2-\psi_1)+c(\dot{\psi}_2-\dot{\psi}_1)$, $s_2 = k(\psi_1+\psi_3-\psi_2)+c(\dot{\psi}_1+\dot{\psi}_3-\dot{\psi}_2)$, and $s_3 = k(\psi_2 - \psi_3) + c(\dot{\psi}_2 - \dot{\psi}_3)$, where k and c are the spring constant and the damping constant, respectively. Additionally, J is the moment of inertial, M is the mass of the cart, m is rod mass, l is rod length, g is the gravitational acceleration, F_ϑ and F_ψ are the friction coefficients. The model parameters are: $M = 10\,\mathrm{kg}$, $m = 0.535\,\mathrm{kg}$, $J = 0.62\,\mathrm{kg\,m^2}$, $l = 0.365\,\mathrm{m}$, $F_\psi = 0.062\,\mathrm{kg/s}$, $F_\vartheta = 0.09\,\mathrm{kg\,m^2}$ and $g = 9.8\,\mathrm{m/s^2}$, $k = 1.5$, and $c = 0.2$.

For each subsystem, we assume the cart position, pendulum angle, and pendulum angular velocity are measured. By using a change of coordinates defined by $x_i = [x_{i1}\ x_{i2}\ x_{i3}\ x_{i4}]^\top = T_i[\psi_i\ \vartheta_i\ \dot{\psi}_i\ \dot{\vartheta}_i]^\top$ with $T_i = [-1.5\ \ 0\ \ 1.5\ \ 3.175/\cos\vartheta_i;\ 1\ \ 0\ \ 0\ \ 0;\ 0\ \ 1\ \ 0\ \ 0;\ 0\ \ 0\ \ 0\ \ 1]$, a state space model in the form of (5.2) can be obtained.

The modeling uncertainty is assumed to be up to 5% inaccuracy in the friction constant F_ψ (In the simulation, the actual modeling uncertainty considered is 2% inaccuracy). We consider a sensor fault which may occur to the first output of the ith subsystem, i.e., a constant bias in y_{i1} with $\theta_{i1} \in [\,0,\ 0.4\,]$.

Figure 5.1, Figure 5.2, and Figure 5.3 show the simulation results when a constant bias with $\theta_2 = [\,0.3\ 0\ 0\,]^\top$ occurs in the second subsystem at $T_2 = 5$ second. Specifically, the fault detection residual (solid line) associated with $\dot{\vartheta}_i$ and its threshold (dashed line) generated by each local FDE are shown in Figure 5.1. As can be seen, the fault is detected almost immediately by each FDE. Then, the three local FIEs are activated to determine the particular faulty subsystem. Selected fault isolation residuals (solid line) and the corresponding thresholds (dashed line) generated by the FIE1 and FIE3 are shown in Figure 5.2.

It can be seen that the residuals associated with $\dot{\vartheta}_i$ generated by FIE 1 and FIE 3 exceed their thresholds at approximately $t = 5.2$ second. Meanwhile, all three residual components (solid line) generated by FIE 2 always remain below their thresholds (dashed line), as shown in Figure 5.3. Thus, we conclude the sensor fault is in subsystem 2. It is worth noting that for FIE 1 and FIE 3, only the residuals and thresholds associated with y_{13} and y_{33} are shown, since it is sufficient to exclude the possibility of occurrence of any sensor fault in subsystem 1 and subsystem 3 based on the presented fault isolation decision scheme.

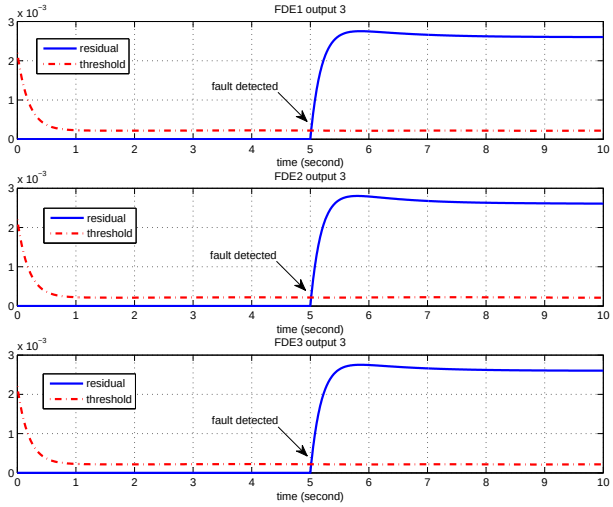

Figure 5.1: Selected detection residual generated by each FDE.

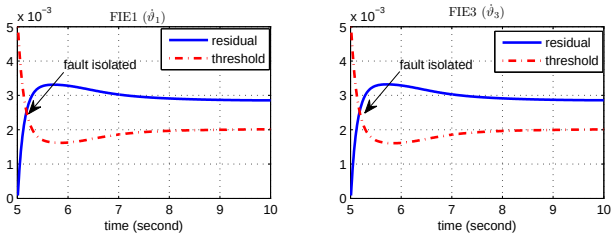

Figure 5.2: Selected isolation residuals generated by FIE 1 and FIE 3 (for subsystems 1 and 3, respectively).

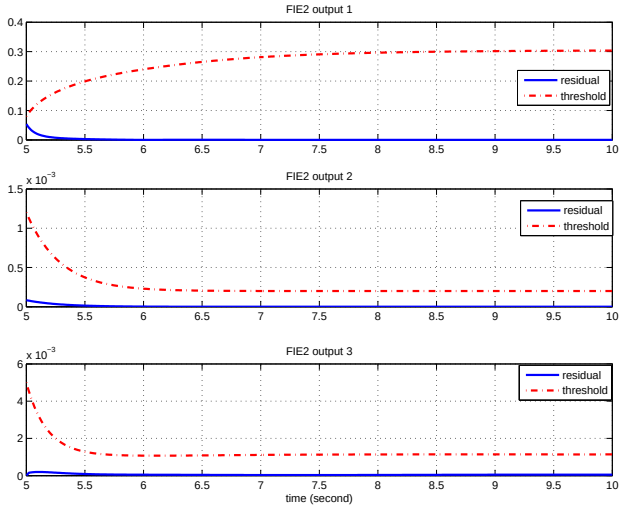

Figure 5.3: Isolation residuals generated by FIE 2 (associated with subsystem 2).

Chapter 6

A Distributed Detection Scheme for Process Faults and Sensor Faults in a Class of Interconnected Nonlinear Uncertain Systems

6.1 Introduction

In the Chapter 3, Chapter 4 and Chapter 5, the design and analysis of distributed faut diagnosis in interconnected input-output nonlinear systems are presented. However, such systems are assumed to satisfy certain structural assumptions. Specifically, the system models considered in the above three chapters are based on the assumptions that the system states in each subsystem can be decomposed into an unknown part and a measurable part. In this chapter, we significantly extend the previous results in the above three chapters by removing this restrictive limitation on system model structure.

In the presented distributed fault detection architecture, a local fault detection component is designed for each subsystem under consideration by utilizing local measurements and

certain communicated information from neighboring fault detection components associated with its directly interconnected subsystems. The distributed fault detection method is presented with an analytical framework aiming at characterizing its important properties. Specifically, the analysis focuses on: (i) derivation of adaptive thresholds for distributed fault detection, ensuring the robustness property with respect to interactions among interconnected subsystems and modeling uncertainty; (ii) investigation of fault detectability conditions, characterizing the class of process faults and sensor faults that are detectable by the proposed method.

This chapter is organized as follows. In Section 6.2, the problem of distributed fault detection for a class of interconnected nonlinear uncertain systems is formulated. Section 6.3 describes the distributed fault detection method, including the design of local fault detection component for each subsystem and the derivation of adaptive thresholds for fault isolation. In Section 6.4, the fault detectability conditions are analyzed, characterizing the class of sensor faults and process faults that are detectable by the proposed method, respectively. Simulation results of an example of multi-machine power systems is presented in Section 6.5.

6.2 Problem Formulation

Consider a nonlinear dynamic system composed of M interconnected subsystems with the dynamics of the ith subsystem, $i = 1, \cdots, M$, being described by the following differential equation

$$\begin{aligned} \dot{x}_i &= A_i x_i + \phi_i(x_i, u_i) + \beta_{ix}(t - T_{ix}) f_i(x_i, u_i) + D_i \eta_i(x_i, u_i, t) + \xi_i(z_i, u_i, t) \\ &\quad + \sum_{j=1}^{M} h_{ij}(y_i, x_j, u_j) \\ y_i &= C_i x_i + \beta_{iy}(t - T_{iy})\theta_i \end{aligned} \tag{6.1}$$

where $x_i \in \Re^{n_i}$, $u_i \in \Re^{m_i}$, and $y_i \in \Re^{l_i}$ are the state vector, input vector, and output vector of the ith subsystem, respectively, $z_i \in \Re^{r_i}$ is the combined state vectors of the

ith subsystem and its directly interconnected subsystems. $\phi_i : \Re^{n_i} \times \Re^{m_i} \mapsto \Re^{n_i}$, $\eta_i : \Re^{n_i} \times \Re^{m_i} \times \Re^{+} \mapsto \Re^{q_i}$, $f_i : \Re^{n_i} \times \Re^{m_i} \mapsto \Re^{n_i}$, $\xi_i : \Re^{r_i} \times \Re^{m_i} \times \Re^{+} \mapsto \Re^{n_i}$, $h_{ij} : \Re^{l_i} \times \Re^{n_j} \times \Re^{m_j} \mapsto \Re^{n_i}$ are smooth vector fields. Specifically, the model given by

$$\begin{aligned} \dot{x}_{Ni} &= A_i x_{Ni} + \phi_i(x_{Ni}, u_i) \\ y_{Ni} &= C_i x_{Ni} \end{aligned}$$

is the *known nominal* model of the ith subsystem with ϕ_i being the known nonlinearity. The modeling uncertainty consists of two parts. First, the vector field η_i in (6.1) represents the modeling uncertainty in the local dynamics of the ith subsystem, and $D_i \in \Re^{n_i \times q_i}$is a modeling uncertainty distribution matrix. Second, the vector field ξ_i in (6.1) represents the modeling uncertainty in the interconnections between the ith subsystem and its directly interconnected subsystems.

The term $\beta_{ix}(t - T_{ix}) f_i(x_i, u_i)$ denotes the changes in the dynamics of ith subsystem due to the occurrence of a process fault in the local subsystem. Specifically, $\beta_{ix}(t - T_{ix})$ describes the time profile of a fault which occurs at some unknown time T_{ix}, and $f_i(x_i, u_i)$ is a nonlinear fault function. The change in the dynamics of ith subsystem due to the occurrence of a sensor fault in the local subsystem is represented by $\beta_{iy}(t - T_0)\theta_i$ in (6.1). Specifically, $\theta_i \in \Re^{l_i}$ represents the magnitude of a constant sensor bias fault, and the function β_{iy} characterize the time profile of the sensor fault in ith subsystem with the unknown fault occurrence time T_{iy}. In this chapter, both the time profile functions $\beta_{ix}(\cdot)$ and $\beta_{ix}(\cdot)$ are considered as a step function β_i (i.e., $\beta_i(t - T_0) = 0$ if $t < T_0$, and $\beta_i(t - T_0) = 1$ if $t \geq T_0$, where $T_0 = T_{ix}$ for process faults, and $T_0 = T_{iy}$ for sensor faults).

The objective of this chapter is to develop a robust distributed fault detection scheme for the class of interconnected nonlinear uncertain systems in the form of (6.1). We consider the case of a single process fault represented by $f_i(x_i, u_i)$ and the case of a single sensor fault represented by θ_i. Note that the sensor fault can possibly affect multiple output components (i.e., $\theta_i \in \Re^{l_i}$). The following assumptions are made throughout this chapter

Assumption 6.1. *The function η_i in (6.1), representing the modeling uncertainty in the*

local dynamics of the ith subsystem, is an unknown nonlinear function of x_i, u_i and t, but bounded. Also, the functions ξ_i in (6.1), describing unknown part of the interaction between ith subsystem and other directly interconnected subsystems, is an unknown nonlinear function of z_i, u_i and t, but bounded. Specifically,

$$\begin{aligned} |\eta_i(x_i, u_i, t)| &\leq \bar{\eta}_i(y_i, u_i, t)\,, \\ |\xi_i(z_i, u_i, t)| &\leq \bar{\xi}_i(y, u_i, t), \end{aligned} \tag{6.2}$$

where y is combined output vectors of the ith subsystem and its directly interconnected subsystems, the the bounding functions $\bar{\eta}_i$ and $\bar{\xi}_i$ are known and uniformly bounded in the corresponding compact sets of admissible state variables, inputs, and outputs with appropriate dimensions, respectively.

Assumption 6.2 *The system state vector x_i of each subsystem remains bounded before and after the occurrence of a fault, i.e., $x_i(t) \in L_\infty$, $\forall t \geq 0$.*

Assumption 6.3 *The nonlinear terms $\phi_i(x_i, u_i)$ in (6.1) satisfy a Lipschitz condition: $\forall u_i \in \mathcal{U}_i$ and $\forall x_i$, $\hat{x}_i \in \mathcal{X}_i$,*

$$|\phi_i(x_i, u_i) - \phi_i(\hat{x}_i, u_i)| \leq \sigma_i |x_i - \hat{x}_i| \tag{6.3}$$

where σ_i is a known Lipschitz constant, $\mathcal{X}_i \subset \Re^{n_i}$ and $\mathcal{U}_i \subset \Re^{m_i}$ are compact sets of admissible state variables and inputs, respectively.

Assumption 6.4 *The interconnection terms $h_{ij}(y_i, x_j, u_j)$ is Lipschitz in x_j with a known Lipschitz constant γ_{ij}, i.e., $\forall x_j$, $\hat{x}_j \in \mathcal{X}_j$,*

$$|h_{ij}(y_i, x_j, u_j) - h_{ij}(y_i, \hat{x}_j, u_j)| \leq \gamma_{ij} |x_j - \hat{x}_j|\,. \tag{6.4}$$

Assumption 6.1 characterize the class of modeling uncertainty under consideration, including various modeling errors in the system's local dynamics and the unknown part of interconnection between subsystems. The bounds on the modeling uncertainties are necessary for distinguishing between the effects of faults and modeling uncertainty (see [79, 84]).

Assumption 6.2 requires the boundedness of the state variables before and after the occurrence of a fault in each subsystem. Hence, it is assumed that the distributed feedback control system is capable of retaining the boundedness of the state variables of each subsystem even in the presence of a fault. This is a technical assumption required for well-posedness since the distributed FDI design under consideration does not influence the closed-loop dynamics and stability. The design of distributed fault-tolerant controllers is beyond the scope of this paper. However, it is important to note that the proposed distributed FDI design does not depend on the structure of the distributed controllers.

Assumption 6.4 requires the nominal interconnection term h_{ij} between subsystems is Lipschitz in x_j. In literature, several examples of distributed nonlinear systems with Lipschitz interconnection terms have been considered (see, for instance, the automated highway system [58], interconnected inverted pendulums [63], and large-scale power systems [25]).

Remark 6.1 The nonlinear fault diagnosis schemes presented in previous papers [82, 84] are based on a *centralized* architecture. In this chapter, the problem of *distributed* fault detection for interconnected nonlinear uncertain systems is investigated. Moreover, in [85, 77, 78], a distributed fault diagnosis method was developed for a class of interconnected nonlinear systems satisfying certain structural assumptions. Moreover, it is assumed the fault only affect measurable state variables. In the dissertation, we consider a class of more general interconnected nonlinear uncertain systems, and the faults are allowed to affect all the state variables.

6.3 Distributed Fault Detection Method

The distributed fault detection architecture is comprised of M local FDE, with one FDE designed for each of the M subsystems. Specifically, each local FDE monitors the corresponding local subsystem to detect the occurrence of any fault.

In this section, we investigate the distributed fault detection method, including the designs of each local FDE for residual generation and the corresponding adaptive thresholds for residual evaluation.

6.3.1 Distributed Fault Detection Estimators

Based on the subsystem model described by (6.1), the FDE for each local subsystem is chosen as:

$$\begin{aligned}\dot{\hat{x}}_i &= A_i\hat{x}_i + \phi_i(\hat{x}_i, u_i) + L_i(y_i - \hat{y}_i) + \sum_{j=1}^{M} h_{ij}(y_i, \hat{x}_j, u_j) + D_i\bar{\eta}_i(y_i, u_i)sgn(E_i\tilde{y}_i) \\ \hat{y}_i &= C_i\hat{x}_i\,, \end{aligned} \tag{6.5}$$

where $\hat{x}_i$ and $\hat{y}_i$ denote the estimated local state and output variables of the ith subsystem, $i = 1, \cdots, M$, respectively, $\tilde{y}_i \stackrel{\triangle}{=} y_i - \hat{y}_i$ denotes the output estimation error, $L_i \in \Re^{n_i \times l_i}$ is a design gain matrix, E_i is a design matrix defined later on (in Lemma 6.2), $\hat{x}_j$ is the estimate of state vector x_j of the jth interconnected subsystem. It is worth noting that the distributed FDE given by (6.5) for the ith subsystem is constructed based on local input and output variables (i.e., u_i and y_i) and the communicated information $\hat{x}_j$ and u_j from the FDE associated with the jth directly interconnected subsystem. Note that many distributed estimation and diagnostic methods in literature allow certain communication among interconnected subsystems (see, e.g., [58, 60, 20]).

For each local FDE, let $\tilde{x}_i \stackrel{\triangle}{=} x_i - \hat{x}_i$ denote the state estimation error of the ith subsystem. Then, before fault occurrence (i.e., for $t < T_0$), by using (6.1) and (6.5), the estimation error dynamics are given by

$$\begin{aligned}\dot{\tilde{x}}_i &= \bar{A}_i\tilde{x}_i + \phi_i(x_i, u_i) - \phi_i(\hat{x}_i, u_i) + \xi_i + \sum_{j=1}^{M}[h_{ij}(y_i, x_j, u_j) - h_{ij}(y_i, \hat{x}_j, u_j)] \\ &\quad + D_i\eta_i - D_i\bar{\eta}_i(y_i, u_i)sgn(E_i\tilde{y}_i) \end{aligned} \tag{6.6}$$

$$\tilde{y}_i = C_i(x_i - \hat{x}_i) = C_i\tilde{x}_i\,, \tag{6.7}$$

where $\bar{A}_i \stackrel{\triangle}{=} A_i - L_iC_i$.

6.3.2 Adaptive Thresholds for Distributed Fault Detection

Next, we investigate the design of adaptive thresholds for distributed fault detection in each subsystem. The following Lemma will be needed in the subsequent analysis:

Lemma 6.1 [35]. *Let* $z(t)$, $r(t) : [0, \infty) \mapsto \Re$. *Then*

$$\dot{z}(t) \leq -\alpha z(t) + r(t), \quad \forall t \geq t_0 \geq 0$$

implies that

$$z(t) \leq e^{-\alpha(t-t_0)} z(t_0) + \int_{t_0}^{t} e^{-\alpha(t-\tau)} r(\tau) d\tau, \quad \forall t \geq t_0 \geq 0$$

for any finite constant α.

Then, a bounding function on the state estimation error vector

$$\tilde{x}(t) \stackrel{\triangle}{=} [(\tilde{x}_1)^\top, \cdots, (\tilde{x}_2)^\top, \cdots, (\tilde{x}_M)^\top]^\top \tag{6.8}$$

before fault occurrence (i.e., for $0 \leq t < T_0$) can be derived. Specifically, we have the following results:

Lemma 6.2 *For the system described by (6.1) and the fault detection estimator described by (6.5). If there exists a symmetric positive definite matrix* $P_i \in \Re^{n_i \times n_i}$, *a gain matrix* $L_i \in \Re^{n_i \times l_i}$, *and a matrix* $E_i \in \Re^{q_i \times l_i}$ *such that,*

$$Q_i \stackrel{\triangle}{=} -\bar{A}_i^\top P_i - P_i \bar{A}_i - (2 + \sum_{j=1}^{M} \gamma_{ij}) P_i P_i - (2\sigma_i ||P_i|| + \sum_{j=1}^{M} \gamma_{ji}) I > 0 \tag{6.9}$$

$$P_i D_i = C_i^\top E_i^\top, \tag{6.10}$$

where I *is the identity matrix,* γ_{ij} *and* γ_{ji} *are the Lipschitz constants introduced in (6.4). Then, for* $0 \leq t < T_0$, *the state estimation error vector* $\tilde{x}(t)$ *defined by (6.8) satisfies*

$$|\tilde{x}|^2 \leq \frac{\bar{V}_0 e^{-at}}{\lambda_{min}(P)} + \frac{1}{2\lambda_{min}(P)} \int_0^t e^{-a(t-\tau)} \sum_{i=1}^{M} |\bar{\xi}_i|^2 \, d\tau \,, \tag{6.11}$$

where the constant $a \triangleq \lambda_{min}(Q)/\lambda_{max}(P)$, $P \triangleq \mathrm{diag}\{P_1, \cdots, P_M\}$, $Q \triangleq \mathrm{diag}\{Q_1, \cdots, Q_M\}$, $\bar{\xi}_i$ *is defined in Assumption 6.1 , and* $\bar{V}_0$ *is a positive constant to be defined later on.*

Proof: For the ith subsystem, let us consider a Lyapunov function candidate $V_i = \tilde{x}_i^\top P_i \tilde{x}_i$. Then the time derivative of V_i along the solution of (6.6) is given by

$$\begin{aligned}\dot{V}_i &= \tilde{x}_i^\top \left[\bar{A}_i^\top P_i + P_i \bar{A}_i\right] \tilde{x}_i + 2\tilde{x}_i^\top P_i \xi_i + 2\tilde{x}_i^\top P_i [D_i \eta_i(x_i, u_i) - D_i \bar{\eta}_i(y_i, u_i) sgn(E_i \tilde{y}_i)] \\ &\quad + 2\tilde{x}_i^\top P_i \sum_{j=1}^{M} [h_{ij}(y_i, x_j, u_j) - h_{ij}(y_i, \hat{x}_j, u_j)] \\ &\quad + 2\tilde{x}_i^\top P_i [\phi_i(x_i, u_i) - \phi_i(\hat{x}_i, u_i)] \,. \end{aligned} \tag{6.12}$$

Based on (6.4), we have

$$\begin{aligned} 2\tilde{x}_i^\top P_i \sum_{j=1}^{M} [h_{ij}(y_i, x_j, u_j) - h_{ij}(y_i, \hat{x}_j, u_j)] &\leq 2|\tilde{x}_i^\top P_i| \sum_{j=1}^{M} \gamma_{ij} |\tilde{x}_j| \\ &\leq \sum_{j=1}^{M} \gamma_{ij} \tilde{x}_i^\top P_i P_i \tilde{x}_i + \sum_{j=1}^{M} \gamma_{ij} \tilde{x}_j^\top \tilde{x}_j \,. \end{aligned} \tag{6.13}$$

Moreover, based on (6.3) and (6.6), we obtain

$$2\tilde{x}_{i1}^\top P_i \left[\phi_i(x_i, u_i) - \phi_i(\hat{x}_i, u_i)\right] \leq 2|\tilde{x}_i| \, ||P_i|| \, \sigma_i \, |\tilde{x}_i| = \tilde{x}_i^\top \left[2\sigma_i ||P_i|| I\right] \tilde{x}_i \,. \tag{6.14}$$

Furthermore, based on (6.10), and by using the property that $(E_i C_i \tilde{x}_i)^\top sgn((E_i C_i \tilde{x}_i)) \geq |E_i C_i \tilde{x}_i|$, we obtain

$$\begin{aligned} 2\tilde{x}_i^\top P_i \left[D_i \eta_i(x_i, u_i) - D_i \bar{\eta}_i(y_i, u_i) sgn(E_i \tilde{y}_i)\right] &= 2(E_i C_i \tilde{x}_i)^\top \eta_i(x_i, u_i) \\ &\quad - 2\bar{\eta}_i(y_i, u_i) \cdot (E_i C_i \tilde{x}_i)^\top sgn(E_i C_i \tilde{x}_i) \\ &\leq 2|E_i C_i \tilde{x}_i| \left[\, |\eta_i(x_i, u_i)| - \bar{\eta}_i(y_i, u_i) \,\right] \\ &\leq 0 \,. \end{aligned} \tag{6.15}$$

Additionally, we have

$$2\tilde{x}_i^\top P_i \xi_i \;\le\; |2P_i\tilde{x}_i|\,|\xi_i| \;\le\; 2\tilde{x}_i^\top P_i P_i \tilde{x}_i + \frac{1}{2}|\bar{\xi}_i|^2\,, \tag{6.16}$$

where $\bar{\xi}_i$ is the upper bound of $|\xi_i|$ defined in Assumption 6.1. By substituting (6.13), (6.14), (6.15) and (6.16) into (6.12), we obtain

$$\dot{V}_i \le \tilde{x}_i^\top \left[\bar{A}_i^\top P_i + P_i\bar{A}_i + 2\sigma_i||P_i||\,I + (2+\sum_{j=1}^{M}\gamma_{ij})P_iP_i\right]\tilde{x}_i + \sum_{j=1}^{M}\gamma_{ij}\tilde{x}_j^\top\tilde{x}_j + \frac{1}{2}|\bar{\xi}_i|^2\,. \tag{6.17}$$

Now, let us consider the following overall Lyapunov function candidate for the interconnected system: $V \stackrel{\triangle}{=} \sum_{i=1}^{M} V_i \;=\; \sum_{i=1}^{M}\tilde{x}_i^\top P_i\tilde{x}_i = \tilde{x}^\top P\tilde{x},$ where P is defined in Lemma 6.2. Let us denote $\Gamma \stackrel{\triangle}{=} \mathrm{diag}\{\sum_{j=1}^{M}\gamma_{j1},\cdots,\sum_{j=1}^{M}\gamma_{jM}\}$ and $R \stackrel{\triangle}{=} \mathrm{diag}\{R_1,\cdots,R_M\}$, where

$$R_i \stackrel{\triangle}{=} \bar{A}_i^\top P_i + P_i\bar{A}_i + (2+\sum_{j=1}^{M}\gamma_{ij})P_iP_i + 2\sigma_i||P_i||\,I. \tag{6.18}$$

Therefore, based on (6.17) and (6.9), we have

$$\dot{V} \le \tilde{x}^\top R\tilde{x} + \tilde{x}^\top\Gamma\tilde{x} + \sum_{i=1}^{M}\frac{1}{2}|\bar{\xi}_i|^2 = -\tilde{x}^\top Q\tilde{x} + \sum_{i=1}^{M}\frac{1}{2}|\bar{\xi}_i|^2\,, \tag{6.19}$$

where the matrix Q is defined by (6.9). By using the Rayleigh principle (i.e., $\lambda_{min}(P)|\tilde{x}|^2 \le V(t) \le \lambda_{max}(P)|\tilde{x}|^2$) and the definition of $V(t)$, we have

$$\dot{V} \le -\lambda_{min}(Q)|\tilde{x}|^2 + \sum_{i=1}^{M}\frac{1}{2}|\bar{\xi}_i|^2 \le -aV + \sum_{i=1}^{M}\frac{1}{2}|\bar{\xi}_i|^2\,, \tag{6.20}$$

where $\tilde{x}$ and the constant a are defined in (6.8) and Lemma 6.2, respectively. Now, based on Lemma 6.1, it can be easily shown that

$$V(t) \le V(0)e^{-at} + \frac{1}{2}\int_0^t e^{-a(t-\tau)}\sum_{i=1}^{M}|\bar{\xi}_i|^2\,d\tau\,.$$

Note that we can always choose a positive constant $\bar{V}_0$ such that $V(0) < \bar{V}_0$. Thus, based on the definition of $V(t)$ and the Rayleigh principle, the proof of (6.11) can be immediately concluded. □

Remark 6.2: Note that conditions (6.9) and (6.10) can be transformed into standard linear matrix inequalities (See , e.g., [69, 76]). Then, a feasible solution to (6.9) and (6.10) can possibly be found by using the linear matrix inequality (LMI) toolbox.

Specifically, the following procedure can be adopted:

- By using the Schur complements, the nonlinear inequalities $-\bar{A}_i^\top P_i - P_i\bar{A}_i - (2 + \sum_{j=1}^{M}\gamma_{ij})P_iP_i - (2\sigma_i||P_i|| + \sum_{j=1}^{M}\gamma_{ji})I > 0$ can be converted to a LMI form as

$$\begin{bmatrix} -\bar{A}_i^\top P_i - P_i\bar{A}_i - 2\sigma_i\varsigma_i I - \sum_{j=1}^{M}\gamma_{ji} I & (2 + \sum_{j=1}^{M}\gamma_{ij})^{\frac{1}{2}} P_i \\ (2 + \sum_{j=1}^{M}\gamma_{ij})^{\frac{1}{2}} P_i & I \end{bmatrix} > 0 \tag{6.21}$$

  and

$$\begin{bmatrix} \varsigma_i I & P_i \\ P_i & \varsigma_i I \end{bmatrix} > 0\,, \tag{6.22}$$

  where ς_i is a positive constant. Then, a suitable solution of P_i can be obtained by solving (6.21) and (6.22) using the LMI toolbox.

- Based on the matrix P_i found in the above step, the matrix E_i can be obtained by using (6.10).

Now, we analyze the output estimation error $\tilde{y}_i(t)$ (see (6.7)) of the ith subsystem. For $0 \le t < T_0$, the solution of (6.6) is given by

$$\begin{aligned} \tilde{x}_i(t) &= \int_0^t e^{\bar{A}_i(t-\tau)}\left[\phi_i(x_i,u_i) - \phi_i(\hat{x}_i,u_i) + \xi_i + D_i\eta_i(x_i,u_i) - D_i\bar{\eta}_i(y_i,u_i)sgn(E_i\tilde{y}_i)\right]d\tau \\ &\quad + \int_0^t e^{\bar{A}_i(t-\tau)}\sum_{j=1}^{M}\left[h_{ij}(y_i,x_j,u_j) - h_{ij}(y_i,\hat{x}_j,u_j)\right]d\tau\,. \end{aligned} \tag{6.23}$$

Therefore, for each component of the output estimation error, i.e., $\tilde{y}_{ip}(t) \stackrel{\triangle}{=} C_{ip}\tilde{x}_i(t)$, $p = 1, \cdots, l_i$, where C_{ip} is the pth row vector of matrix C_i, by applying the triangle inequality, we have

$$\begin{aligned} |\tilde{y}_{ip}(t)| \;\leq\; & \left| \int_0^t C_{ip} e^{\bar{A}_i(t-\tau)} \left[\phi_i(x_i, u_i) - \phi_i(\hat{x}_i, u_i) + \xi_i\right] d\tau \right| \\ & + \left| \int_0^t C_{ip} e^{\bar{A}_i(t-\tau)} \sum_{j=1}^{M} [h_{ij}(y_i, x_j, u_j) - h_{ij}(y_i, \hat{x}_j, u_j)] d\tau \right| \\ & + \left| \int_0^t C_{ip} e^{\bar{A}_i(t-\tau)} [D_i \eta_i(x_i, u_i) - D_i \bar{\eta}_i(y_i, u_i) sgn(E_i \tilde{y}_i)] d\tau \right|. \end{aligned}$$

Therefore, based on (6.2), (6.3), (6.4), and (6.6), we have

$$|\tilde{y}_{ip}(t)| \leq k_{ip} \int_0^t e^{-\lambda_{ip}(t-\tau)} \left[\sigma_i \, |\tilde{x}_i| + 2||D_i|| \, \bar{\eta}_i + |\xi_i| + \sum_{j=1}^{M} \gamma_{ij} |\tilde{x}_j| \right] d\tau \,, \tag{6.24}$$

where k_{ip} and λ_{ip} are positive constants chosen such that $|C_{ip} e^{\bar{A}_i t}| \leq k_{ip} e^{-\lambda_{ip} t}$ (since $\bar{A}_i$ is stable, constants k_{ip} and λ_{ip} satisfying the above inequality always exist [35]). By defining

$$\varrho_i \stackrel{\triangle}{=} [\gamma_{i1}, \, \cdots \, , \gamma_{i(i-1)}, \, \sigma_i, \, \gamma_{i(i+1)}, \, \cdots \, , \gamma_{iM}]^\top \,, \tag{6.25}$$

(that is, the components of ϱ_i are given by $\varrho_{ii} = \sigma_i$, and $\varrho_{ij} = \gamma_{ij}$ for $j \neq i$), the inequality (6.24) can be rewritten as

$$|\tilde{y}_{ip}(t)| \leq k_{ip} \int_0^t e^{-\lambda_{ip}(t-\tau)} \left[|\varrho_i| \, |\tilde{x}| \; + \; 2||D_i|| \, \bar{\eta}_i + \bar{\xi}_i \right] d\tau. \tag{6.26}$$

Now, based on (6.26) and (6.11), we obtain

$$|\tilde{y}_{ip}(t)| \leq k_{ip} \int_0^t e^{-\lambda_{ip}(t-\tau)} \left[|\varrho_i| \, \chi(\tau) + 2||D_i|| \, \bar{\eta}_i + \bar{\xi}_i \right] d\tau \,.$$

where

$$\chi(t) \stackrel{\triangle}{=} \left\{ \frac{\bar{V}_0 e^{-at}}{\lambda_{min}(P)} + \frac{1}{2\lambda_{min}(P)} \int_0^t e^{-a(t-\tau)} \sum_{i=1}^{M} |\bar{\xi}_i|^2 \, d\tau \right\}^{\frac{1}{2}} . \tag{6.27}$$

Therefore, based on the above analysis, we have the following result

Distributed Fault Detection Decision Scheme: *The decision on the occurrence of a fault (detection) in the ith subsystem is made when the modulus of at least one component of the output estimation error (i.e., $\tilde{y}_{ip}(t)$) generated by the local FDE exceeds its corresponding threshold $\nu_{ip}(t)$ given by*

$$\nu_{ip}(t) \triangleq k_{ip} \int_0^t e^{-\lambda_{ip}(t-\tau)} \left[|\varrho_i| \, \chi(\tau) + 2||D_i|| \, \bar{\eta}_i + \bar{\xi}_i \right] d\tau. \tag{6.28}$$

The fault detection time T_d is defined as the first time instant such that $|\tilde{y}_{ip}(T_d)| > \nu_{ip}(T_d)$, for some $T_d \geq T_0$ and some $p \in \{1, \cdots, l_i\}$, that is, $T_d \triangleq \inf \bigcup_{p=1}^{l_i} \{ t \geq 0 : \ |\tilde{y}_{ip}(t)| > \nu_{ip}(t) \}$.

Remark 6.3 It is worth noting that $\nu_{ip}(t)$ given by (6.28) is an adaptive threshold for fault detection, which has obvious advantage over a constant one. Moreover, the threshold $\nu_{ip}(t)$ can be easily implemented using linear filtering techniques [83]. Additionally, the constants $\bar{V}_0$ in (6.27) is a (possibly conservative) bound for the unknown initial conditions $V(0)$. However, note that, since the effect of this bound decreases exponentially (i.e., it is multiplied by e^{-at}), the practical use of such a conservative bound will not affect significantly the performance of the distributed fault detection algorithm.

6.4 Fault Detectability Analysis

As is well known in the fault diagnosis literature, there is an inherent tradeoff between robustness and fault sensitivity. Below, we studied the fault detectability property of the proposed distributed fault detection method, which characterizes the class of detectable sensor faults and process faults.

6.4.1 Sensor Fault Detectability Condition

In this section, the fault detectability condition of sensor faults are derived. Specifically, the following theorem characterizes the class of sensor faults that are detectable by the proposed distributed fault detection method.

Theorem 6.1: *For the distributed fault detection method described by (6.5) and (6.28), suppose that a sensor fault occurs in the ith subsystem at time T_{iy}, where $i \in \{1, \cdots, M\}$. Then, if there exist some time instant $T_d > T_{iy}$ and some $p \in \{1, \cdots, l_i\}$, such that the sensor bias θ_i satisfies*

$$|\theta_i| \geq \frac{1}{N_i(T_d)} \left[\left| \frac{C_{ip}|\varrho_i|}{\sqrt{2\lambda_{min}(P)}} \int_{T_{iy}}^{T_d} e^{\bar{A}_i(t-\tau)} ||\bar{\xi}_i||_{2a} d\tau \right| + 2\nu_{ip}(T_d) \right], \tag{6.29}$$

where $||(\cdot)||_{2a}$ is the exponentially weighted L_2 norm [35],

$$N_i(t) \triangleq \left| C_{ip} \int_{T_{iy}}^{t} e^{\bar{A}_i(t-\tau)} L_i d\tau - F_{ip} \right| - \left| \frac{C_{ip}|\varrho_i|}{\sqrt{a\lambda_{min}(P)}} \int_{t_{iy}}^{t} e^{\bar{A}_i(t-\tau)} ||L_i|| d\tau \right|,$$

and F_{ip} is a constant matrix defined later on in the proof. Then, the sensor fault will be detected at time $t = T_d$, i.e., $|\tilde{y}_{ip}(T_d)| > \nu_{ip}(T_d)$.

Proof: In the presence of a sensor fault (i.e., for $t \geq T_{iy}$) in ith subsystem, base on (6.1) and (6.5), the dynamics of the state estimation error $\tilde{x}_i \triangleq x_i - \hat{x}_i$ satisfies

$$\begin{aligned} \dot{\tilde{x}}_i &= \bar{A}_i \tilde{x}_i + \phi_i(x_i, u_i) - \phi_i(\hat{x}_i, u_i) + \xi_i + D_i \eta_i(x_i, u_i) - D_i \bar{\eta}_i(y_i, u_i) sgn(E_i \tilde{y}_i) - L_i \beta_{iy} \theta_i \\ &\quad + \sum_{j=1}^{M} [h_{ij}(y_i, x_j, u_j) - h_{ij}(y_i, \hat{x}_j, u_j)] \end{aligned} \tag{6.30}$$

$$\tilde{y}_i = C_i \tilde{x}_i + \beta_{iy} \theta_i \tag{6.31}$$

First, let us consider the Lyapunov function candidate $V_i = \tilde{x}_i^\top P_i \tilde{x}_i$ for the ith subsystem. By following similar reasoning logic as reported in the proof of Lemma 6.2, we can show that the time derivative of V_i along the solution of (6.30) satisfies

$$\dot{V}_i \leq \tilde{x}_i^\top R_i \tilde{x}_i + \sum_{j=1}^{M} \gamma_{ij} \tilde{x}_j^\top \tilde{x}_j + \frac{1}{2} |\xi_i - L_i \beta_{iy} \theta_i|^2,$$

where R_i is defined in (6.18). Note that

$$|\xi_i - L_i \beta_{iy} \theta_i|^2 \leq (|\xi_i| + |L_i \beta_{iy} \theta_i|)^2 \leq 2(|\bar{\xi}_i|^2 + |L_i \beta_{iy} \theta_i|^2).$$

Then, based on two above inequalities, we have:

$$\dot{V}_i \leq \tilde{x}_i^\top R_i \tilde{x}_i + \sum_{j=1}^{M} \gamma_{ij} \tilde{x}_j^\top \tilde{x}_j + |\xi_i|^2 + |L_i \beta_{iy} \theta_i|^2 \,. \tag{6.32}$$

Second, for the interconnected kth subsystem which is healthy, where $k \in \{1, \cdots, M\} \backslash \{i\}$, we also define a Lyapunov function $V_k = \tilde{x}_k^\top P_k \tilde{x}_k$. Analogously, the time derivative of V_k along the solution of (6.6) satisfies:

$$\dot{V}_k \leq \tilde{x}_k^\top R_k \tilde{x}_k + \sum_{j=1}^{M} \gamma_{kj} \tilde{x}_j^\top \tilde{x}_j + \frac{1}{2} |\bar{\xi}_k|^2 \,. \tag{6.33}$$

Next, we consider an overall Lyapunov function candidate $V = \sum_{j=1}^{M} V_j = \sum_{j=1}^{M} \tilde{x}_j^\top P_j \tilde{x}_j = \tilde{x}^\top P \tilde{x}$ for all the interconnected subsystems, where $P = \text{diag}\{P_1, \cdots, P_M\}$, and $\tilde{x}$ is defined in (6.8). From (6.32) and (6.33), we have

$$\dot{V} \leq -\tilde{x}^\top Q \tilde{x} + \sum_{i=1}^{M} \frac{1}{2} |\bar{\xi}_i|^2 + \frac{1}{2} |\bar{\xi}_i|^2 + |L_i \beta_{iy} \theta_i|^2 \,. \tag{6.34}$$

where Q is defined in Lemma 6.2.

Then, by following similar reasoning logic as reported in the proof of Lemma 6.2, based on (6.34), we can obtain:

$$|\tilde{x}|^2 \leq \frac{\bar{V}_0 e^{-at}}{\lambda_{min}(P)} + \frac{1}{2\lambda_{min}(P)} \int_0^t e^{-a(t-\tau)} \sum_{i=1}^{M} |\bar{\xi}_i|^2 d\tau + \frac{1}{\lambda_{min}(P)} \int_0^t e^{-a(t-\tau)} \left(\frac{|\bar{\xi}_i|^2}{2} + |L_i \beta_{iy} \theta_i|^2 \right) d\tau \,. \tag{6.35}$$

By substituting (6.27) into (6.35), we have

$$\begin{aligned} |\tilde{x}|^2 &\leq \chi^2 + \frac{1}{\lambda_{min}(P)} \int_0^t e^{-a(t-\tau)} \left(\frac{|\bar{\xi}_i|^2}{2} + |L_i \beta_{iy} \theta_i|^2 \right) d\tau \\ &\leq \chi^2 + \frac{1}{\lambda_{min}(P)} \int_0^t e^{-a(t-\tau)} \left(\frac{|\bar{\xi}_i|}{\sqrt{2}} + |L_i \beta_{iy} \theta_i| \right)^2 d\tau \,. \end{aligned} \tag{6.36}$$

From (6.36), we know

$$\begin{aligned} |\tilde{x}| &\leq \left\{ \frac{1}{\lambda_{min}(P)} \int_0^t e^{-a(t-\tau)} (\frac{|\bar{\xi}_i|}{\sqrt{2}} + |L_i \beta_{iy} \theta_i|)^2 \, d\tau \right\}^{\frac{1}{2}} + \chi \\ &= \chi + \frac{1}{\sqrt{\lambda_{min}(P)}} \big|\big| (\frac{|\bar{\xi}_i|}{\sqrt{2}} + |L_i \beta_{iy} \theta_i|) \big|\big|_{2a} , \end{aligned} \tag{6.37}$$

where $||(\cdot)||_{2a}$ is the exponentially weighted L_2 norm [35]. By using the property $||x+y||_{2a} \leq ||x||_{2a} + ||y||_{2a}$, the above inequality can be rewritten as

$$|\tilde{x}| \leq \chi + \frac{||\bar{\xi}_i||_{2a}}{\sqrt{2\lambda_{min}(P)}} + \frac{||L_i \beta_{iy} \theta_i||_{2a}}{\sqrt{\lambda_{min}(P)}} . \tag{6.38}$$

Note that

$$||L_i \beta_{iy} \theta_i||_{2a} = \left\{ \frac{|L_i \beta_{iy} \theta_i|^2}{a} (1 - e^{-at}) \right\}^{\frac{1}{2}} \leq \frac{||L_i \beta_{iy}|| \, |\theta_i|}{\sqrt{a}} .$$

Thus, we have

$$|\tilde{x}| \leq \chi + \frac{||\bar{\xi}_i||_{2a}}{\sqrt{2\lambda_{min}(P)}} + \frac{||L_i \beta_{iy}|| \, |\theta_i|}{\sqrt{a \lambda_{min}(P)}} . \tag{6.39}$$

Now we analyze the output estimation error. Specifically, for each component of the output estimation error, i.e., $\tilde{y}_{ip}(t) \triangleq C_{ip} \tilde{x}_i(t) + \beta_{iy} F_{ip} \theta_i$, where for the constant matrix $F_{ip} \in \Re^{l_i \times l_i}$, only its $(p,\ p)$th entry takes the value of 1 , while all the remaining entries are 0. Based on (6.30) and (6.31), we have

$$\begin{aligned} \tilde{y}_{ip} &= C_{ip} \int_0^t e^{\bar{A}_i (t-\tau)} \big[- L_i \beta_{iy} \theta_i + \xi_i + \sum_{j=1}^{M} [h_{ij}(y_i, x_j, u_j) - h_{ij}(y_i, \hat{x}_j, u_j)] \big] d\tau + \beta_{iy} F_{ip} \theta_i \\ &\quad + [\phi_i(x_i, u_i) - \phi_i(\hat{x}_i, u_i)] + C_{ip} \int_0^t e^{\bar{A}_i (t-\tau)} \Big[D_i \eta_i(x_i, u_i) - D_i \bar{\eta}_i(y_i, u_i) sgn(E_i \tilde{y}_i) \Big] d\tau . \end{aligned}$$

By applying the triangle inequality, based on Assumption 6.1, Assumption 6.3 and Assump-

tion 6.4, we obtain:

$$|\tilde{y}_{ip}(t)| \geq \left| \int_0^t C_{ip} e^{\bar{A}_i(t-\tau)} L_i \beta_{iy} \theta_i d\tau - \beta_{iy} F_{ip} \theta_i \right| - \left| \int_0^t C_{ip} e^{\bar{A}_i(t-\tau)} \big[|\varrho_i||\tilde{x}| + D_i \eta_i - D_i \bar{\eta}_i sgn(E_i \tilde{y}_i) + \xi_i \big] d\tau \right|, \quad (6.40)$$

where ϱ_i is defined in (6.25). Then by using (6.39) and (6.40), we have

$$|\tilde{y}_{ip}(t)| \geq \left| \int_0^t C_{ip} e^{\bar{A}_i(t-\tau)} L_i \beta_{iy} \theta_i d\tau - \beta_{iy} F_{ip} \theta_i \right| - \left| \int_0^t C_{ip} e^{\bar{A}_i(t-\tau)} \big[|\varrho_i| \chi + 2||D_i||\, \bar{\eta}_i + \bar{\xi}_i \big] d\tau \right| - \left| \int_0^t C_{ip} e^{\bar{A}_i(t-\tau)} \frac{|\varrho_i|\, ||\bar{\xi}_i||_{2a}}{\sqrt{2\lambda_{min}(P)}} d\tau \right| - \left| \int_0^t C_{ip} e^{\bar{A}_i(t-\tau)} \frac{|\varrho_i|\, ||L_i \beta_{iy}||\, |\theta_i|}{\sqrt{a\lambda_{min}(P)}} d\tau \right|. \quad (6.41)$$

By rearranging the terms involving θ_i and by substituting (6.28) into (6.41), we have

$$|\tilde{y}_{ip}(t)| \geq \left| \int_0^t C_{ip} e^{\bar{A}_i(t-\tau)} L_i \beta_{iy} d\tau - \beta_{iy} F_{ip} \right| |\theta_i| - \left| \frac{|\varrho_i|}{\sqrt{a\lambda_{min}(P)}} \int_0^t C_{ip} e^{\bar{A}_i(t-\tau)} ||L_i \beta_{iy}|| d\tau \right| |\theta_i| - \left| \frac{|\varrho_i|}{\sqrt{2\lambda_{min}(P)}} \int_0^t C_{ip} e^{\bar{A}_i(t-\tau)} ||\bar{\xi}_i||_{2a} d\tau \right| - \nu_{ip}\,. \quad (6.42)$$

Based on the property of the step function β_{iy}, we can rewrite the above inequality as follows:

$$|\tilde{y}_{ip}(t)| \geq \left| \int_{T_{iy}}^t C_{ip} e^{\bar{A}_i(t-\tau)} L_i d\tau - F_{ip} \right| |\theta_i| - \left| \frac{|\varrho_i|}{\sqrt{a\lambda_{min}(P)}} \int_{T_{iy}}^t C_{ip} e^{\bar{A}_i(t-\tau)} ||L_i|| d\tau \right| |\theta_i| - \left| \frac{|\varrho_i|}{\sqrt{2\lambda_{min}(P)}} \int_0^t C_{ip} e^{\bar{A}_i(t-\tau)} ||\bar{\xi}_i||_{2a} d\tau \right| - \nu_{ip}\,. \quad (6.43)$$

Now, from (6.43), we can see that if there exists $T_d > T_{iy}$, such that condition (6.29) is satisfied, then it is concluded that $|\tilde{y}_{ip}(T_d)| > \nu_{ip}(T_d)$, i.e., the sensor fault is detected at time $t = T_d$.

□

6.4.2 Process Fault Detectability Condition

In this section, we derive the fault detectability condition for process fault $f_i(x_i, u_i)$. Specifically, the following theorem characterizes the class of process faults that are detectable by the proposed distributed fault detection method.

Theorem 6.2: *For the distributed fault detection method described by (6.5) and (6.28), suppose that a process fault $f_i(x_i, u_i)$ occurs in the ith subsystem at time T_{ix}, where $i \in \{1, \cdots, M\}$. Then, if there exist some time instant $T_d > T_{ix}$ and some $p \in \{1, \cdots, l_i\}$, such that the fault function $f_i(x_i, u_i)$ satisfies*

$$\begin{aligned} &\left| \int_{T_{ix}}^{T_d} C_{ip} e^{\bar{A}_i(t-\tau)} f_i(x_i, u_i) d\tau \right| - \left| \frac{|\varrho_i|}{\sqrt{\lambda_{min}(P)}} \int_{T_{ix}}^{T_d} C_{ip} e^{\bar{A}_i(t-\tau)} ||f_i(x_i, u_i)||_{2a} d\tau \right| \\ &\geq \left| \frac{|\varrho_i|}{\sqrt{2\lambda_{min}(P)}} \int_{0}^{T_d} C_{ip} e^{\bar{A}_i(t-\tau)} ||\bar{\xi}_i||_{2a} d\tau \right| + 2\nu_{ip} \,. \end{aligned} \tag{6.44}$$

Then, the process fault will be detected at time $t = T_d$, i.e., $|\tilde{y}_{ip}(T_d)| > \nu_{ip}(T_d)$.

Proof: In the presence of a process fault (i.e., for $t \geq T_{ix}$) in ith subsystem, base on (6.1) and (6.5), the dynamics of the state estimation error $\tilde{x}_i \stackrel{\triangle}{=} x_i - \hat{x}_i$ satisfies

$$\begin{aligned} \dot{\tilde{x}}_i &= \bar{A}_i \tilde{x}_i + \phi_i(x_i, u_i) - \phi_i(\hat{x}_i, u_i) + \xi_i + \beta_{ix} f_i(x_i, u_i) \\ &\quad + \sum_{j=1}^{M} [h_{ij}(y_i, x_j, u_j) - h_{ij}(y_i, \hat{x}_j, u_j)] \\ &\quad + D_i \eta_i(x_i, u_i) - D_i \bar{\eta}_i(y_i, u_i) sgn(E_i \tilde{y}_i) \end{aligned} \tag{6.45}$$

$$\tilde{y}_{ip} = C_{ip} \tilde{x}_i \tag{6.46}$$

First, we consider the Lyapunov function candidate $V_i = \tilde{x}_i^\top P_i \tilde{x}_i$ for the ith subsystem. By following similar reasoning logic reported in the proof of Theorem 6.1, we can show the time derivative of V_i along the solution of (6.45) satisfies

$$\dot{V}_i \leq \tilde{x}_i^\top R_i \tilde{x}_i + \sum_{j=1}^{M} \gamma_{ij} \tilde{x}_j^\top \tilde{x}_j + |\bar{\xi}_i|^2 + |\beta_{ix} f_i(x_i, u_i)|^2 \,. \tag{6.47}$$

Second, for the interconnected kth subsystem which is healthy, where $k \in \{1, \cdots, M\} \backslash \{i\}$, the time derivative of the Lyapunov function $V_k = \tilde{x}_k^\top P_k \tilde{x}_k$ along the solution of (6.6) is the same as (6.33).

Next, for an overall Lyapunov function candidate $V = \sum_{j=1}^{M} V_j = \sum_{j=1}^{M} \tilde{x}_j^\top P_j \tilde{x}_j = \tilde{x}^\top P \tilde{x}$, where $P = \text{diag}\{P_1, \cdots, P_M\}$, and $\tilde{x}$ is defined in (6.8). Based on the (6.47) and (6.33), we have

$$\dot{V} \leq -\tilde{x}^\top Q \tilde{x} + \sum_{i=1}^{M} \frac{1}{2}|\bar{\xi}_i|^2 + \frac{1}{2}|\bar{\xi}_i|^2 + |\beta_{ix} f_i(x_i, u_i)|^2 \,. \tag{6.48}$$

Then, by following a similar reasoning logic as reported in the proof of Theorem 6.1, we have

$$\begin{aligned} |\tilde{x}|^2 &\leq \frac{\bar{V}_0 e^{-at}}{\lambda_{min}(P)} + \frac{1}{2\lambda_{min}(P)} \int_0^t e^{-a(t-\tau)} \sum_{i=1}^{M} |\bar{\xi}_i|^2 d\tau \\ &\quad + \frac{1}{\lambda_{min}(P)} \int_0^t e^{-a(t-\tau)} \big[\frac{|\bar{\xi}_i|^2}{2} + |\beta_{ix} f_i(x_i, u_i)|^2 \big] \, d\tau \\ &\leq \chi + \frac{||\bar{\xi}_i||_{2a}}{\sqrt{2\lambda_{min}(P)}} + \frac{||\beta_{ix} f_i(x_i, u_i)||_{2a}}{\sqrt{\lambda_{min}(P)}} \,. \end{aligned} \tag{6.49}$$

Now, we analyze the output estimation error, for each component of the output estimation error, i.e., $\tilde{y}_{ip}(t) \triangleq C_{ip} \tilde{x}_i(t)$, $p = 1, \cdots, l_i$, we have

$$\begin{aligned} \tilde{y}_{ip} &= C_{ip} \int_0^t e^{\bar{A}_i (t-\tau)} \Big[\phi_i(x_i, u_i) - \phi_i(\hat{x}_i, u_i) + \xi_i + [D_i \eta_i(x_i, u_i) - D_i \bar{\eta}_i(y_i, u_i) sgn(E_i \tilde{y}_i)] \\ &\quad + \beta_{ix} f_i(x_i, u_i) \Big] d\tau + C_{ip} \int_0^t e^{\bar{A}_i (t-\tau)} \sum_{j=1}^{M} [h_{ij}(y_i, x_j, u_j) - h_{ij}(y_i, \hat{x}_j, u_j)] d\tau \,. \end{aligned} \tag{6.50}$$

By applying the triangle inequality, based on Assumption 6.1, Assumption 6.3, and Assumption 6.4, we have:

$$\begin{aligned} |\tilde{y}_{ip}(t)| &\geq \left| \int_0^t C_{ip} e^{\bar{A}_i (t-\tau)} \beta_{ix} f_i(x_i, u_i) d\tau \right| - \left| \int_0^t C_{ip} e^{\bar{A}_i (t-\tau)} \big[\, |\varrho_i| \, |\tilde{x}| + \xi_i \, \big] d\tau \right| \\ &\quad - \left| \int_0^t C_{ip} e^{\bar{A}_i (t-\tau)} \big[D_i \eta_i - D_i \bar{\eta}_i sgn(E_i \tilde{y}_i) \big] d\tau \right|, \end{aligned} \tag{6.51}$$

where ϱ_i is defined in (6.25). Based on (6.49) and (6.51), we have

$$\begin{aligned}|\tilde{y}_{ip}(t)| \;\geq\; & \left|\int_0^t C_{ip}e^{\bar{A}_i(t-\tau)}\beta_{ix}f_i(x_i,u_i)d\tau\right| - \left|\int_0^t C_{ip}e^{\bar{A}_i(t-\tau)}\left[|\varrho_i|\chi + 2||D_i||\,\bar{\eta}_i + \bar{\xi}_i\right]d\tau\right| \\ & -\left|\int_0^t C_{ip}e^{\bar{A}_i(t-\tau)}\frac{|\varrho_i|\,||\bar{\xi}_i||_{2a}}{\sqrt{2\lambda_{min}(P)}}d\tau\right| - \left|\int_0^t C_{ip}e^{\bar{A}_i(t-\tau)}\frac{|\varrho_i|\,||\beta_{ix}f_i(x_i,u_i)||_{2a}}{\sqrt{\lambda_{min}(P)}}d\tau\right|.\end{aligned}$$

By substituting (6.28) and using the property of the step function β_{ix} and we can rewrite the above inequality as follows:

$$\begin{aligned}|\tilde{y}_{ip}(t)| \;\geq\; & \left|\int_{T_{ix}}^t C_{ip}e^{\bar{A}_i(t-\tau)}f_i(x_i,u_i)d\tau\right| - \left|\frac{|\varrho_i|}{\sqrt{\lambda_{min}(P)}}\int_{T_{ix}}^t C_{ip}e^{\bar{A}_i(t-\tau)}||f_i(x_i,u_i)||_{2a}d\tau\right| - \nu_{ip} \\ & -\left|\frac{|\varrho_i|}{\sqrt{2\lambda_{min}(P)}}\int_0^t C_{ip}e^{\bar{A}_i(t-\tau)}||\bar{\xi}_i||_{2a}d\tau\right|.\end{aligned}$$

Now, we can see that if there exists $T_d > T_{ix}$, such that condition (6.44) is satisfied, then it is concluded that $|\tilde{y}_{ip}(T_d)| > \nu_{ip}(T_d)$, i.e., the process fault is detected at time $t = T_d$.

□

6.5 Simulation Results

A two-machine infinite bus power system shown in Figure 6.1 is used to demonstrate the effectiveness of the proposed distributed fault detection and isolation method. Specifically,

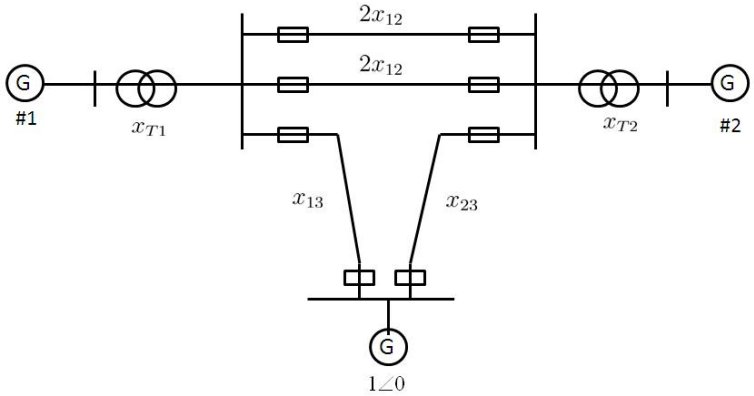

Figure 6.1: A two-machine infinite bus power system [26].

we consider a two machine infinite bus power system consisting of 2 interconnected machines under turbine / governor control. Based on the dynamics of such power systems [25, 26, 71, 9, 41, 57], by defining the state variables as $x_i = [\delta_i \;\; \omega_i \;\; P_{mi} \;\; X_{e_i}]^\top$, we can obtain a state space model of the ith subsystem $i = 1\,, 2$ as follows [40]:

$$\begin{aligned} \dot{x}_i &= A_i x_i + B_{i1} u_{i1} + B_{i2} h_{ij}(y_i, x_j) \\ y_i &= C_i x_i \end{aligned} \tag{6.52}$$

where

$$A_i = \begin{bmatrix} 0 & 1 & 0 & 0 \\ 0 & -\frac{D_i}{2H_i} & \frac{\omega_0}{2H_i}(1 - F_{IP_i}) & \frac{\omega_0}{2H_i} F_{IP_i} \\ 0 & 0 & -\frac{1}{T_{m_i}} & \frac{K_{m_i}}{T_{m_i}} \\ 0 & -\frac{K_{e_i}}{T_{e_i} R_i \omega_o} & 0 & \frac{1}{T_{e_i}} \end{bmatrix}$$

$B_{i1} = [\,0 \;\; 0 \;\; 0 \;\; \frac{1}{T_{e_i}}\,]^\top$, $B_{i2} = [\,0 \;\; -1 \; 0 \; 0\,]^\top$ and

$$C_i = \begin{bmatrix} 1 & 0 & 0 & 0 \\ 0 & 1 & 0 & 0 \\ 0 & 0 & 0 & 1 \end{bmatrix}$$

and the interconnection term $h_{ij} = \sum_{j=1, j\neq i}^{N} \frac{\omega_o E'_{q_i} E'_{q_j} B_{ij}}{2H_i} \sin(\delta_i - \delta_j)$ and the known terms E'_{qi}, E'_{q_j} and B_{ij}, i, j = 1, 2, are assumed to be constants [25]. The parameters for each machine are the same as given in [40] and are shown in Table 6.1.

Table 6.1 System parameters

	machine 1	machine 2
$H(s)$	4	5.1
$D(p.u.)$	5	3
k_c	1	1
F_{IP}	0.3	0.3
T_m	0.35	0.35
$\omega_0(rad/s)$	314.159	314.159

For simplicity, the input to each subsystem consists of two parts: a stabilizing part based on state feedback design and a sinusoidal signal causing each subsystem to deviate from steady-state linear dynamics. The modeling uncertainty under consideration consists of two parts. First, the modeling uncertainty in the local dynamics of the two subsystems are assumed to be up to 5% inaccuracy in the gain of the speed governor of the machine, which are represented as $D_1\eta_1$ and $D_2\eta_2$, respectively, where $D_1 = D_2 = [0 \;\; 0 \;\; 0 \;\; 1]^\top$, $\eta_1 = \eta_2 = \frac{\varphi_i K_{e_i}}{T_{e_i} R_i \omega_0}\omega_i$, and $\varphi_i \in [-0.05 \;\; 0.05]$, which lead to $\bar{\eta}_i = |\frac{0.05 K_{e_i}}{T_{e_i} R_i \omega_0}\omega_{i_{max}}|$, where $\omega_{i_{max}}$ is upper bound of $|\omega_i|$ obtained based on the prior knowledge of the system. In the simulation, the unknown modeling uncertainty in the local dynamics of the two subsystems are assumed to be $\eta_1 = \eta_2 = \frac{0.03 K_{e_i}}{T_{e_i} R_i \omega_0}\omega_i$.

Second, for the uncertainty in the interconnection term, we consider up to 5% inaccuracy in the interconnection term $\sum_{j=1, j\neq i}^{N} \frac{\omega_o E'_{q_i} E'_{q_j} B_{ij}}{2H_i} \sin(\delta_i - \delta_j)$ (corresponding to ξ_i in (6.1)). In the simulation, the unknown part in the interconnection term is assumed to be 4% inaccuracy in the term $\sum_{j=1, j\neq i}^{N} \frac{\omega_o E'_{q_i} E'_{q_j} B_{ij}}{2H_i} \sin(\delta_i - \delta_j)$.

In addition, the following two types of faults are considered in each subsystem:

1. *An actuator fault.* A simple multiplicative actuator fault by letting $u_i = \bar{u}_i + \vartheta_i \bar{u}_i$ is considered, where $\bar{u}_i$ is the nominal control input in the non-fault case, and $\vartheta_i \in [-1 \;\; 0]$ is the unknown fault magnitude. For instance, the case $\vartheta_i = 0$ represents the normal operation condition, while the case $\vartheta_i = -1$ corresponds to a complete failure of the actuator.

2. *A sensor bias fault.* A sensor bias in the first output is represented as θ_i, $\theta_i \in [\,0,\ 10\,]$ (i.e., up to 20% of the maximum value of the first output of each machine).

By using the LMI toolbox introduced in the Section (4.2.1), the design parameters can be obtained as follows:

$$L_1 = \begin{bmatrix} 13.5 & 1 & 0 \\ -1.034 & 23.718 & 11.781 \\ -0.404 & 4.195 & 2.857 \\ 0 & -0.6366 & 23.7 \end{bmatrix}$$

$$L_2 = \begin{bmatrix} 13.5 & 1 & 0 \\ -0.850 & 24.050 & 9.24 \\ -0.423 & 5.349 & 2.857 \\ 0 & -0.6366 & 23.7 \end{bmatrix}$$

$$P_1 = \begin{bmatrix} 0.0614 & 0.0002 & 0.004 & 0 \\ 0.0002 & 0.03 & -0.006 & 0 \\ 0.004 & -0.006 & 0.188 & 0 \\ 0 & 0 & 0 & 0.0604 \end{bmatrix}$$

$$P_2 = \begin{bmatrix} 0.0669 & 0 & 0.004 & 0 \\ 0 & 0.037 & -0.012 & 0 \\ 0.004 & -0.0122 & 0.184 & 0 \\ 0 & 0 & 0 & 0.0658 \end{bmatrix}$$

$E_1 = [\,0\ \ 0\ \ 0.066\,]$, and $E_2 = [\,0\ \ 0\ \ 0.0604\,]$. Consequently, the related design constants are $k_{i1} = k_{i2} = k_{i3} = 1$, $\lambda_{i1} = 13.5$ and $\lambda_{i2} = 13.3$ and $\lambda_{i3} = 13.9$. Thus

$$Q_1 = \begin{bmatrix} 1.044 & -0.004 & -0.008 & 0 \\ -0.004 & 0.828 & -0.212 & 0 \\ -0.008 & -0.212 & 0.7155 & 0 \\ 0 & 0 & 0 & 1.045 \end{bmatrix}$$

$$Q_2 = \begin{bmatrix} 1.041 & -0.01 & -0.0015 & 0 \\ -0.007 & 0.948 & -0.357 & 0 \\ -0.008 & -0.366 & 0.8158 & 0 \\ 0 & 0 & 0 & 1.042 \end{bmatrix}$$

and $a = 2.73$.

First, the case of a *sensor fault* in machine 2 is illustrated in Figure 6.2 and Figure 6.3. Specifically, we consider a sensor fault with $\theta_2 = [10\ 0\ 0\ 0]^\top$ occurs to machine 2 at $T_{2y} = 5$ second. As we can see, in Figure 6.2, although there is no fault in machine 1, the residual in the second output generated by FDE 1 exceeds its corresponding threshold approximately at $t = 5\,\text{sec}$, indicating that the effect of the sensor bias in machine 2 has been propagated into the machine 1 due to the interconnection. In Figure 6.3 the residuals in the first and the second outputs generated by FDE 2 exceeds their corresponding thresholds immediately after sensor bias occurrence. Therefore, the sensor bias fault in machine 2 is timely detected.

Then, we consider an *actuator fault* in machine 1. Figure 6.4 shows the fault detection results when a partial actuator fault with $\vartheta_1 = -0.25$ occurs to machine 1 at $T_{1x} = 5$ second. As can be seen from Figure 6.4, the residual in the third output generated by FDE 1(i.e., the local FDE designed for machine1) exceeds its threshold immediately after fault occurrence. Therefore, the actuator fault in machine 1 is also timely detected.

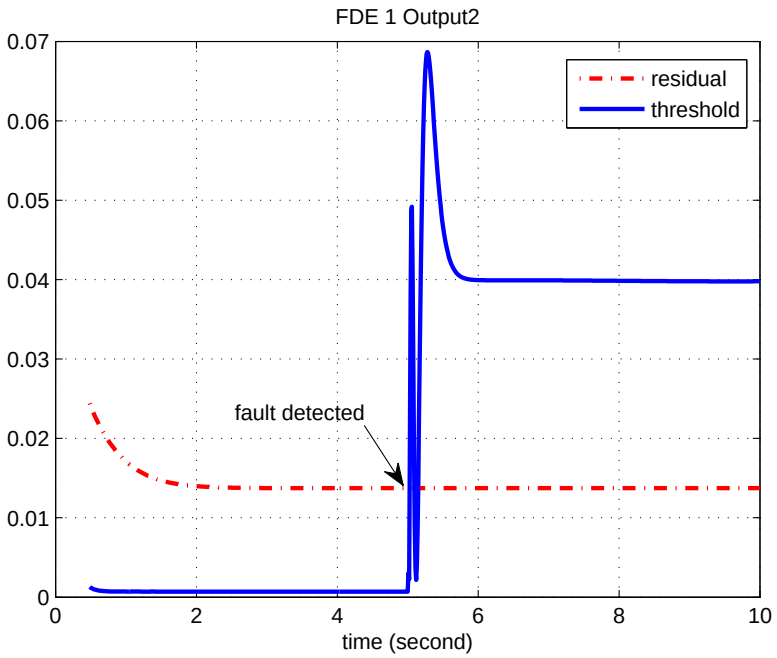

Figure 6.2: The case of a sensor fault in machine 2: fault detection residuals (solid and blue line) associated with y_{12} and the corresponding threshold (dashed and red line) generated by the FDE 1

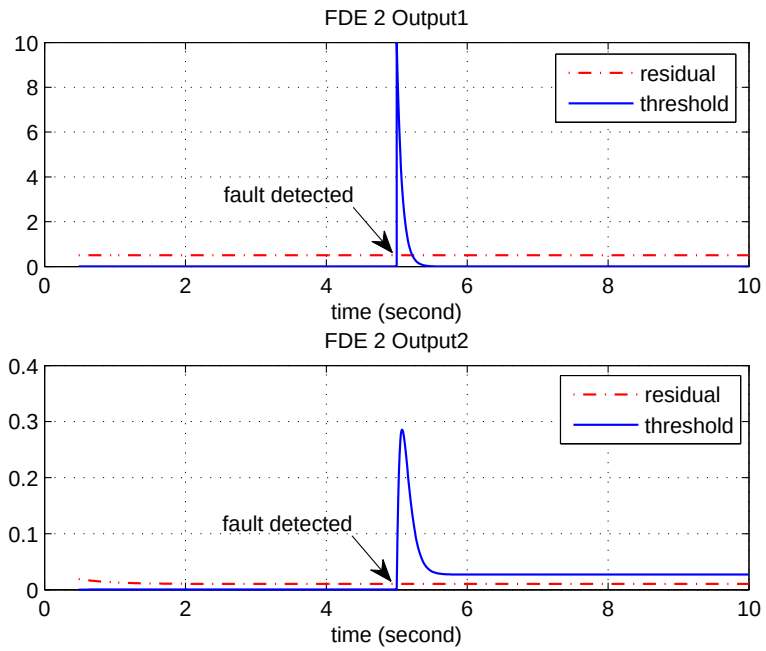

Figure 6.3: The case of a sensor fault in machine 2: the fault detection residuals (solid and blue line) associated with y_{21} and y_{22} and the corresponding threshold (dashed and red line) generated by the FDE 2

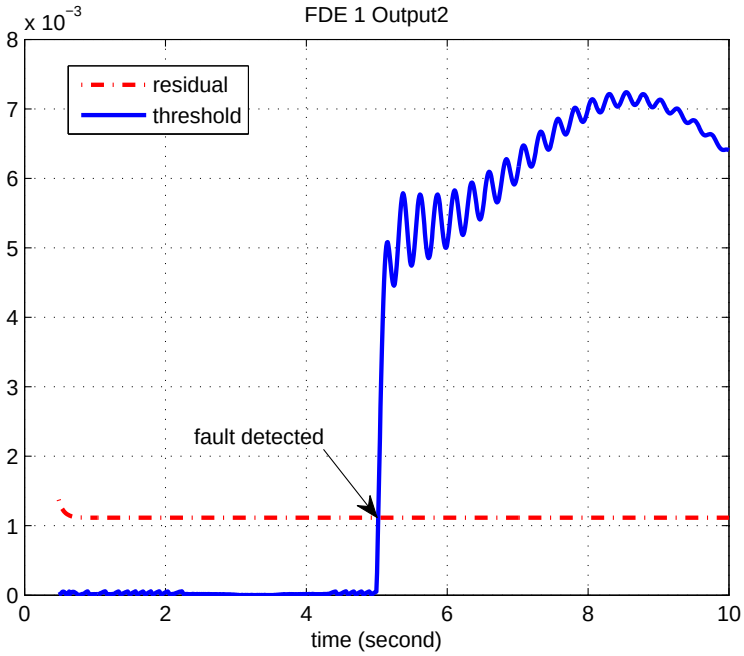

Figure 6.4: The case of an actuator fault in machine 1: the fault detection residuals (solid and blue line) associated with y_{13} and the corresponding threshold (dashed and red line) generated by the FDE 1

Chapter 7

Conclusions and Future Work

7.1 Conclusions

In this dissertation, the problem of fault diagnosis of interconnected nonlinear uncertain systems is investigated. In the presented distributed FDI architecture, a fault diagnostic component is designed for each subsystem in the interconnected system by utilizing local measurements and certain communicated information from neighboring FDI components associated with its directly interconnected subsystems. Each local FDI component consists of two modules: a fault detection module is used to detect an occurrence of any fault in the corresponding subsystem, and a fault isolation module is used to determining the type of the fault among a set of partially known possible fault types in each subsystem or determining the actual faulty subsystem among all the subsystems.

First, a distributed fault detection and isolation method is developed for process faults in a class of interconnected nonlinear uncertain systems. In the fault diagnostic component associated with each subsystem, a fault detection estimator is used for fault detection and activation of fault isolation, and a bank of fault isolation estimators are used to determine the particular type of fault that has occurred in the subsystem. Under certain assumptions, adaptive thresholds are designed for distributed fault detection and isolation in each subsystem. The important properties of robustness and fault sensitivity (fault detectability and

isolability) of the distributed FDI algorithm are investigated. In addition, the stability and learning capability of local adaptive fault isolation estimators designed for each subsystem are also established.

Second, a distributed sensor FDI scheme is developed for a class of interconnected input-output nonlinear systems where only the measurable part of state variables are directly affected by the interconnections between subsystems. A class of multi-machine power systems is used as an application example to illustrate the effectiveness of the proposed approach. The general theory can be easily extended to other system. For each subsystem, a local FDI component comprised of a fault detection estimator and a fault isolation estimators is designed to detect sensor faults and determine the particular subsystem where the sensor fault actually occurs. The adaptive thresholds for distributed sensor fault detection and isolation in each subsystem are derived and some important properties of FDI methods are analyzed, including fault detectability, fault isolability, and the stability and learning capability of the distributed adaptive fault isolation estimators

Third, we extend the above sensor FDI results by considering a class of interconnected input-output nonlinear systems where both the unknown and the measurable parts of system states of each subsystem are directly affected by the interconnection between subsystems. In this case, due to the fault effect propagation, the estimation error of the unknown state variables in each subsystem is also affected by the sensor fault. Thus, the problem considered is more challenging than what is described above

Fourth, a fault detection scheme is presented for a more general distributed nonlinear systems. We significantly extend the research work in Chapter 3, Chapter 4 and Chapter 5 by removing some restrictive limitations on system model structure. In the distributed detection scheme, a fault detection component is associated with each subsystem. Adaptive thresholds for fault detection is derived, ensuring robustness with respect to interconnections among subsystems and modeling uncertainty. Moreover, the fault detectability conditions are rigorously investigated, characterizing the class of detectable process faults and sensor faults in each subsystem.

7.2 Future Research Work

For the problem of sensor fault diagnosis in interconnected nonlinear systems discussed in Chapter 5, the issue of the fault isolability condition still needs further investigation. The fault isolability condition is a critical property in characterizing the class of sensor faults that are isolable by the proposed fault isolation method. Additionally, after a faulty subsystem is successfully isolated by using the proposed sensor fault isolation scheme discussed in Chapter 5, we can extend the presented fault isolation method to construct a hierarchical method which allows the isolation of both the faulty subsystem and the particular faulty sensor as well. Also, the fault isolation issue for the system model given in Chapter 6 needs investigation in the future.

As described in Section 2.3, malicious attacks on the interconnection or communication link between subsystems is a typical fault needs to be considered in the fault diagnosis of interconnected systems. The issue of detection and isolation of malicious attacks in the communication link are interesting topics for future research. The robustness to communication delay and packet dropouts is also worth investigating.

In this work, the interconnections among subsystems are assumed to be partially known. However, in some applications, the interconnection information of interconnected systems is difficult to model due to the complexity of the overall systems. Thus, the case of interconnection effects with significant modeling uncertainties should be investigated to extend the applicability of the distributed FDI method proposed in this dissertation.

Bibliography

[1] A. R. Behbahani. Adaptive distributed intelligent control architecture for future propulsion systems. Technical Report PR-WP-TP-2007-22, U.S. Air Force Research Laboratory, April 2007.

[2] A.R. Bergen. *Power systems analysis.* Prentice Hall, Englewood Cliffs, New Jersey, 1986.

[3] M. Blanke, M. Kinnaert, J. Lunze, and M. Staroswiecki. *Diagnosis and Fault-Tolerant Control.* Springer, Berlin, 2006.

[4] Francesca Boem, Riccardo MG Ferrari, and Thomas Parisini. Distributed fault detection and isolation of continuous-time non-linear systems. *European Journal of Control*, 17(5):603–620, 2011.

[5] J. Chen and R. J. Patton. *Robust Model-Based Fault Diagnosis for Dynamic Systems.* Kluwer Academic Publishers, London, 1999.

[6] W. Chen and M. Saif. Adaptive actuator fault detection, isolation and accommodation in uncertain systems. *International Journal of Control*, 80(1):45–63, 2007.

[7] Mo-Yuen Chow and Yodyium Tipsuwan. Network-based control systems: a tutorial. In *Industrial Electronics Society, 2001. IECON'01. The 27th Annual Conference of the IEEE*, volume 3, pages 1593–1602. IEEE, 2001.

[8] Mariesa L Crow and MD Ilić. The waveform relaxation method for systems of differential/algebraic equations. *Mathematical and computer modelling*, 19(12):67–84, 1994.

[9] D. M. Stipanovic D. D. Siljak and A. I. Zecevic. Robust decentralized turbine/governor control using linear matrix inequalities. *IEEE Trans. Power System*, 17(3):715–722, 2002.

[10] Supratim Deb and R Srikant. Rate-based versus queue-based models of congestion control. *ACM SIGMETRICS Performance Evaluation Review*, 32(1):246–257, 2004.

[11] F Dorfler, Fabio Pasqualetti, and Francesco Bullo. Distributed detection of cyber-physical attacks in power networks: A waveform relaxation approach. In *Communication, Control, and Computing (Allerton), 2011 49th Annual Allerton Conference on*, pages 1486–1491. IEEE, 2011.

[12] Nicola Elia and Jeff N Eisenbeis. Limitations of linear control over packet drop networks. *Automatic Control, IEEE Transactions on*, 56(4):826–841, 2011.

[13] D. G. Eliades and M. M. Polycarpou. A fault diagnosis and security framework for water systems. *IEEE Transactions on Control Systems Technology*, 18(6):1254–1265, 2010.

[14] A. Emami-Naeini, M. M. Akhter, and S. M. Rock. Effect of model uncertainty on failure detection: the threshold selector. *IEEE Transactions on Automatic Control*, 33:1106–1115, 1988.

[15] J. Farrell and M. M. Polycarpou. *Adaptive Approximation Based Control*. J. Wiley, Hoboken, NJ, 2006.

[16] M Farsi, K Ratcliff, and Manuel Barbosa. An overview of controller area network. *Computing & Control Engineering Journal*, 10(3):113–120, 1999.

[17] James P Farwell and Rafal Rohozinski. Stuxnet and the future of cyber war. *Survival*, 53(1):23–40, 2011.

[18] R. Ferrari, T. Parisini, and M. M. Polycarpou. Distributed fault diagnosis of large-scale discrete-time nonlinear systems: New results on the isolation problem. In *49th IEEE Conference on Decesion and Control*.

[19] R. Ferrari, T. Parisini, and M. M. Polycarpou. A fault detection scheme for distributed nonlinear uncertain systems. In *Proceedings of the 2006 IEEE International Symposium on Intelligent Control*.

[20] R. Ferrari, T. Parisini, and M. M. Polycarpou. Distributed fault diagnosis with overlapping decompositions: an adaptive approximation approach. *IEEE Trans. on Automatic Control*, 54:794–799, 2009.

[21] R. Ferrari, T. Parisini, and M. M. Polycarpou. Distributed fault detection and isolation of large-scale discrete-time nonlinear systems:an adaptive approximation approach. *IEEE Trans. on Automatic Control*, 57:275–290, 2012.

[22] P. M. Frank. Fault diagnosis in dynamic systems using analytical and knowledge-based redundancy - a survey and some new results. *Automatica*, 26:459–474, 1990.

[23] Emilia Fridman, Alexandre Seuret, and Jean-Pierre Richard. Robust sampled-data stabilization of linear systems: an input delay approach. *Automatica*, 40(8):1441–1446, 2004.

[24] J. J. Gertler. *Fault Detection and Diagnosis in Engineering Systems*. Marcel Dekker, New York, NY, 1998.

[25] Y. Guo, D. J. Hill, and Y. Wang. Nonlinear decentralized control of large-scale power systems. *Automatica*, 36:1275–1289, 2000.

[26] Y. Wang. G. Guo and D. J. Hill. Robust decentralized nonlinear controller design for multimahine power systems. *Automatica*, 33:1725–1733, 1997.

[27] Rachana Ashok Gupta and Mo-Yuen Chow. Networked control system: Overview and research trends. *Industrial Electronics, IEEE Transactions on*, 57(7):2527–2535, 2010.

[28] M.F. Hassan, M.A.Sultan, and M.S.Attia. Fault detection in large-scale stochastic dynamic systems. In *IEE PROCEEDINGS -D*, volume 139, 1992.

[29] Joao P Hespanha, Margaret McLaughlin, Gaurav S Sukhatme, Minoo Akbarian, Rajiv Garg, and Weirong Zhu. Haptic collaboration over the internet. In *The Fifth PHANTOM Users Group Workshop*, volume 40, 2000.

[30] Joao P Hespanha, Payam Naghshtabrizi, and Yonggang Xu. A survey of recent results in networked control systems. *Proceedings of the IEEE*, 95(1):138–162, 2007.

[31] Kenji Hikichi, Hironao Morino, Isamu Arimoto, Kaoru Sezaki, and Yasuhiko Yasuda. The evaluation of delay jitter for haptics collaboration over the internet. In *Global Telecommunications Conference, 2002. GLOBECOM'02. IEEE*, volume 2, pages 1492–1496. IEEE, 2002.

[32] N. Hovakimyan, E. Lavretsky, B. Yang, and A.J.Calise. Coordinated decentralized adaptive output feedback control of interconnected systems. *IEEE Transactions on Nerural Networks*, 16:185–194, 2005.

[33] I. Hwang, S. Kim, Y. Kim, and C. E. Seah. A survey of fault detection, isolation, and reconfiguration methods. *IEEE TRANSACTIONS ON CONTROL SYSTEMS TECHNOLOGY*, 18(3):636–653, 2010.

[34] M. IKEDA and D.D.Siljak. Overlapping decomposition expansion and contraction of dynamic systems. *J. Large Scale Syst*, 1:2938, 1980.

[35] P. A. Ioannou and J. Sun. *Robust Adaptive Control*. Prentice Hall, Englewood Cliffs, NJ, 1996.

[36] R. Isermann. *Fault-Diagnosis Systems: An Introduction from Fault Detection to Fault Tolerance*. Springer, Berlin, 2006.

[37] B. Jiang, M. Staroswiechi, and V. Cocquempot. Fault diagnosis based on adaptive observer for a class of nonlinear systems with unknown parameters. *International Journal of Control*, 77(4):415–426, 2004.

[38] Karl Henrik Johansson, Martin Törngren, and Lars Nielsen. Vehicle applications of controller area network. In *Handbook of Networked and Embedded Control Systems*, pages 741–765. Springer, 2005.

[39] P. Kabore and H. Wang. Design of fault diagnosis filters and fault tolerant control for a class of nonlinear systems. *IEEE Transactions on Automatic Control*, 46:1805–1810, 2001.

[40] Jianming Lian Karanjit Kalsi and Stanislaw H.Zak. Decentralized control of multi-machine power systems. In *2009 American Control Conference*, pages 2122–2127, St. Louis, MO, USA, 2009.

[41] P. Kundur. *Power system stability and control*. McGrawHill, New York, NY, 1994.

[42] S Kuvshinkova. Sql slammer worm lessons learned for consideration by the electricity sector. *North American Electric Reliability Council*, 2003.

[43] Ekachai Lelarasmee, Albert E Ruehli, and Alberto L Sangiovanni-Vincentelli. The waveform relaxation method for time-domain analysis of large scale integrated circuits. *IEEE Transactions on Computer-Aided Design of Integrated Circuits and Systems*, 1(3):131–145, 1982.

[44] Derong Liu. *Networked control systems: theory and applications*. Springer, 2008.

[45] N. Meskin and K. Khorasani. Actuator fault detection and isolation for a network of unmanned vehicles. *IEEE Transactions on Automatic Control*, 54(4):835–840, 2009.

[46] Reza Olfati-Saber and Richard M Murray. Consensus problems in networks of agents with switching topology and time-delays. *Automatic Control, IEEE Transactions on*, 49(9):1520–1533, 2004.

[47] P. Panagi and M. M. Polycarpou. Decentralized adaptive approximation based control of a class of large-scale systems. pages 4191–4196, June 2008.

[48] P. Panagi and M. M. Polycarpou. Distributed fault detection and accommodation with partial communication. March 2010.

[49] Fabio Pasqualetti, Florian Dörfler, and Francesco Bullo. Attack detection and identification in cyber-physical systems–part i: Models and fundamental limitations. *arXiv preprint arXiv:1202.6144*, 2012.

[50] Fabio Pasqualetti, Florian Dörfler, and Francesco Bullo. Attack detection and identification in cyber-physical systems–part ii: Centralized and distributed monitor design. *arXiv preprint arXiv:1202.6049*, 2012.

[51] Fabio Pasqualetti, Florian Dorfler, and Francesco Bullo. Cyber-physical security via geometric control: Distributed monitoring and malicious attacks. In *Decision and Control (CDC), 2012 IEEE 51st Annual Conference on*, pages 3418–3425. IEEE, 2012.

[52] G. K. A. Rao and N. Viswanadham. Decentralized fault detection and diagnosis in large linear stochasitc systems. *J.I. Electr. Telecommun. Eng*, 39:143–148, 1993.

[53] K. Reif, K. Schmidt, F. Gesele, S. Reichelt, M. Saeger, and N. Seidler. Networked control systems in motor vehicles. *ATZelektronik Worldwide*, 3(4):18–23, 2008.

[54] Wei Ren and Randal W Beard. Consensus seeking in multiagent systems under dynamically changing interaction topologies. *Automatic Control, IEEE Transactions on*, 50(5):655–661, 2005.

[55] Michael Rotkowitz and Sanjay Lall. Affine controller parameterization for decentralized control over banach spaces. *Automatic Control, IEEE Transactions on*, 51(9):1497–1500, 2006.

[56] G. P. Sallee. Performance deterioration based on existing (historical) data JT9D jet engine diagnostics program. Technical Report NASA CR135448, PWA551221, United Technologies Corporation, Pratt & Whitney Aircraft Group, 1978.

[57] P. W. Sauer and M. A. Pai. *Power systems dynamics and stability*. Prentice-Hall, Englewood Cliffs, New Jersey, 1998.

[58] S. Shankar, S. Darbha, and A. Datta. Design of a decentralized detection filter for a large collection of interacting LTI systems. *Mathematical Problems in Engineering*, 8:233–248, 2002.

[59] Shervin Shirmohammadi and N Ho Woo. Evaluating decorators for haptic collaboration over internet. In *Haptic, Audio and Visual Environments and Their Applications, 2004. HAVE 2004. Proceedings. The 3rd IEEE International Workshop on*, pages 105–109. IEEE, 2004.

[60] D. D. Siljak, editor. *Decentralization, Stabilization and Estimation of Large-Scale Linear Systems*. Academic Press Inc., Boston, 1990.

[61] M. G. Singh, M. F. Hassan, Y. L. Chen, and Q. R. Pan. New approach to failure detection in large-scale systems. In *IEE PROCEEDINS,*, volume 130, pages 243–249, 1983.

[62] J. T. Spooner and K. M. Passino. Adaptive control of a class of decentralized nonlinear systems. *IEEE Transactions on Automatic Control*, 41(2):280–284, 1996.

[63] J. T. Spooner and K. M. Passino. Decentralized adaptive control of nonlinear systems using radial basis neural networks. *IEEE Transactions on Automatic Control*, 44(11):2050–2057, 1999.

[64] Ao Tang, Krister Jacobsson, Lachlan LH Andrew, and Steven H Low. An accurate link model and its application to stability analysis of fast tcp. In *INFOCOM 2007. 26th*

IEEE International Conference on Computer Communications. IEEE, pages 161–169. IEEE, 2007.

[65] L. Tang, X. Zhang, J. A. DeCastro, L. Farfan-Ramos, and D. Simon. A unified nonlinear adaptive approach for detection and isolation of engine faults. In *Proceedings of the ASME Turbo Expo 2010*, Glasgow, Scotland, June 2010.

[66] X. Tang, G. Tao, and S. M. Joshi. Adaptive actuator failure compensation for nonlinear MIMO systems with an aircraft control application. *Automatica*, 43:1869–1883, 2007.

[67] Yodyium Tipsuwan and Mo-Yuen Chow. Control methodologies in networked control systems. *Control engineering practice*, 11(10):1099–1111, 2003.

[68] Nikolai Vatanski, Jean-Philippe Georges, Christophe Aubrun, Eric Rondeau, and Sirkka-Liisa Jämsä Jounela. Control compensation based on upper bound delay in networked control systems. *arXiv preprint cs/0609151*, 2006.

[69] K. Vijayaraghavan, R. Rajamani, and J. Bokor. Quantitative fault estimation for a class of nonlinear systems. *International Journal of Control*, 80(1):64–74, 2007.

[70] A. Xu and Q. Zhang. Nonlinear sysem fault diagnosis based on adaptive estimation. *Automatica*, 40:1181–1193, 2004.

[71] D. J. Hill Y. Wang and G. Guo. Robust decentralized control for multimachine power systems. *IEEE Trans. Circuits System*, 45(3):271–279, 1998.

[72] X. Yan and C. Edwards. Robust decentralized actuator fault detection and estimation for large-scale systems using a sliding-mode observer. *International Journal of Control*, 81(4):591–606, 2008.

[73] Tai C Yang. Networked control system: a brief survey. *IEE Proceedings-Control Theory and Applications*, 153(4):403–412, 2006.

[74] Lei Ying, Geir E Dullerud, and Rayadurgam Srikant. Global stability of internet congestion controllers with heterogeneous delays. *IEEE/ACM Transactions on Networking (TON)*, 14(3):579–591, 2006.

[75] Sandro Zampieri. Trends in networked control systems. In *17th IFAC World Congress*, pages 2886–2894, 2008.

[76] Ke Zhang, Bin Jiang, and Peng Shi. Fast fault estimation and accommodation for dynamical systems. *Control Theory & Applications, IET*, 3(2):189–199, 2009.

[77] Q. Zhang and X. Zhang. Distributed sensor fault diagnosis in a class of interconnected nonlinear uncertain systems. In *the 2012 IFAC Symposium on Fault Detection, Supervision and Safety of Technical Processes*, pages 1101–1106, Mexico City, Mexico, August 2012.

[78] Q. Zhang and X. Zhang. Distributed sensor fault diagnosis in a class of interconnected nonlinear uncertain systems. *Annual Reviews in Control*, 37:170–179, 2013.

[79] X. Zhang. Sensor bias fault detection and isolation in a class of nonlinear uncertain systems using adaptive estimation. *IEEE Transactions on Automatic Control*, 56:1220–1226, 2011.

[80] X. Zhang, H.Uliyar, L.Farfan-Ramos, Y.Zhang, and M.Salman. Fault diagnosis of automotive electric power generation and storage systems. In *2010 IEEE International Conference on Control Applicaitons, Part of 2010 IEEE Multi-Conference on Systems and Control*, Yokohama, Japan, September 2010.

[81] X. Zhang, T. Parisini, and M. M. Polycarpou. Sensor bias fault isolation in a class of nonlinear systems. *IEEE Transactions on Automatic Control*, 50:370–376, 2005.

[82] X. Zhang, M. M. Polycarpou, and T. Parisini. Robust fault isolation of a class of nonlinear input-output systems. *International Journal of Control*, 74(13):1295–1310, 2001.

[83] X. Zhang, M. M. Polycarpou, and T. Parisini. A robust detection and isolation scheme for abrupt and incipient faults in nonlinear systems. *IEEE Transactions on Automatic Control*, 47(4):576–593, 2002.

[84] X. Zhang, M. M. Polycarpou, and T. Parisini. Fault diagnosis of a class of nonlinear uncertain system with lipschitz nonlinearities using adaptive estimation. *Automatica*, 46:290–299, 2010.

[85] X. Zhang and Q.Zhang. Distributed fault detection and isolation in a class of large-scale nonlinear uncertain systems. *International Journal of Control*, 85(11):1644–1662, 2012.

[86] X. Zhang and Q. Zhang. Distributed fault detection and isolation in a class of large-scale nonlinear uncertain systems. In *18th IFAC World Congress*, pages 4302–4307, Milano, Italy, August 2011.

Appendix A

Notation of Chapter 6

δ_i the power angle of the ith generator, in rad

ω_i the relative speed of the ith generator, in rad/s

P_{mi} the mechanical input power, in p.u.

P_{ei} the electrical power, in p.u

ω_0 the synchronous machine speed in rad/s

D_i the per unit damping constant

H_i the inertia constant, in s

E'_{qi} the transient EMF in the quadrature axis, in p.u

E_{qi} EMF in the quadrature axis, in p.u

E_{fi} the equivalent EMF in the excitation coil, in p.u

T'_{doi} the direct axis transient short-circuit time constant, in s

x_{di} the direct axis reactance, in p.u.

x'_{di} the direct axis transient reactance, in p.u.

B_{ij} the ith row and jth column element of nodal susceptance matrix at the internal nodes after eliminating all physical buses, in p.u.

Q_{ei} the reactive power, in p.u.

I_{fi} the excitation current, in p.u.

I_{di} the direct axis current, in p.u.

I_{qi} the quadrature axis current, in p.u.

k_{ci} the gain of excitation amplifier, in p.u.

u_{fi} the input of the SCR amplifier, in p.u.

x_{adj} the mutual reactance between the excitation coil and the stator coil, in p.u.

x_{ij} the transmission line reactance between the ith generator and the jth generator, in p.u.